1997 Annual water column monitoring report

Massachusetts Water Resources Authority
Environmental Quality Department
Report ENQUAD 1998-19

1997 Annual Water Column Monitoring Report

submitted to

MASSACHUSETTS WATER RESOURCES AUTHORITY
Environmental Quality Department
100 First Avenue
Charlestown Navy Yard
Boston, MA 02129
(617) 242-6000

prepared by

Stephen J. Cibik
Kristyn B. Lemieux
Joan K. Tracey
Stephanie J. Kelly

ENSR
35 Nagog Park
Acton, MA 01720
(978) 635-9500

and
Brian L. Howes
CMAST
New Bedford, MA 02744
and

Cabell Davis
Craig D. Taylor
Woods Hole Oceanographic Institution
Woods Hole, MA 02543

and

Theodore C. Loder, III
University of New Hampshire
Durham, NH 03824

December 1998

Citation:

Cibik SJ, Lemieux KB, Tracey JK, Kelly SJ, Howes BL, Taylor CD, Loder TC, III. 1998. 1997 Annual water column monitoring report. Boston: Massachusetts Water Resources Authority. Report ENQUAD 98-19. 258 p.

Acknowledgements

The authors wish to acknowledge the innumerable people who contributed to the monitoring studies presented in this annual report. First and foremost, we recognize the scientific teams fielded by the many organizations who participated in the MWRA's monitoring program, both at sea and in the laboratory. It was their expertise and dedication which produced the high-quality data reported herein, despite working frequently under exceedingly difficult conditions. Special recognition is given to Mr. Steven Wolf, ENSR Operations Manager, and Mr. Don Boyé, ENSR Chief Scientist, for their logistical abilities that made it all happen. We also thank Mr. Mel Higgins and Dr. Joshua Lieberman for their database expertise.

We additionally recognize Ms. Dale Goehringer of WHOI, Mr. Rob Boudrow of UNH, and Mr. Richard Lacouture of the Academy of Natural Sciences' Estuarine Research Center for coordinating the various laboratory efforts. We also thank the masters and crews of the vessels *Isabel S* and *Christopher Andrew*, with special thanks to Mr. Frank Mirarchi and Mr. Chip Rhyther of CR Environmental for their capable support of our sea operations.

The authors also received generous technical support and information from numerous agencies outside of the program. We thank in particular Ms. Fran Hotchkiss, Mr. Bill Strahle, and Dr. Rich Signell of the USGS Woods Hole office for providing data and information on mooring deployments. We thank Mr. Tom Shepard, Mr. Russell Gadoury, and Ms. Jessica Stock-Alvarez of the USGS Marlborough, Massachusetts, Office for providing river discharge data. Thanks also to Douglas Hankins of WETLabs for providing timely data for continuous chlorophyll monitoring, and to Kathy Vreeland of the Northeast Regional Climate Center for meteorological data.

Thanks are also extended to Dr. Don Anderson of WHOI for additional data on the occurrence and distribution of *Alexandrium tamarense* in Massachusetts Bay during the monitoring period, Dr. Steve Bates of the Bedford Institute of Oceanography, Marine Environmental Sciences Division for consultations on domoic acid and *Pseudo-nitzschia*, and to Dr. David Taylor of the MWRA Central Laboratory for chlorophyll data from Boston Harbor. Thanks also to Dr. Bernie Gardner of UMass Boston for his input on the interpretation of physical oceanography data.

Finally, we acknowledge that there are certainly several people we have overlooked who deserve specific mention, to whom we extend our thanks and our apologies for our momentary lapse in memory.

1997 ANNUAL WATER COLUMN REPORT
EXECUTIVE SUMMARY

The Massachusetts Water Resources Authority (MWRA) Harbor and Outfall Monitoring (HOM) Program has collected water quality data in Massachusetts and Cape Cod Bays since 1992. This monitoring is in support of the HOM Program mission to assess the potential environmental effects of effluent discharge relocation from Boston Harbor into Massachusetts Bay. The data are being collected to establish baseline water quality conditions and ultimately to provide the means to detect significant departure from that baseline. The data include physical water properties, nutrients, biological production and respiration, and plankton measurements. Two types of surveys are performed: nearfield surveys with stations located in the area around the future outfall site, and more comprehensive combined nearfield/farfield surveys that include stations in Boston Harbor, Massachusetts Bay, and Cape Cod Bay.

This report presents the results of the sixth continuous year of water column monitoring. The data presented in this report were collected throughout 1997 (February to December) in the Massachusetts Bay system. The scope of this annual report is to provide a comprehensive review of the 1997 data, to provide an integrative synthesis of results across the various technical disciplines, and to provide a comparison of results with data collected during previous monitoring years.

The Massachusetts Bay system undergoes strong seasonal stratification of the water column, and the timing of the onset and breakdown of vertical stratification influences seasonal nutrient cycling and its effect on critical issues such as dissolved oxygen depletion in stratified bottom water. The interpretation of monitoring data is thus intricately associated with the physical characteristics of the Massachusetts Bay environment. This summary first presents an overview of events that occurred during 1997, and then provides a comparison with monitoring data collected in previous years.

1997 Monitoring Results

During early February the water column was well mixed and replete with nutrients. Minimal autotrophic and heterotrophic activity was evident throughout Massachusetts Bay, whereas lower nutrient concentrations and somewhat elevated chlorophyll and phytoplankton densities in Cape Cod Bay indicated that the late winter bloom was already underway there. By the second survey in late February, the bloom in Cape Cod Bay was fully developed. Primary productivity at the outer nearfield (station N04) reached its annual peak during this survey, and evidence from several supporting parameters indicated heightened activity throughout Massachusetts Bay except in Boston Harbor.

Surface algal activity in the center of the nearfield (station N18) declined substantially in mid-March compared with the more seaward station N04. Nutrient uptake and productivity in general slowed, and surface chlorophyll and phytoplankton results were lower relative to the preceding survey. A prolonged 10-

day period of cloudy skies during early March may have been responsible for the curtailed production. Primary production rebounded at station N18 during the early April combined survey and was more comparable to station N04. Chlorophyll and carbon concentrations in the deeper samples from N18 reached their seasonal peak concentrations, and high respiration rates were noted during both March surveys.

A system-wide bloom of *Phaeocystis pouchetii* which began in late February reached its maximum concentrations during early April, with Cape Cod Bay densities reaching 15 million cellsL^{-1} and nearfield densities peaking around 7 million cellsL^{-1}. There was evidence that nutrient-limiting conditions had begun in the nearfield during this survey. Some settling of the *Phaeocystis* bloom in the nearfield was evident during early April as cell densities, chlorophyll, and particulate carbon reached peak concentrations at a depth of 20-30m (station N18). The *Phaeocystis* bloom had largely ended by late April, which may have resulted from dispersal by a strong northeaster that passed through on April 20th, and possibly grazing pressure imparted by a seasonal peak in zooplankton abundance during early April.

The onset of vertical stratification occurred in the inner nearfield by late April and was fully developed throughout the nearfield by mid-May. Stratification was augmented by an intrusion of low salinity surface water to the nearfield during late April and May resulting from a spring freshet. A chlorophyll peak below the developing pycnocline reached more than 12 μgL^{-1}, producing substantial increases in primary production and respiration. Centric diatoms of the genus *Chaetoceros* were the dominant taxon responsible for this activity, and the resultant carbon delivery to the bottom layer, together with the earlier biomass from the *Phaeocystis* bloom, may have contributed substantially to subsequent dissolved oxygen depression in bottom water and to a higher 1997 sediment oxygen demand rate.

Following the onset of stratification, photosynthetic activity diminished in the more offshore regions of the nearfield, although heightened activity by the centric diatom *Rhizosolenia fragilissima* and the dinoflagellate *Ceratium longipes* occurred offshore around the third week in June. In Boston Harbor and coastal stations, a bloom developed at this time that continued through the summer. The Harbor bloom heavily influenced the inner nearfield stations in June and was comprised primarily of *Chaetoceros* and *R. fragilissima*.

Peak bottom water dissolved oxygen (DO) concentrations were documented in late March, after which a sharp seasonal decline in DO began. Following the mid-June survey the decline in average nearfield bottom water DO reversed itself, and both DO concentration and saturation were observed to increase for the next two surveys (W9708 in late June and W9709 in mid-July). While localized primary productivity which was evident at mid-depth may have contributed to the observed increase, evidence from the USGS mooring also suggested that a large-scale advection occurred in the bottom water of the nearfield during the period. This reversal in DO decline resulted in an increase in average bottom water DO concentration of 1.5 mgL^{-1}. Mixing associated with Tropical Storm Danny on July 25th may have altered water column conditions, and bottom water DO characteristics appeared to return to a more normal scenario by month's end.

A strong phytoplankton bloom continued to occur through August in Boston Harbor and along the coast, with maximum chlorophyll concentration >7 μgL^{-1} and areal production rates of 2,200 $mgCm^{-2}d^{-1}$. More seaward areas of Massachusetts Bay exhibited relatively low phytoplankton activity, apparently a result of a continued strong horizontal gradient in surface water nutrients. Evidence of coastal upwelling during the period included decreasing bottom water temperature and increasing bottom salinity, areas of colder, more saline surface water at coastal stations, and prolonged onshore bottom water currents. The phytoplankton assemblage in the Harbor and adjacent stations (dominated by *Skeletonema costatum* and cryptophytes) differed substantially from the bloom in western Cape Cod Bay and adjacent coastal stations (dominated by *R. fragilissima*). The more southerly bloom may thus have developed separately in response to nutrient release from the coastal upwelling. It is perhaps worthy to note here that the high rates of exchange between Harbor and coastal waters often result in a similar phytoplankton assemblage between the two regions. However, the Harbor assemblage may often be temporally different from the nearfield, as was the case in 1997 when *Chaetoceros* was prevalent in the nearfield during April and May but didn't succeed as a dominant in the Harbor until June.

Between the August and October combined nearfield/farfield surveys, primary production rates in the outer nearfield remained relatively low, but rates continuously increased at the more inshore station N18. Both sensor data and nutrient chemistry results indicated that the nearfield remained stratified through September and into October. However, vertical cast data from the shallower inshore stations of the nearfield and current meter data again indicated partial mixing, onshore advection and potential upwelling conditions occurred during September. Although survey data indicated little nearfield chlorophyll activity (<1.5 μgL^{-1}) during the late September nearfield survey (W9713), primary production rates at N18 exceeded 3,000 $mgCm^{-2}d^{-1}$. Continuously recorded data from the USGS mooring also showed a substantial increase in chlorophyll shortly after the late September survey.

Survey data documented a strong fall bloom during early October (W9714), particularly along the coast, in the nearfield, and in northern Massachusetts Bay. Chlorophyll concentrations at the more offshore stations in Massachusetts Bay remained relatively low. Vertical water column mixing in the nearfield progressed slowly seaward throughout October, with stratification at the deeper nearfield stations still evident by the late October survey (W9715). The fall bloom thus appears to have developed inshore in late September, perhaps in response to near-coastal phenomena and subsequently progressed further into Massachusetts Bay as nutrients trapped below the pycnocline were released. Chlorophyll concentrations in the nearfield had declined by the end of October, perhaps due to grazing by zooplankton that concurrently reached a seasonal peak at month's end. This latter observation may imply continued bloom conditions during mid-October; however, there are no supporting data to directly document the magnitude of chlorophyll activity during this period.

The protracted sequence of water column mixing also affected results for bottom water DO concentration. The minimum average nearfield bottom water concentration (7.3 mgL^{-1}) was reported during early October (W9714). The average bottom water concentration over the nearfield rose by the late October survey

(W9715), but since vertical mixing had yet to reach the deeper stations, individual minima for concentration (6.4 mgL^{-1}) and saturation (68.5 percent) were recorded during late October. These late-season minima caused by the delayed mixing might have very well been even lower had not the seasonal decline in bottom water DO concentration been mitigated by large-scale advection during July.

1992-1997 Interannual Comparisons

The key parameters for assessing potential eutrophic impacts to the water column from the outfall relocation are chlorophyll and dissolved oxygen. This summary therefore focuses on the interannual variability seen during the baseline monitoring for these two parameters. Despite the large winter/spring bloom of *Phaeocystis pouchetii* and *Chaetoceros*, and the occurrence of a fairly strong fall bloom, 1997 ranked lowest of the six-year baseline in terms of annual average chlorophyll concentration in the nearfield, and fifth for the annual average all of Massachusetts Bay samples combined. In terms of seasonal nearfield averages, the spring and summer averages ranked third, while the fall average was the lowest of the baseline. Interestingly, 1997 produced the highest single chlorophyll concentration of the monitoring program (29.2 μgL^{-1}), which was 40 percent higher than the previous maximum reported in 1993.

These summary statistics further demonstrate the different scales of variability inherent to the Massachusetts Bay system. Seasonal blooms vary in magnitude and duration, and are controlled by a variety of physical, chemical and biological factors. Predictive capability is thus extremely constrained, and post-relocation impact assessments will require a detailed, integrated investigation of potential causality. The spring bloom appeared to be "interrupted" by an extended period of cloudy days, which may have imparted light-limiting conditions during a period when the bloom is typically undergoing strong development. Grazing pressure in early April may have also controlled the bloom's development and reduced the magnitude of the overall seasonal average. The largest spring bloom of the baseline occurred in 1996 and was characterized by almost two continuous months of high chlorophyll biomass.

The fall bloom yielded high densities of centric and pennate diatoms, but elevated chlorophyll results captured by the monitoring were largely restricted to a single survey. However, productivity rates were documented to initially increase in September in the nearfield. By contrast, the largest fall bloom of the baseline period, which occurred during 1993, developed substantial chlorophyll biomass during September that continued to increase into October.

With respect to bottom water dissolved oxygen minima, 1997 ranked third in the baseline record for low DO. Although the *Phaeocystis* bloom (which was the largest *Phaeocystis* bloom of the baseline period) did not contribute to a substantial seasonal chlorophyll average, it did appear to contribute to a potentially record-setting dissolved oxygen scenario. Together with the late spring *Chaetoceros* bloom that was located below the developing pycnocline, the carbon associated with these two events produced high water column respiration rates. The net result was the lowest bottom water DO concentration of the baseline period for the beginning of the summer (mid-June). Given the "extended season" resulting from the late turnover,

moderately high bottom water temperatures, and high water column and sediment respiration rates, 1997 would likely have been the worst year on record for low bottom water DO had the bottom water re-aeration event in late June and July not occurred.

Carbon cycling in western Massachusetts Bay appears to be driven by internal recycling of nutrients based on parallel measurements of production and respiration. The regenerated nutrients support continued high production rates even during the stratified period. It is clear that the input of additional nutrients to the euphotic zone results in increased production, particularly in late spring and during the stratified period. Production-driven respiration in the bottom water and sediments determines the potential oxygen depletion. The oxygen depletion that actually occurs depends on the set-up conditions, the duration of stratification, and perhaps most importantly based on 1997 results the degree of mitigation imparted by advection or other physical influences. Again, post-relocation impact assessment will require an evaluation of both statistically significant change in threshold parameters, as well as a detailed investigation of the rate-dependent processes that impact these thresholds.

CONTENTS

CONTENTS (Cont'd)

CONTENTS (Cont'd)

CONTENTS (Cont'd)

LIST OF TABLES

LIST OF FIGURES

LIST OF FIGURES (Cont'd)

LIST OF FIGURES (Cont'd)

LIST OF FIGURES (Cont'd)

LIST OF FIGURES (Cont'd)

LIST OF FIGURES (Cont'd)

LIST OF FIGURES (Cont'd)

1.0 INTRODUCTION

The Massachusetts Water Resources Authority (MWRA) has implemented a long term monitoring plan for the proposed MWRA wastewater outfall in Massachusetts Bay. The purpose of the Harbor and Outfall Monitoring (HOM) Program is to verify compliance with the discharge permit and to assess the potential effects of the relocated discharge of treated effluent into Massachusetts Bay. To help establish the present conditions, ENSR conducted the baseline water quality monitoring in 1997. This report represents the sixth continuous year of monitoring results since the program was established in February 1992.

The objective of this report is to describe the 1997 seasonal baseline conditions of the water column in Boston Harbor and Massachusetts and Cape Cod Bays. Vertical profiles of the water column, along with discrete water samples obtained at predetermined depths, provide the basis to identify the predominant spatial scales of variability, the sources of the variability, and the general features of circulation and mixing at the time of the measurements. Analysis of seasonal fluctuations is performed to assess the temporal variability of each of the water properties, as well as the primary mechanisms responsible for the variability. Comparison to data collected in previous years is made to help establish interannual variability and to distinguish discernible trends.

The water quality data presented herein include the physical characteristics of temperature, salinity and density, annual nutrient cycling, chlorophyll, dissolved oxygen, productivity and respiration, and phytoplankton and zooplankton. Each are discussed in separate sections. A concluding section summarizes the principal events/observations noted within each section.

2.0 DATA SOURCES AND 1997 PROGRAM OVERVIEW

This section identifies the various sources of information and data integrated within this annual report. The MWRA has a comprehensive bibliography of technical reports generated by the HOM Program. A general description of the documents associated with the 1997 water column monitoring tasks is provided below, along with an overview of the sampling program.

2.1 Data Sources

Full details of technical procedures, equipment, and quality controls are presented in the Combined Work/Quality Assurance Project Plan (CW/QAPP) for Water Quality Monitoring: 1995-1997 (Bowen *et al.*, 1997). This includes descriptions of standard survey methods, instrument specifications, laboratory support, and quality control procedures. Individual survey locations and descriptions, sampling methodologies, sequences of events, navigational and vessel information, and scientific crew are documented in individual survey plans prior to each survey and confirmed in survey reports. These reports also describe deviations in standard methods, detail any marine mammal observations, and present raw sensor data after each survey is completed.

Detailed summaries of water column survey data are available in three data reports (nutrient, plankton, and productivity/respiration) that are issued five times a year. Nutrient reports include sensor and chemistry data and plankton reports cover whole-water phytoplankton, screened phytoplankton, and zooplankton results. Finally, semi-annual reports integrate results and provide initial interpretation of data. All quantitative data generated by the program are available in the MWRA HOM Program Database.

2.2 1997 Monitoring Program Overview

There were 17 water quality monitoring surveys conducted in Boston Harbor and Massachusetts and Cape Cod Bays during 1997. They were divided into two main types of surveys: combined nearfield/farfield surveys, which comprehensively sample all stations in the monitoring program (Figures 2-1 and 2-2) over a period of several days, and nearfield surveys to sample the stations in the nearfield grid (Figure 2-2). Additional components were included within this framework to meet specific objectives. These included a survey in Stellwagen Basin, conducted in late fall to monitor dissolved oxygen levels at station F12 (located in Stellwagen Basin, see Figure 2-1), and a winter nutrients survey to determine the levels of nutrients in the Massachusetts Bay area after the fall mixing event.

The nearfield stations are located in a grid pattern over the future outfall site to provide a detailed picture of conditions in the water column in the vicinity of the discharge (Figure 2-2). The farfield stations are located throughout Boston Harbor, Cape Cod Bay and Massachusetts Bay in a strategic pattern that is intended to provide an overall characterization of the area. Stations are grouped into six regions in the farfield area according to their location (Figure 2-1). These include Boston Harbor (stations F23, F30 and F31), Coastal region (stations F18,

F24, F25, F14, F13, and F05), Offshore region (stations F22, F19, F16, F15, F10, F06 and F07, and F17), Boundary region (stations F26, F27, F28, F12, and F29), and Cape Cod Bay (stations F01, F02, and F03).

The combined nearfield/farfield surveys were conducted six times during the course of the year, intended to capture periods of peak activity in the Massachusetts coastal waters. Two surveys during February and one during April encompassed the spring bloom, while a survey in June captured the onset of stratification. A survey during late August captured conditions in summer when the water column was strongly stratified, and a final survey during early October investigated seasonal dissolved oxygen minima and the onset of fall water column mixing. The nearfield-only surveys were performed an additional eleven times throughout the year (February through early December) at intervals of every two to three weeks (Table 2-1).

Altogether there are 42 stations located in the nearfield and farfield survey areas, 17 in the nearfield and 25 in the farfield. N16 is sampled as both a nearfield and farfield station. Stations are assigned categories that signify the types of analyses conducted at that station, with each category represented by a letter (A, D, E, F, G, R, and P, Table 2-2). These station categories are also depicted in the station maps (Figures 2-1 and 2-2).

At each station, five depths are typically sampled (surface, mid-surface, middle, mid-bottom, and bottom, designated A, B, C, D and E, respectively). Respiration were measured at two additional depths during stratified conditions. Shallower inshore stations were only sampled at three depths (surface, middle, and bottom). Detailed descriptions of station coverage and individual analyses performed are available in each of the survey plans and in the CW/QAPP.

TABLE 2-1

1997 Schedule of Survey Events

Event Number	Type of Survey	Date
W9701	Nearfield/Farfield	February 1-5
W9702	Nearfield/Farfield	February 25-March 1
W9703	Nearfield	March 17-18
W9704	Nearfield/Farfield	March 30-April 6
W9705	Nearfield	April 22-23
W9706	Nearfield	May 12-13
W9707	Nearfield/Farfield	June 16-20
W9708	Nearfield	June 30-July 1
W9709	Nearfield	July 21-22
W9710	Nearfield	August 5-6
W9711	Nearfield/Farfield	August 18-23
W9712	Nearfield	September 4-5
W9713	Nearfield	September 22-25
W9714	Nearfield/Farfield	October 6-10
W9715	Nearfield	October 29-30
W9716	Nearfield/Stellwagen Bank	November 21- December 4
W9717	Nearfield/Winter Nutrients	December 15-16

TABLE 2-2

Station Types and Analyses
(& Number of Depths Sampled)

Analysis	A	D	E	F	G	P	R
Dissolved Inorganic Nutrients (NH_4, NO_3, NO_2, PO_4, SiO_4)	5	5	5	5	3		
Other Nutrients (DOC, TDN, TDP, PC, PN, PP, Biogenic Si)	2	3			2		
Chlorophyll	5	5			3	1*	
Total Suspended Solids	3	3			3		
Dissolved Oxygen	4	4		4	3		2*
Phytoplankton and Urea		2			2		
Zooplankton		1			1		
Respiration							3/5*
Productivity						5	

*Additional measurements performed under supplementary task order number 97-3

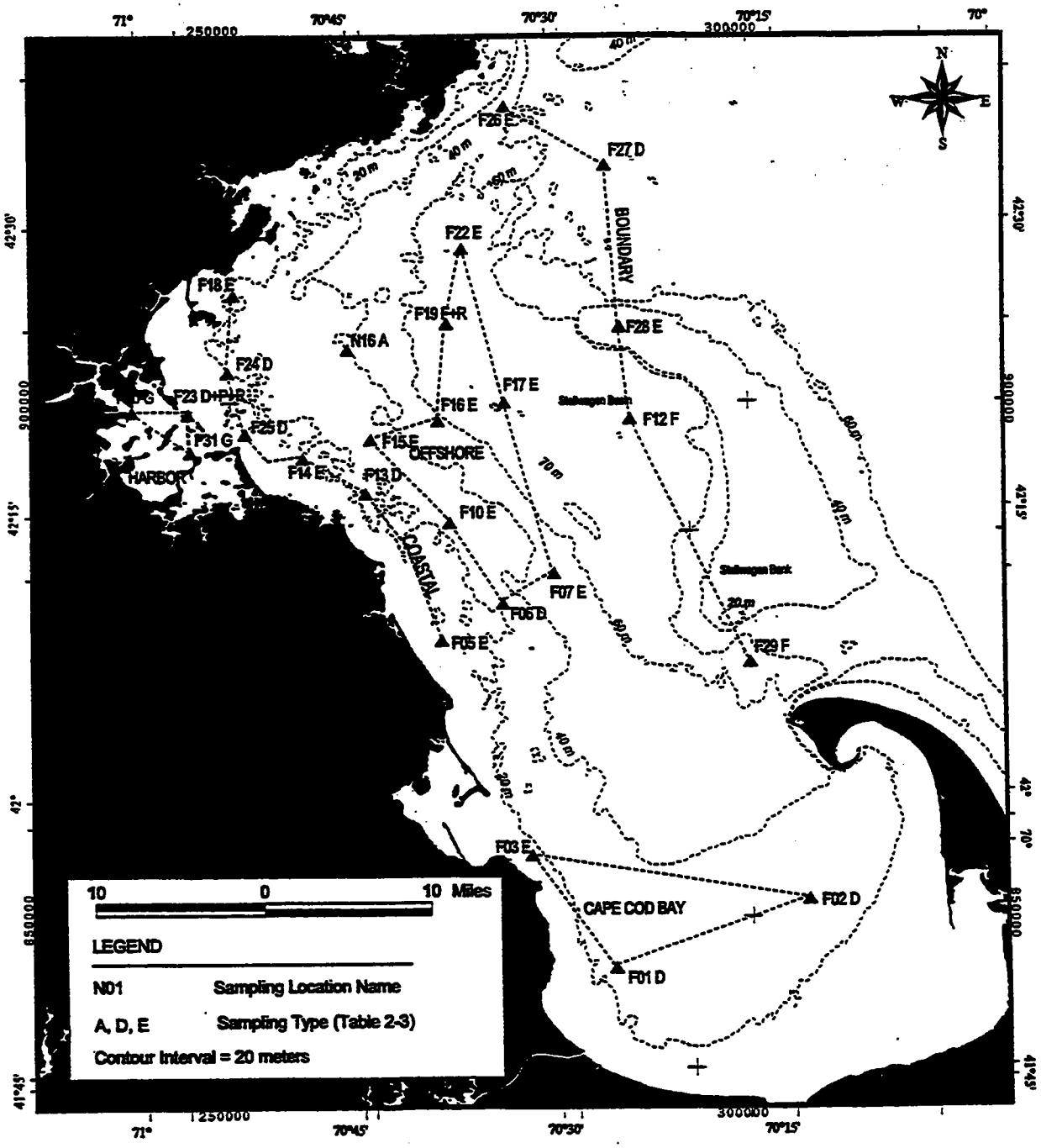

FIGURE 2-1
Location of Farfield Stations Showing Regional Geographic Classifications

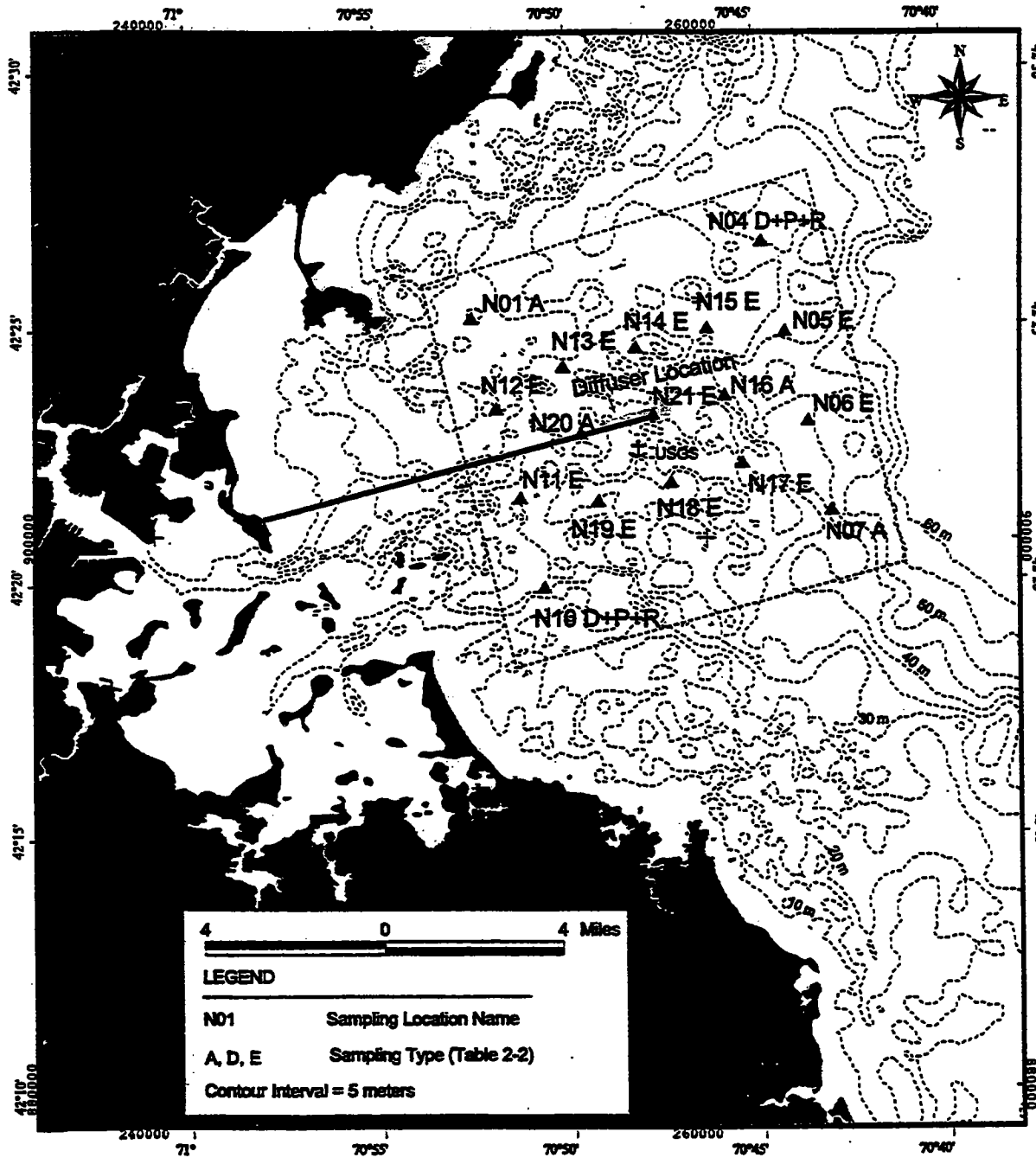

FIGURE 2-2
Location of Nearfield Stations Stations and USGS Mooring

3.0 PHYSICAL CHARACTERIZATION OF SYSTEM

This section provides a basic overview of the physical structure of the water column in the Massachusetts Bay system as it relates to key chemical and biological processes. Data from the 1997 monitoring period are illustrated to contrast conditions in the various regions within the monitoring area, and to provide the context for presentations in later sections of chemical and biological processes also sampled by the HOM program. For easy reference and to facilitate integration of results from the various ecosystem components represented by sections in this annual review, significant events throughout the year are summarized in Table 9-1. The 1997 record is also compared with 1992-1996 baseline monitoring data to support inter-annual comparisons of monitoring results.

3.1 1997 Meteorological Overview

This section presents a basic overview of weather conditions in Massachusetts during 1997. An effort was made to focus on information that occurred in coastal Massachusetts during the 1997 calendar year, including precipitation, temperature, stream flows (see section 3.3.3 for river discharge data), and major storm events. The data, obtained from the Northeast Regional Climate Center (NRCC, 1998a), are used in later sections of this report to evaluate the influence that specific meteorological events may have had on the physical, biological, or chemical characteristics of the water column of Massachusetts Bay.

3.1.1 January

Temperatures for the month of January departed little from the historical monthly average for Massachusetts. Temperatures across the entire Northeast averaged 0.8°F above normal. Precipitation and steam flow also fell within normal ranges for eastern Massachusetts. No significant weather events occurred along the Massachusetts coast during this period.

3.1.2 February

February was unseasonably warm, averaging 6.3°F above the monthly average. Precipitation was only 57 percent of the long-term average for February. One storm event occurred between February 4th and 5th generating snow, sleet and rain. Sustained winds of 72mph were recorded on the 21st and 22nd of the month. In spite of the below-average monthly precipitation, stream flows were reported as being normal for the month.

3.1.3 March

In contrast to February's unseasonably warm temperatures, March temperatures dropped slightly below the long-term average. Precipitation exceeded 127 percent of the monthly average. Both rain and snow contributed to this departure from the average, resulting in above average stream flows for southeastern Massachusetts. The surrounding regions of Massachusetts reported normal stream flows.

March 1997 was an active month for major storm events throughout the Northeast. Two storms directly affected coastal Massachusetts, with the first bringing damaging winds in excess of 65mph on March 6th. A second nor'easter hit the area on March 14th. The April Fools Nor'easter (March 31st – April 1st) was the third greatest snowstorm ever to hit Boston, producing 25.4 inches of snowfall over the two day period. Peak wind gusts in Boston were recorded at 53mph, while a peak of 72mph was recorded at the Blue Hill Observatory.

3.1.4 April

The average temperature during April was 1.2°F below normal for the month. Precipitation for April was 98 percent of the historical average despite the heavy snowstorm at the beginning of the month and the major rainstorm that occurred in mid-month (April 20th). High winds (with a peak gust of 97mph recorded in Falmouth) accompanied the heavy rains during the mid-month storm. Stream flow was above normal for eastern Massachusetts as a result of the rain and melting snow.

3.1.5 May

The average temperature for May was 4.4°F cooler than historical averages for the Northeast, making the spring 2.6°F cooler than average. Precipitation was low, reported as 81 percent of the long-term average. Stream flows throughout Massachusetts were normal with the exception of Boston, which fell slightly below the average.

May saw little significant storm activity for coastal Massachusetts. The severe weather remained to the west and southwest, except for reports of 2-inch diameter hail that occurred on the 1st of the month.

3.1.6 June

In contrast to cooler conditions in May, June showed temperatures slightly above the long-term average (0.6°F) for the Northeast. June's precipitation was only 44 percent of the norm in 1997, and stream flows were below normal. A low-pressure system which passed south of the region early in the month generated 2-3m swells in the nearfield over several days (USGS, 1998a). Wind damage from severe thunderstorms was reported on the 22nd of June.

3.1.7 July

Although parts of Massachusetts experienced somewhat cooler than normal temperatures for July, a small heat wave between 13th-18th compensated to yield average monthly temperatures. As with June, Massachusetts underwent an unusually dry month (74 percent of average for July), with a 5.71-inch year to date deficit from the normal precipitation. Monthly stream flow averages were below normal for the second consecutive month.

Several storms prevailed throughout July, beginning with thunderstorms and accompanying high winds, hail and tornadoes on the 3rd, and damaging winds and hail on the 9th. Rainfall on July 25th (associated with Tropical Storm Danny) exceeded four inches on Cape Cod, and produced prolonged wind gusts of 20-40mph.

3.1.8 August

August temperatures were slightly cooler than normal. Precipitation varied widely throughout the Northeast, but was average for the month (101 percent of the norm) in Massachusetts. Stream flow was below average for the third consecutive month in eastern Massachusetts. Rain and thunderstorms were recorded on the 9th and 22nd.

3.1.9 September

September fell slightly below the long-term average for temperature throughout the region. September was another dry month in a dry summer, with coastal areas receiving only half of the normal precipitation. This dry weather produced lower than normal stream flows for eastern Massachusetts for the fourth consecutive month. Significant weather events were isolated to the western and southwestern areas of the Northeast.

3.1.10 October

October temperatures were unseasonably warm during the first half of the month, followed by unseasonably cold temperatures during the latter half. Precipitation continued to be below the normal rainfall average, with only 57 percent of the long-term norm for Massachusetts being recorded for October. The continued low rainfall amounts yielded a cumulative deficit of 14 inches compared with the same ten months of 1996. Monthly stream flow averages remained below normal for the fifth consecutive month. Coastal New England experienced severe weather on the 27th in association with a low-pressure system.

3.1.11 November

Temperatures in November were colder than normal, averaging 3.0°F below average for Massachusetts. Precipitation levels were 153 percent of the average. For the sixth consecutive month, stream flow levels remained below normal in eastern Massachusetts. Coastal storms brought wind damage to the eastern part of the state on the 1st and on the 27th. A storm produced a mixture of sleet and snow for eastern Massachusetts on the 14th.

3.1.12 December

December was 2.3°F higher than the long-term average in December, which is not considered unusual during an El Niño winter. Precipitation levels were only 77 percent of the average for Massachusetts, resulting in continued below-average stream flow levels. Low stream flow was a consistent feature of 1997, with low flows recorded from June to December. Three significant weather events occurred during December. Snowstorms

with high winds prevailed on the 1st and 22nd-23rd of the month, with the latter producing as much as 6-8 inches around Boston. Winds with gusts as high as 68 mph in New Bedford struck the coast between the 29th and 30th.

3.2 Annual Temperature Cycle

3.2.1 Nearfield

The 21 monitoring stations in the nearfield were vertically sampled with ship-based sensors at a relatively high frequency in 1997 (n=17), providing the best resolution for the annual temperature cycle throughout western Massachusetts Bay. Additional continuously recorded temperature data were collected by the USGS from a sensor array moored within the central region of the nearfield (Figure 2-2). During the 1997 monitoring period, these sensors were located 22.4m and 27.8m below the surface (USGS, 1998b). Unfortunately, sensor data typically available from the 5m depth are not available for 1997.

Nearfield temperature data from the 1997 HOM sampling program are presented for three regions (Figure 3-1a, b, and c): inner nearfield stations (stations N10 and N11, see Figure 2-2), which are shallower and are tidally influenced by Boston Harbor; Broad Sound (as represented by Station N01 off Winthrop and Nahant); and the outer nearfield (stations N04, N07, N16, and N20).

Data from the first survey in February indicated that surface water (typically 2.5-5m depth) temperatures were slightly colder in the inner nearfield (Figure 3-1). Surface temperatures were also cooler than the bottom except in Broad Sound, where surface and bottom temperatures were similar. By late February and throughout March, average water temperatures were uniform both horizontally and vertically across the nearfield (ca. 4°C). In early April, surface temperatures began to rise more quickly than bottom water, initiating the seasonal thermal stratification. Maximum temperatures had been reached by August (W9710) throughout the nearfield, averaging between 19°C (outer nearfield) and 20°C (inner nearfield).

While surface temperatures began to cool after early August, bottom temperatures continued to warm through the end of October (W9715). Highest average bottom temperatures were recorded in the inner nearfield (around 11°C), while the average in the deeper water of the outer nearfield reached a peak of around 9.5 °C. The water column was isothermal by early December (W9716), though strong November storm activity beginning on the first of November (Section 3.1.11) likely produced substantial mixing soon after survey W9715.

Plots of continuously recorded data from the USGS mooring (located in Figure 2-2) provided additional resolution (Figure 3-2). Temperature data from station N16, including surface data, were included to permit comparisons with ship-based survey data. The continuous measurements indicated that bottom water temperature in the central nearfield region reached its annual minimum during mid-February. After a two-week warming period in late February, bottom temperature again declined to <4°C until early April.

Beginning in early April, bottom water temperatures exhibited a steady increase through early June, at which point a rapid increase in temperature was recorded by the USGS sensors (of ca. 3°C at 22m and around 2°C at the

bottom) just prior to the mid-June survey (W9707, Figure 3-2). This was likely due to storm-induced mixing (Section 3.1.6). More substantial mixing was observed during late July, when high winds associated with Tropical Storm Danny increased the temperature at the bottom by 3°C and at 22m by 6°C.

While bottom water temperatures continued to rise through mid-October, there were two periods of prolonged temperature declines. The first was evident during early August when decreasing temperatures (1-2°C) occurred over about a one-week period (Figure 3-2). The second event occurred in late September, when temperatures declined by 2-3°C over a two-week period and remained low for an additional week into early October. These data would indicate that colder water from offshore was advecting into the nearfield during these two periods. This phenomenon will be further examined with respect to salinity (Section 3.3.1) and currents (Section 3.5).

The September/October decline in bottom temperature was abruptly reversed during mid-October, with a 3-4°C increase in temperature recorded by the USGS sensors (Figure 3-2). At this point the bottom temperature approached the trend line for decreasing surface temperatures, suggesting that the water column mixed completely in the center of the nearfield around this time.

3.2.2 Regional Comparisons

Regional trends in water column temperature were compared using data collected during the six farfield surveys. Average regional surface and bottom temperature data were calculated for the regions defined in Section 2 and illustrated in Figure 2-1.

In late winter, average regional temperatures remained relatively uniform throughout the water column, but with a slight increasing temperature gradient from the Harbor to the Boundary region (Figure 3-3a through d). Cape Cod Bay was most similar to the coastal stations. Towards the end of March, surface waters in all regions began to rise and followed a similar pattern over the summer. Bottom waters reflected the differences in regional depths, with the shallow bottom water of the Harbor reaching maximum temperature (around 15.2°C) in late August, while bottom water in deeper offshore and boundary regions warmed more slowly and reached maxima of only around 8.7°C in October. Bottom water in Cape Cod Bay was slightly cooler than the coastal region during the summer, remaining at or below 8°C through the August survey. Maximum bottom water temperatures in Cape Cod Bay (10°C in early October) were similar to the coastal region maximum.

A well-defined summer thermocline was evident in all regions except for the Harbor stations. The thermocline in Massachusetts Bay was well established by the time of the fourth combined survey event in mid-June (Figure 3-3b-e), but given the evidence from the higher-frequency nearfield data, stratification most likely began during late April or May. The Harbor stations (Figure 3-3a) typically do not develop a well-defined thermocline due to strong tidal mixing.

3.2.3 1992-1997 Interannual Comparisons

Average nearfield surface and bottom water temperatures for the period 1992 to 1997 were plotted to examine interannual differences (Figure 3-4a). Surface temperature trends were generally similar for each year, with maximum temperatures between 19°C and 20°C typically recorded during August or early September. The lowest maximum average surface temperature for the six-year baseline period was in 1994 (17.8°C), while the highest was in 1995 (19.6°C). The surface temperature pattern during 1997 was most comparable with 1995. Other notable features were the colder winter surface temperatures in 1993-94 and in 1996, and periodic drops in surface temperature during mid-summer which were observed in 1992, 1993, and 1996.

The most prominent feature of the six-year record for bottom water temperature was the relatively high late-season bottom temperatures evident in 1994-96 (Figure 4-3a). Maximum average bottom temperatures during these three years were around 12°C, whereas bottom temperatures during 1992-93 and in 1997 did not exceed 9.5°C. This observation is perhaps most curious for 1997, when initial bottom temperatures during late winter and early spring were the highest of the baseline period (around 4°C). More importantly, the average bottom temperature in the nearfield during 1994 exceeded the 9.5°C maxima for over four months. Although peak bottom temperatures were slightly higher in 1995 and 1996, the duration of temperatures above 9.5°C was shorter (around two and three months, respectively). The potential for high metabolic activity and respiration, and a potentially more significant reduction in dissolved oxygen concentration, was therefore greatest during 1994. This potential is discussed in greater detail in Sections 6 and 7.

A similar scenario was evident in Stellwagen Basin (Figure 3-4b). In summer the average surface temperatures were coolest during 1994 (16°C) and warmest in 1995 (19.5°C). Maximum surface temperatures in 1997 were the second coolest of the baseline period (Figure 3-4b). The Stellwagen Basin data also indicated that early season temperatures during 1993, 1994 and 1996 were the lowest of the baseline period.

Maximum average bottom temperatures in Stellwagen Basin were typically observed during October, however, extended survey coverage between 1995 and 1997 showed that maximum temperatures can occur as late as December (1997, Figure 4-3b). The maximum average bottom water temperature in Stellwagen Basin (10°C) was recorded during 1994, followed by a maximum of 9.5°C during 1996 and 9.0°C in 1997. The coolest years during the baseline were 1992 (6.5°C) and 1993 (7.5°), although higher temperatures may have been reached after survey coverage ceased.

3.3 Salinity

3.3.1 Nearfield

As with the temperature data, surface and bottom salinity profiles were plotted for the three regions of the nearfield (Figure 3-5). In general, surface water salinity is more variable due to influx of fresher water from coastal runoff, while the bottom water salinity exhibits seasonal trends but is more uniform throughout the year.

During 1997, surface salinity rose slightly by the second survey in February, after which salinity declined through June. This decline was temporarily reversed during mid-May (survey W9706), which was particularly evident in the inner nearfield and Broad Sound regions (Figures 3-5a and b). The nature of this reversal is uncertain given the relatively calm conditions during the period. After the overall decline ended in June, surface salinity generally rose throughout the rest of the year, with slight declines noted in late October and at year's end (e.g. Figure 3-5a).

Average bottom water salinity also increased in late February and, after a general decline through April, remained fairly stable through August. Average bottom salinity then generally increased through the fall, with the notable exception of a decrease in the inner nearfield during late October (Figure 3-5a).

Continuously recorded data from the USGS mooring (22.4m and 27.8m depths, USGS 1998c) were plotted along with ship-based survey measurements, including surface readings (Figure 3-6). USGS and HOM records for bottom salinity were similar through late April (W9705), when the USGS captured a rapid decrease in bottom salinity just after survey W9705. This event coincided with the storm that produced 97-mph winds and 8m waves (Section 3.1.4). The salinity results indicated that substantial water column mixing occurred, as the minimum bottom salinity matched the surface salinity recorded by survey W9705.

Bottom salinity reached its seasonal maximum during mid-May, which was only surpassed by results from late in the year (Figure 3-6). Following this peak, a second rapid decrease in bottom water salinity was observed around the beginning of June, an event also documented as an increase in bottom temperature (Figure 3-2). Together with the temperature data, salinity results indicate that water column mixing occurred during the period between HOM surveys W9706 and W9707. Another notable decrease in bottom water salinity (and increase in temperature, Figure 3-2) was documented during mid-July following survey W9709, representative of the mixing that was produced by Tropical Storm Danny (Section 3.1.7).

There were two periods of prolonged increases in bottom water salinity, which appeared to coincide with the declines observed in bottom temperature in early August and late September (Section 3.1.1). These data would further suggest advection of more saline bottom water from offshore into the nearfield during these two periods. Bottom salinity generally increased through the remainder of the year, although decreases in bottom salinity during mid-October and the first half of November were indicative of storm-related mixing.

3.3.2 Regional Comparisons

Salinity generally increased throughout the study area through time (Figure 3-7). Harbor stations had the lowest regional averages, with surface salinity of 30 PSU early in the year increasing to almost 32 PSU by year's end (Figure 3-7a). Bottom salinity in the Harbor also increased during the year, from 31 PSU to 32 PSU by year's end. Coastal and Cape Cod Bay stations followed patterns similar to each other (Figures 3-7b and e), although Cape Cod Bay appeared to be better mixed during the early part of the year (Figure 3-7e). The average surface salinity in Cape Cod Bay remained above 31 PSU throughout the year.

The Offshore and Boundary regions exhibited a slightly different pattern, with a more stable bottom salinity of ≥32 PSU throughout the year, while surface salinity fell in mid-year to match the Harbor and Coastal values (Figures 3-7 c and d).

3.3.3 Influence of Precipitation and River Discharge on Salinity

Precipitation data from Logan International Airport, obtained from the Northeast Regional Climate Center (NRCC, 1998b), documented only three precipitation events yielding greater than one inch of rainfall per day throughout 1997 (Figure 3-8a). The first of these three events was associated with the April Fools Nor'easter (Section 3.1.3), which produced 25.4 inches of snowfall over a two day period. Rainfall during mid-April, combined with the meltdown from this snowfall, resulted in the only month of the year with above normal stream flow (NRCC 1998a). Peak annual flow rates from the Merrimack River (ca. 42,600 cfs)[1] and the Charles River (ca. 1,020 cfs)[1] occurred during mid-April, after which discharge rates declined through the end of June (Figure 3-8b and c).

Surface salinity data were consistent with this pattern, with declining salinity from late March through June, followed by a continual increase from July through the end of the year. Additional periods of heavy rain in late October and early November also resulted in increased discharge rates from the two rivers, with the Merrimack reaching 12,200 cfs and the Charles peaking at 280 cfs. The effects of this late-season rainfall were evident in the near-shore surface salinity data from station N10 and from the USGS mooring (e.g. Figures 3-5a, 3-6, and 3-8b).

3.3.4 Interannual Comparisons

Interannual plots of surface and bottom salinity in the nearfield and Stellwagen Basin indicated that the highest average salinities occurred between July 1994 and July 1995 (Figure 3-9a and b). Average nearfield surface salinity values >32 PSU were only occasionally evident in other years, but the data suggest that the surface average in the nearfield exceeded 32 PSU from October 1994 to March 1995 (Figure 3-9a). The average nearfield surface salinity did not go below 31 PSU during 1995. With the exception of one survey, the average nearfield bottom salinity exceeded 32 PSU for all of 1994 and through April 1995, and remained at or above 32 PSU through the remainder of 1995.

By contrast, average surface salinity readings in the nearfield did not exceed 32 PSU during 1996 and during only two surveys in 1997. In fact, the average surface salinity fell below 31 PSU for most of the spring and summer in 1996, reflecting its status as the wettest year on record (NRCC, 1998c). However, the lowest average surface

[1]Charles R. data from gage 01104500 at Waltham, MA., multiplied by 1.27 to estimate discharge at mouth of river (USGS, 1997)

[2] Merrimack R. data from gage 01100000 in Lowell, MA., multiplied by 1.08 to estimate discharge at mouth of river (USGS, 1997)

readings were recorded during the spring of 1993, when the average nearfield salinity fell below 29.5 PSU during April and May, yielding an overall baseline range of average surface salinity of 29.2 to around 32.5 PSU.

The readings in Stellwagen Basin showed a similar pattern, but note that bottom salinities varied by only around 1 PSU. Even during the wettest year in 1996, the average bottom salinity was barely below 32 PSU. Surface averages ranged from around 30 PSU to about 32.6 PSU.

3.4 Water Column Stratification

Massachusetts Bay is typically characterized by a seasonal cycle from cold, well-mixed waters during winter months to strong vertical stratification during summer. Early stratification during spring is salinity-driven due to freshwater runoff from the major rivers to the north and from coastal runoff, while temperature dominates the density structure during summer and fall (Geyer *et al.*, 1992). In the following sections, the water column structure in the nearfield during 1997 is compared with other regions within the system, as well as with previous baseline monitoring years.

3.4.1 1997 Nearfield Stratification

The density data for the inner nearfield indicated some degree of salinity stratification inshore during February and March (Figure 3-10, see also Figures 3-1 and 3-5). By mid-April, thermal stratification began to contribute to the vertical structure of the water column, but the large vertical salinity difference observed during the period suggested a substantial contribution from salinity into the summer (Figures 3-1 and 3-5, Section 3.3.3). Temperature certainly was an important factor by mid-June (Figure 3-1), and likely dominated the water column structure through early October.

By late October, the shallower inner nearfield stations N10 and N11 appeared to be vertically homogenous (Figure 3-10a), while the rest of the nearfield still appeared to have some vertical structure. By late November, complete mixing throughout the nearfield had occurred. Further discussion of nearfield stratification is included with the regional comparisons in the following section.

3.4.2 Regional Comparisons

With the exception of the Cape Cod Bay, most regions appeared to exhibit salinity-driven stratification early in the year (Figure 3-11a through e). Well-mixed conditions in Cape Cod Bay appeared to continue through March (Figure 3-11e). Vertical differences in density evident by late March in other regions appeared to be due to the influx of fresh water from riverine discharge (see Figures 3-3 and 3-7). Even as surface temperatures increased in early summer, concurrent reductions in surface salinity at the Offshore and Boundary stations lent further structure to the water column. With the exception of Boston harbor, the water column remained stratified in all regions through the final farfield surveys in early October.

Further insight into the vertical structure of the water column and the seasonal progression of stratification throughout Massachusetts Bay is available from vertical density profiles from hydrocast data (Figures 3-12 through 3-17). Density profiles were plotted for several stations to represent a transect from inshore to offshore. Stations selected included the three productivity (F23, N18, and N04) and four respiration stations (F23, N18, N04, and F19), permitting reference to water column structure in later discussions in Section 7. Station N10 was included in this transect to demonstrate the tidal influence from the harbor on water column structure in the inner nearfield, while station N07 was included to permit a comprehensive evaluation of the nearfield.

Harbor station F23 exhibited a shallow halocline during the first survey (W9701), apparently a result of fresh water discharge from the Charles River (Figure 3-12, using Figures 3-3a, 3-7a, and 3-8b for reference). A vertical salinity gradient remained for the next two surveys, however it was much more gradual over depth. A weak pycnocline was evident at F23 at a depth of around 18m during the June survey (W9707), but the water column was vertically uniform during the August and October surveys (W9711and W9714). A shallow surface lens of fresh water from the Harbor was evident during the December survey (W9717).

Nearfield station N10 also showed salinity-driven stratification during the two February surveys (W9701 and W9702), but it was much less pronounced by the next survey (Figures 3-13). Vertical structure was more pronounced by mid-April (W9705) during the large-scale advection of riverine discharge into Massachusetts Bay (Section 3.3.3). Curiously, the survey in early May (W9706) revealed an increase in density due to increasing salinity throughout the water column (Figures 3-5 and 3-6), despite the continued output of fresh water from the two rivers (Figure 3-8). Note that temperatures remained roughly similar to the previous survey (Figures 3-1 and 3-2), and there were no significant storms during the period (Section 3.1.5). This observation would suggest that the circulation in Massachusetts Bay may have changed for a period of a few weeks and countered the influence of the spring freshet. Interpreting the course of events during the period is further complicated by the apparent mixing event which occurred during the first part of June prior to W9707 (Figures 3-2 and 3-6), and the possible return of the spring freshet into the nearfield in late May and June (as evidenced by further decreases in salinity).

Density profiles at station N10 from surveys W9708 through W9712 indicated modest vertical stratification during July and August, however strong stratification appeared to be precluded by Tropical Storm Danny in late July (Figures 3-2 and 3-6). A strong storm on August 22nd also appeared to cause some vertical mixing immediately after W9711. Further evidence of mixing prior to W9712 (see Figures 3-2 and 3-6) may have precluded stronger stratification during early September. Potential upwelling conditions during mid-August and late September (as evidenced by prolonged decreases in bottom temperature and increases in bottom salinity in Figures 3-2 and 3-6, respectively; Cibik *et al.*, 1998a) also appeared to influence the inshore water column structure (see density profiles for W9711 and W9713-14 in Figure 3-13). By late October, the water column at station N10 was vertically homogenous (W9715 in Figure 3-13), with evidence that strong vertical mixing occurred during the middle of the month (Figure 3-2).

Station N18, N04, and N07 showed more distinctive patterns of water column stratification throughout the year (Figures 3-14 through 3-16). Late-winter (i.e. survey W9701) salinity stratification was evident at stations N18 and N04 but not at N07. After a period of vertically homogenous conditions through mid-March (W9703) at all

three nearfield stations, the onset of the spring freshet was quite evident at the northeastern-most nearfield station N04 (see Figure 2-2) by early April (W9704), but not at stations N18 and N07 until mid-April (W9705).

Strong stratification was evident at all three stations by mid-June (W9707). Relative to the profiles from mid-June (W9707), the pycnocline seemed to lift at all three stations (particularly at N18) around the end of June (W9708). By early August (W9710), there was a strong, well-pronounced pycnocline at around 15m at all three stations. Note however that the pycnocline depth had raised by around 5m by August 21 (W9711), which may have be a result of onshore advection and perhaps upwelling conditions. The pycnocline then re-established itself at a depth of 15-20m during September (W9712 and W9713), a period of relatively calm, dry weather.

In early October (W9714), the pycnocline lifted at the more inshore station N18 (Figure 3-14) and at N07 (Figure 3-16). Weather conditions continued to be calm and dry throughout this period. The USGS sensors did record a two-week period of decreasing bottom temperature and increasing bottom salinity (Figures 3-2 and 3-6, respectively), suggesting that large-scale advection into the nearfield may have been responsible for the change in water column structure. Curiously, the profile at station N04 (Figure 3-15) did not show a similar pattern. What is clear from the profiles is that the mixing which appeared to occur in mid-October, coupled with the storm activity on October 27th, resulted in a homogenous water column by W9715 at the more inshore stations N18 (Figure 3-14). Mixing was only evident to a depth of around 36m at the deeper outer nearfield stations N04 and N07. Again, this delayed mixing of the deeper bottom water of the nearfield has implications on the magnitude of seasonal dissolved oxygen declines in the nearfield, which will be addressed in Sections 6 and 7.

Vertical density profile at station F19 in Stellwagen Basin also showed an early season halocline near the surface, and the onset of the spring freshet by W9704 (Figure 3-17). A strong 5-10m deep pycnocline was evident during surveys W9707 and W9711, with only a modest decrease in depth by the later survey compared with that seen at the nearfield stations. Vertical mixing had only occurred to a depth of 12m by early October (W9714), and it is not clear when the bottom water of Stellwagen Basin experienced complete mixing. Several periods of storm-related wave activity were evident at almost weekly intervals during November (USGS, 1998a), thus vertical stratification likely did not persist through the month. The water column was vertically homogenous by the final survey of the year in mid-December (W9717).

3.4.3 1992-1997 Interannual Comparisons

The dry weather that was characteristic of the last seven months of 1997 appeared to result in one of the more stable water column structures of the 1992-1997 monitoring period based on surface and bottom water densities (Figure 3-18a). Intra-annual ranges in bottom water densities ($\Delta\sigma_t$) prior to 1997 were as much as 2 kgm^{-3}, and short-term changes documented by successive surveys were as much as 0.4 kgm^{-3}. During 1997, the range in $\Delta\sigma_t$ for bottom water densities was <0.8 kgm^{-3}, and there was little short-term variability based on HOM shipboard measurements. Surface densities exhibited the typical seasonal cycle, but also showed comparatively little short-term variability (e.g., compared with 1992, 1993, and 1996). Surface densities were most similar to 1994 and 1995, years when dissolved oxygen minima in bottom water were of concern (Kelly and Turner, 1995; Cibik *et al.*, 1996).

Baseline density results for Stellwagen Basin appear more comparable, however, this may be in part due to the lower temporal coverage of farfield surveys (6-8 times per year) as well as the less variable nature of the deeper, more seaward Stellwagen Basin stations. As with the nearfield results, it does appear that the bottom water in Stellwagen Basin exhibited little variability throughout 1997.

3.5 Currents

Current meter data during the six-year baseline period were collected by the USGS at their mooring near the center of the nearfield in Massachusetts Bay (Figure 2.2). Current data were available at two depths in the water column (approximately 22 and 30 meters, USGS, 1998d). Current meter data were not available at the surface depth (<5 meters) during 1997, and the mid-depth data were only available through mid-September (W9712). The availability of current meter data coinciding with the nearfield sampling surveys is provided in Table 1 of Appendix A.

In order to visualize the large volume of data collected by the current meters, and to help conceptualize the potential movement of water within the nearfield around the time of each survey, progressive vector plots were developed for each survey (Appendix A). These plots project the progressive movement of a hypothetical particle within the water column at the depth of each sensor based on measurements taken at the mooring. However, as the particle travels further away from the mooring its projection becomes less reliable as it assumes that the water movement at locations increasingly distant from the mooring remains the same. In order to minimize this potential error, the plots use the survey date as time zero, and project particle movement both backward and forward in time. Another way to illustrate current data is through the use of stick plots, which are comprehensively available for the baseline period (see USGS, 1998e).

Table 3-1 summarizes the net movement of water around the time of each survey for 1997, and estimates the residence time of a water particle in the nearfield at both depths. In general, the mid-depth layer had higher current velocities than the bottom layer, particularly during the stratified period (see estimated residence times in Table 3-1 and plots in Appendix A). It is expected that this was also true for the surface layer. Also evident from the plots and discussion in Appendix A is that the currents at the two depths do not move in the same directions. The bottom water mass tends to hold a more stable course, while the mid-depth is more variable, which also contributes to the differences in residence times.

Residence times at the mid-depth varied from 2 to >14 days (Table 3-1), with the longer residence times often due to frequent reversals in current direction (e.g. survey W9701 in Appendix A). The shortest residence time at the mid-depth was during late April (W9705) and during August (W9710-11) when strong southeasterly flow patterns were evident (Table 3-1, Appendix A). Residence times at the bottom depth ranged from 4 to >14 days, and were longest during the summer stratified period when oxygen depletion in bottom water is most critical (Sections 6 and 7).

For convenience of reference in the ensuing discussion, please refer to Table 9-1 to visually correlate water column characteristics throughout the year. It is interesting to note that during the major nor'easters which occurred on April 1st and April 20th (approximately the time of surveys W9704 and W9705), the mid-depth current meter indicated net water movement to the southeast while the bottom water was shown to be moving to the east. Perhaps coincidentally, this was also the case during Tropical Storm Danny in late July. In addition to the substantial mixing which occurred during the nor'easters due to the high waves (USGS, 1998a), these storms apparently resulted in downwelling along the coast from the northeasterly winds producing the offshore movement of bottom water. Thus the observed decrease in bottom water salinity during the period (Figure 3-6) was likely due to both vertical mixing and downwelling of fresher surface water.

The increase in bottom salinity documented during W9706 and recorded by the USGS sensors appeared to result from a prolonged onshore movement of bottom water into the nearfield. This would be consistent if the less saline bottom water in western Massachusetts Bay resulting from the April storms was being displaced by more saline bottom water from Stellwagen Basin or further offshore. The subsequent decline in bottom salinity during the first 10 days of June can only be explained by wave-generated mixing (see USGS, 1998a), although a southeasterly flow at the 20m-depth during the 10-day period was reminiscent of the apparent downwelling that occurred during the two nor'easters (see USGS, 1998e).

The other events observed in the physical data that warrant further examination through the current meter data were periods suggestive of onshore advection during late June (W9708), early August (between W9710-11), and late September (around the time of W9713). In each instance, bottom currents were moving in a westerly direction. In fact, with the exception of the brief reversal associated with the storm in late August, the predominant direction for the bottom currents throughout August and September was onshore (Tables 3-1 and 9-1).

The results from the various physical data are used in the following sections to help interpret the chemical and biological results, and provide a better understanding of the processes and events that occurred in Massachusetts Bay during 1997.

SURVEY	DEPTH			
	Mid-depth		Bottom	
	Direction of travel	R.T.	Direction of travel	R.T.
W9701	Variable	>14	SW	>11
W9702	NW	>9	W	4
W9703	SW	>8	W	>14
W9704	SE-NW	7	E-W	8
W9705	SE	2	E-NE	4
W9706	NW	>9	W	9
W9707	N-S	>14	SW	10
W9708	E-N	>10	E-W	>14
W9709	SE	5	E-W	>13
W9710	SE	4	W	>11
W9711	SE	2	W-E	>13
W9712	N-SE	8	SW	>14
W9713	X	X	SW	8
W9714	X	X	W	13
W9715	X	X	NW	11
W9716	X	X	SW-NW	>13
W9717	X	X	SE-SW	>14

Notes:
R.T. = Residence time (reported in days)
X - mid-depth current velocity not recorded

TABLE 3-1
Net water movement and residence time within the nearfield

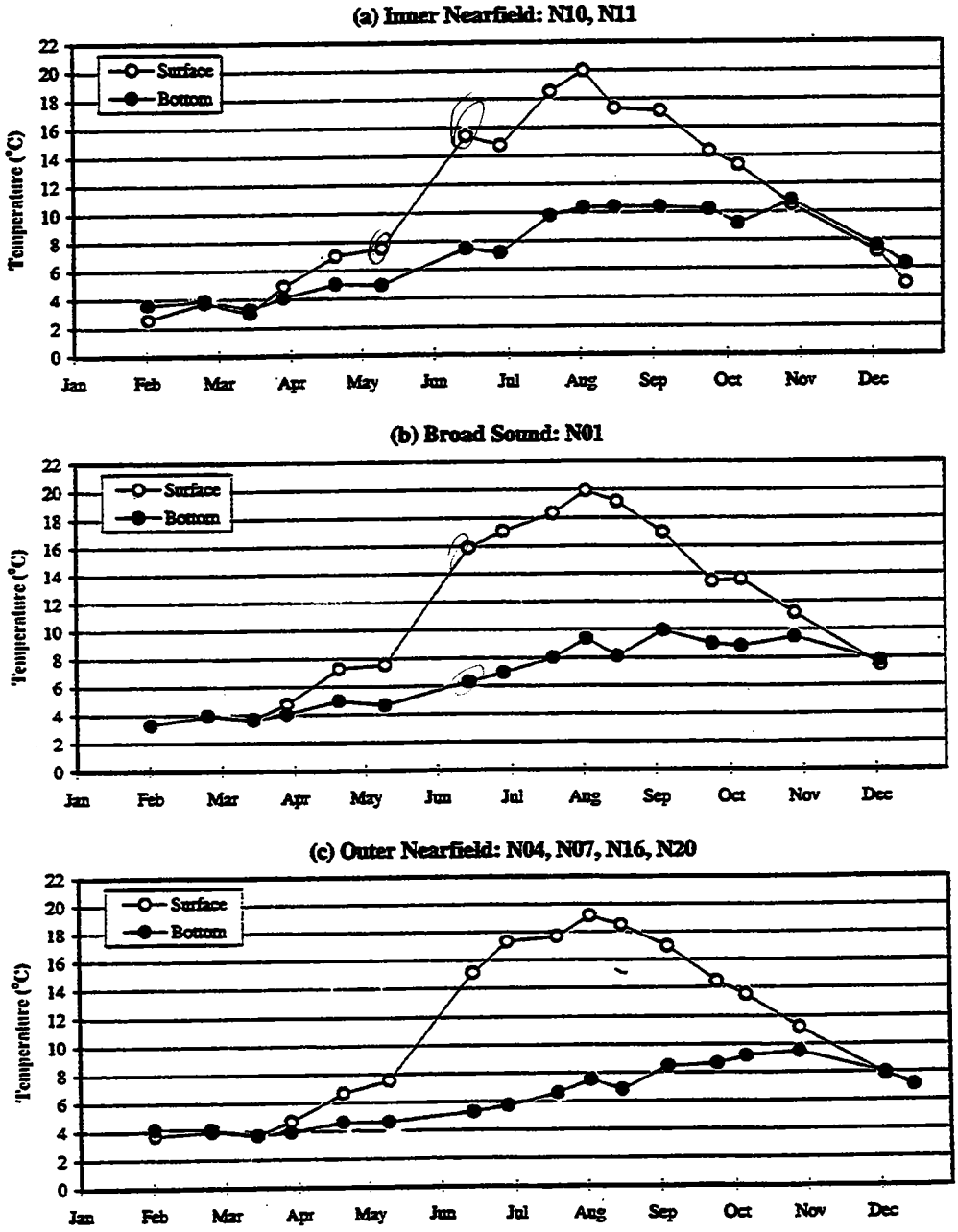

FIGURE 3-1

1997 Nearfield Temperature Cycle

Surface, Bottom, and Delta (Surface - Bottom) Survey Averages

F3-1_97.xls

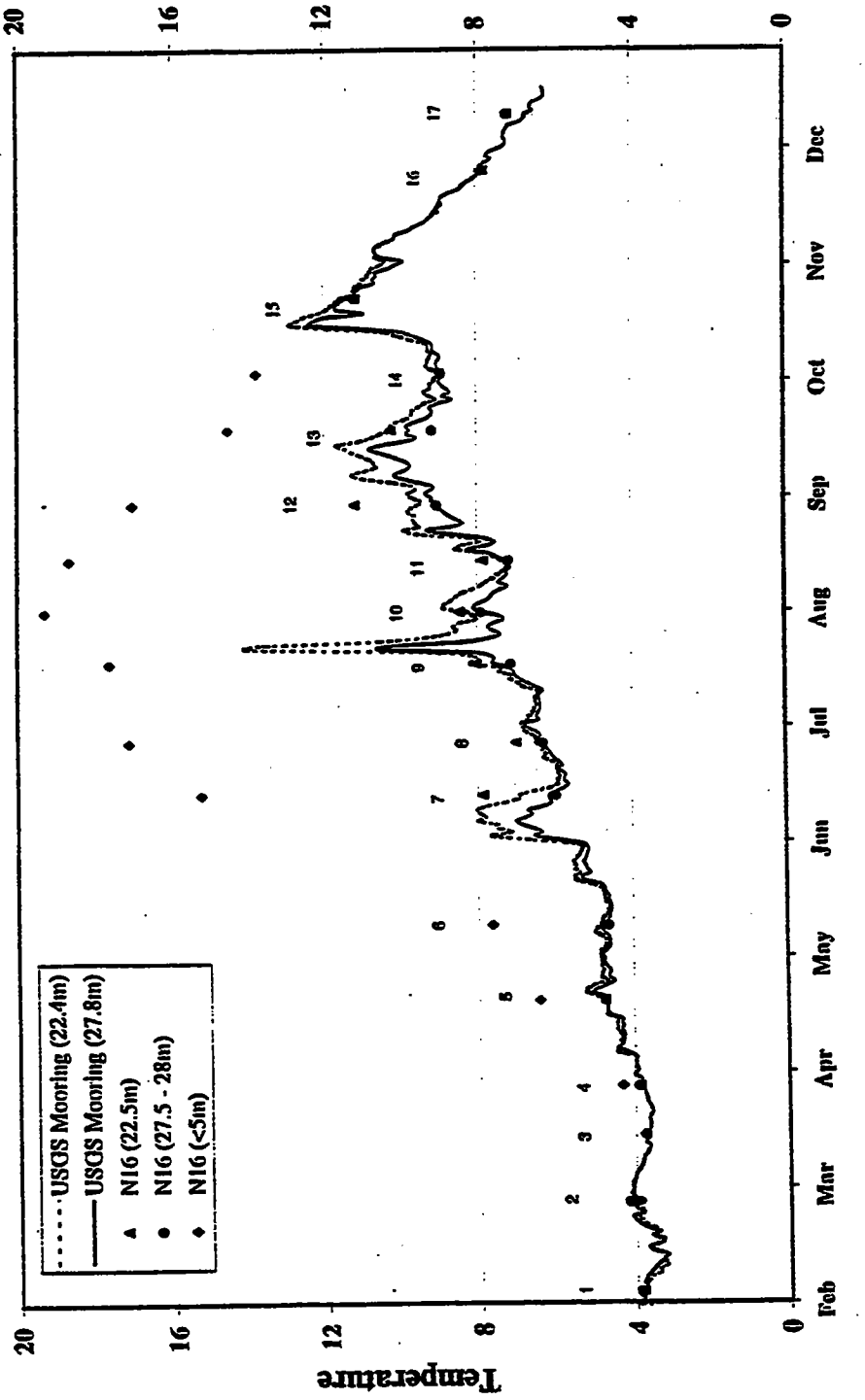

FIGURE 3-2
1997 Temperature Data at the USGS Mooring and Nearfield Station N16

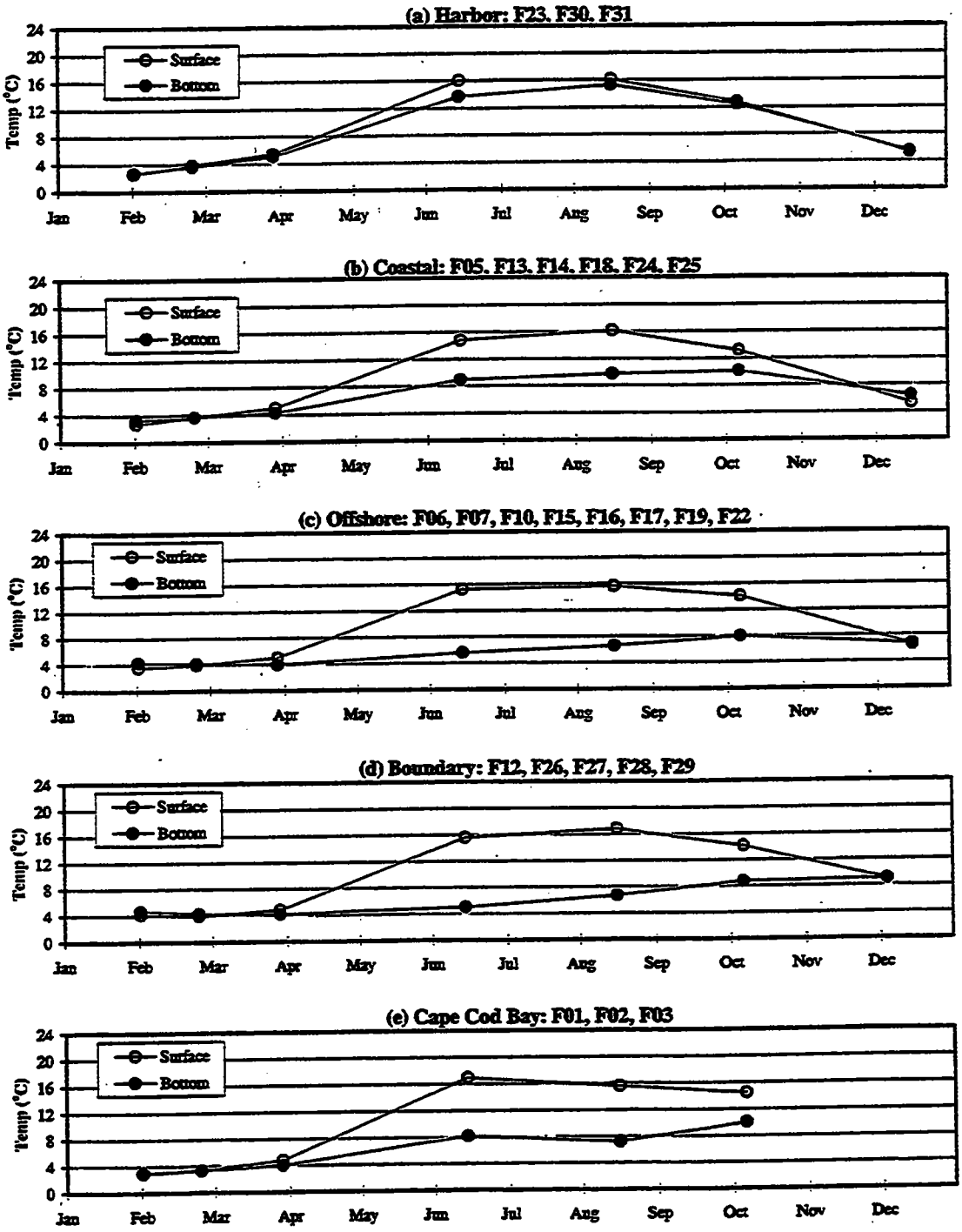

FIGURE 3-3

1997 Regional Temperature Averages

Surface, Bottom, and Delta (Surface - Bottom) Survey Averages

F3-3_97.xls

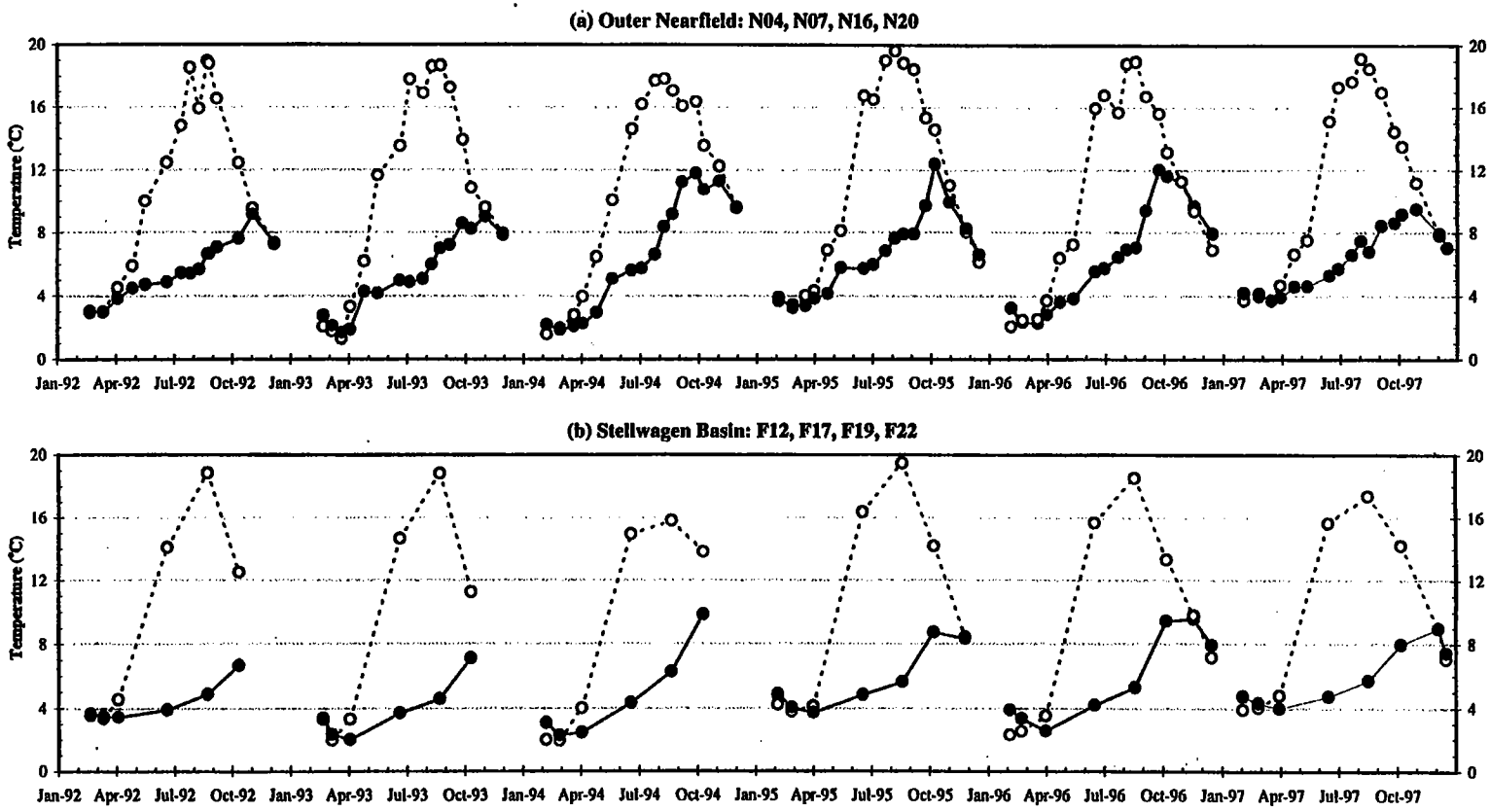

FIGURE 3-4

Interannual Comparison of Temperature in the Nearfield and Stellwagen Basin Regions

Surface (A, open symbols) and Bottom (B, solid symbols) depths averaged over stations as indicated.

F3-4_97.xls

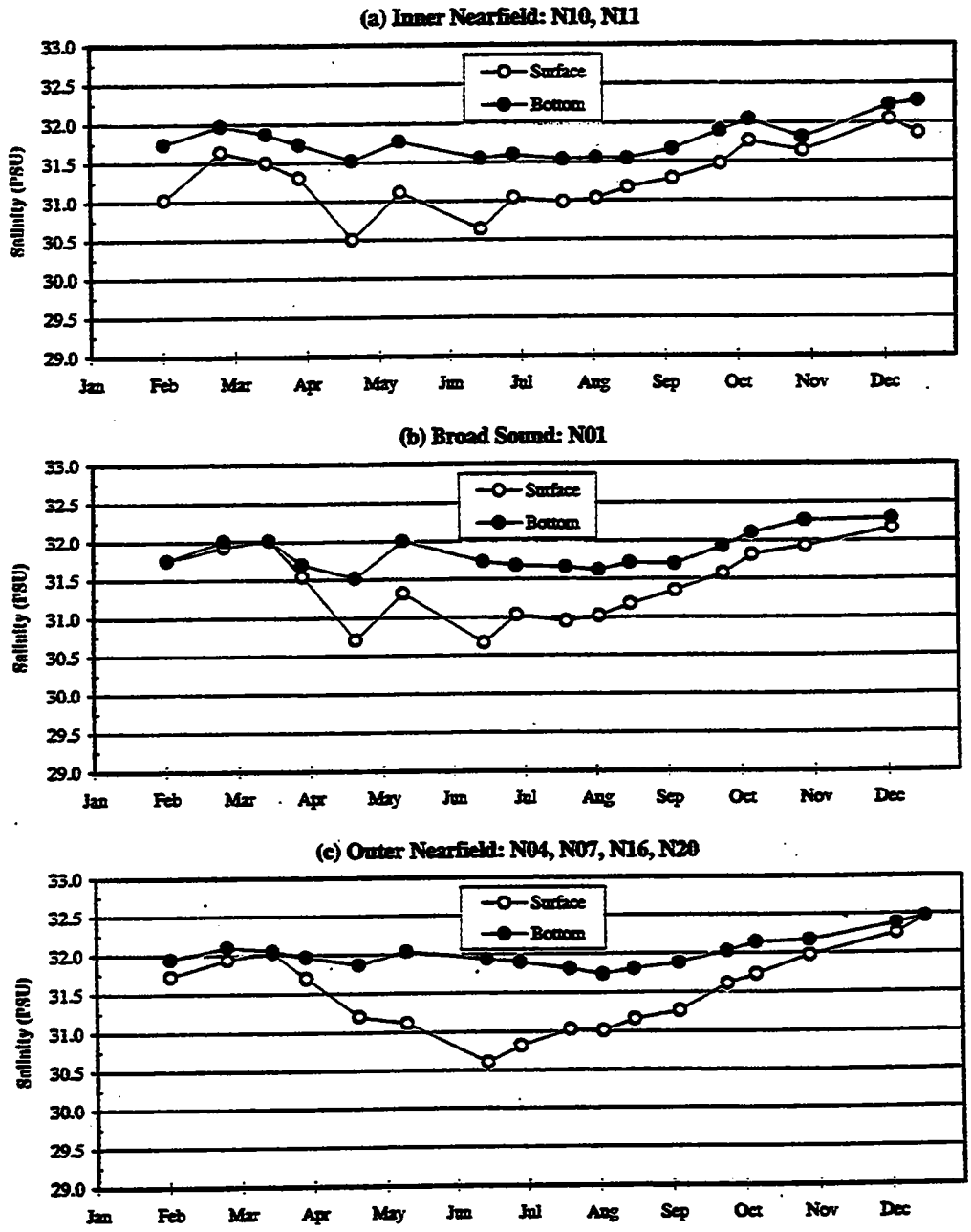

FIGURE 3-5

1997 Nearfield Salinity Cycle

Surface, Bottom, and Delta (Surface - Bottom) Survey Averages

F3-5_97.xls

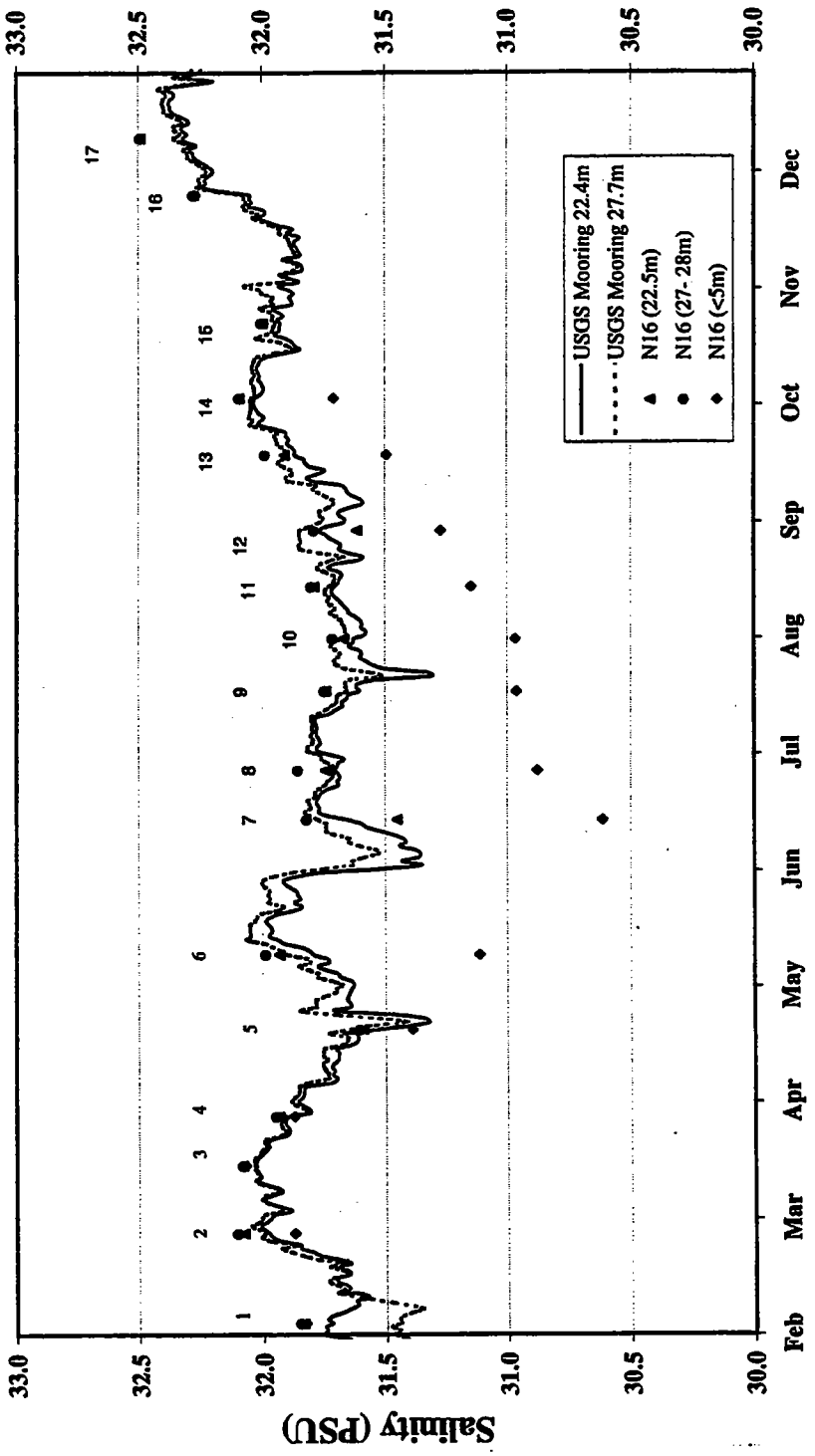

FIGURE 3-6

1997 Water Column Salinity at the USGS Mooring and Nearfield Station N16

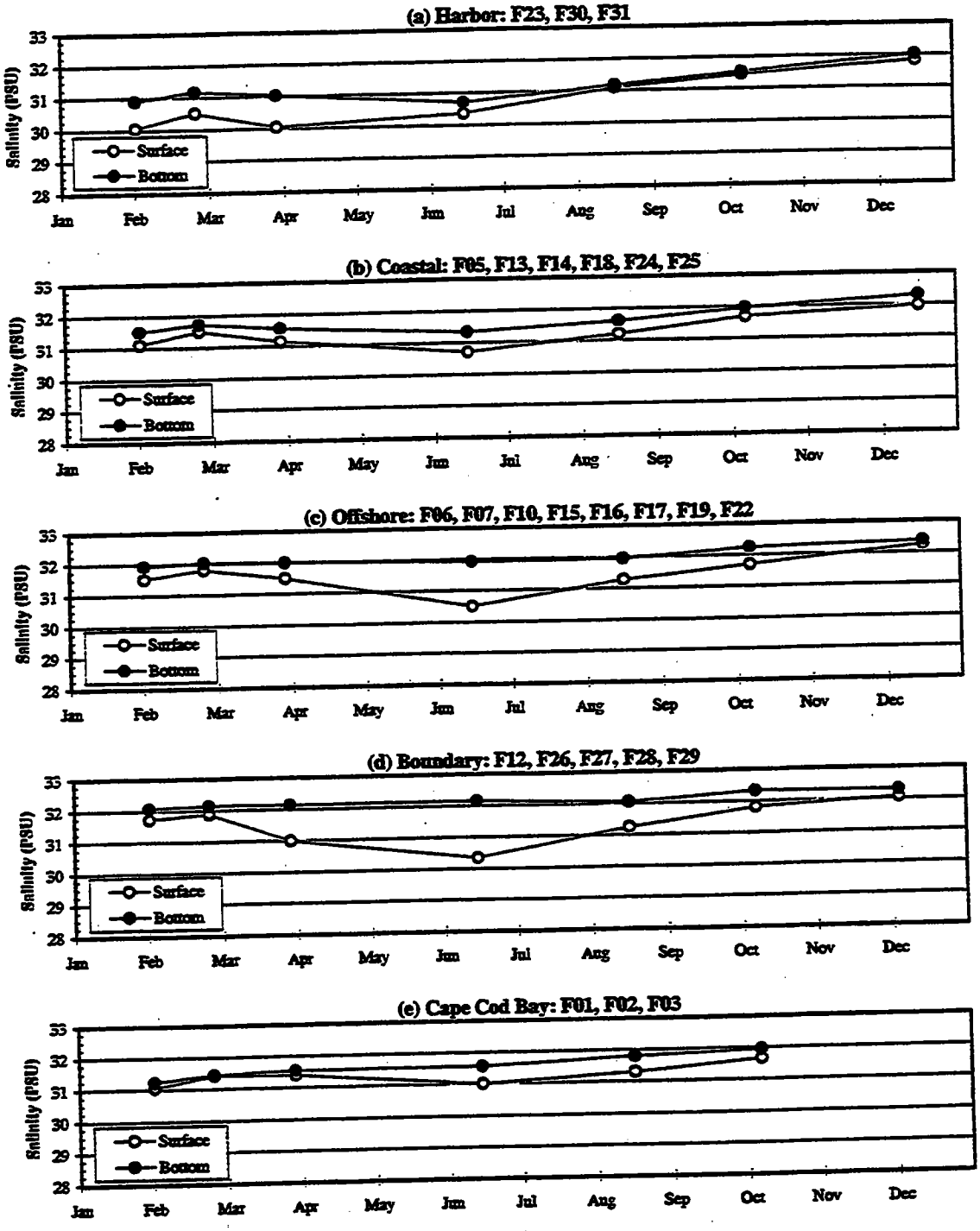

FIGURE 3-7

1997 Regional Salinity Averages

Surface, Bottom, and Delta (Surface - Bottom) Survey Averages

F3-7_97.xls

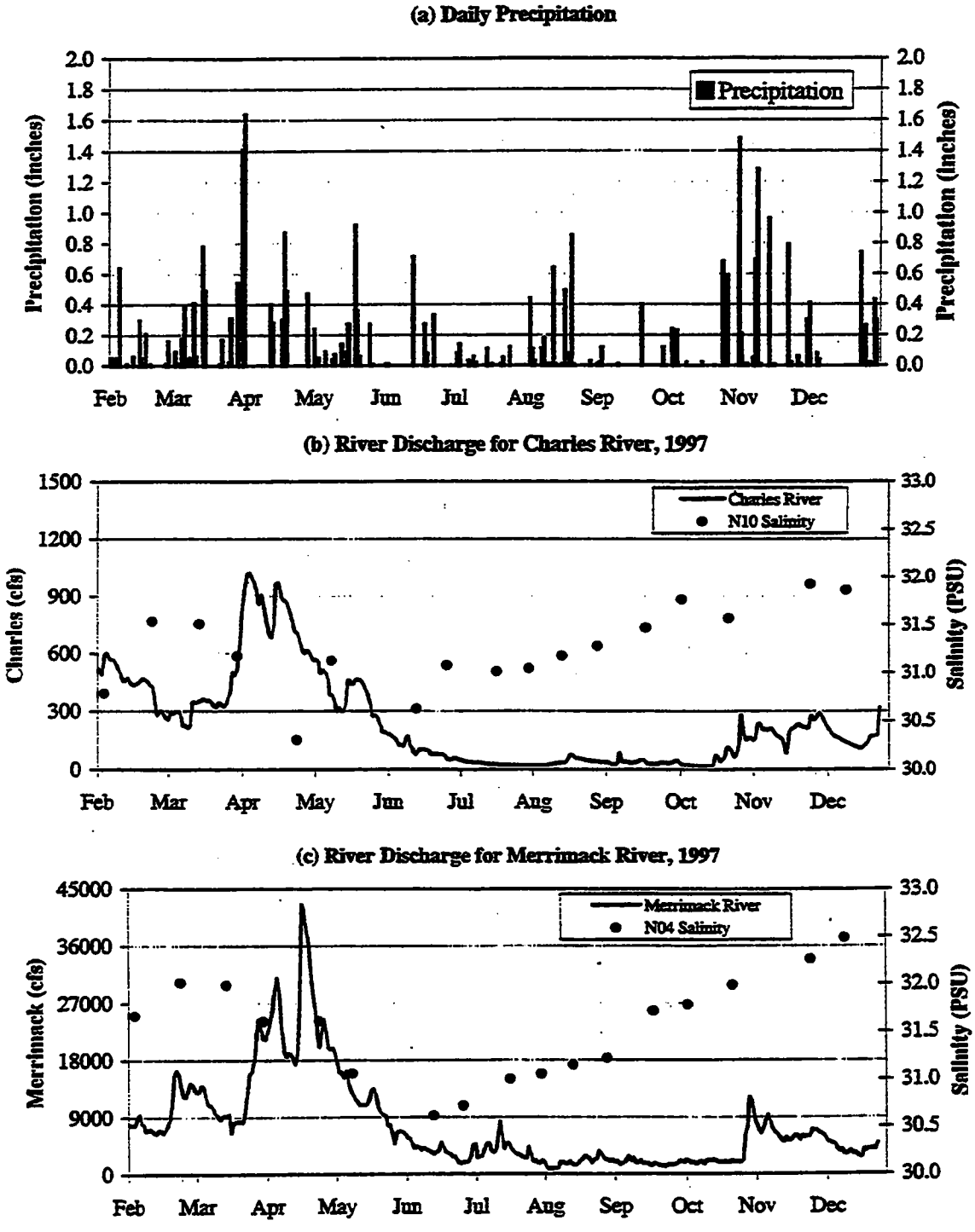

Figure 3-8

1997 Daily Precipitation (Logan International Airport) and River Discharge for Merrimack and Charles Rivers

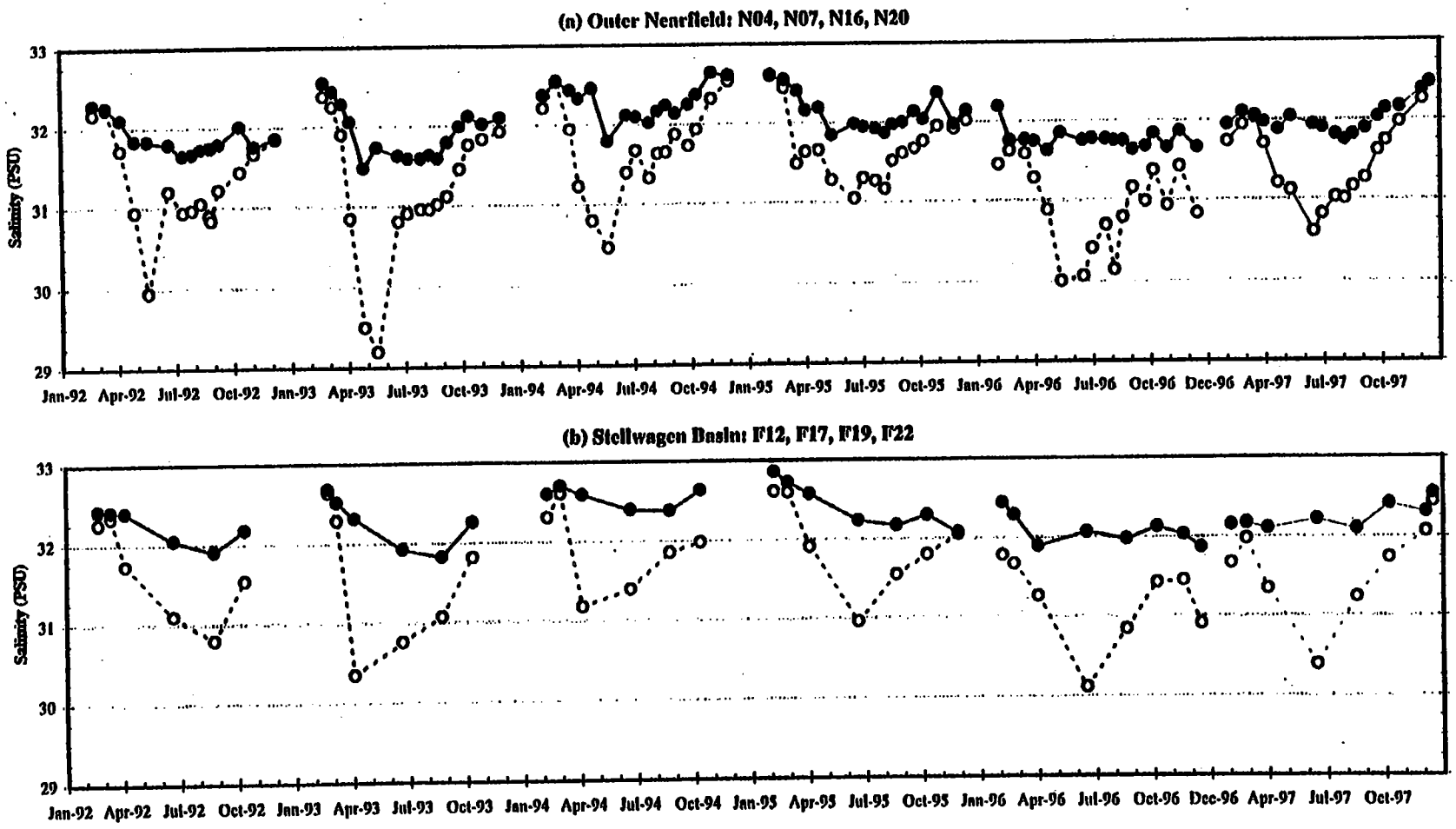

FIGURE 3-9

Interannual Comparison of Salinity in the Nearfield and Stellwagen Basin Regions

Surface (A, open symbols) and Bottom (B, solid symbols) depths, Stations as indicated.

F3-9.xls

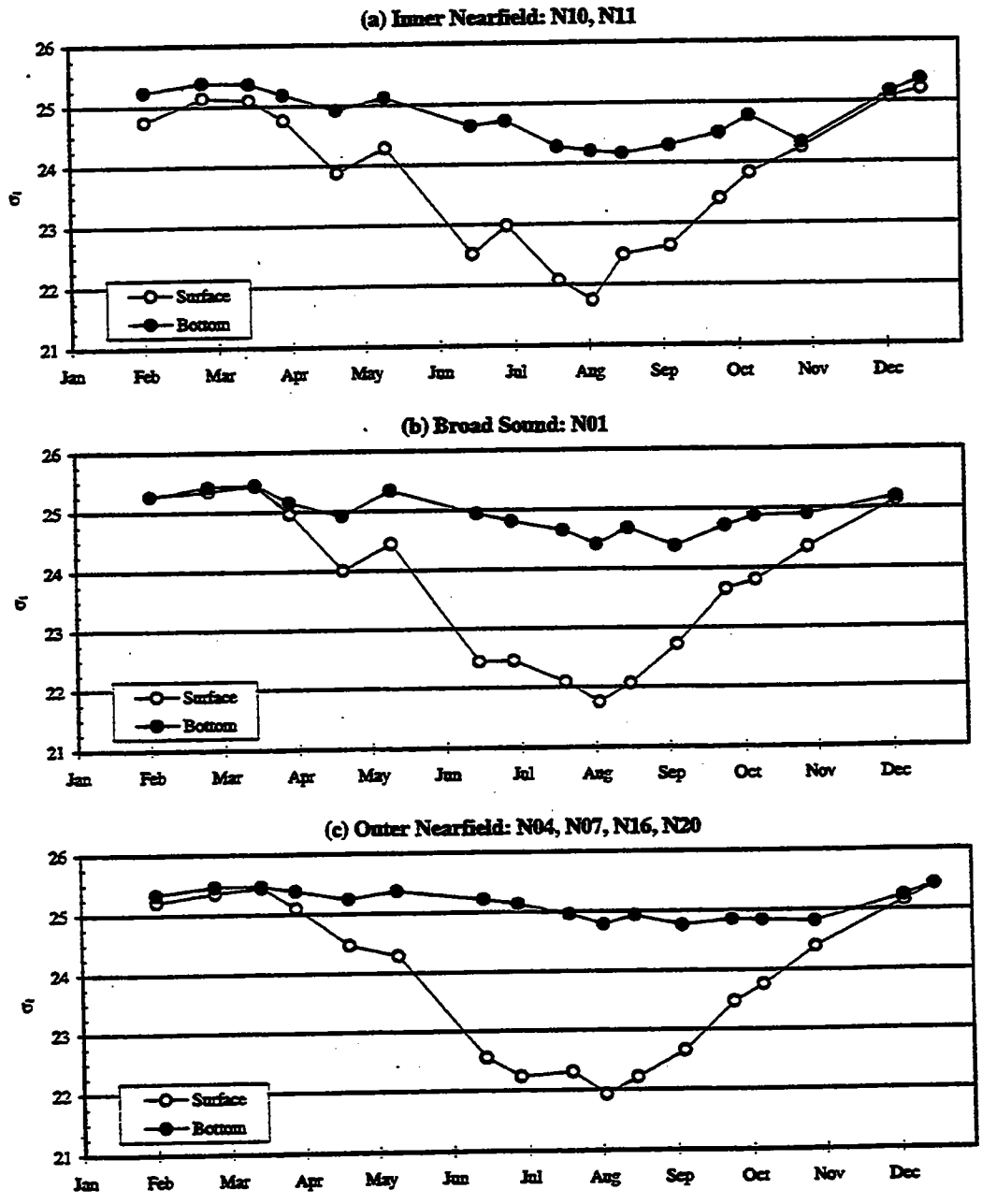

FIGURE 3-10

1997 Nearfield Density (σ_t) Cycle

Surface, Bottom, and Delta (Surface - Bottom) Survey Averages

F3-10_97.xls

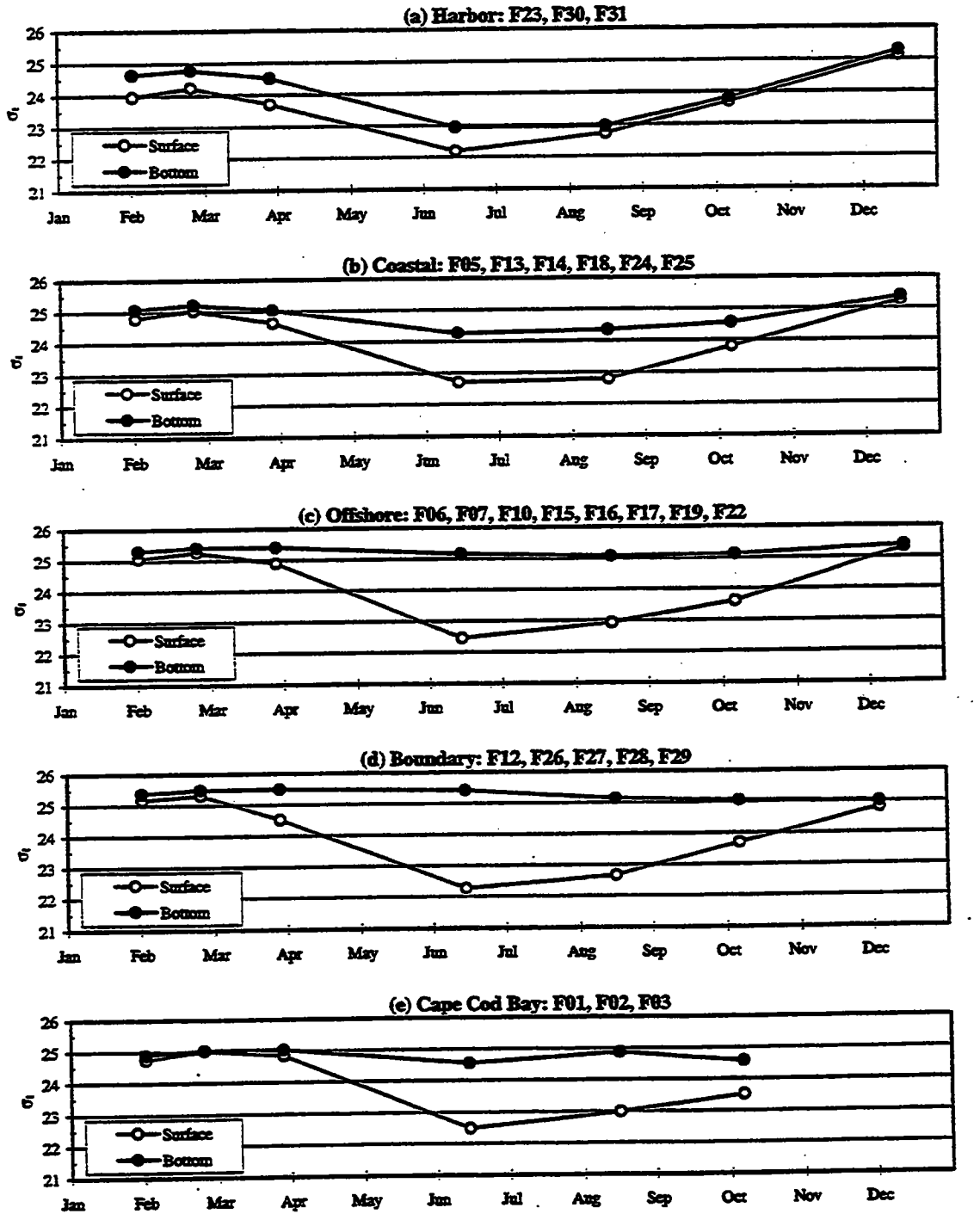

FIGURE 3-11

1997 Regional Density (σ_t) Averages

Surface, Bottom, and Delta (Surface - Bottom) Survey Averages

F3-11_97.xls

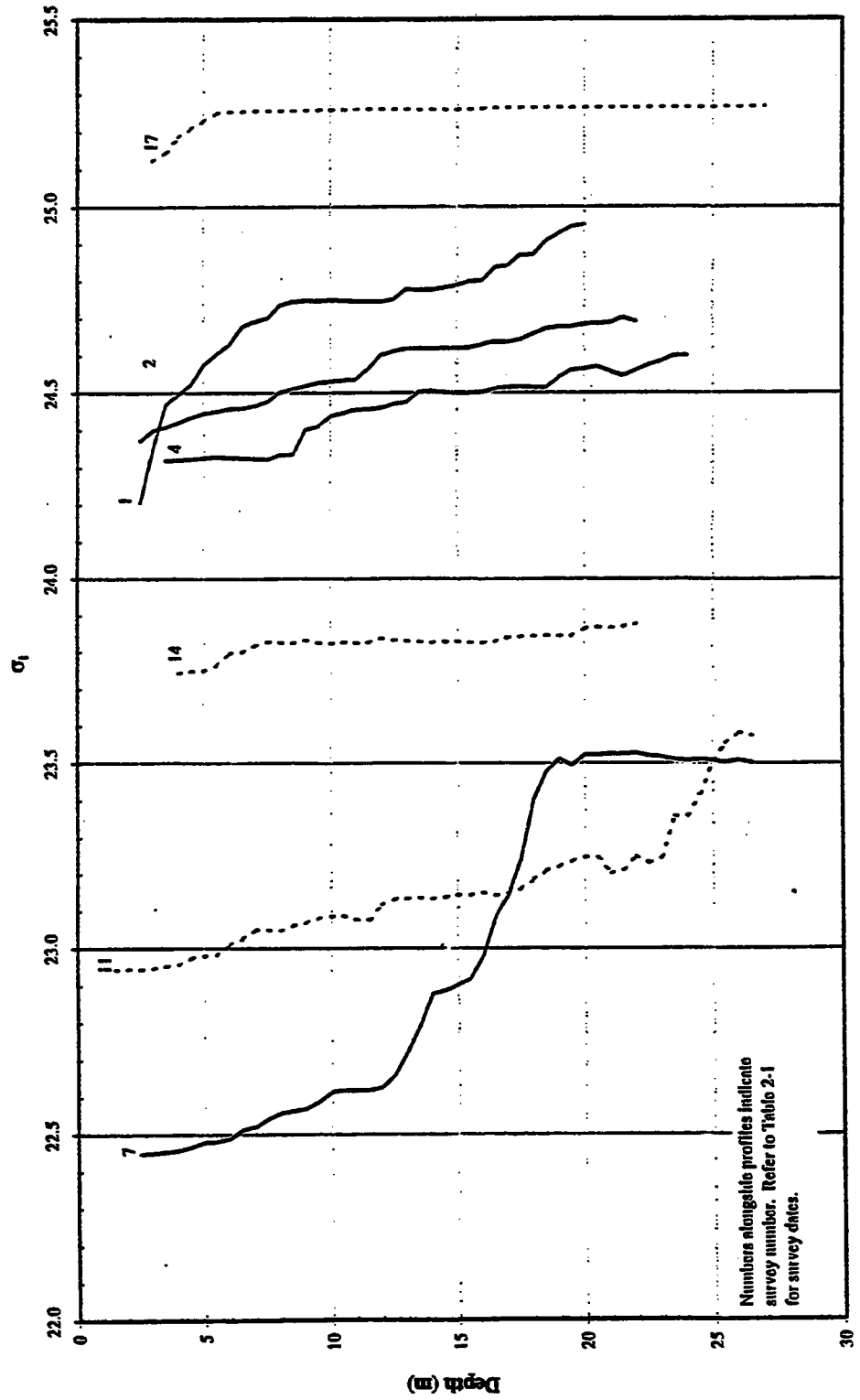

FIGURE 3-12
1997 Seasonal Density (σ_t) Cycle at Productivity/Respiration Station F23

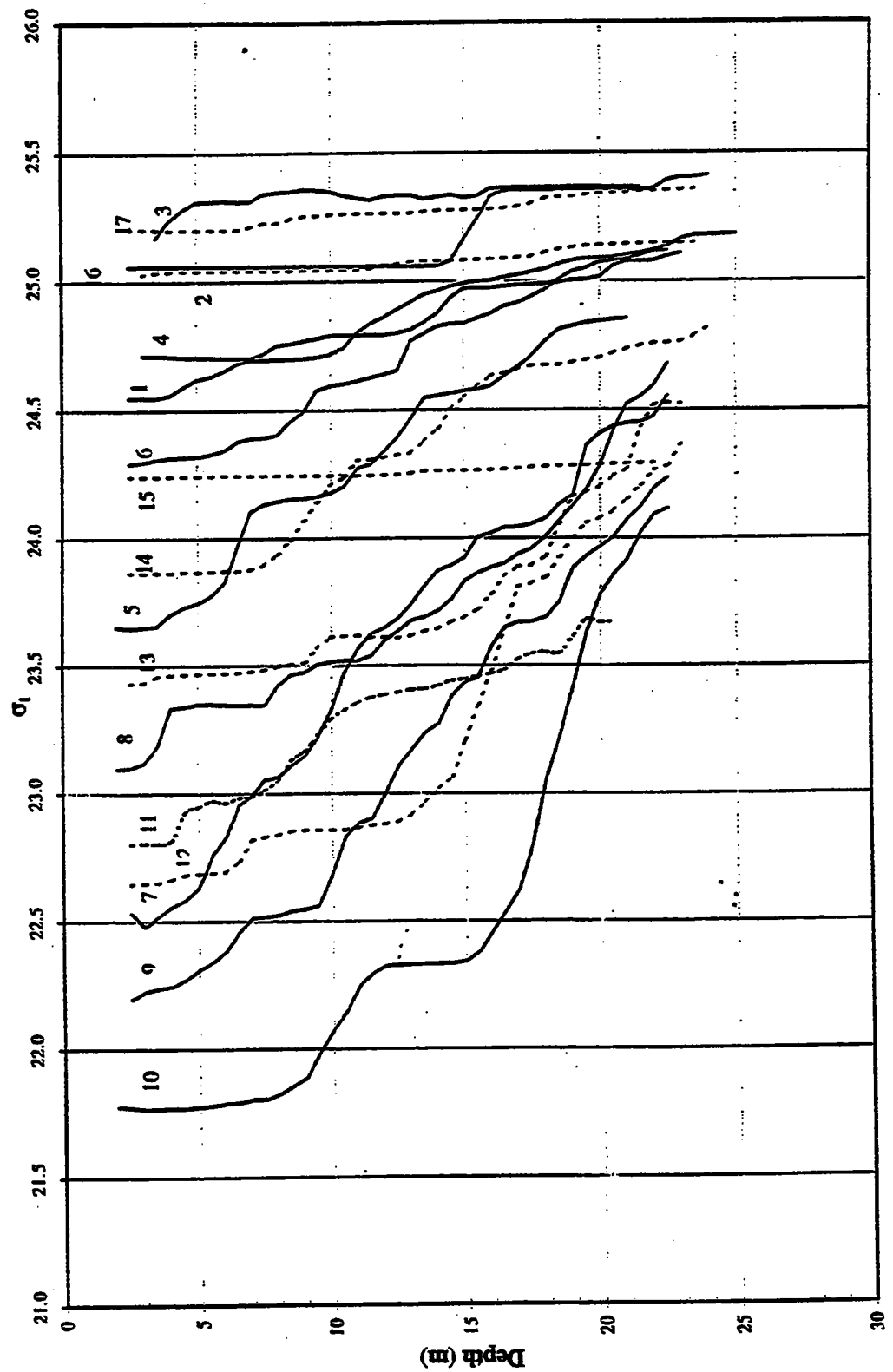

FIGURE 3-13
1997 Seasonal Density (σ_t) Cycle at Station N10

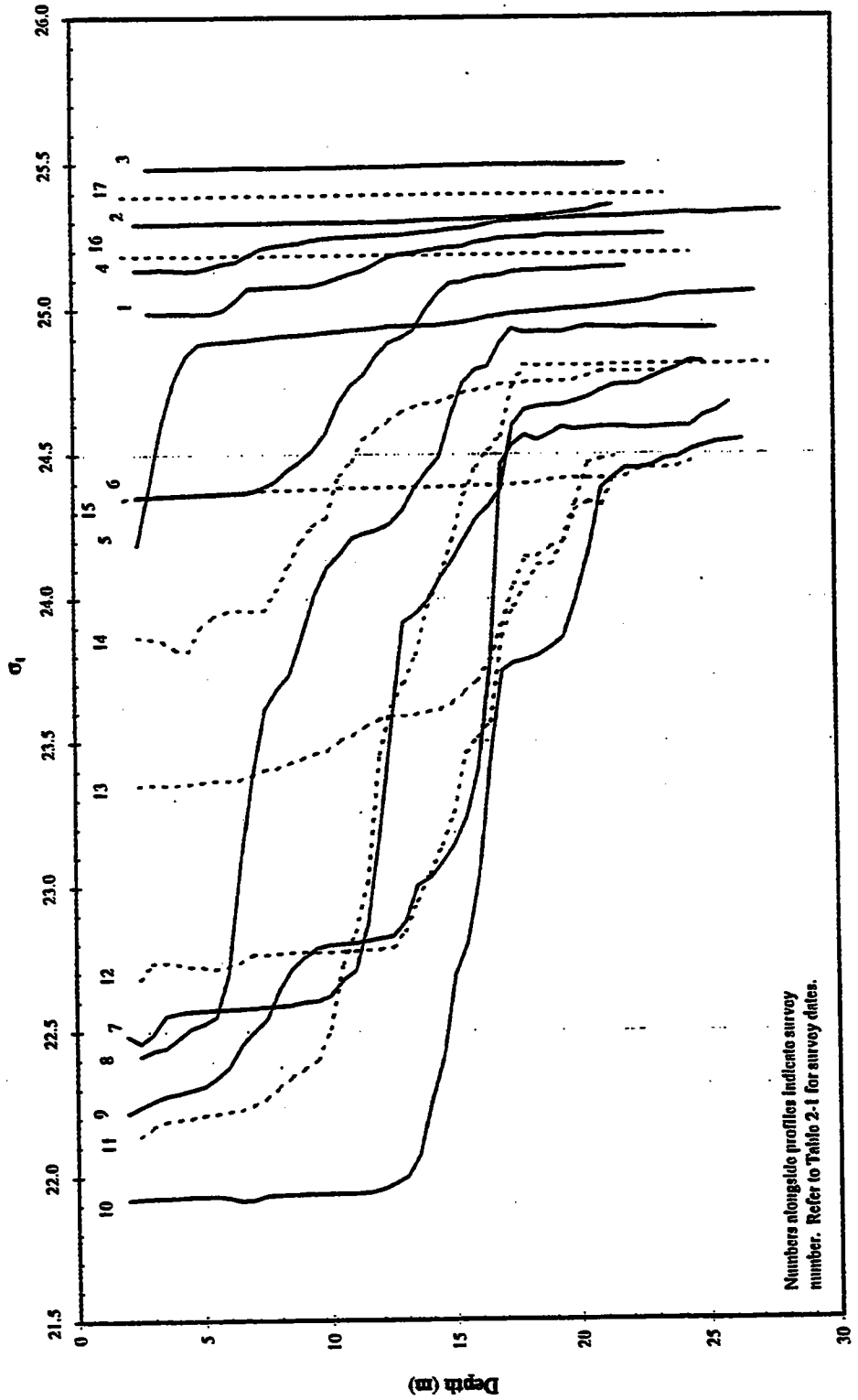

3-14elg2.xls

FIGURE 3-14
1997 Seasonal Density (σ_t) Cycle at Productivity/Respiration Station N18

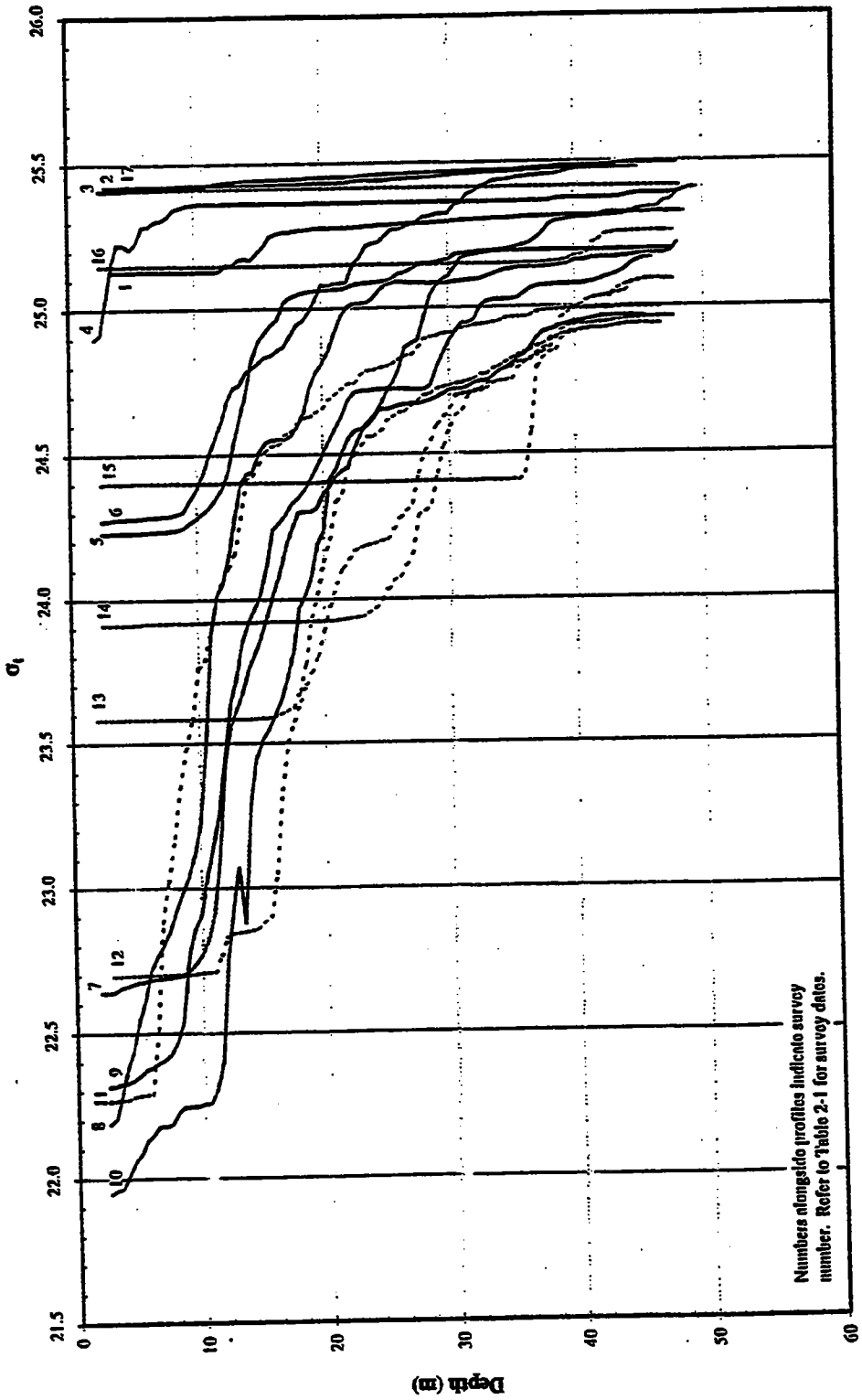

3-16ilg.xls

FIGURE 3-15
1997 Seasonal Density (σ_t) Cycle at Productivity/Respiration Station N04

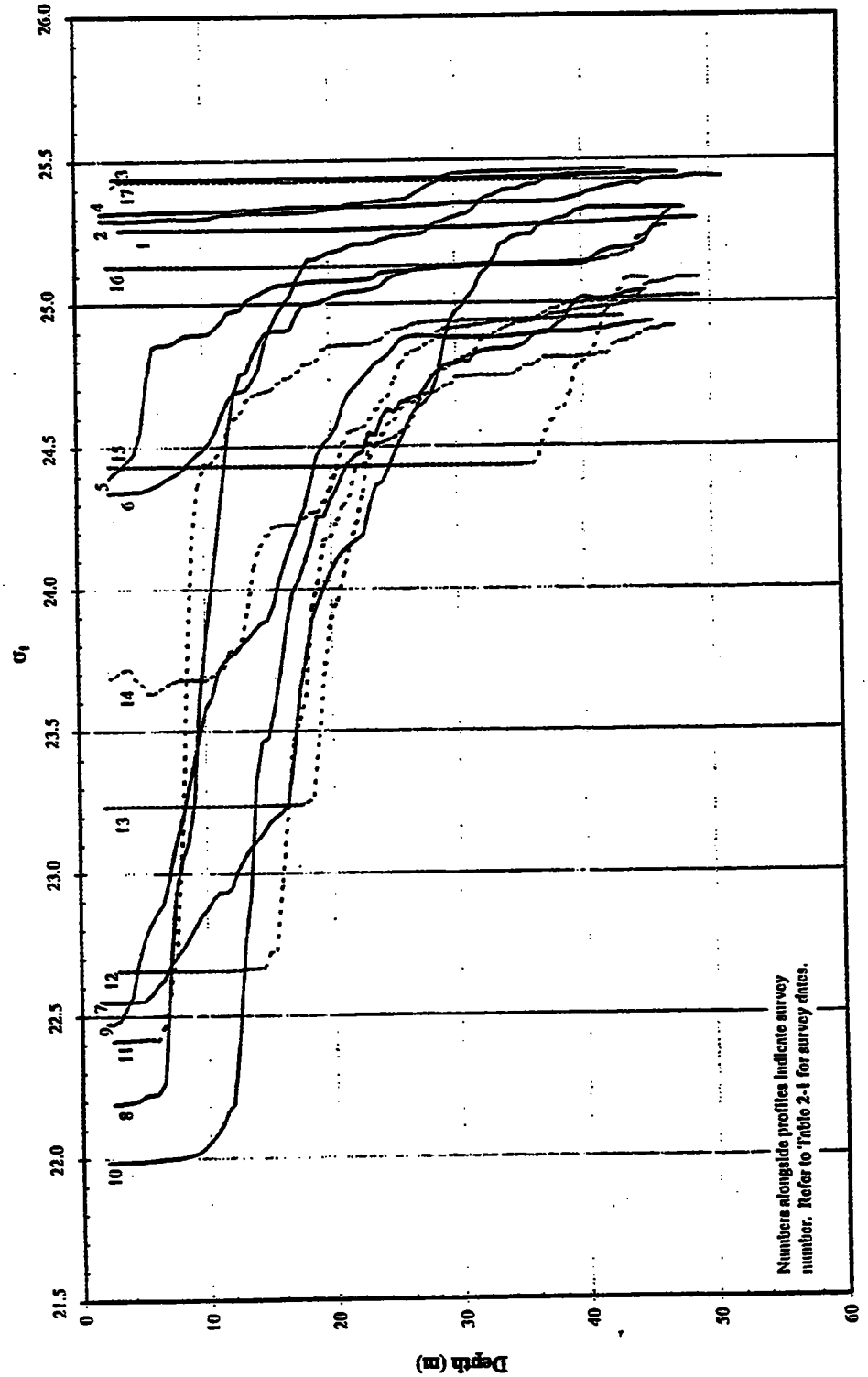

3-16slg.xls

FIGURE 3-16
1997 Seasonal Density (σ_t) Cycle at Productivity/Respiration Station N07

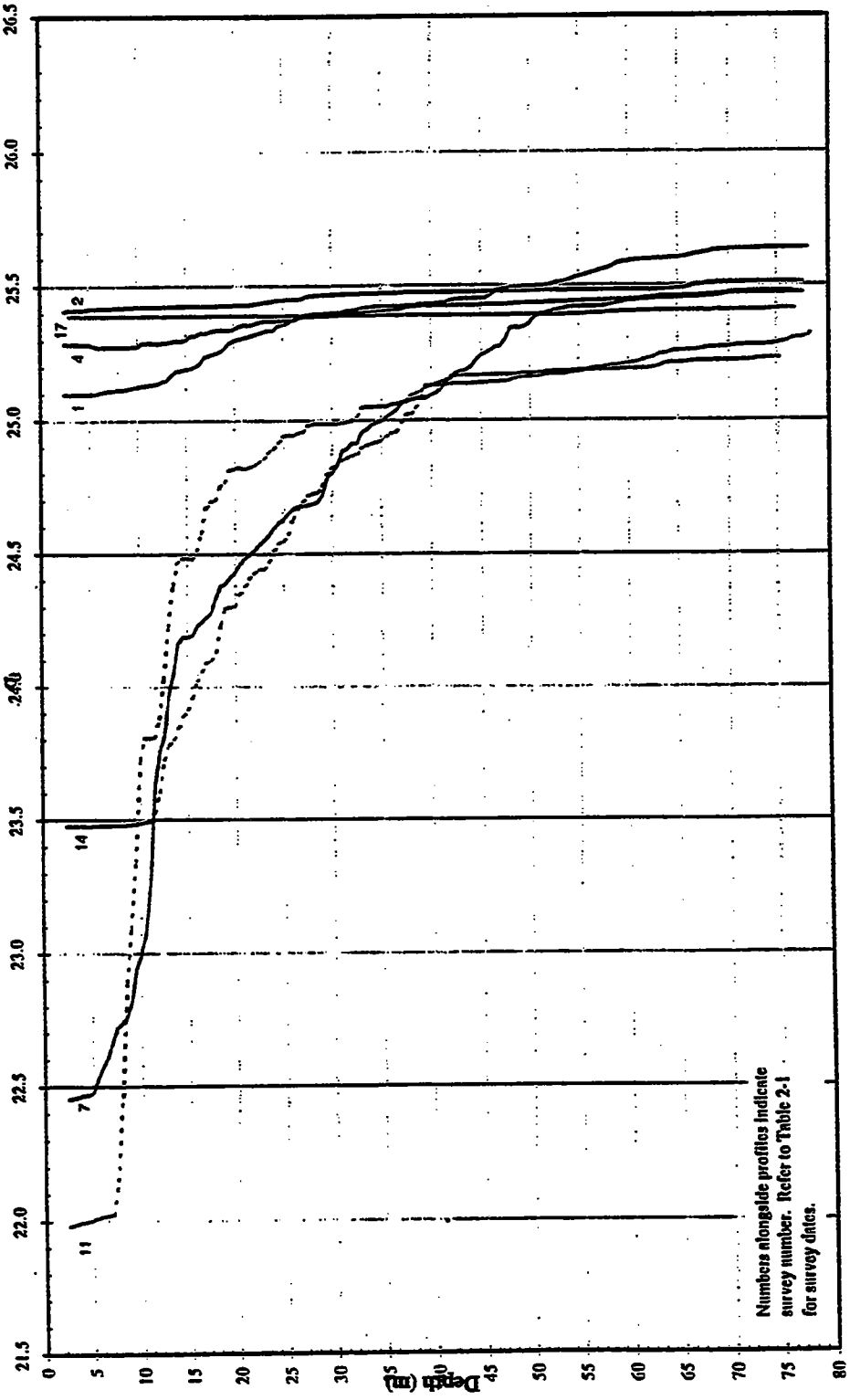

F3-17a(g.xls

FIGURE 3-17
1997 Seasonal Density (σ_t) Cycle at Respiration Station P19

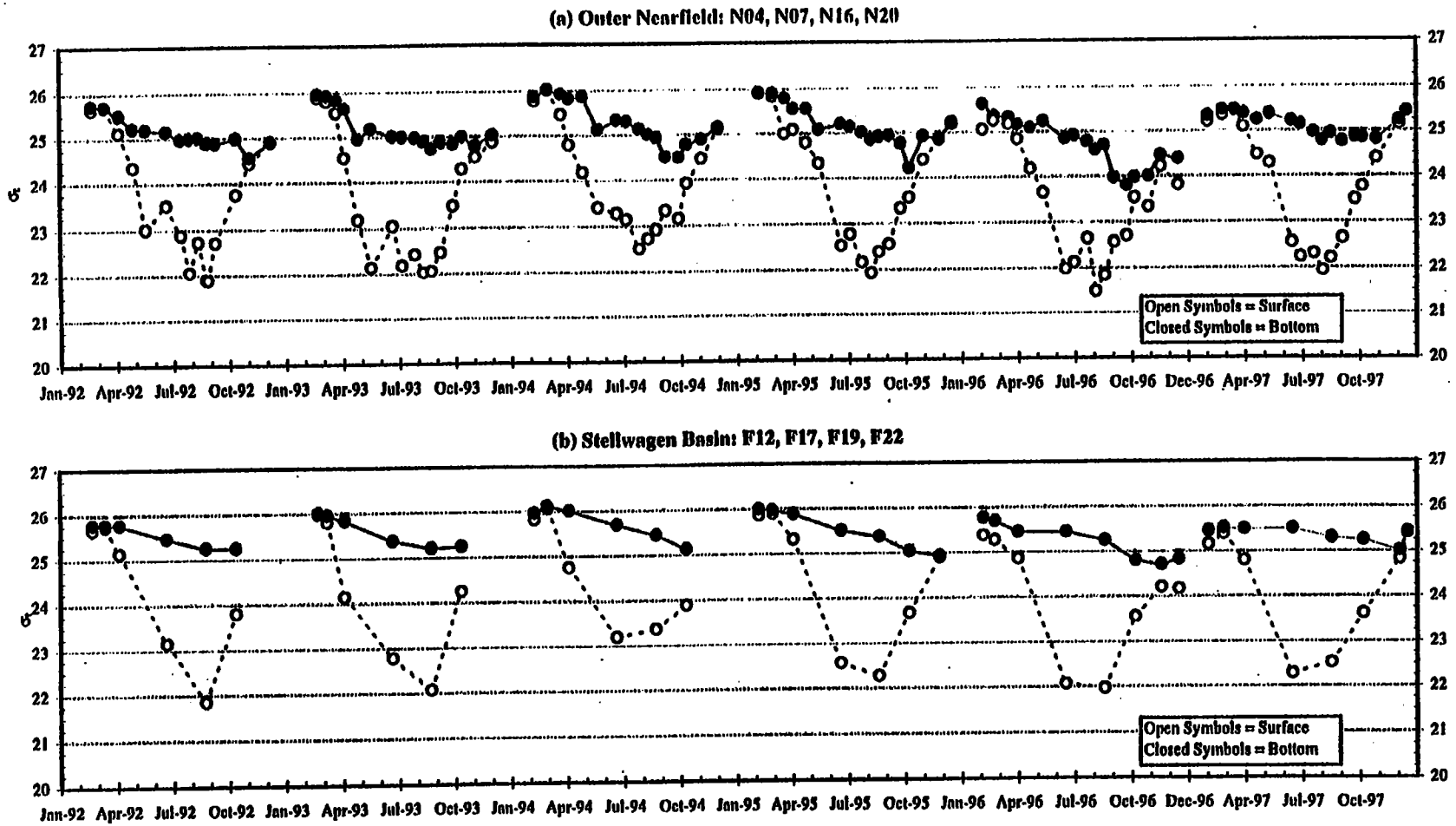

FIGURE 3-18

Interannual Comparison of Density (σ_t) in the Nearfield and Stellwagen Basin Regions

A and B depths, Stations as indicated

F3-19_97.xls

4.0 NUTRIENTS

This section provides an overview of the distribution of dissolved nutrients in the water column of the Massachusetts Bay system in 1997 based upon nearfield and farfield surveys conducted from February to December and February to October, respectively. Selected data from the 1997 samplings are presented and discussed both with regard to seasonal changes in the nearfield region and to spatial gradients between the various regions of the Bays. The 1997 nutrient record for the nearfield region surrounding the new outfall site is compared with data from the same stations throughout 1992-1996 to illustrate interannual variability at this location. The nutrient data presented here include water column concentrations for nitrate + nitrite, ammonium, phosphate (sometimes termed soluble reactive phosphorus), and silicate, as well as combined data such as DIN (nitrate + nitrite + ammonium), and ratios of DIN:phosphate and DIN:silicate.

Included also are analysis and discussion of dissolved parameters associated with water column carbon cycling such as dissolved organic carbon (DOC), dissolved organic nitrogen (DON), dissolved organic phosphorus (DOP), total dissolved nitrogen (TDN=DIN+DON), and total dissolved phosphorus (TDP). Similarly, particulate parameters such as particulate organic carbon (POC), particulate organic nitrogen (PON), particulate phosphorus (PP), biogenic silica (BioSi) and total suspended solids (TSS) are presented. Although discussed elsewhere in detail, *in vivo* chlorophyll fluorescence (Chapter 5) and dissolved oxygen (DO, Chapter 6) have been included to aid in data interpretation.

4.1 Annual Nutrient Cycle in the Nearfield

Several nearfield stations were sampled for nutrients more consistently than others throughout this study, due to either sampling design or weather related problems. To reduce bias, a subset of the routinely sampled stations was chosen for analysis of temporal and spatial changes during 1997. In the following sections, the nearfield nutrient and related data were plotted in several forms to help elucidate seasonal cycles, including both temporal vertical and horizon distributions, and to support interannual comparisons (1992-1997). The stations chosen and their rationale are presented in each subsection below.

4.1.1 Vertical Distribution of Nutrients in Nearfield

In order to show nutrient trends in the water column for the entire nearfield region during 1997, nutrient concentrations were plotted vs. time (Figures 4-1, 4-2, 4-3). In addition, fluorescence and DO concentrations were also plotted in the same manner to allow direct comparisons with these parameters (Figure 4-4a and b). Each individual nearfield station result was plotted in order to show data variability more clearly than would be shown by simple standard deviation brackets. In addition, averages of the surface, mid-depth and bottom samples were plotted to indicate average seasonal trends. Data from the A and B depths (Section 2) were pooled as they represent the mixed layer and show little difference in nutrient levels throughout the year. Bottom data represent the D and E depths, which during stratification were sub-pycnocline samples. The mid-depth average consists only of the C depth, which during stratification was near the pycnocline depth.

The observed differences reflect the integration of the effects of vertical mixing, stratification, and the different rates of phytoplankton uptake and nutrient regeneration in the surface and bottom layers. The vertical distribution of nutrients in the nearfield can also be observed in contour plots which show levels in profile over time with interpolation between each of the 17 field surveys and over depth (Figures 4-5 to 4-8, discussed further in section 4.1.2). Note that the contour plots contain only a subset of the nearfield data, while Figures 4-1 through 4-4 use all nearfield sample results. Clear seasonal differences were evident in all plots, with generally higher nutrient levels during spring and fall versus summer in both the surface and bottom waters. However, during the stratified interval, depletion of surface water nutrients was much more intense than in bottom waters, most likely due to the higher photosynthetic uptake in the surface waters for regenerated nutrients.

Between early February and late-March (surveys W9701 through W9704), when the water column was well mixed, nutrients were removed from the water column due to the late winter/spring phytoplankton bloom (Figures 4-1 through 4-3, Figure 4-5). This removal occurred for all nutrient parameters, although the trend in ammonium concentrations is less clear due to its lower initial concentration (Figure 4-1b and 4-5). During this interval, surface concentrations for nitrate + nitrite, phosphate and silicate were on average slightly lower than the bottom water concentrations (Figures 4-1a, 4-3a and b), again most likely due to the concentration of photosynthetic uptake in the surface waters (Section 7.1), even in the unstratified water column (Section 3). However, mixing was sufficient to produce nutrient removal rates that were apparently similar throughout the water column as evidenced by the similar slopes of surface and deep-water concentrations vs. time for the three major nutrients.

After the March survey (W9704), when the water column had begun to stratify (Figures 3-4 and 3-9), the average nutrient concentrations in the surface water became substantially lower than bottom water due to the continued high removal rates at the surface. However, surface layer concentrations of nitrate + nitrite, phosphate, and silicate did not reach their typical summer time minimum concentrations until mid June (W9707, Figures 4-1 through 4-3, Figure 4-5). This nutrient removal pattern is typical of a year in which the late winter bloom is relatively weak, such that the nutrients are not stripped from the water column by the onset of water column stratification (see Section 4.1.3).

The higher initial levels of ammonium in the surface water compared with the bottom at some stations (Figure 4-1b) was likely due to the influence of Boston Harbor and other coastal sources, but the difference was not apparent by the end of February. By late March, the average ammonium concentration for the bottom layer was higher than the surface, which is typical for ammonium. The increase in bottom water ammonium from late March to mid May (Figures 4-1b and 4-5) was potentially due to the initial ammonification of the organic matter produced during the late winter/spring bloom and the diminished uptake resulting from the onset of stratification.

As mentioned above, once the water column began to stratify in late March, the concentrations of nitrate + nitrite, phosphate, and ammonium continued to decrease in the surface water until they reached their annual minima by mid June (Figure 4-5). Surface water silicate showed a single-survey spike in April (W9705, Figures 4-3b and 4-5) due to storm-driven vertical mixing (Section 3.3.1), but also reached its annual minimum by mid June. In the

bottom layer, nitrate + nitrite, phosphate, and ammonium all showed a short-lived increase in mid May. This increase may have resulted from nutrient regeneration of settled organic matter from the late winter bloom, particularly evidenced by the increase in bottom water ammonium concentrations (Figures 4-1b and 4-5). In addition, both salinity data (Figure 3-6) and current meter data (Section 3.5) indicated that large-scale advection may have occurred prior to survey W9706, potentially introducing different water quality characteristics into the region. Afterward, nutrient concentrations in bottom water continued to decline to their seasonal minima in mid July.

In the bottom water, concentrations of nitrate + nitrite, phosphate, and silicate all increased rapidly after their July minima as nutrient regeneration, including nitrification, continued into the fall (Figures 4-1a, 4-3, and 4-5). The higher bottom water temperatures during this period enhance nutrient regeneration relative to the pre-stratified interval (bottom panel of Figure 4-6, also see Section 7.2). During the late summer and fall, bottom layer concentrations of ammonium remained low. The mid-depth concentrations of all the nutrients typically fell between the surface and bottom concentrations, though nitrogen concentrations were more similar to surface averages.

By early October (W9714), bottom water levels of nitrate + nitrite, phosphate, and silicate had all reached concentrations equal to or higher than their late winter values. In contrast, the phytoplankton uptake associated with the fall bloom (Figure 4-4a, Sections 5 and 8.1) reduced the average surface water nutrient concentrations (Figures 4-1 through 4-3, Figure 4-5). Water column mixing in October reduced mid-depth and bottom water concentrations by month's end (W9715) while surface levels rose slightly. As photosynthetic uptake declined, nutrient levels increased in late November and December through continued regeneration and water column mixing, although both silicate and fluorescence data indicated modest algal uptake during December (W9717, Figures 4-3b and 4-4a).

Average ammonium concentrations remained low during the fall and early winter period, except for late October (W9715) when ammonium concentrations rose temporarily. The increased scatter in elevated surface ammonium concentrations during this period (Figure 4-1b) was partly attributable to the high concentrations of ammonium from coastal sources, which typically influence the surface water of the inner nearfield during the fall. A similar degree of scatter in bottom depth results was testament to the degree of mixing occurring inshore at the time (Section 3.4.2). Degradation of the fall bloom material also likely contributed to the observed peak (Section 7.2).

Nutrient ratios are useful tools for assessing the sources and sinks of nutrients in coastal waters and for gaining insight into which nutrients might be limiting phytoplankton production. Within Massachusetts Bay in 1997, dissolved inorganic nitrogen (DIN = nitrate + nitrite + ammonium) to phosphate ratios (DIN:PO_4) in both surface and bottom water were typically much lower than the Redfield ratio of 16:1, indicating that nitrogen rather than phosphorus is more likely to be limiting to phytoplankton production. The DIN:PO_4 ratios ranged on average from ~9-12:1 during the winter months throughout the water column, while summer ratios were even lower (~4-10:1 for bottom water and ~1-5:1 for the mixed layer; see top panel of Figure 4-6). Overall, the water column in the nearfield is depleted in nitrogen relative to phosphorus throughout the whole year, especially at the surface

during the summer months. During the summer, sufficient phosphate (0.2-0.3 μM) typically remained available to support phytoplankton production as DIN concentrations approached zero (Cibik *et al*, 1998a & b).

DIN to silicate ratios (DIN:SiO_4) remained below 1:1 throughout most of the year, with the exception of the spring bloom period of March to May when average values were from ~1:1 to 2:1 (Cibik *et al*, 1998a). During the late spring (W9706), when diatoms were a major contributor to phytoplankton production, both DIN and silicate were removed in an approximately 1:1 ratio from the water column and were almost completely removed from the surface water (Figure 4-5). However, in general there is sufficient SiO_4 to allow photosynthetic uptake of all of the DIN pool.

In the surface layer, the DIN:SiO_4 ratios slowly increased from late summer values of ~ 0.1:1 to 0.3:1 to about ~ 1:1 in the late fall due to the greater increase in DIN over SiO_4 in the water column during the late fall (Figure 4-6). There was typically a surplus amount of silicate (1-4 μM) in the water column as DIN concentrations approached zero due to the relative dominance of non-diatom species. However, note the occasional depletion of surface silicate during the summer in Figure 4-5 (e.g., mid-August and mid-September) when periodic diatom growth occurred (Section 8.1).

4.1.2 Vertical Distribution of Nutrient-Related Parameters in Nearfield

Further analysis of the nutrient trends in the nearfield was undertaken through the use of contour plots of data collected throughout 1997. As indicated previously, the contour plots show the parameter levels in profile over time with interpolation between each of the 17 field surveys and over depth. Stations N04, N07, N16 and N20 were selected for this analysis as they integrate the area of the future outfall site (Figure 2-2) and had the most complete data sets. This approach was used for dissolved inorganic nutrients (Figure 4-5); DIN:PO_4 and DIN:SiO_4 ratios, fluorescence, DO and temperature (Figure 4-6); the particulate parameters POC, PON, PP, BioSi, and TSS (Figure 4-7); and dissolved organic parameters, DOC, DON, DOP, TDN, and TDP (Figure 4-8).

General seasonal trends for all the nutrients (Figure 4-5) and for DIN:PO4 and DIN:SiO4 ratios (Figure 4-6) were discussed above in section 4.1.1. Note however the relationship between nutrients and chlorophyll fluorescence (Figures 4-5 and 4-6). The typical sequence observed in 1997 was depletion of nutrient pools as the chlorophyll levels increase, which occurred during March, May, and early October. Also note also the deepening of the surface DIN depletion (i.e., nutricline) through July.

The May mid-depth chlorophyll maximum (15-20m) was centered below the 10-15m pycnocline (see Figures 3-15 and 3-16), and thus had access to relatively high concentrations of DIN and phosphate in the bottom waters. This suggests that mid-water blooms can occur in late spring after the water column has stratified as long as there is adequate light penetration and a nutrient supply in the mid and bottom layers. This latter feature will be the norm once the new outfall is operating. Similarly high concentrations of chlorophyll occurred during the fall bloom in early October (W9714) and were also associated with increasing levels of both DIN and phosphate in the mid-depth and bottom layers. Dissolved oxygen and temperature (Figure 4-6) were plotted at this set of stations for later reference and are discussed elsewhere in this report.

Given the dominance of phytoplankton production in the carbon cycle of western Massachusetts Bay (Cibik *et al.* 1996, 1998c, Section 7), it is not surprising that total particulate levels (which consist almost wholly of organic matter) largely follow plankton blooms and the amount of plankton in the water column. Hence the patterns for POC, PON and PP are all very similar, with highest concentrations associated with the spring and fall blooms (Figure 4-7). There were also relatively high concentrations related to production during a bloom in early August, also apparently centered below the pycnocline.

PON concentrations of 3-5 μM (during maximum bloom periods, Figure 4-7) indicated that about 20-30 percent of the total nitrogen (sum of all forms) in the water column was particulate, compared to about 10 percent in early summer and 5 percent during winter. Both POC and PON showed similar percentages of the totals (TOC and TN). Concentrations of POC, PON and PP were similar in both the May and fall blooms. Similar to PON, the concentration of PP during the blooms was about 30 percent of the total phosphorus. In contrast to PON, during the summer months PP accounted for about 40% of the TP, a much higher fraction compared to the PON:TN pool. Additional analysis of transformations of these nitrogen and phosphorus forms is detailed by Z. Wang (UNH Master's thesis, in review).

The concentration of BioSi, which mainly represents silica bound in diatom frustules, was clearly highest during the intense May diatom bloom (Figure 4-7, bottom panel). Concentrations also showed maxima during the earlier spring bloom and the fall bloom. The concentrations of BioSi during the summer period were consistently very low, reflecting lower diatom biomass and dominance by non-diatom species (see Section 8.1). Note again the apparent accumulation of diatom-bound silicate at depth during early August, which may have been associated with the increases in POC and PON also noted at depth (Figure 4-7).

TSS concentrations were typical for this area of Massachusetts Bay, ranging from about 0.5 to 3 mgL^{-1} (Figure 4-7). In addition to phytoplankton biomass, TSS concentrations are also affected by resuspension of bottom material during storms and transformations due to zooplankton grazing. Hence, concentrations are typically highest during the winter months and during periods of high production (spring and fall blooms). Concentrations tend to be lower during the summer months when there is little storm activity, the water column is stratified, and zooplankton grazing rates keep pace with primary production. TSS in 1997 followed these general trends, with the lowest concentrations were found during July in the surface water and the highest were found at mid-depths during the spring bloom and in June associated with a water column mixing event. The June mixing event is clearly seen in the temperature data from the USGS mooring (Figure 3-2), and given the TSS results, it appears to have been strong enough to resuspend sediments. This latter conclusion stems from the apparent inorganic nature of the TSS as evidenced by the lack of a parallel increase in POC, PON or POP concentration in June.

Dissolved organic carbon (DOC) concentrations (Figure 4-8) were relatively constant during most of the year and generally fell between 60-100 μM. During mid-summer (W9709), DOC concentration appear to have reached an annual maximum, but the effect is generated by only a few high DOC samples on a single survey. The fall bloom DOC concentrations were relatively low. Dissolved organic nitrogen (DON) concentrations (Figure 4-8) were also relatively constant during most of the year with most values falling between 6-9 μM. The highest

concentrations were observed during the May and October bloom periods and likely resulted from leaching from senescent phytoplankton or from grazing.

DON is often the predominant form of nitrogen in the water column and can range from about 50 percent of the total nitrogen to nearly 80 percent during summer months. By contrast, the dissolved organic phosphorus (DOP) usually represented only about 15-30 percent of the total phosphorus in the water column (Figure 4-8). Both the total dissolved nitrogen (TDN) and total dissolved phosphorus (TDP) plots show highest concentrations in the bottom water during May and October and throughout the entire water column during winter. This is due mainly to the increase in dissolved inorganic forms during these time periods.

4.1.3 Interannual Nutrient Variability in the Nearfield

Inter-annual variability of nutrients and chlorophyll in the area of the future discharge in the nearfield was illustrated by using the same four stations (N04, N07, N16 and N20). This approach was also used in Section 4.1.2 since these stations have the most complete data coverage over the baseline monitoring period. Data from these stations were averaged for each of the five discrete sampling depths (A-E) and then plotted in profile for the 17 sampling surveys. A contouring program was used to interpolate concentrations between the average survey profiles throughout the baseline period (1992-1997, Figures 4-9 through 4-14).

The average depth of the bottom samples at these stations among the surveys was 38-42m. Note that the sampling season was longer (started earlier and ended later) during 1995-1997 than in the previous three years. Care must be taken or this subtle difference in timing of sampling can result in substantial bias, particularly when using seasonal averaging schemes. For example, it appears that there were much higher winter DIN concentrations in the water column during 1995-1997 than during 1992 (Figure 4-9). However, this apparent difference may have been due to the earlier sampling in the later monitoring years before nutrient depletion by the bloom.

Plots for each nutrient show there were substantial differences in the concentration patterns over the six years presented, although each year does reflect a consistent trend of declining nutrient levels from initial winter maxima due to the onset of the late winter/spring bloom in each year. In 1997 the initial nutrient uptake rates during the late winter bloom appeared low, similar to 1993 and 1995 (e.g. Figures 4-9 and 4-10). Consequently, the concentration of DIN and nitrate + nitrite did not approach total depletion prior to water column stabilization as was observed in earlier years such as 1992, 1994 and 1996. The nitrate + nitrite concentration increase in the bottom waters in mid May probably helped fuel 1997's unusually intense mid-water bloom. Similar late spring bottom water concentration increases were observed in other years (e.g., 1994 and 1995), with similar production of mid-depth blooms.

The late-season increase in nitrate + nitrite concentration observed in 1997 was evident in most of the other years (Figure 4-10). The pattern in 1996 was slightly different in that there was no subsequent decline in concentration; instead concentration rose continuously from September onward. It is worth noting here that the timing of the fall bloom appears to be a more consistent than that of the spring bloom in the nearfield area (Figure 4-11),

although even here it can vary by a month or more (e.g., 1995 vs. 1993). However, the relative uniformity in the timing of the fall bloom is almost certainly due to its association with the regular breakdown of stratification.

Trends in both phosphate and silicate agreed well with nitrate + nitrite (Figures 4-12 and 4-13). Silicate concentration patterns were similar to other years in which there were spring diatom blooms (e.g., 1994 and 1996). Ammonium concentration patterns were similar to most of the prior years in that there were relatively high concentrations in the bottom waters in May and June, reflecting regeneration of organic matter from spring bloom period (Figure 4-14). These high concentrations were observed later in the season in 1997 compared to years with early intense blooms such as in 1996. The increase in ammonium concentrations in the surface layers in late October likely reflects the losses from the intense early October bloom.

4.2 Annual Nutrient Cycle in Massachusetts and Cape Cod Bays

The annual nutrient cycle in Massachusetts and Cape Cod Bays was examined using both nutrient vs. depth plots and nutrient vs. nutrient plots for all nearfield and farfield stations. In order to distinguish regional concentration differences and processes, the data were plotted using different symbols for each of six regions: Boundary, Cape Cod Bay, Coastal, Harbor, Nearfield, and Offshore (see Figures 2-1 and 2-2). The data were not averaged because of the large differences between stations within each of the areas.

The different regions often act as semi-independent or independent systems with regards to temporal and spatial variability of nutrient concentrations as well as other parameters. Only a few of the nutrient vs. depth plots (available comprehensively in Cibik *et al.*, 1998a & b) are presented here to make specific points about regional processes and differences (Figures 4-15 to 4-22). It is important to note that sampling of the entire bay occurred only six times during the year.

4.2.1 Regional Nutrient Variability with Depth

Within the Massachusetts Bays system, nutrient levels change over an annual cycle due to different biological regimes and different nutrient sources within various sub-areas. During 1997, as in previous years, several trends were apparent. In early February (W9701), nutrient concentrations were relatively high in most regions of Massachusetts Bay (Figures 4-15 to 4-17). During survey W9701, all nutrients were somewhat lower in the deeper waters compared to 1996 with the exceptions that all nutrient levels were slightly higher in the Harbor area. Cape Cod Bay showed concentrations of nitrate + nitrite and silicate just slightly lower than the other regions, due to earlier initiation of the late winter bloom (Section 8.1). The elevated nutrient concentrations in the Harbor were associated with lower salinity water. These higher concentrations of nutrients, especially ammonium and phosphate, can typically be used as markers to track plumes of harbor water.

For the farfield surveys W9702, W9704, W9707, W9711, and W9714, only the DIN vs. depth plots are shown (Figures 4-18 to 4-20). By late February (W9702), the late winter bloom had started in much of Massachusetts Bays and nutrient concentrations had begun to decrease regionally (Figure 4-18a). There was also more scatter in nutrient concentrations due to different timings of the onset of the spring bloom in the different regions. Thus

DIN values were lowest in the Cape Cod Bay and the nearfield while concentrations were at intermediate levels in the Offshore and Coastal areas and still high in the Harbor and adjacent stations. The relative distributions of phosphate and silicate were similar to DIN (not shown). BioSi values, which were initially around 2μM, began to decrease in eastern Cape Cod Bay while increasing in other regions as a spring diatom bloom began to spread throughout the system (Figure 4-21a).

By April (W9704), vertical gradients were developing in DIN concentrations in the deeper water regions (Figure 4-18b). DIN levels were higher in the bottom versus surface layers, but bottom concentrations had declined to about 30-60 percent of their winter values (W9701). DIN values from the surface down to 20-30m in depth were depleted to less than 5 μM, except for some Harbor and Coastal stations where levels remained slightly higher (due to ammonium). Again, the spatial and temporal patterns for phosphate and silicate were similar to DIN. BioSi values (Figure 4-21b) had nearly doubled compared to their early February concentrations especially in the Harbor and Coastal regions. The observed reductions in concentrations of all nutrients during W9704, as well as high BioSi concentrations, are consistent with the observed widespread diatom bloom (Sections 7.1 and 8.1).

By June (W9707), surface DIN concentrations were highly depleted compared to April, though a couple of Harbor and Coastal stations had slightly elevated concentrations due to nearshore inputs (Figure 4-19a). In contrast, nearfield bottom waters showed higher DIN values than in April (~7-9 μM), approaching winter levels. Bottom water DIN concentrations in the Boundary and Offshore areas nearly doubled as nitrate + nitrite was regenerated. Silicate and phosphate distributions (not shown) were similar to DIN, also nearly doubling in the deeper waters especially in the boundary and offshore regions.

In August (W9711), surface DIN concentrations in the nearfield were still low and similar to the concentrations in June (Figure 4-19a and b). However, there was increased scatter due to higher levels in the Coastal and Harbor stations. Concentrations of DIN in the deeper waters changed little from the June sampling. Deep-water concentrations of phosphate and silicate (not shown) showed similar trends to the DIN, except that concentrations of silicate in the bottom water below 40 m were quite variable (5-13μM). Although BioSci concentrations in the nearfield were quite low, concentrations in the harbor areas were the highest observed during the year for all of Massachusetts Bay (Figure 4-22a and b).

The October survey (W9714) indicated that DIN concentrations in surface waters (top 10m) remained low at all of the nearfield stations. In contrast, the Harbor and Coastal stations showed elevated DIN concentrations (8-17 μM) due to the increased influence of coastal sources of ammonium and nitrate + nitrite (Figure 4-20a). There was also evidence of coastal upwelling during the period, which may have contributed to elevated nutrients in surface water (Section 3). In the mid-depth and bottom waters, DIN concentrations were highly scattered. The bottom layer DIN concentrations for the Boundary and Offshore areas were the highest observed during the entire year.

Phosphate during early October (not shown) was also high in the Harbor and Coastal surface water (1-1.5 μM), though it remained relatively low in most of the other areas. Silicate concentrations (also not shown) were generally low in the surface waters with slightly higher concentrations found at the Harbor and Coastal stations.

Concentrations of phosphate and silicate in the bottom layers were quite scattered following the same trends as DIN concentrations. The increase in BioSi values throughout the region indicated a fall bloom dominated by diatoms. The increase was most noticeable in the nearfield and in the Harbor and Coastal regions (Figure 4-22b).

Although the winter nutrients survey in December (W9717) was not as comprehensive as typical farfield surveys, samples were collected in several of the regions around the nearfield. The water column was unstratified and DIN concentrations (mainly nitrate + nitrite) were found to have increased to winter levels of 7-15 μM. Near-surface water concentrations in the harbor and adjacent stations were also quite elevated (Figure 4-20b). The distribution trends of phosphate (not shown) were similar to DIN showing the same surface increases, while silicate was relatively uniform throughout the water column (7-11 μM).

While overall trends in nutrient levels in Cape Cod Bay generally were similar to the rest of the stations there were some notable exceptions. In early February, nitrate + nitrite and silicate concentrations were lower in Cape Cod Bay than in the rest of Massachusetts Bay due to the early onset of the late winter bloom. Although a few near-bottom samples had relatively high silicate values in October (W9714), they were similar in concentration to many stations in the nearfield area and thus did not appear to be unusually high as has been reported in different years by Becker (1992) and Coniaris and Loder (unpublished data).

4.2.2 Nutrient vs. Nutrient Relationships

Nutrient relationships were investigated by comparing nutrient concentrations in each sample (Figures 4-23 through 4-26). Nutrient ratios relating nitrogen to phosphorus (N:P) and nitrogen to silica (N:Si) are useful in determining nutrient limitation of phytoplankton growth. Plots of these nutrient relationships can also be used to identify water masses and provide insights into nutrient sources and removal processes. Using these plots, three distinct systems, Boston Harbor-Coastal, Massachusetts Bays (Nearfield, Offshore, and Boundary), and Cape Cod Bay become evident during certain times of the year.

Surveys during early-February, late February, and early April (surveys W9701-W9704) all showed similar trends with respect to dissolved inorganic nitrogen (DIN) and phosphate, although the overall concentrations were declining. In early February, DIN:DIP ratios were ~10:1 to 14:1 for most of Massachusetts Bays, while the Harbor and adjacent stations exhibited slightly higher ratios due to enrichment of nitrogen from coastal sources (Figure 4-23a). Eastern Cape Cod Bay data were slightly set apart (lower values) from the rest of Massachusetts Bays, indicating earlier uptake activity by the phytoplankton community.

In late February (W9702), the overall concentrations had decreased from the previous survey. The DIN:DIP ratios also decreased slightly (Figure 4-23b), while DIN:Si ratios began a subtle divergence indicating the beginning of two water masses with different characteristics (Figure 4-24b). During this period, the higher DIN:Si water of the Harbor and Harbor-influenced stations, and lower DIN:Si water of the Boundary area mixed with the water in the nearfield region, creating the bifurcated distribution of these properties. Most of the Harbor and Harbor-influenced stations had DIN:Si ratios well above 1:1, while most of Cape Cod Bay exhibited ratios below 1:1 due to depletion by the late winter diatom bloom, with the DIN:Si removed at about a 1:1 ratio.

In early April (W9704), the DIN and phosphate data were tightly clustered with the DIN:DIP ratios for the nearfield scattering about a 16:1 trend line. Most of the Harbor samples fell outside the cluster indicating they were relatively enriched in DIN (Figure 4-23c). The DIN and silicate concentrations were low and relatively scattered (Figure 4-24c).

During the summer months (i. e. W9707 in June) there was a wide range of concentrations of DIN and phosphate, though the data fell in a tight line with a slope of about 16:1. There was a decrease in slope below a phosphate concentration of about 0.4 μM (Figure 4-25a), and data were tightly clustered indicating that as the nitrogen was used up, there is still residual phosphate in the water column. This situation continued throughout the summer, with the DIN:DIP ratios for the nearfield scattering about a 16:1 trend line.

During the October survey (W9714), the DIN and phosphate concentrations continued to co-vary, with a ratio of about 16:1 throughout most of Massachusetts Bay. However, at high concentrations there was some divergence between the Harbor samples and the Offshore and Boundary samples (Figure 4-26a). Most of the nearfield DIN and silicate concentrations fell along a 1:1 trend line, suggesting equal removal rates (i.e., diatom growth). However many Coastal region and Harbor samples fell nearer a 2:1 trend line, indicating additional nitrogen uptake which was suggestive of growth of non-diatom species as well (see Section 8). The DIN:DIP distribution suggests that with complete uptake of the DIN pool, residual phosphate will remain at about 0.2-0.3 μM.

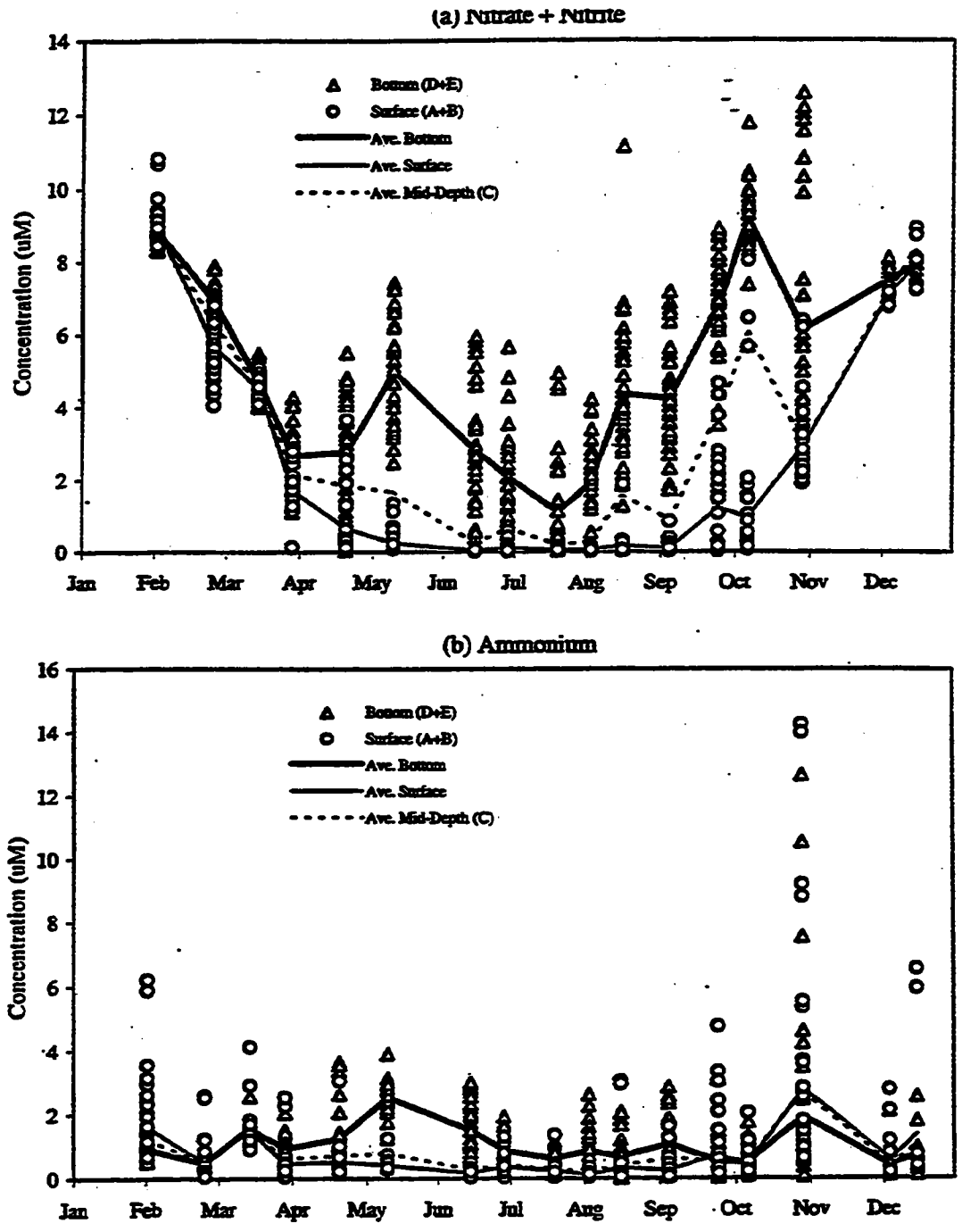

FIGURE 4-1
1997 Nearfield Nutrient Cycles
Surface, Bottom, Surface Averages, Mid-Depth Averages, and Bottom Averages
a) Nitrate + Nitrite, b) Ammonium

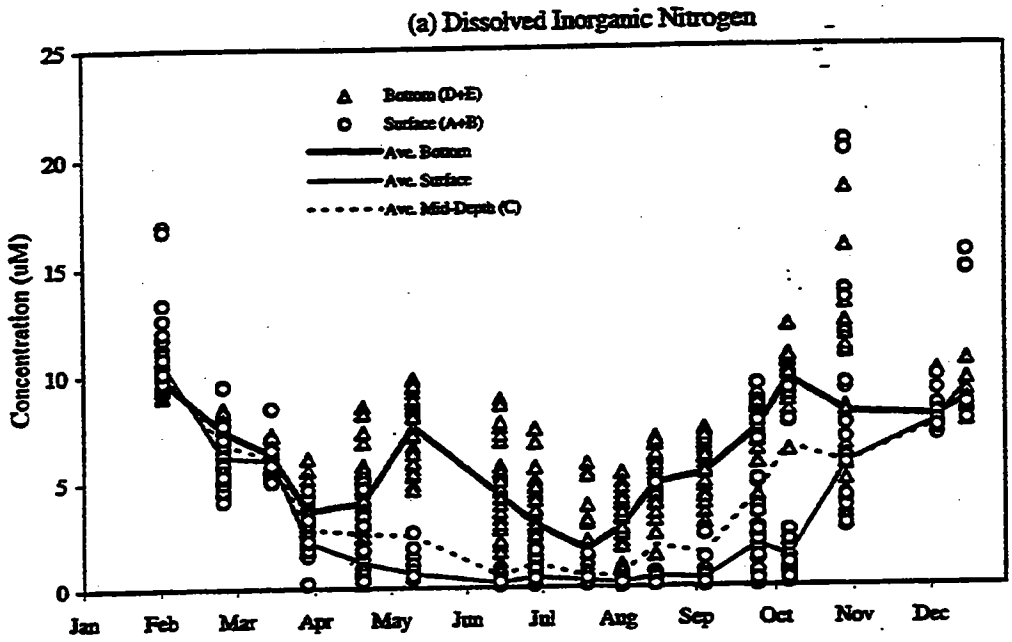

FIGURE 4-2
1997 Nearfield Nutrient Cycles
Surface, Bottom, Surface Averages, Mid-Depth Averages, and Bottom Averages
a) Dissolved Inorganic Nitrogen

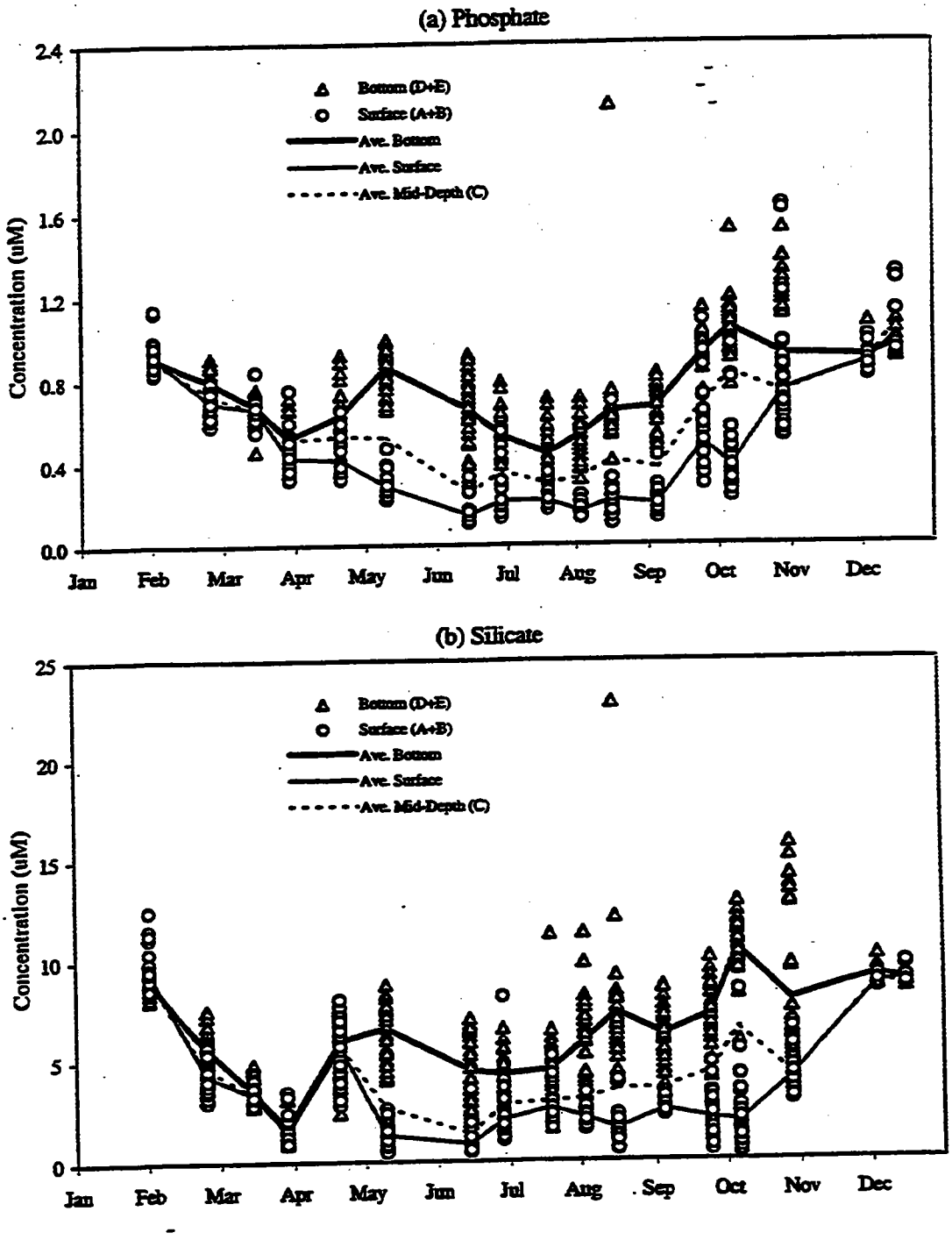

FIGURE 4-3
1997 Nearfield Nutrient Cycles
Surface, Bottom, Surface Averages, Mid-Depth Averages, and Bottom Averages
a) Phosphate, b) Silicate

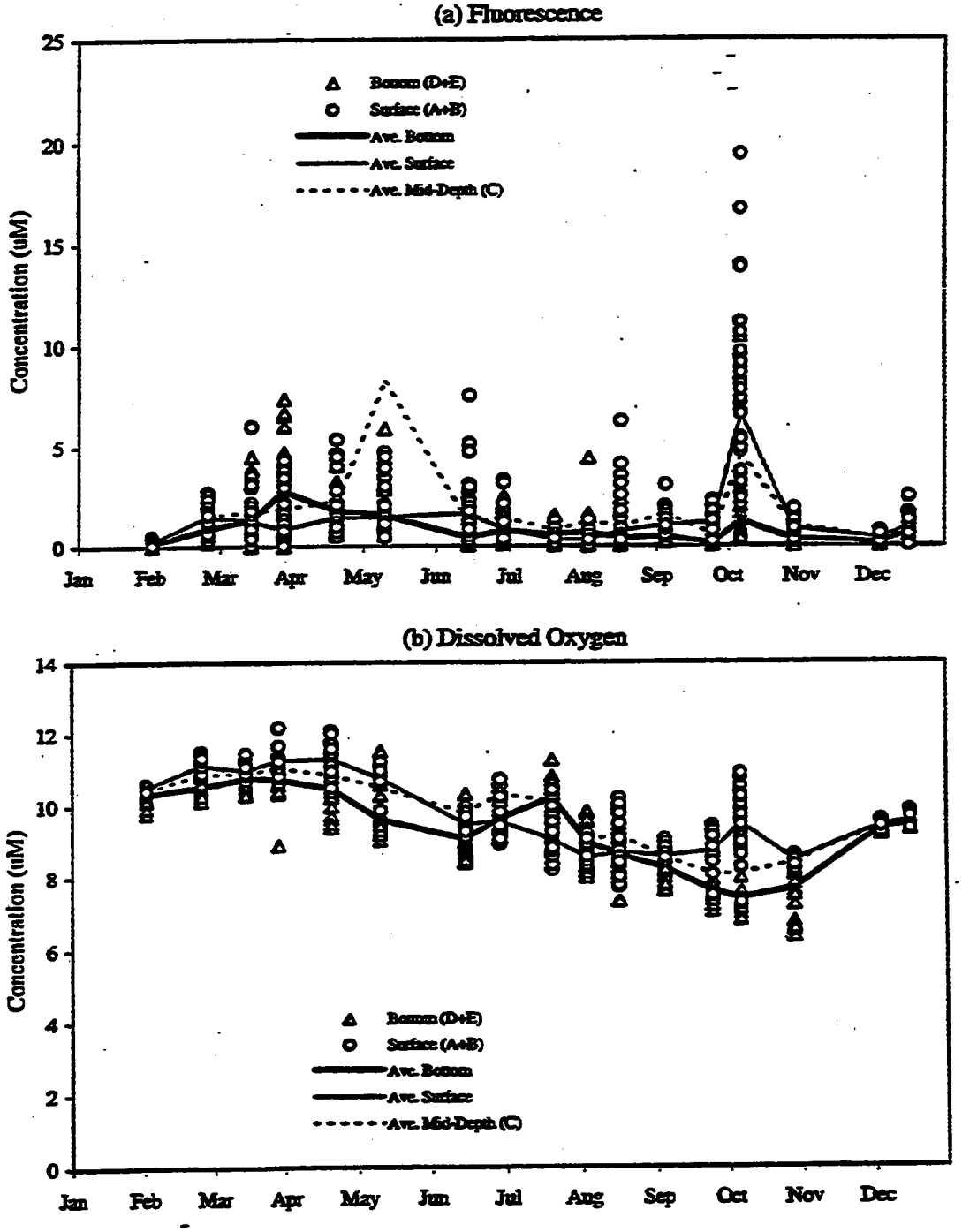

FIGURE 4-4
1997 Nearfield Nutrient Cycles
Surface, Bottom, Surface Averages, Mid-Depth Averages, and Bottom Averages
a) Fluorescence, b) Dissolved Oxygen

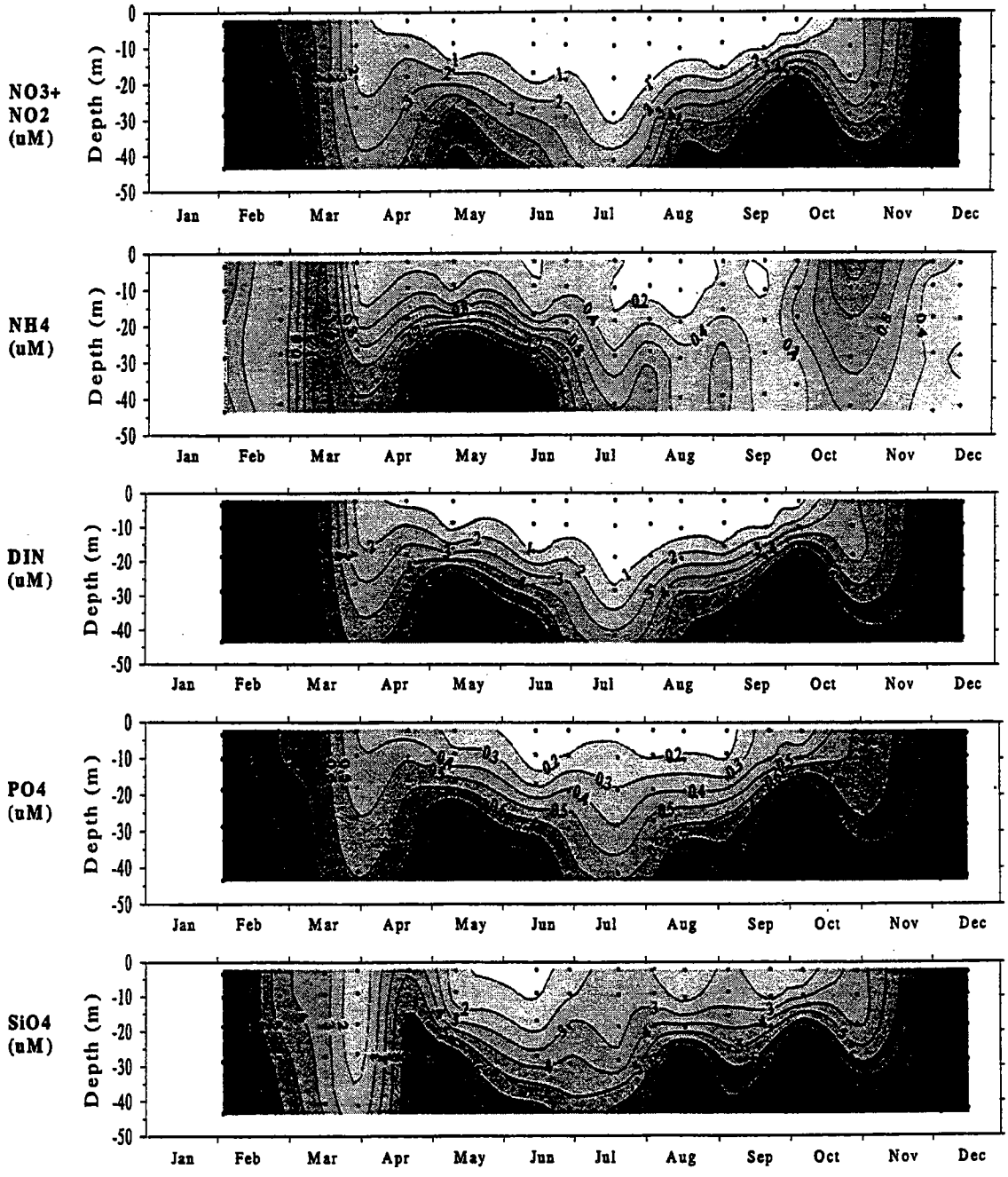

FIGURE 4-5
1997 Nearfield Averaged Nutrient Annual Parameter Distributions
Concentration/Depth/Time contours for NO3+NO2, NH4, DIN, PO4 and SiO4

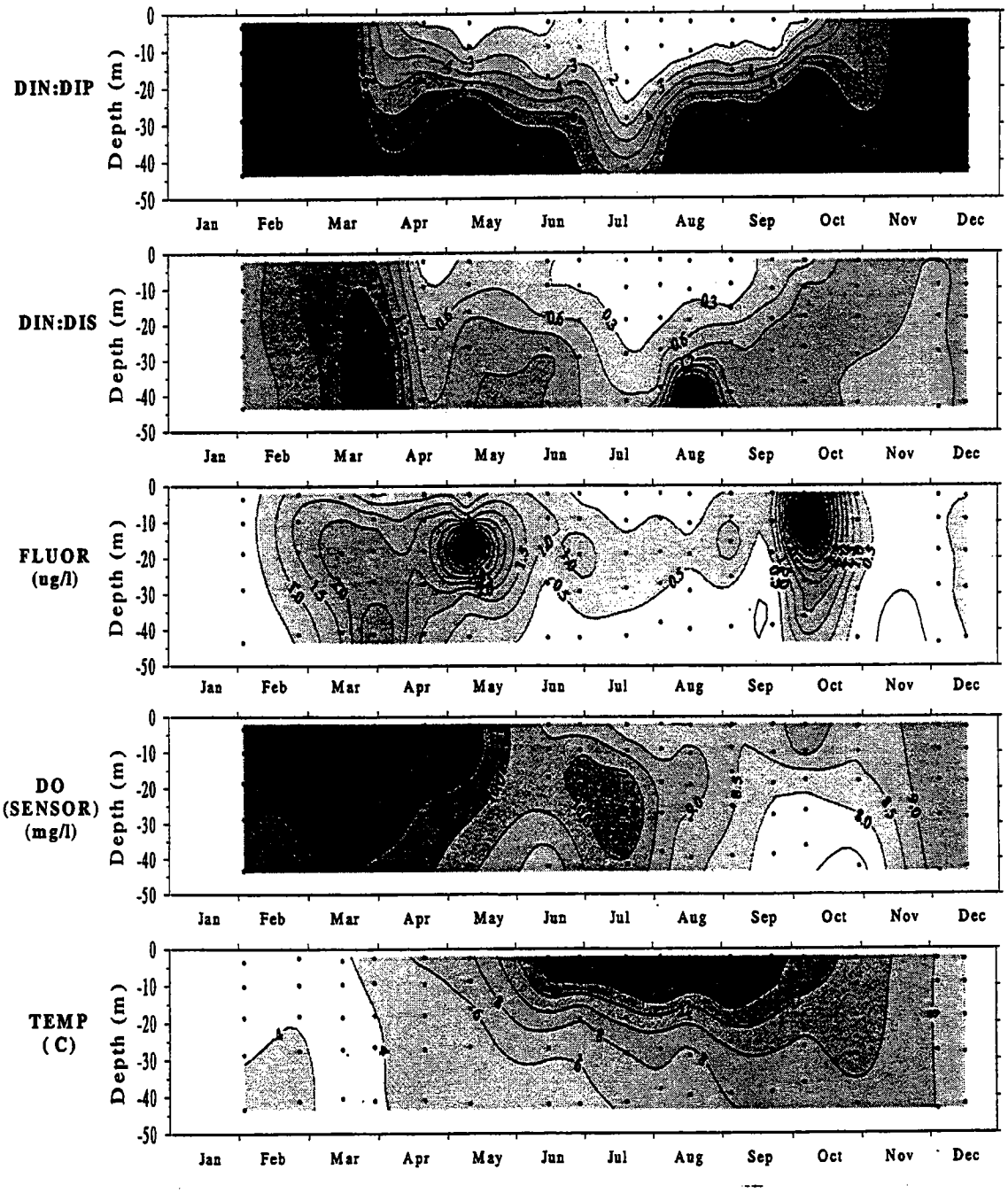

FIGURE 4-6
1997 Nearfield Averaged Nutrient Parameter Annual Distributions
Concentration/Depth/Time contours for DIN/PO4 (DIP), DIN/SiO4 (DIS),
Fluorescence, Dissolved Oxygen and Temperature

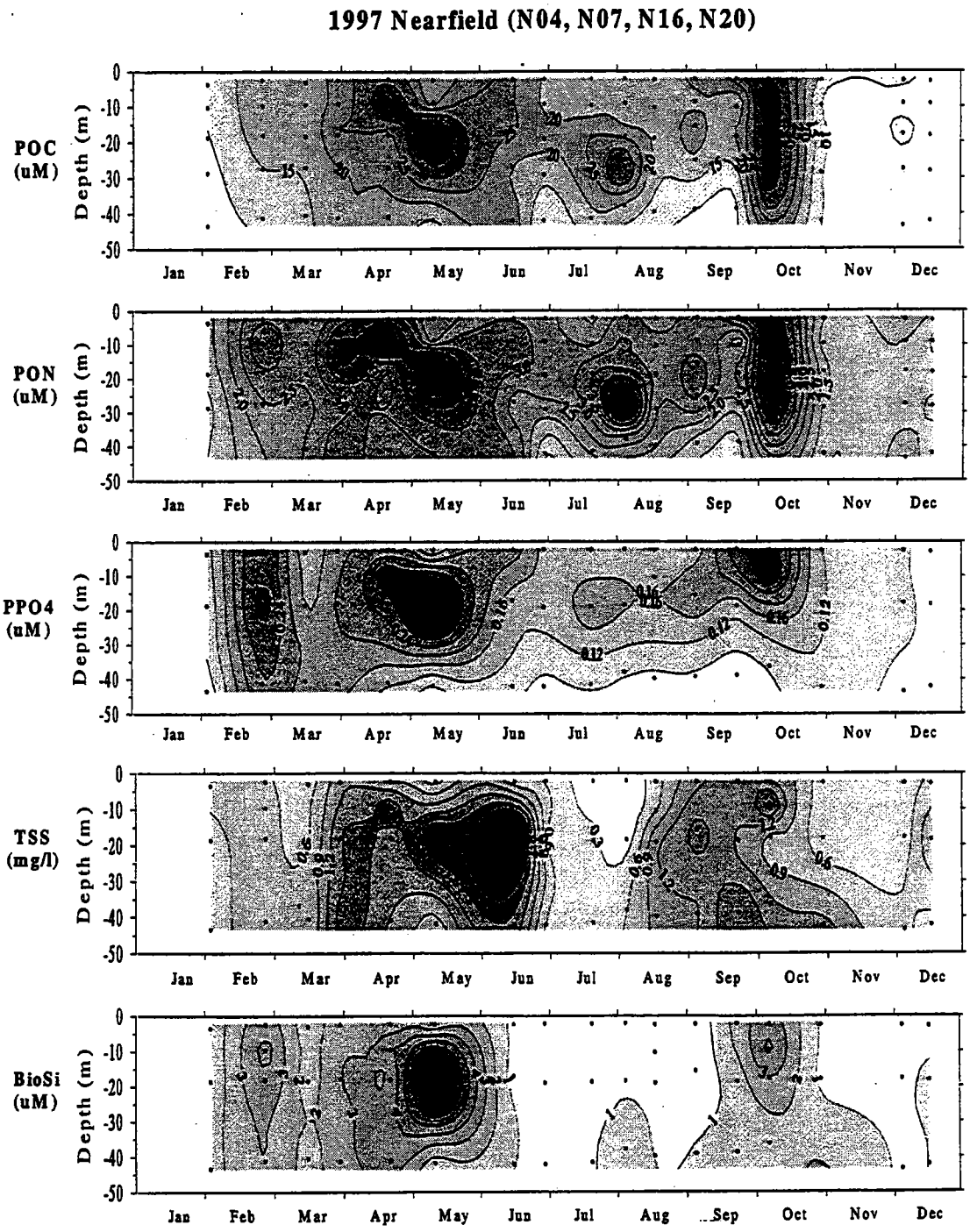

FIGURE 4-7
1997 Nearfield Averaged Particulate Nutrient Parameter Annual Distributions
Concentration/Depth/Time contours for POC, PON, PP, TSS and BioSi

1997 Nearfield (N04, N07, N16, N20)

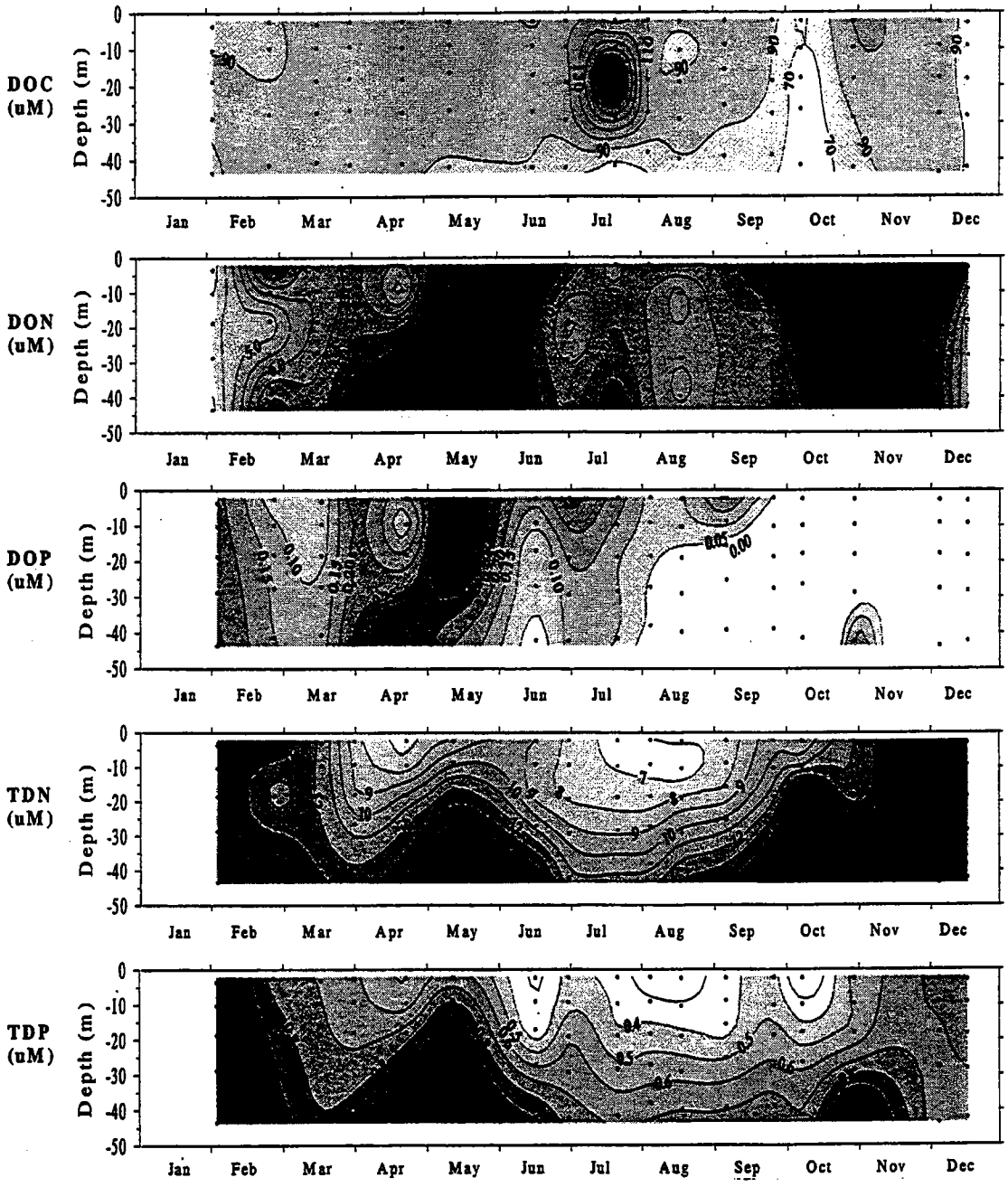

FIGURE 4-8
1997 Nearfield Averaged Dissolved Nutrient Parameter Annual Distributions
Concentration/Depth/Time contours for DOC, DON, DOP, TDN and TDP

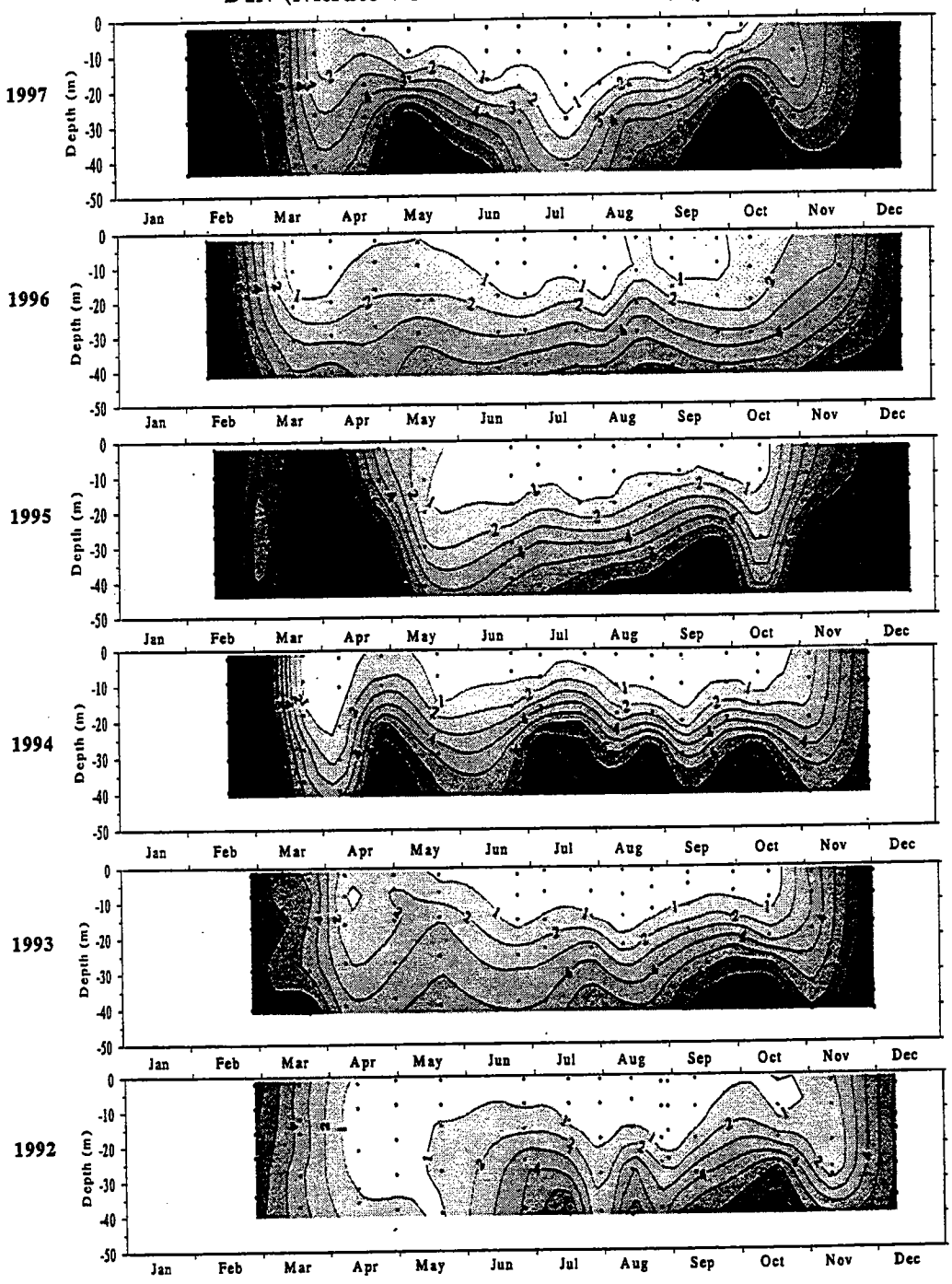

FIGURE 4-9
1992-1997 Nearfield Averaged Nutrient Annual Distributions
Concentration/Depth/Time contours for DIN

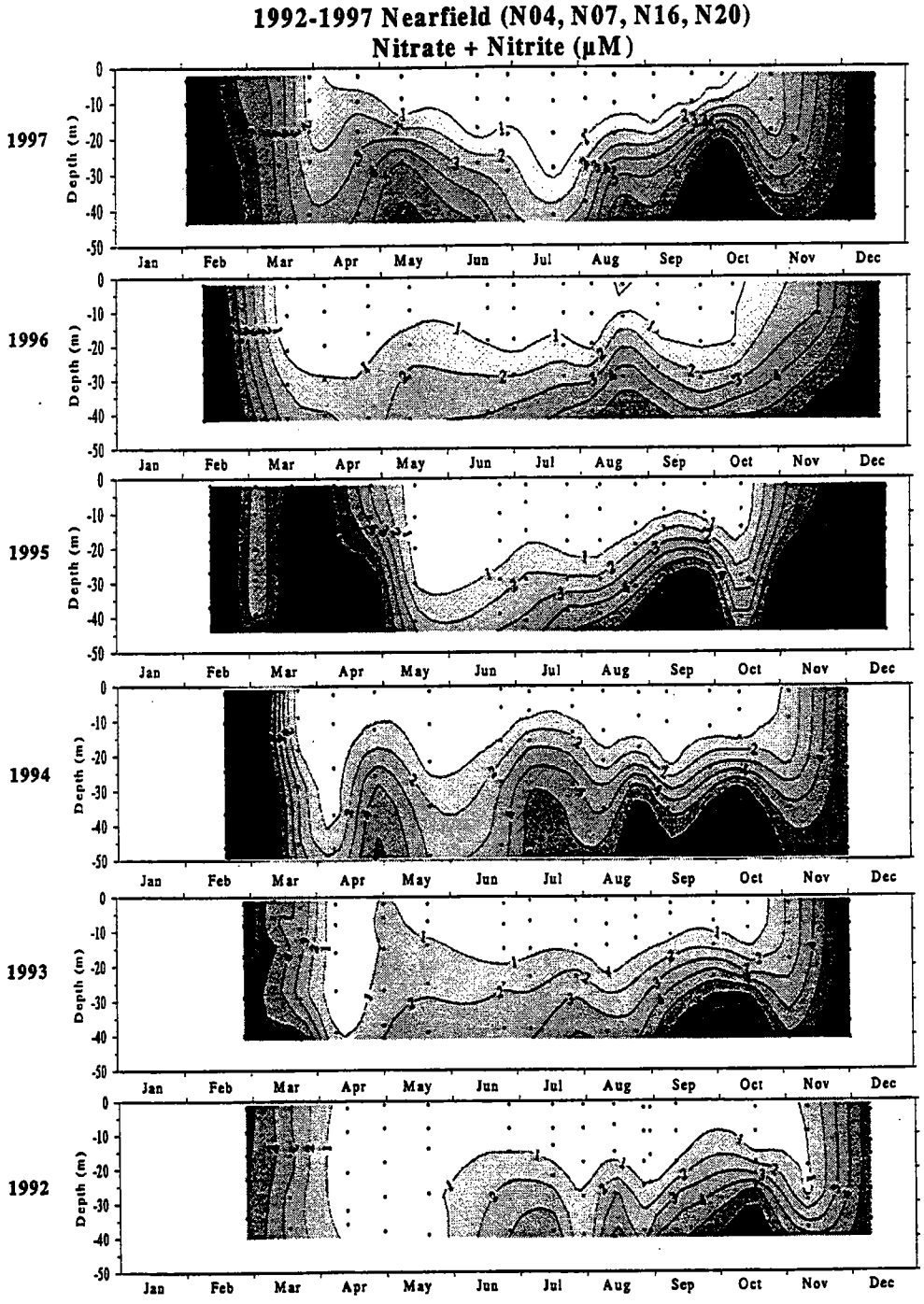

FIGURE 4-10
1992-1997 Nearfield Averaged Nutrient Annual Distributions
Concentration/Depth/Time contours for NO3+NO2

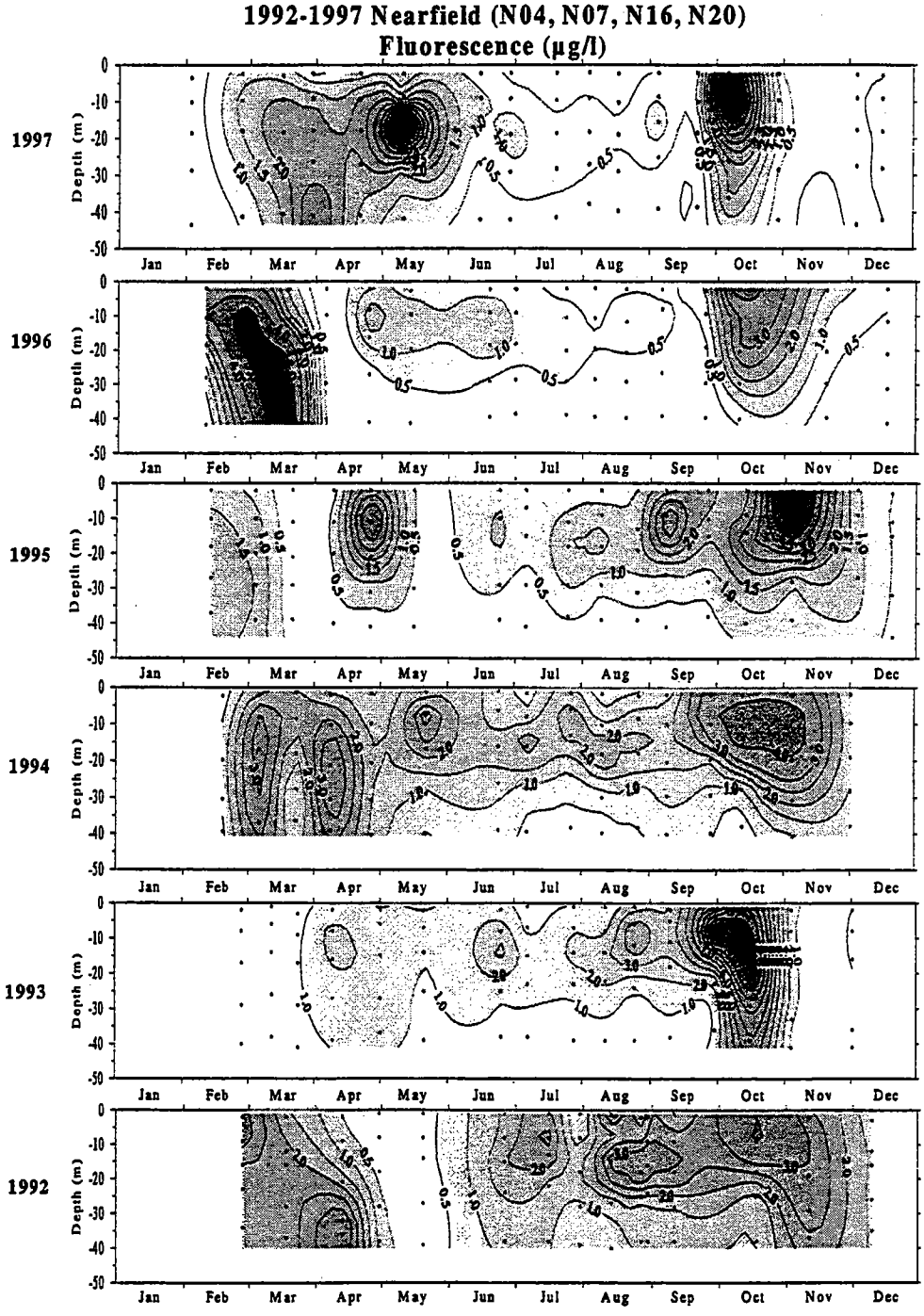

FIGURE 4-11
1992-1997 Nearfield Averaged Nutrient Annual Distributions
Concentration/Depth/Time contours for Fluorescence

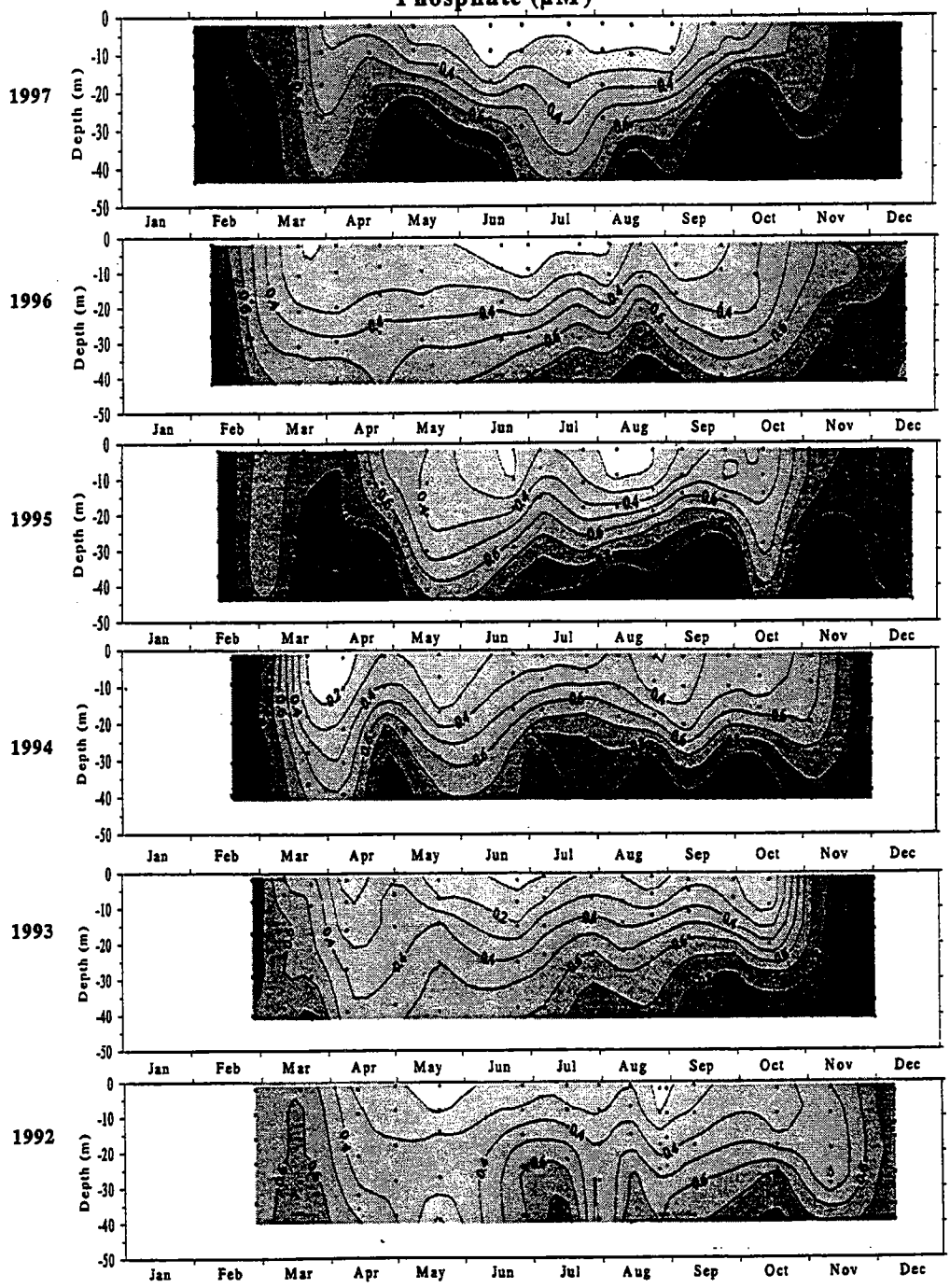

FIGURE 4-12
1992-1997 Nearfield Averaged Nutrient Annual Distributions
Concentration/Depth/Time contours for PO4

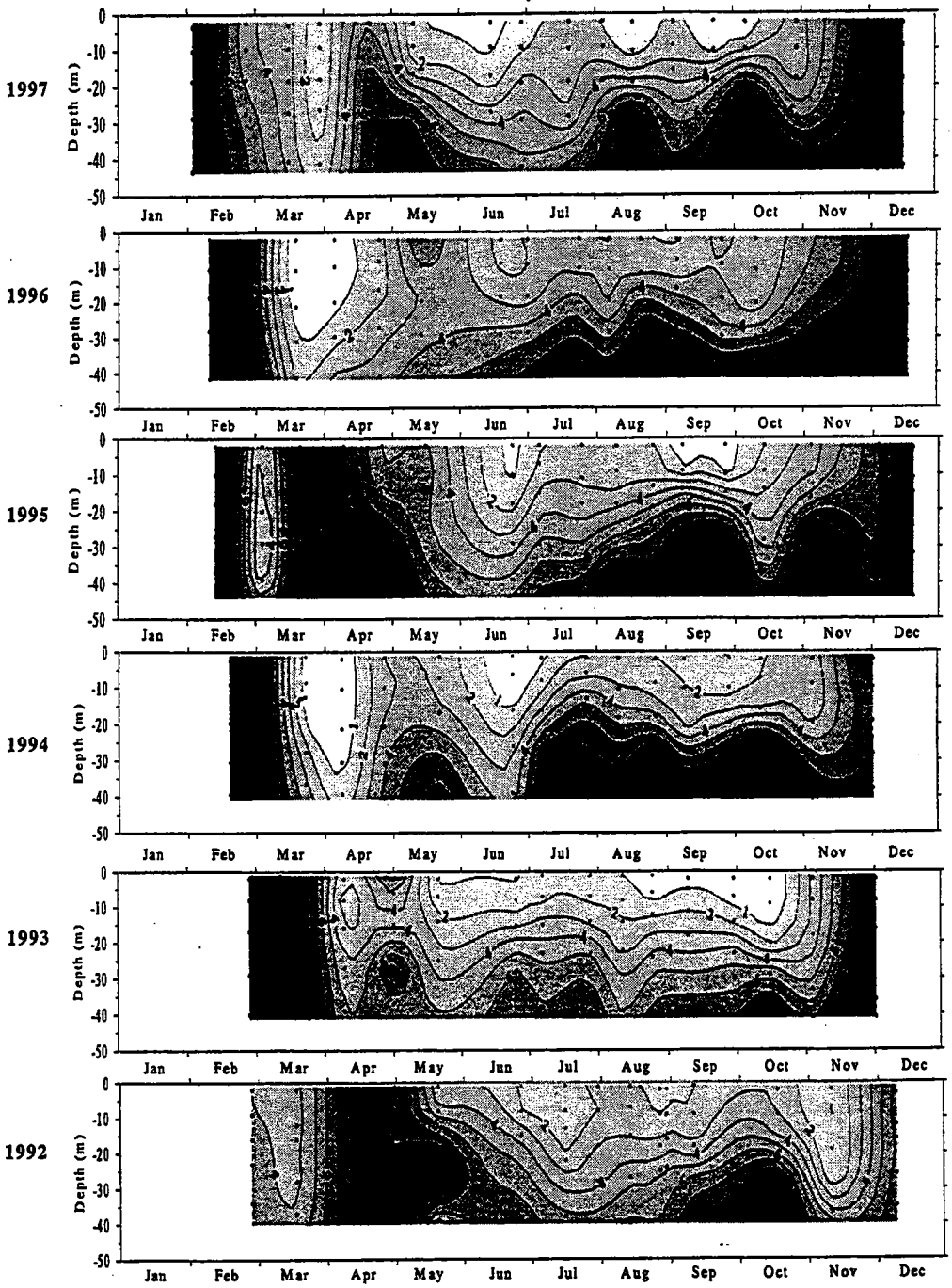

FIGURE 4-13
1992-1997 Nearfield Averaged Nutrient Annual Distributions
Concentration/Depth/Time contours for SiO4

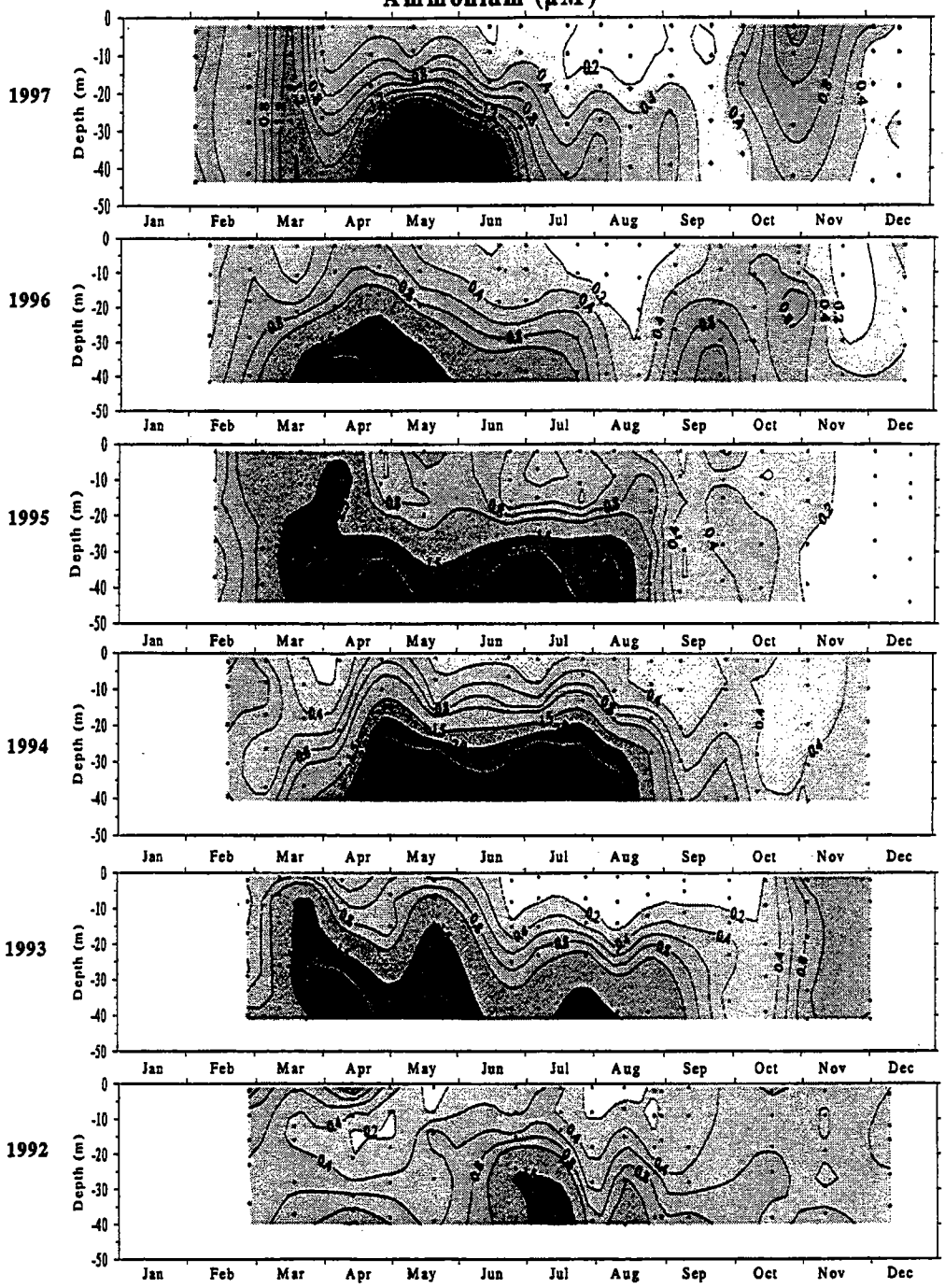

FIGURE 4-14
1992-1997 Nearfield Averaged Nutrient Annual Distributions
Concentration/Depth/Time contours for NH4

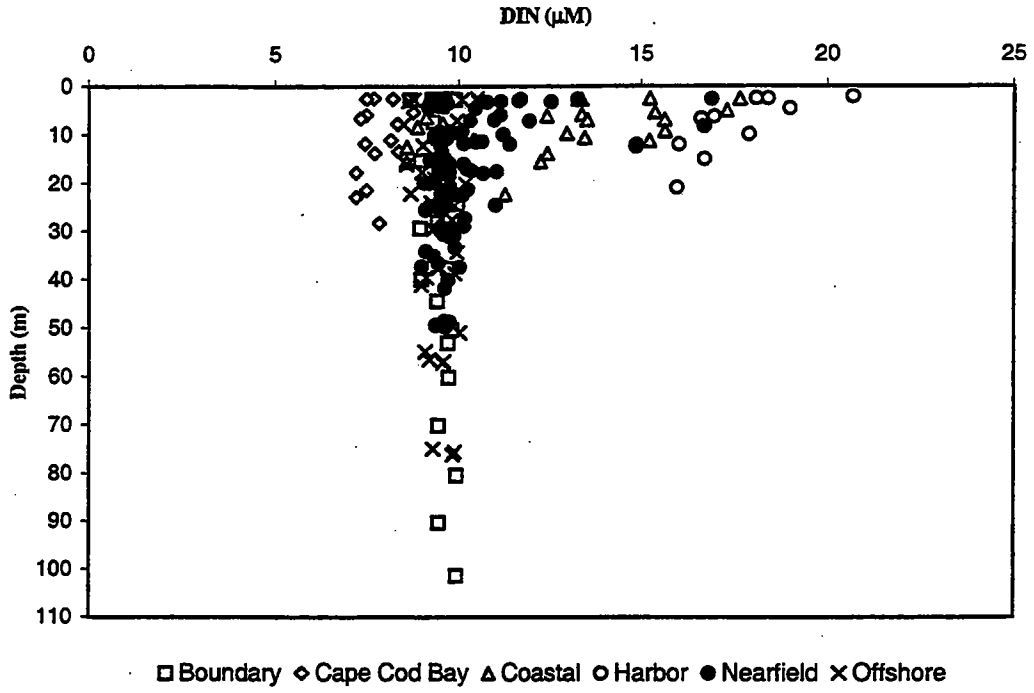

FIGURE 4-15
Depth vs. DIN concentrations for farfield survey W9701, (February 1997)

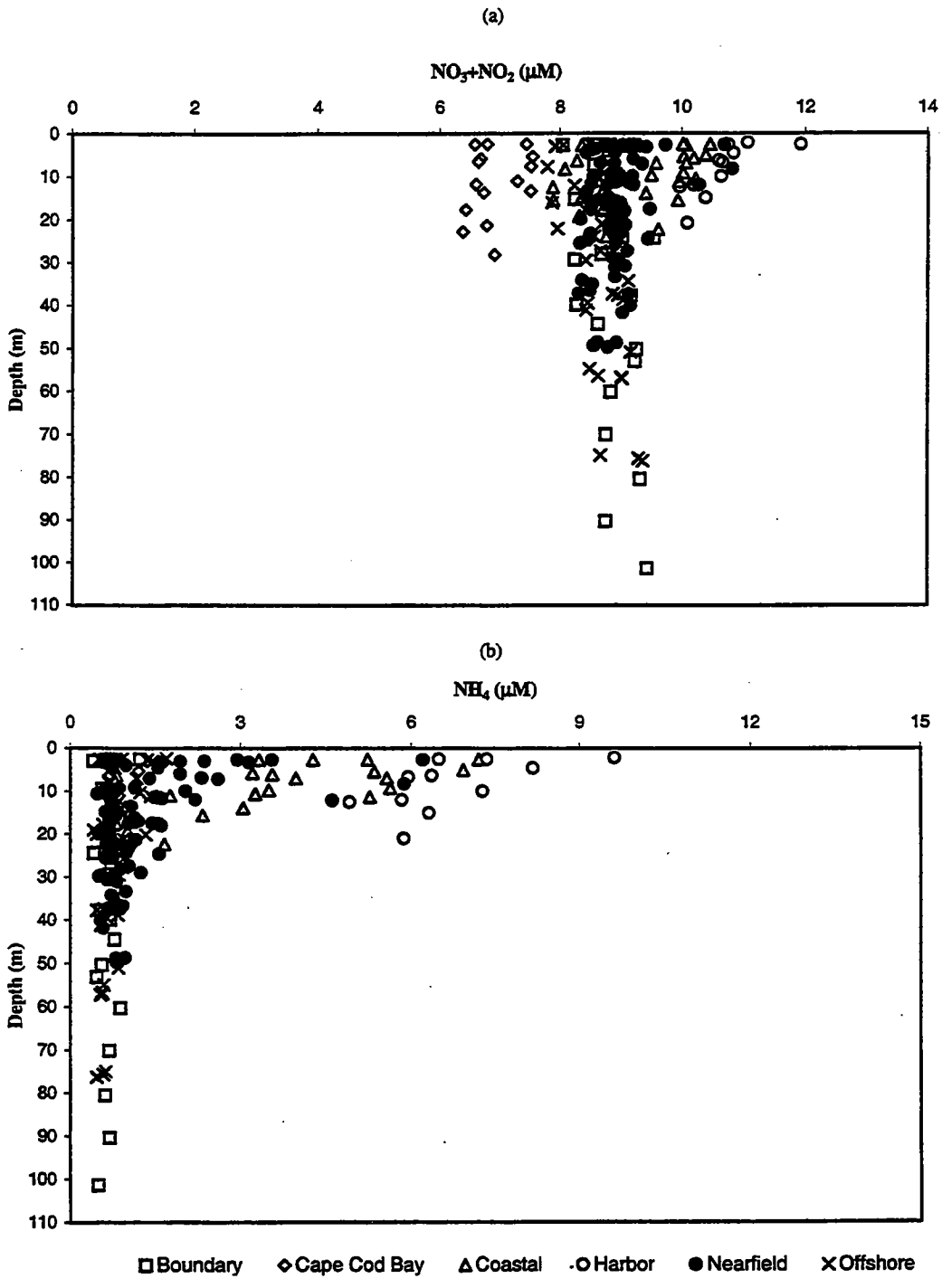

FIGURE 4-16

(a) Depth vs. NO_3+NO_2 concentrations and (b) depth vs. NH_4 concentrations for farfield survey W9701, (February 1997)

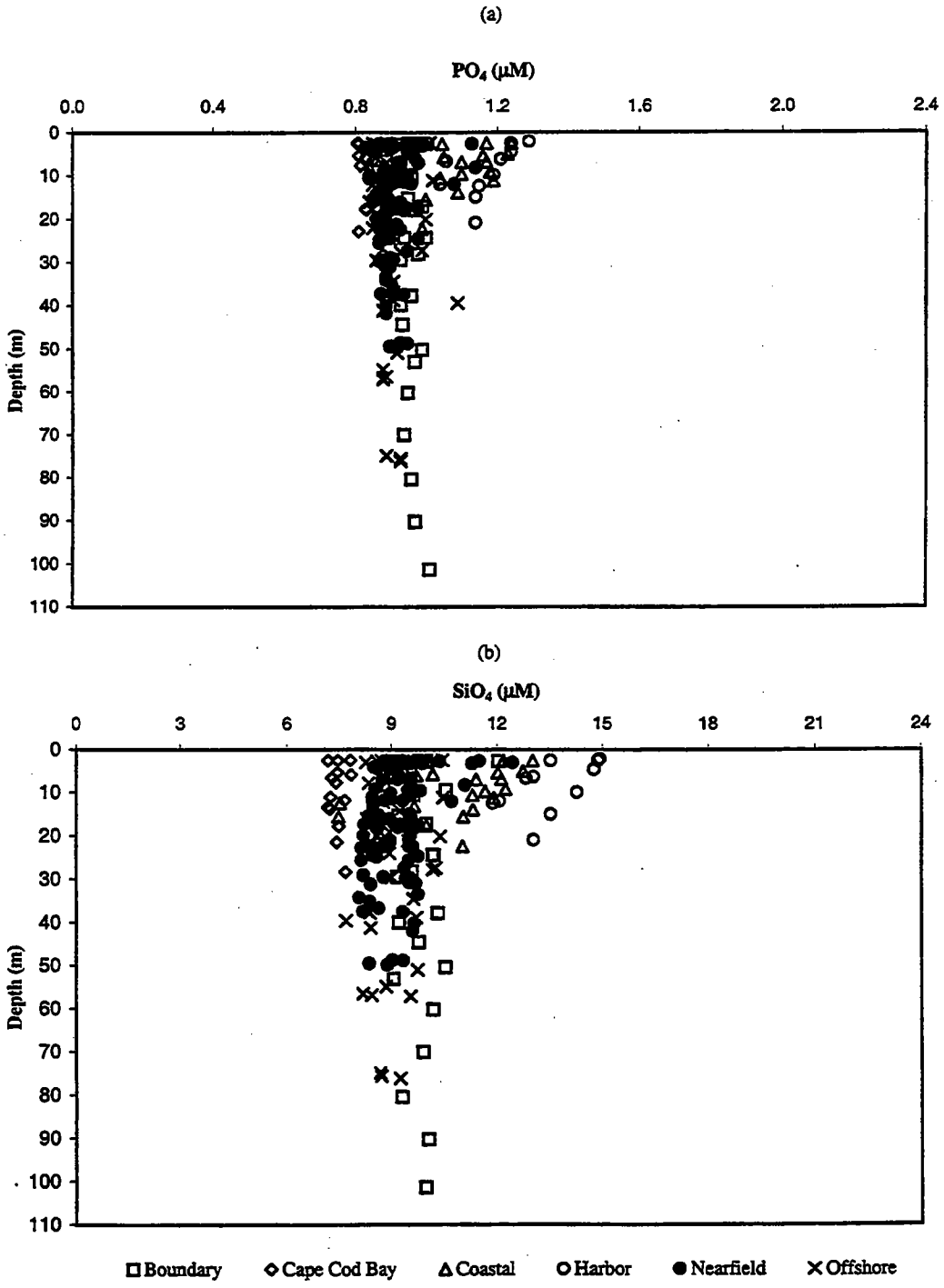

FIGURE 4-17
(a) Depth vs. PO_4 concentrations and (b) Depth vs. SiO_4 concentrations for farfield survey W9701, (February 1997)

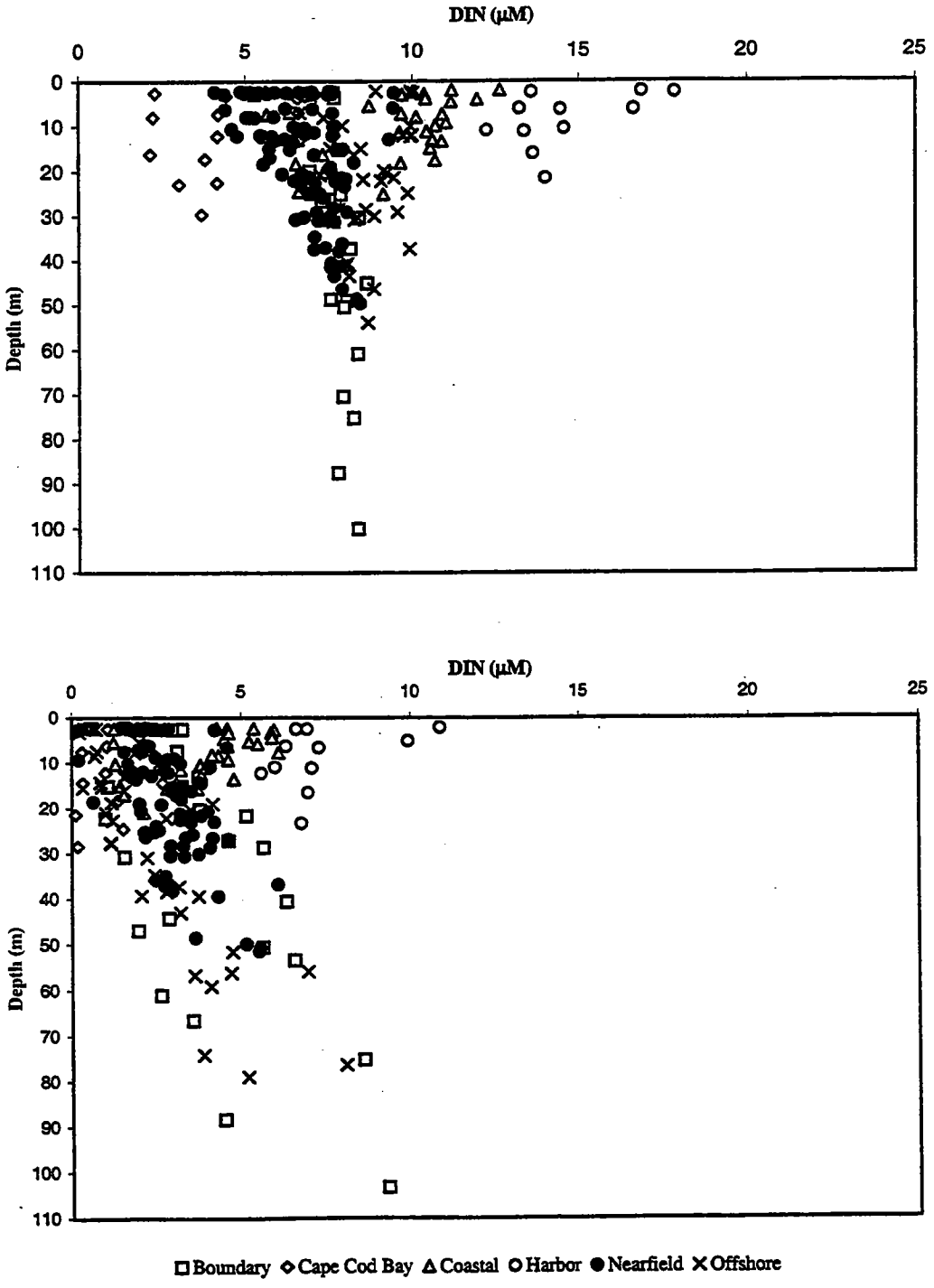

FIGURE 4-18

Depth vs. DIN concentration for farfield surveys (a) W9702, (February 1997) and (b) W9704, (April 1997)

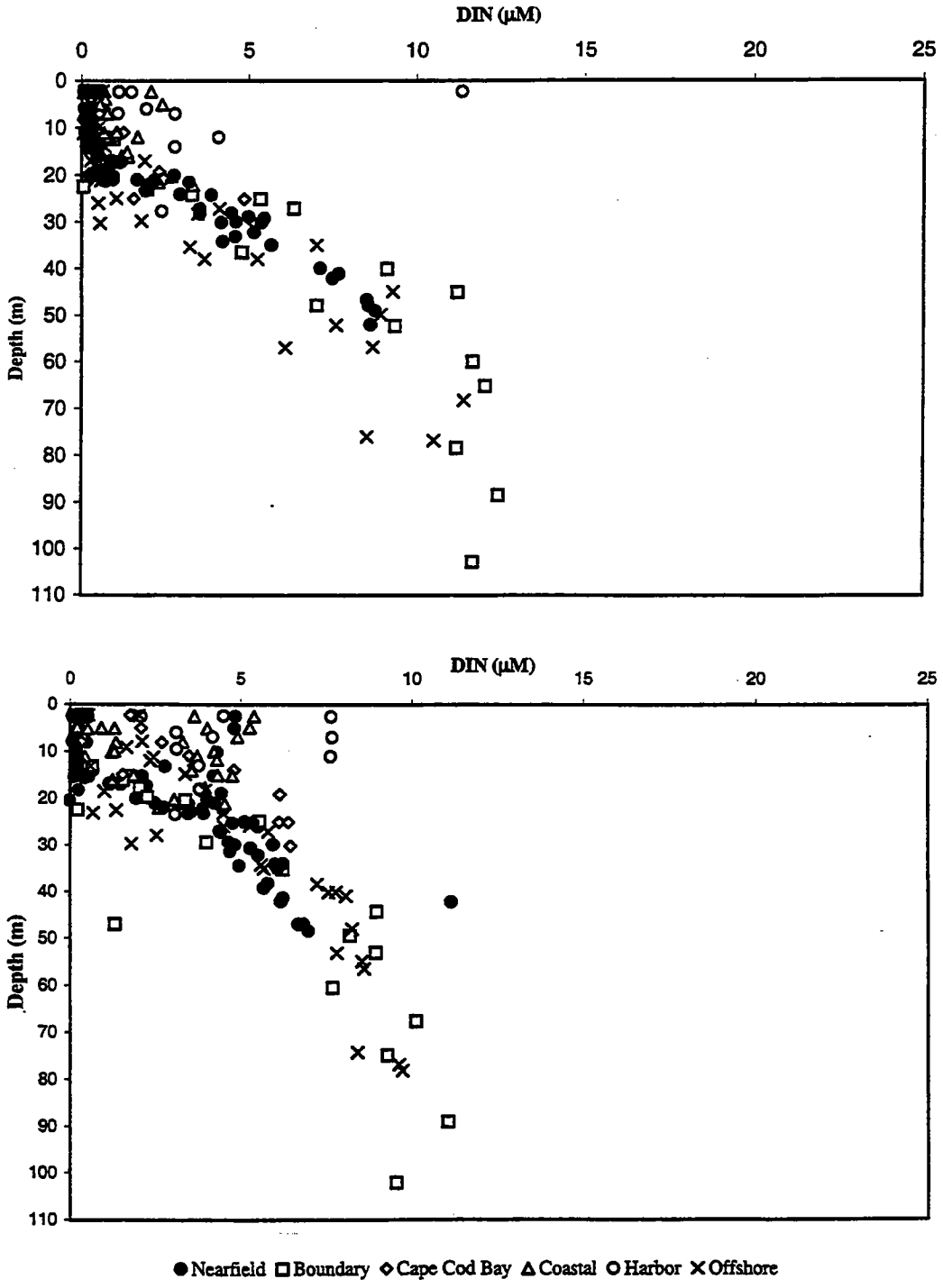

FIGURE 4-19

Depth vs. DIN concentrations for farfield surveys (a) W9707, (June 1997) and (b) W9711, (August 1997)

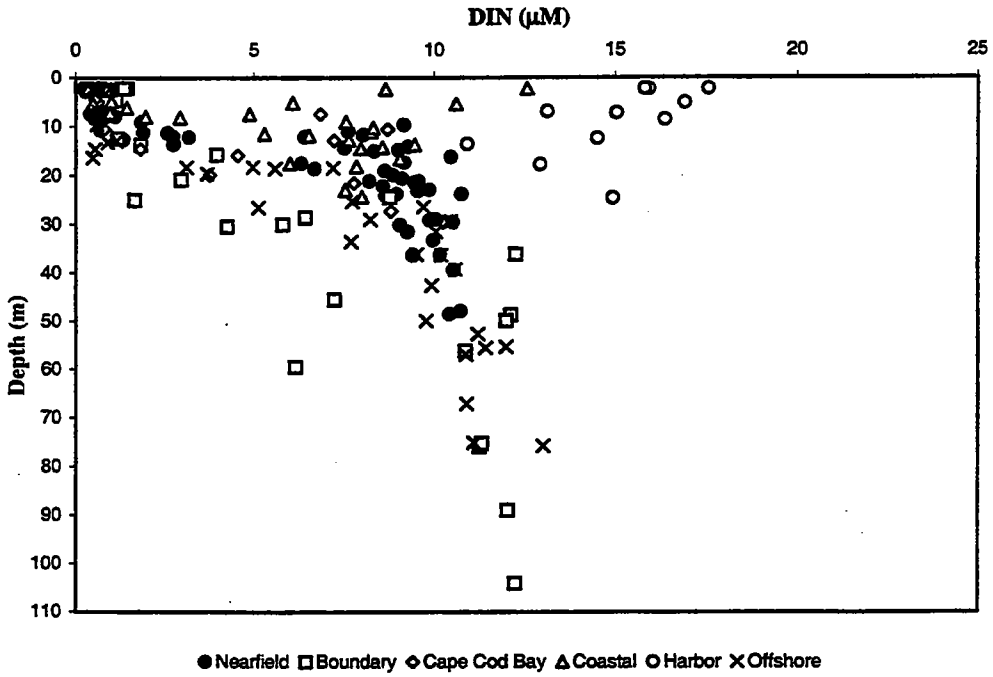

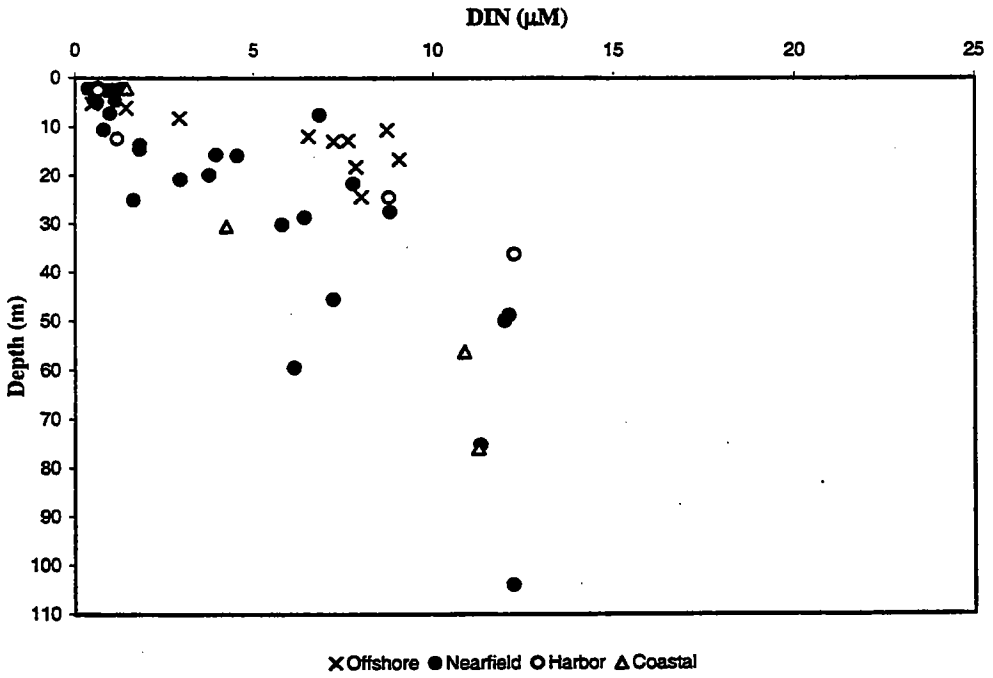

FIGURE 4-20
Depth vs. DIN concentrations for farfield surveys
(a) W9714, (October 1997) and (b) W9717 (December 1997)

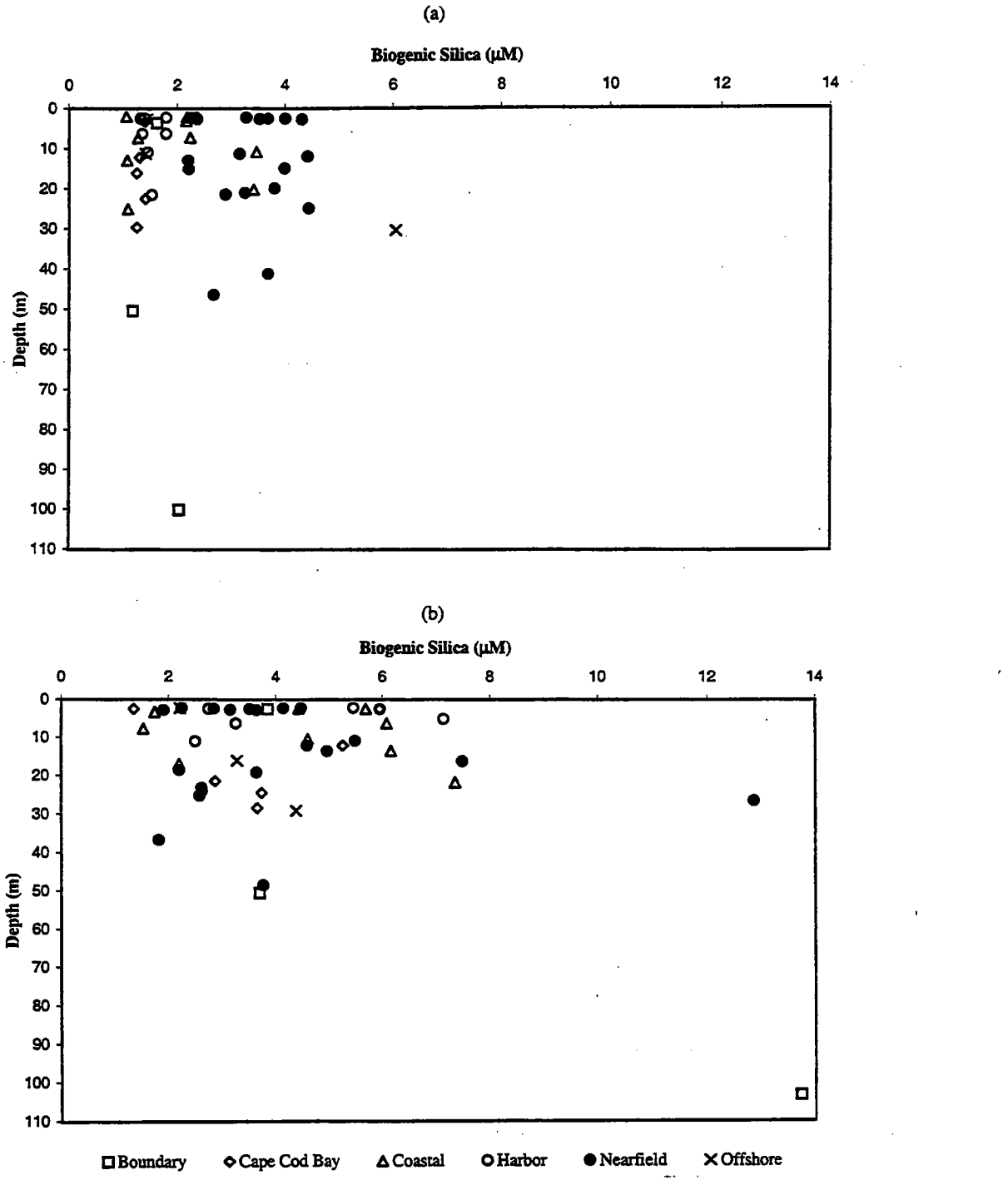

FIGURE 4-21

Depth vs. Biogenic Silica concentrations for farfield surveys (a) W9702, (February 1997) and (b) W9704, (April 1997)

(a)

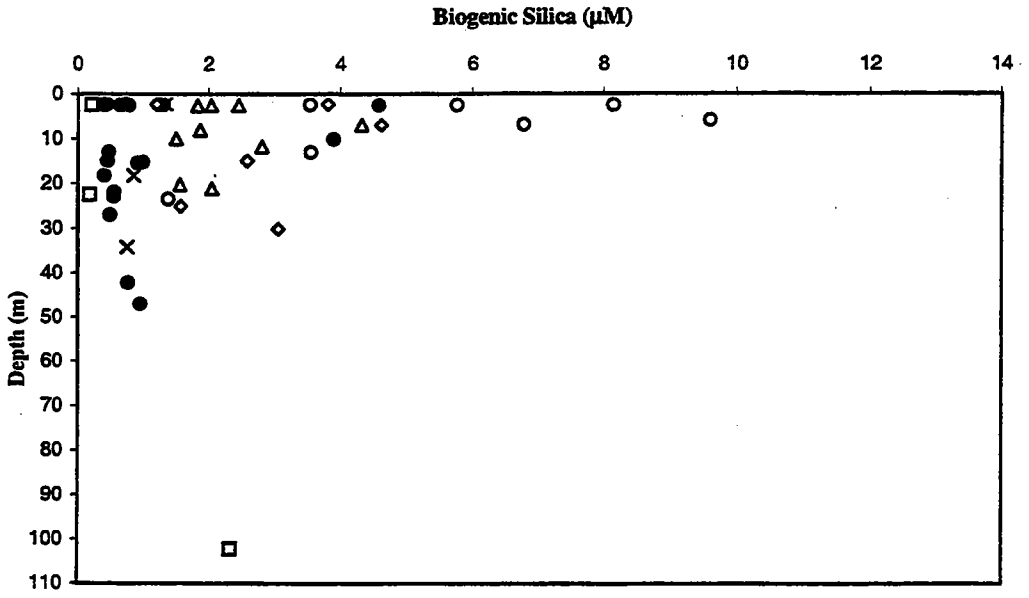

(b)

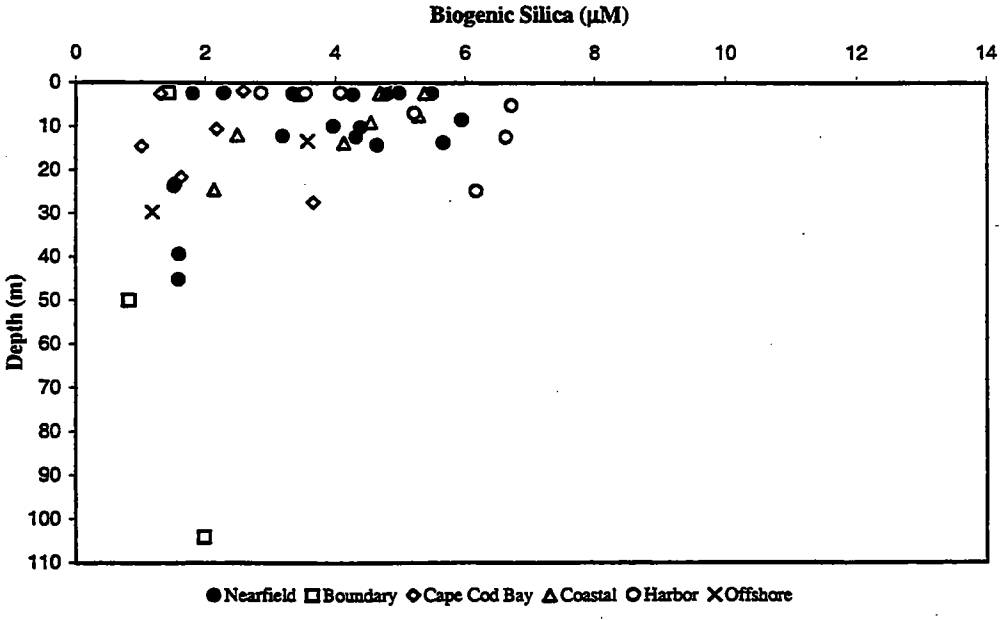

FIGURE 4-22

Depth vs. Biogenic Silica concentrations for farfield surveys (a) W9711, (August 1997) and (b) W9714, (October 1997)

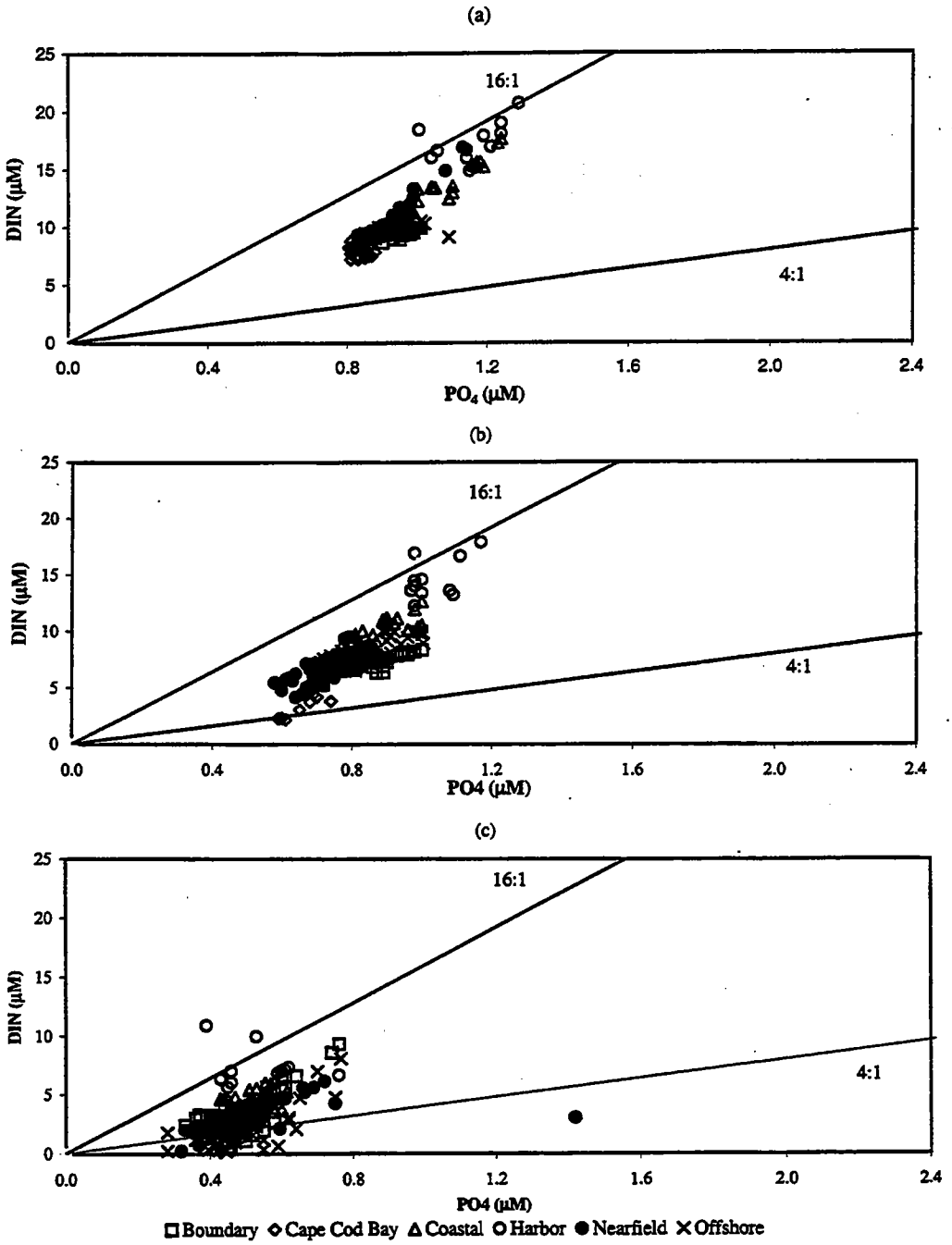

FIGURE 4-23

DIN vs. PO_4 concentrations for farfield surveys

(a) W9701, (February 1997), (b) W9702 (February 1997), and (c) W9704 (April 1997)

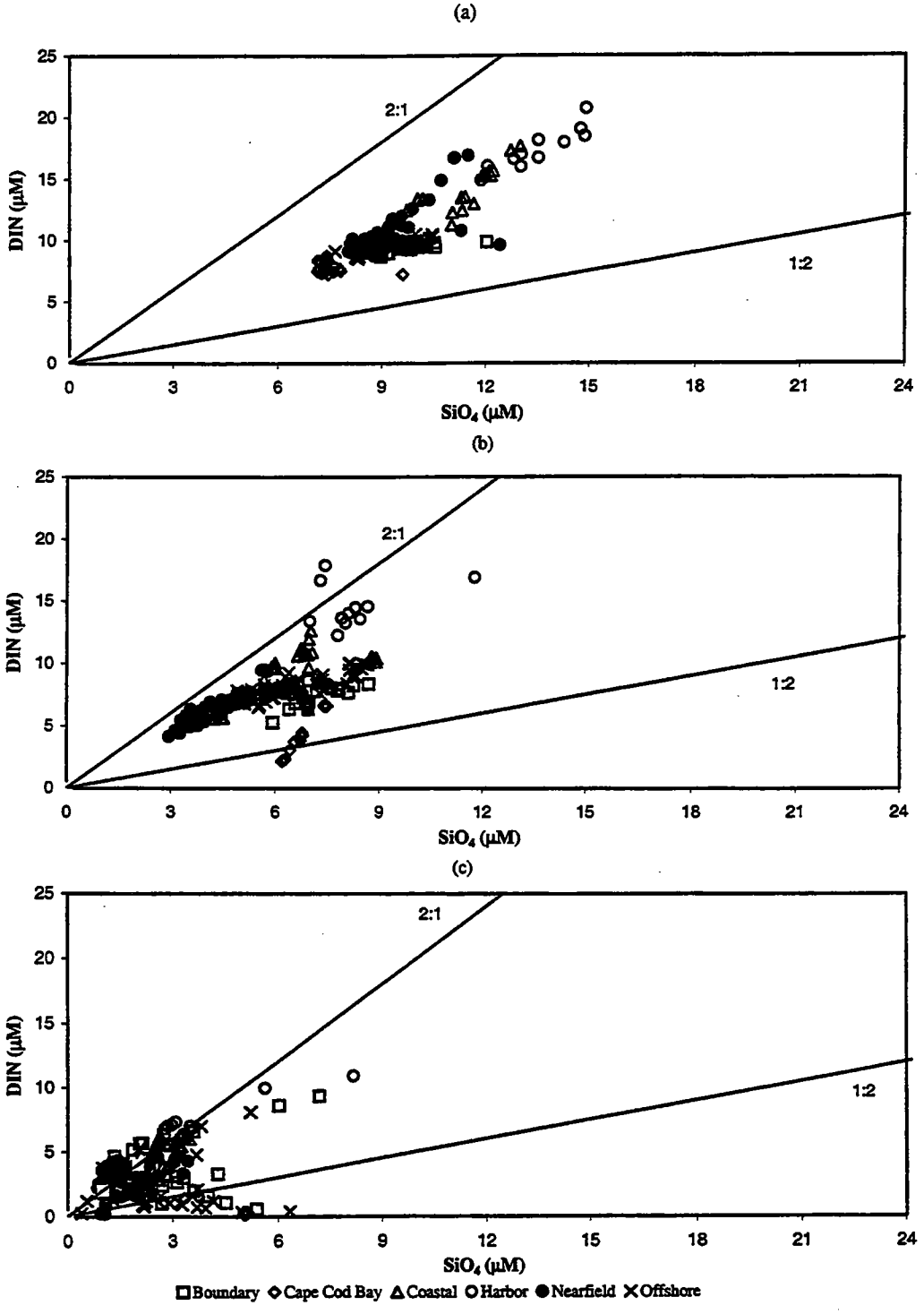

FIGURE 4-24

DIN vs. SiO_4 for farfield surveys

(a) W9701, (February 1997), (b) W9702 (February 1997), and (c) W9704 (April 1997)

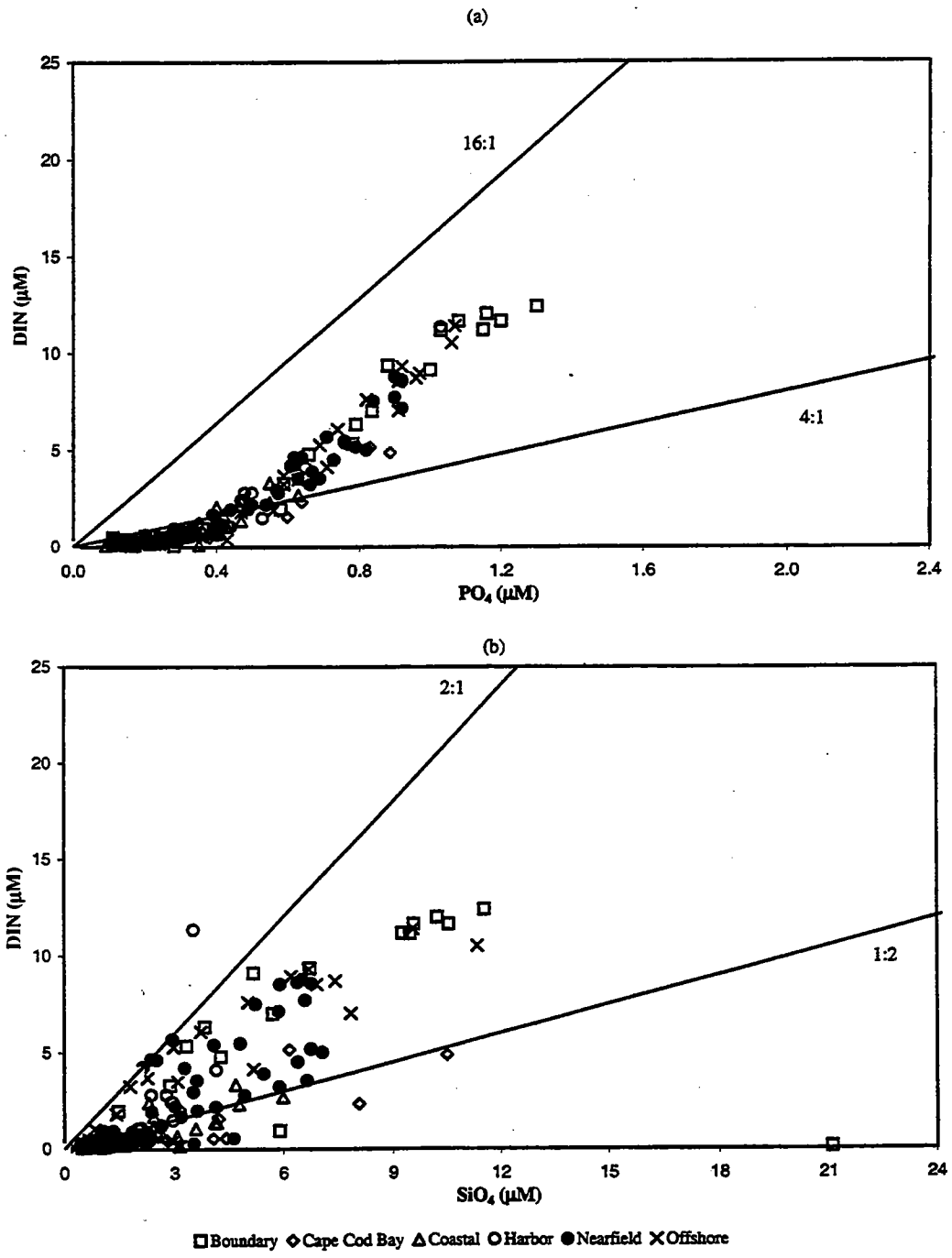

FIGURE 4-25

(a) DIN vs. PO_4 concentrations and (b) DIN vs. SiO_4 concentrations for farfield surveys W9707, (June 1997)

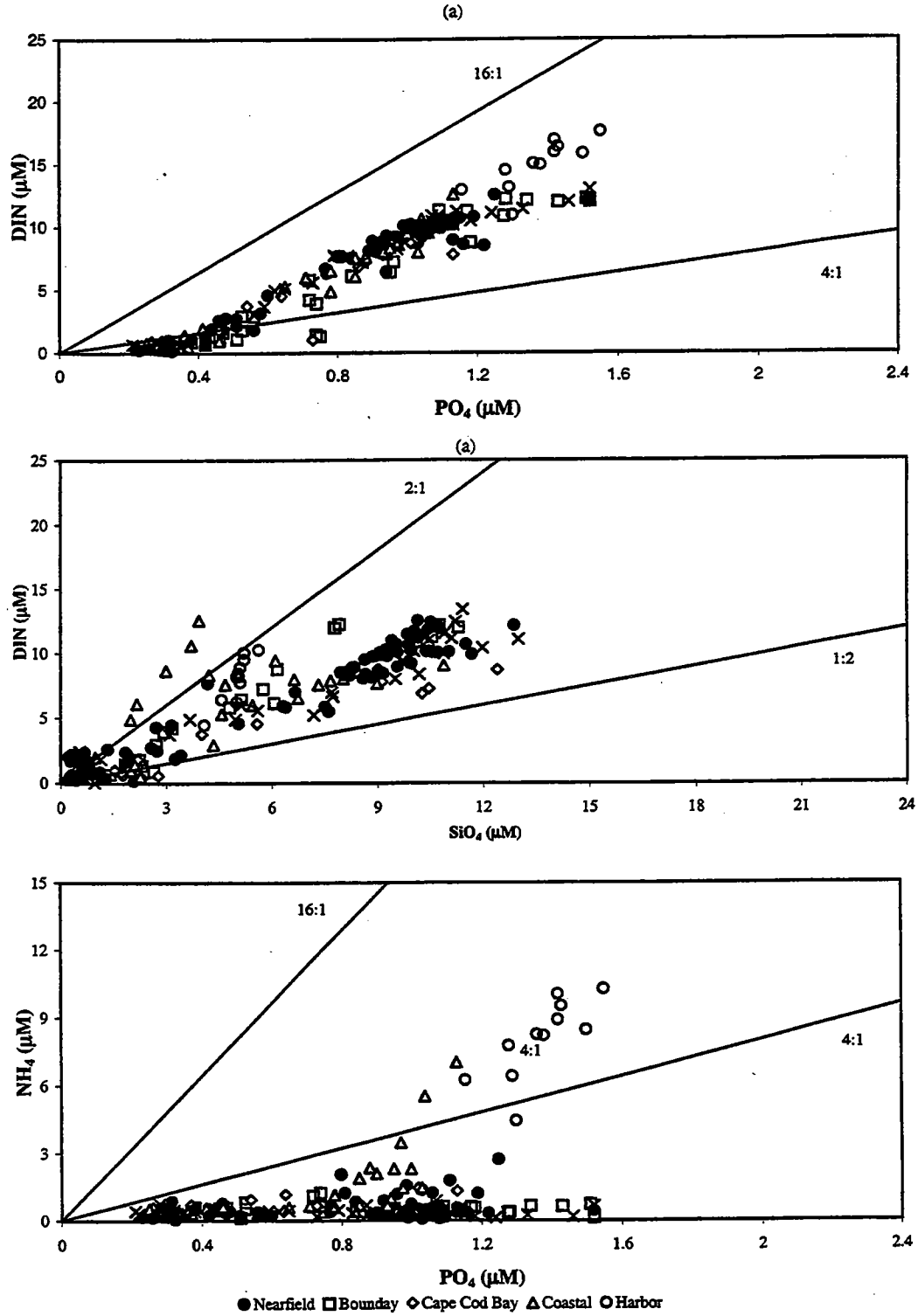

FIGURE 4-26
(a) DIN vs. PO_4 concentrations, (b) DIN vs. SiO_4 concentrations, and (c) NH_4 vs. PO_4 concentrations for farfield survey W9714, (October 1997)

5.0 CHLOROPHYLL

Chlorophyll concentration is an indicator of phytoplankton biomass and thus used in the HOM Program as a surrogate for biomass and phytoplankton standing stock, to normalize productivity measurements, and to ultimately assess the potential for eutrophic effects from the outfall relocation. Chlorophyll was measured on a comprehensive scale by *in-situ* fluorometry during continuous downcasts at each sampling station, and during upcasts when discrete Niskin bottle samples were taken in order to allow comparisons with nutrients, DO, and other parameters.

The *in-situ* fluorometric sensor was calibrated to analytical determinations of chlorophyll *a* from a subset of the discrete samples. Discrete chlorophyll analyses also included determination of the concentration of phaeopigments, which are degradation products of chlorophyll *a*. These results can be used to assess the physiological status of the phytoplankton community, and can be an indicator of zooplankton grazing when productivity is high (breakdown of chlorophyll *a* by digestion leading to proportionally high phaeopigment concentrations).

In this section, chlorophyll results from the 1997 monitoring activities are presented for the nearfield stations and on a regional basis, and are compared with the 1992-1996 data set. Unless otherwise stated, the results presented consist of calibrated *in situ* fluorescence readings taken at the upcast sampling depths. Included is an evaluation of chlorophyll results taken from the surface and at the mid-depth, which we operationally refer to as the chlorophyll maximum (chl_{max}) depth, which are later compared with total phytoplankton densities determined from concurrent samples. Complete presentation of phytoplankton monitoring results is included in Section 8.1. Further detail on chlorophyll concentrations at individual stations within the nearfield grid is included with the discussion of primary productivity in Section 7.1. As with previous sections, significant events in the chlorophyll data are summarized in Table 9-1.

5.1 1997 Nearfield Results

The frequency distribution of chlorophyll results for all nearfield stations and all depths (Figure 5-1) indicated that the majority of samples had relatively low concentrations. During 1997 monitoring, 62 percent of results were less than 1 μgL^{-1}, and just over 97 percent were less than 5 μgL^{-1}. The average nearfield concentration for the year was 1.23 μgL^{-1}, and the maximum concentration was 29.2 μgL^{-1} (Table 5-1). Less than one percent of results exceeded 10 μgL^{-1}. Slightly more than 8 percent of results were categorized as zero, which indicated that the fluorescence recorded by the sensor was predominantly due to the presence of phaeopigments.

The temporal and spatial distributions of chlorophyll within the nearfield were plotted for several stations within the nearfield grid (N10, N16, N04, and N18) to illustrate the response of phytoplankton to the horizontal inshore-offshore nutrient gradient (see Section 4). Surface, mid-depth and bottom concentrations were plotted to evaluate vertical differences. The annual nearfield chlorophyll pattern during 1997 included only a modest late winter bloom, with surface concentrations typically less than 2μgL^{-1} (Figure 5-2). In early March (W9703), nearfield

concentrations typically fell except at station N04, where chlorophyll activity continued through the late March survey (W9704). Station N18 produced a late March peak of around 7 μgL^{-1}, but only in the mid-depth sample (Figure 5-2).

Chlorophyll activity increased during early May throughout most of the nearfield (Figure 5-2). While this late spring peak diminished by the mid-June survey (W9707) in most locations, surface chlorophyll at station N10 increased to around 8 μgL^{-1}. Chlorophyll concentrations generally subsided after mid-June, although a periodic increases at mid-depth were evident at station N16 throughout the summer. A further increase in chlorophyll activity was observed at station N10 during mid-August (W9711). A substantial fall bloom was recorded throughout the nearfield during the early October farfield survey (W9714), with chlorophyll concentrations reaching 6-8 μgL^{-1} at most stations and <11 μL^{-1} at the surface of station N10. This bloom had diminished by the late October survey (W9715), however a late season peak was noted at station N10 during the final survey in December (W9717), and to a much smaller degree at the other more inshore nearfield station N18.

Continuously recorded chlorophyll results from a 12.5m-deep WETLabs sensor on the USGS mooring in the nearfield were available from mid-February through mid-October, although there was a gap in the record during most of September. The WETLabs data were plotted along with results collected from nearfield station N18 during HOM surveys (Figure 5-3). The WETLabs data documented a peak in chlorophyll activity > 4 μL^{-1} following the late February survey (W9702), suggesting that the late-winter bloom in western Massachusetts Bay may have occurred during early March. Subsequent to the diminished chlorophyll concentrations following this event, the WETLabs data indicated a late-March bloom event yielding chlorophyll concentrations approximately double that seen in HOM results (although the surface sample from N18 seemed to capture the magnitude of this event (see Figure 5-2).

After the late March peak, the WETLabs sensor recorded continued chlorophyll activity through mid-May (Figure 5-3). Daily average chlorophyll concentrations increased from around 3 μgL^{-1} the first week of April to a maximum of around 10 μgL^{-1} by mid-May. Individual peaks in concentration were noted to be as high as 20 μgL^{-1} around the mid-May maxima. Coupled with the surface data from the HOM surveys, it appears that this spring bloom was largely a subsurface event. Afterwards, average chlorophyll concentrations recorded by the WETLabs sensor fell to 1-2μgL^{-1} through the rest of the summer.

The WETLabs record indicated that there was substantial chlorophyll activity occurring in the nearfield between the late September and early October HOM surveys (W9713 and W9714, respectively). Average daily chlorophyll concentrations ranged from 3-6 μgL^{-1} for the week following W9713, and after falling to a daily average of 2 μgL^{-1}, peaked again around 8 μgL^{-1} on October 11th. The WETLabs record indicated that chlorophyll concentrations in this region of the nearfield ended within a week of survey W9714.

5.2 1997 Regional Comparisons

A frequency distribution for chlorophyll *a* results was prepared for all stations and all depths sampled in Massachusetts and Cape Cod Bays during the combined nearfield/farfield events (Figure 5-4). These results

indicated that the distribution of chlorophyll concentrations were similar bay-wide as that seen in the nearfield (refer to Figure 5-1). Massachusetts Bay as a whole had a slightly higher average annual concentration (1.29 μgL^{-1}), but yielded a lower maximum concentration (23.7 μgL^{-1}, Table 5-1).

Regional plots of fluorescence data indicated highest chlorophyll concentrations during the late winter bloom (around 6 μgL^{-1} during W9702) in eastern Cape Cod Bay (station F02, Figure 5-5). Surface chlorophyll activity seemed to continue in Cape Cod Bay during the next farfield survey (W9704), with results during this survey only exceeded by those from N18. Over the summer period, regional chlorophyll concentrations were highest in Boston Harbor (Station F23) during June, and later in August at Cape Cod Bay station F02 and the coastal station F13.

During the fall bloom period, highest regional concentrations were seen in the nearfield (station N18), followed by Boston Harbor and the Offshore region station F06 (Figure 5-5). Fall bloom activity was also seen in Cape Cod Bay, but not much activity was evident at the Boundary station F27. During the extended sampling for winter nutrient concentrations conducted during December, increased chlorophyll activity was evident at coastal station F13, and at the Offshore station F06.

5.3 Interannual Comparisons of Chlorophyll Concentration

5.3.1 Nearfield Comparisons

The annual seasonal cycles for chlorophyll (surface and bottom) in the nearfield for the period 1992 to 1997, along with the extent of spatial and temporal variability for nearfield stations as a whole is depicted in Figure 5-6. The size of the error bars (standard deviations) indicates the degree of horizontal and vertical variability encountered during one survey. Large interannual differences were typically seen during both the spring and fall blooms.

The largest spring bloom occurred during 1996 (seasonal average concentration 2.43 μgL^{-1}), followed by 1992 and 1994 (Figure 5-6). For 1997, the spring bloom ranked third in magnitude for the baseline period. The largest fall bloom occurred during 1993 (average = 4.42 μgL^{-1}), with 1997 ranking as the smallest fall bloom on record (average concentration of 1.28 μgL^{-1}. This graphical representation also demonstrates that both the spring and fall events vary considerably in duration, while the timing of the events themselves may shift by a month or more.

Despite the differences observed in the magnitude of bloom events from year to year, annual nearfield averages only differed by around 1 μgL^{-1}, ranging from 1.23 μgL^{-1} in 1997 to 2.36 μgL^{-1} in 1993 (Table 5-1). The overall average calculated for the 1992-1997 baseline period was 1.78 μgL^{-1}. Variability in chlorophyll *a* concentrations was more substantial seasonally. Seasonal *in situ* chlorophyll *a* concentrations were calculated for all years as part of the baseline evaluation (Table 5-2). Spring chlorophyll *a* concentrations ranged from 1.01 μgL^{-1} during 1993 to 2.43 μgL^{-1} during 1996, with a baseline average of 1.61 μgL^{-1}.

As might be expected from previous discussions, seasonal chlorophyll *a* concentrations were generally lowest during the summer, ranging from 0.73 μgL^{-1} in 1995 to 1.88 μgL^{-1} in 1992, and a baseline average of 1.30 μgL^{-1}. The exception to this seasonal trend occurred during the summer 1993, when the average summertime chlorophyll *a* concentration (1.81 μgL^{-1}) was almost double the average for the spring (1.01 μgL^{-1}). The fall produced the overall highest seasonal average for chlorophyll *a* (2.45 μgL^{-1}), with individual years ranging from a low in 1997 of 1.28 μgL^{-1} to a high of 4.42 μgL^{-1} in 1993.

5.3.2 Regional Comparisons

Table 5-1 also provides annual averages for results from the regional stations (Massachusetts and Cape Cod Bays) sampled during the six combined surveys between 1992 and 1997. Average results ranged from 1.20 μgL^{-1} to 2.84 μgL^{-1}, with results from 1995 the lowest of the six-year period. In order to examine these interannual differences on a regional and temporal basis, results from selected stations in each sampling region were plotted for 1992 through 1997 (Figure 5-7). Harbor stations typically increased in concentrations through the summer. The only year in which a pronounced fall bloom was evident in Boston harbor was during 1997 (Figure 5-7), which even exceeded the Harbor's chlorophyll concentration during the large fall bloom in 1993.

A comparison across the baseline period for the six stations plotted in Figure 5-7 emphasizes that 1997 appeared to have few significant bloom events of the magnitude seen in previous years. With the exception of the coastal bloom measured during early October, 1997 appeared to be most similar to 1995. Further assessments of this are included in later sections on productivity (Section 7.1) and plankton (Section 8.)

Year	Mean (µg/L)	Standard Deviation	N	Maximum (µg/L)
Nearfield				
1992	2.08	1.69	1465	17
1993	2.36	3.11	1851	20.5
1994	1.96	1.48	1863	13.7
1995	1.39	2.32	1682	18.1
1996	1.54	1.89	1275	11.5
1997	1.23	1.99	1379	29.2
1992-1997 Baseline	**1.78**	**2.18**	**9515**	**29.2**
Massachusetts Bay				
1992	2.24	1.75	2200	
1993	2.84	3.85	1103	21.1
1994	2.27	2	1132	16.9
1995	1.20	1.74	1102	15.0
1996	1.81	2.18	1275	13.4
1997	1.29	1.97	1386	23.7

Notes:
Nearfield = all Nearfield stations, all depths
Massachusetts Bay = all Farfield stations + 7 Nearfield stations (N01, N04, N07, N10, N16, N18, N20), all depths

TABLE 5-1
Comparison of Annual and Regional In-situ Fluorescence Characteristics

Year	Spring	Summer	Fall
1992	1.97	1.88	2.46
1993	1.01	1.81	4.42
1994	1.95	1.55	2.47
1995	1.02	0.73	2.58
1996	2.43	0.78	1.47
1997	1.29	1.08	1.28
1992-1997			
Mean	1.61	1.30	2.45
Standard Deviation	0.59	0.51	1.11
N	6	6	6
Threshold Concentration	2.58	2.15	4.28
Threshold Concentration = Mean + (1.645) * StDev			

TABLE 5-2
Mean MWRA Baseline Seasonal In-situ Fluorescence Data
17 Nearfield Station (All Depths)

T5-2.xls

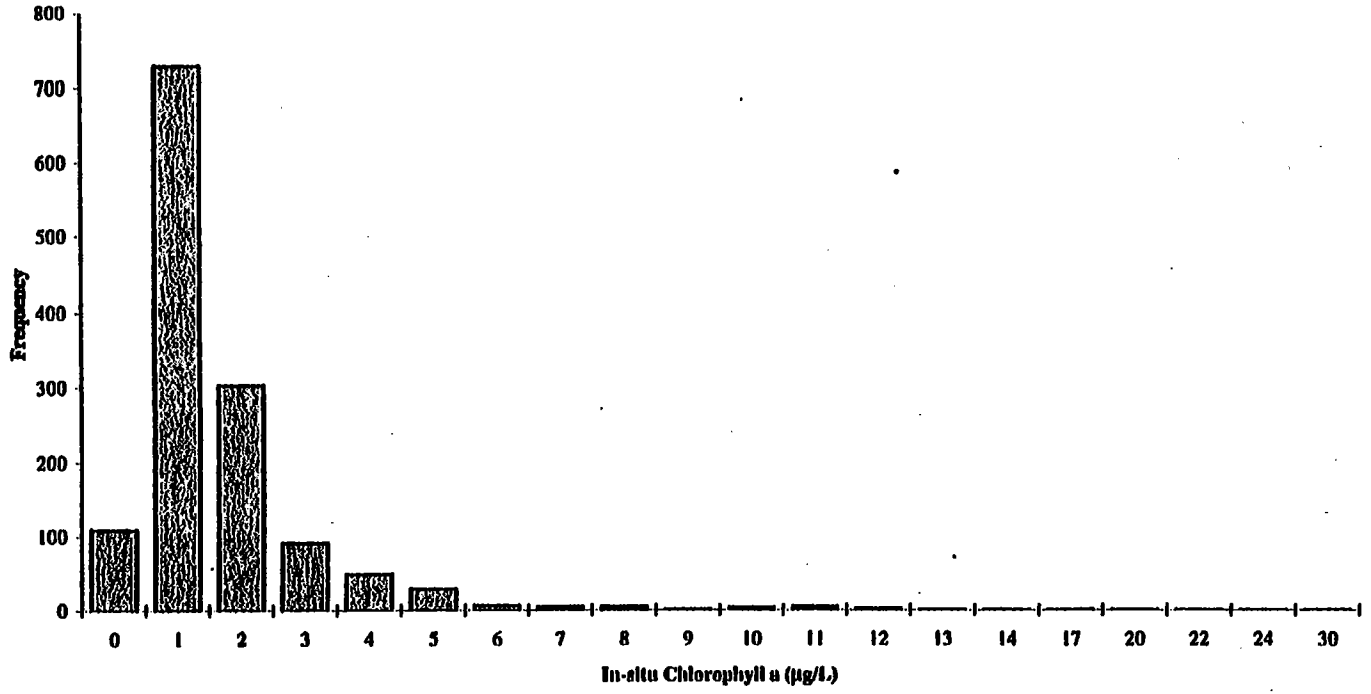

																					Total
Nearfield	109	728	303	91	50	30	7	5	5	2	4	5	3	1	1	1	1	1	1	1	1349
Total Number	109	728	303	91	50	30	7	5	5	2	4	5	3	1	1	1	1	1	1	1	1349
Percent	8.1%	54.0%	22.5%	6.7%	3.7%	2.2%	0.5%	0.4%	0.4%	0.1%	0.3%	0.4%	0.2%	0.1%	0.1%	0.1%	0.1%	0.1%	0.1%	0.1%	100.0%
Cumulative Number	109	837	1140	1231	1281	1311	1318	1323	1328	1330	1334	1339	1342	1343	1344	1345	1346	1347	1348	1349	
Cumulative Percent	8.1%	62.0%	84.5%	91.3%	95.0%	97.2%	97.7%	98.1%	98.4%	98.6%	98.9%	99.3%	99.5%	99.6%	99.6%	99.7%	99.8%	99.9%	99.9%	100.0%	

Note: Bin number denotes upper limit of bin.

Figure 5-1
Frequency Distribution of 1997 Nearfield In-situ Fluorescence Results
All depths at all nearfield stations on all nearfield surveys.

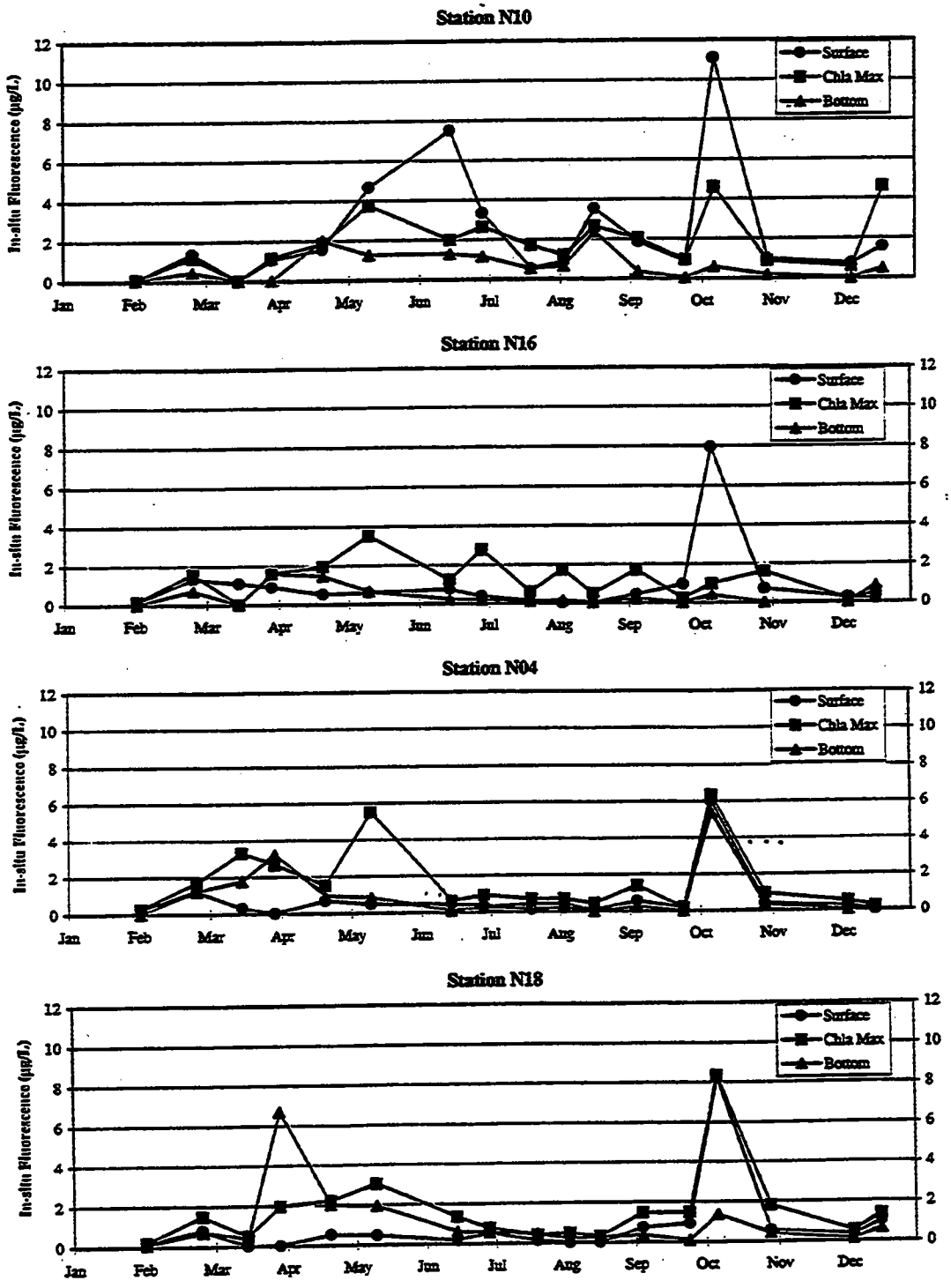

FIGURE 5-2
1997 In-situ Fluorescence in the Nearfield

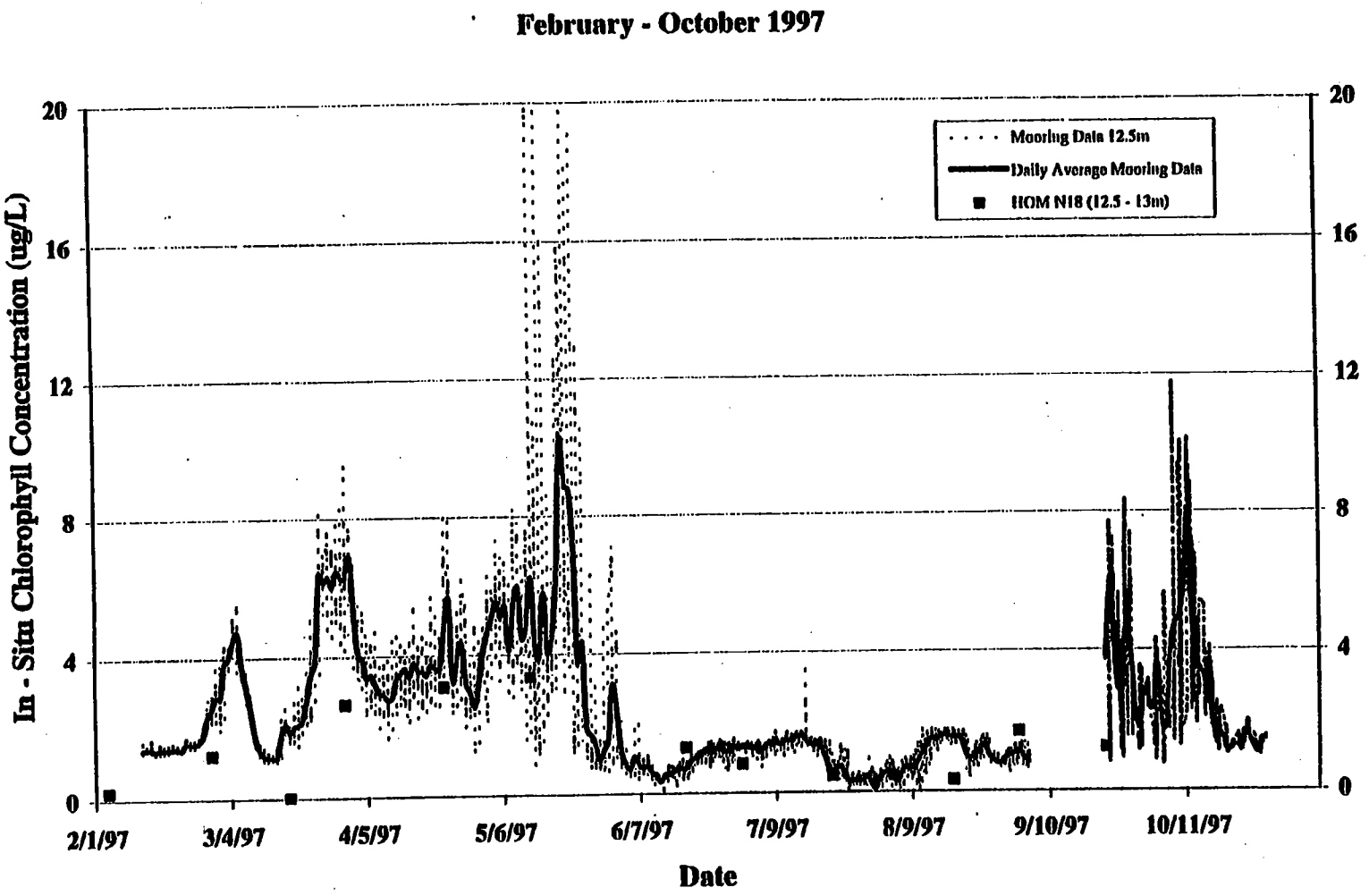

FIGURE 5-3
1997 Moored In-situ Fluorometric Data with Nearfield Station N18

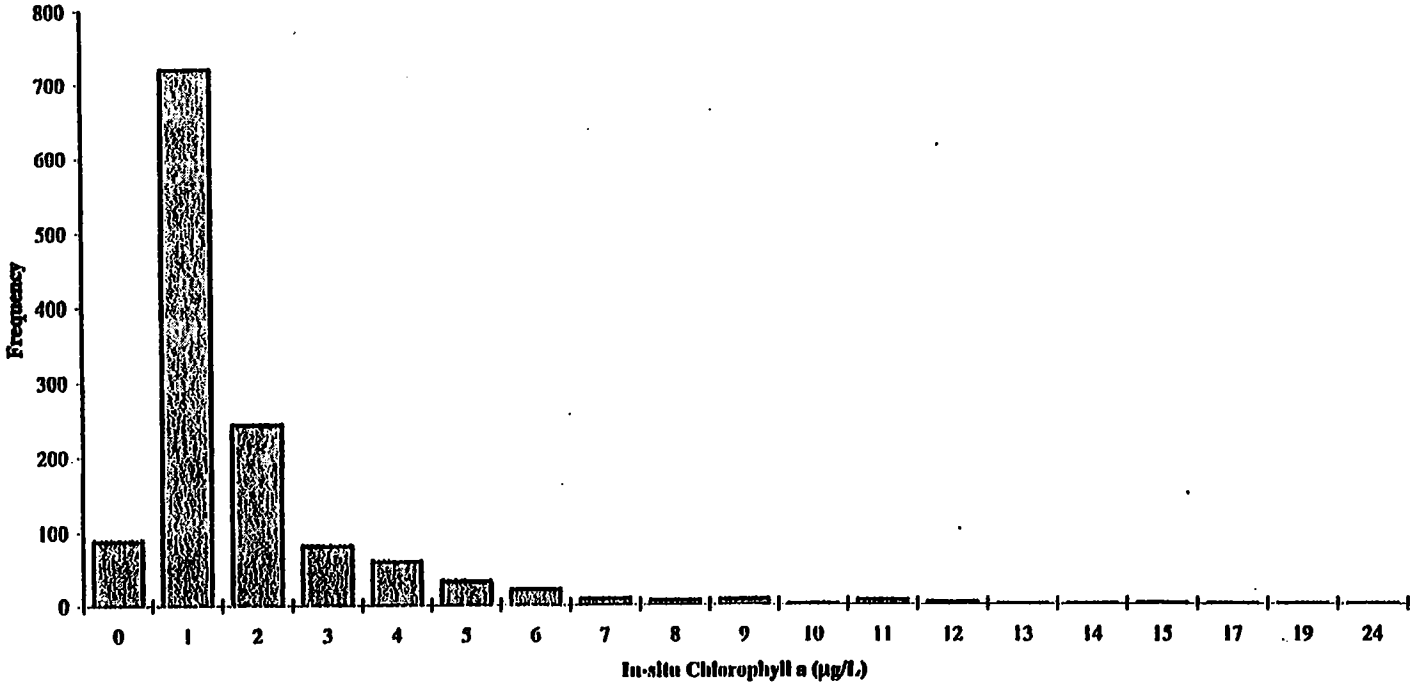

																				Total
Boundary	11	101	34	6	3															155
Cape Cod Bay	1	48	14	6	11	6	2	1												89
Coastal	8	91	33	17	13	7	4	1	1	2	1	2	1		1	2		1		185
Harbor	3	35	3	11	8	5	9	2	1	3										77
Nearfield	44	282	113	34	19	12	2	2	4	1		4	2	1			1		1	521
Offshore	21	164	46	7	8	2	4	2		1										255
Total Number	88	721	243	81	59	32	21	8	6	7	1	6	3	1	1	2	1	1	1	1283
Percent	6.9%	56.2%	18.9%	6.3%	4.6%	2.5%	1.6%	0.6%	0.5%	0.5%	0.1%	0.5%	0.2%	0.1%	0.1%	0.2%	0.1%	0.1%	0.1%	100.0%
Cumulative Number	88	809	1052	1133	1192	1224	1245	1253	1259	1266	1267	1273	1276	1277	1278	1280	1281	1282	1283	
Cumulative Percent	6.9%	63.1%	82.0%	88.3%	92.9%	95.4%	97.0%	97.7%	98.1%	98.7%	98.8%	99.2%	99.5%	99.5%	99.6%	99.8%	99.8%	99.9%	100.0%	

Figure 5-4
Frequency Distribution of 1997 Massachusetts Bay In-situ Fluorescence Results
All depths, all FF and 7 NF stations, all combined surveys.

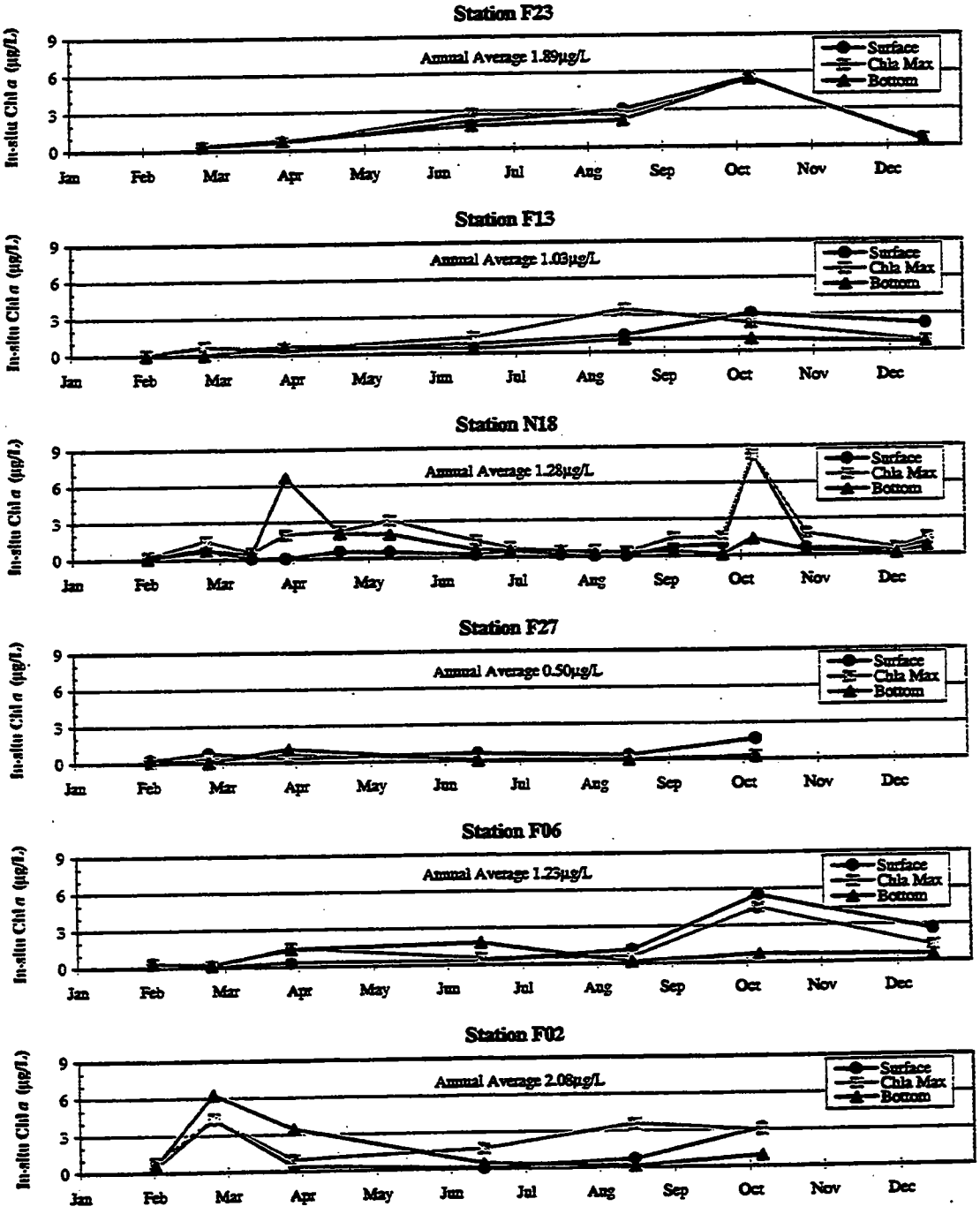

FIGURE 5-5
1997 Regional In-situ Fluorescence

F5-5chla.XLS

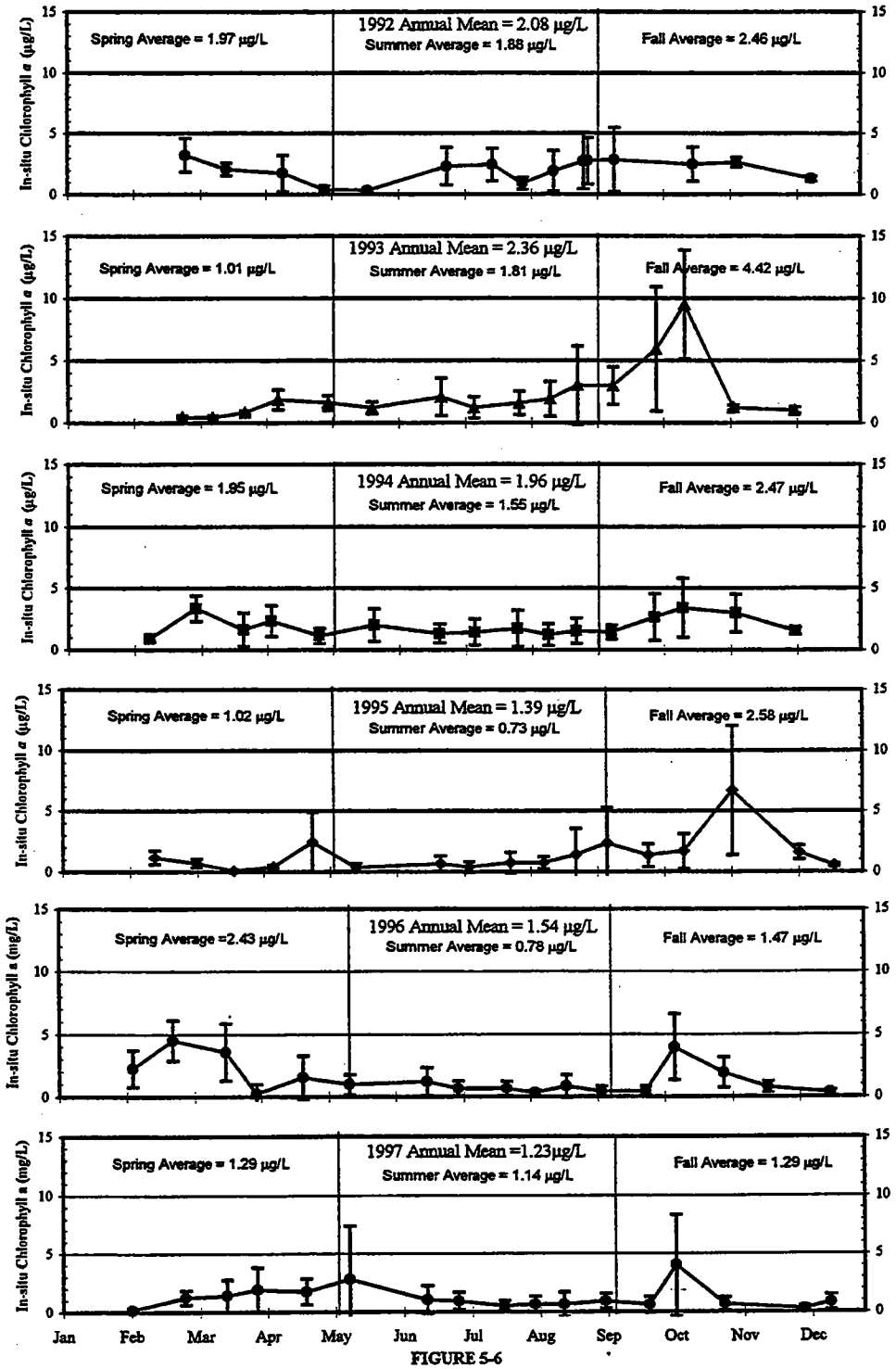

FIGURE 5-6
Interannual Nearfield Survey In-situ Fluorescence Averages
All depths at all nearfield stations included.
Error bars represent +/- one standard deviation.

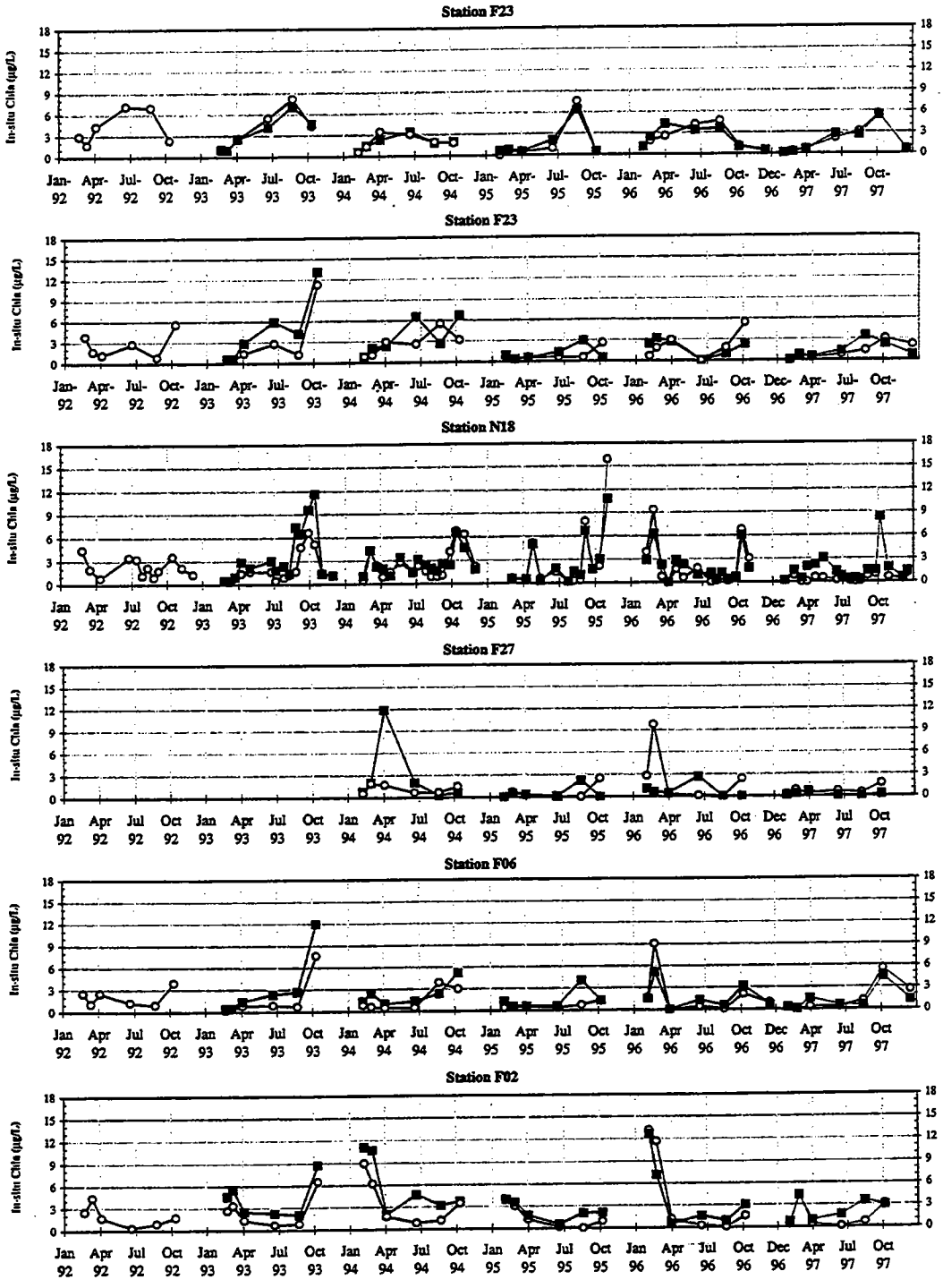

FIGURE 5-7
Interannual In-situ Fluorescence
Circles = Surface (A); Squares = Mid-Depth (C)

6.0 DISSOLVED OXYGEN

Dissolved oxygen (DO) concentrations in the water column and the sediments are important from both a regulatory and an ecological perspective. The Commonwealth of Massachusetts has established water quality standards for minimum water column DO concentrations. The state standard for Class SA water, which includes all of the study area outside of Boston Harbor, is 6 mgL^{-1}. From an ecological perspective, DO in the water column and sediments is of interest not only because it a requisite for the life of aquatic animals, but because it integrates the biological and physical processes which establish a system's habitat quality.

Accordingly, factors that create or increase the level of DO depletion play key roles in the diversity and productivity of the recipient water. These factors are both natural (stratification, primary production, water depth, temperature, etc.) and anthropogenic (wastewater discharges, cultural eutrophication). Fortunately, it is not the sporadic presence of depressed oxygen concentration but the severity, frequency and duration of low DO that affects aquatic health. The HOM program is designed to provide both adequate spatial and temporal coverage of water column DO throughout the year, and especially during the stratified interval. During stratification, the isolation of the bottom water from atmospheric exchange coupled with *in situ* respiration within both bottom water (Chapter 7.2) and sediments (Howes, 1997; 1998), results in oxygen depletion of the bottom water. This depletion is typically most strongly realized at depth in the water column. Increases in oxygen concentration in deeper water result primarily from periodic ventilation through storm-driven mixing, advection of oxygen rich bottom water (Cibik *et al.*, 1996), and de-stratification in the fall.

This section reports the results of MWRA's DO monitoring in Massachusetts and Cape Cod Bays. The focus is on the 1997 results and comparisons to the pattern and extent of DO depletion in the previous years of the HOM program. Since the observed DO depletion is fundamentally related to the stratified water column, the focus is on bottom water concentrations in the nearfield and Stellwagen Basin. The data indicate that over the six years of monitoring, DO depletion and re-aeration in Massachusetts and Cape Cod Bays follows a predictable seasonal pattern that determines the timing, but not the magnitude of the annual DO minimum.

DO results presented in this section consist of calibrated upcast sensor data for the uppermost (surface) and lowest (bottom) sample depths. Downcast vertical profiles of DO and other parameters measured during the 1997 surveys have been reported earlier in periodic nutrient data reports. Additional information on sampling can be found in Section 2, and in the CW/QAPP (Bowen *et al.*, 1997).

6.1 Annual DO Cycle in Nearfield

6.1.1 1997 Results

DO concentration in coastal water is determined by the temperature (and salinity) during atmospheric exchange, inputs through photosynthesis, the level of respiratory uptake, and the time since onset of stratification. It is the interplay of these factors which established the typical seasonal cycle of DO depletion in Massachusetts and Cape

Cod Bays and other temperate coastal water in 1997. The highest average DO concentrations in the nearfield occurred during winter and early spring (Figure 6-1a), when the water column was well mixed, the water temperature was at or near the annual minimum (Figure 3-2), and respiration in the water column was low (Section 7.2). Nearfield DO concentrations peaked in mid-April in the surface water, with an average of around 11.4 mgL^{-1}. DO saturation in surface water exceeded 100 percent from February through April, and reached around 114 percent during the period of peak concentration (Figure 6-1b).

Surface water DO concentrations steadily declined after the spring peak through July, afterwards remaining fairly constant at around 8.4 mgL^{-1} until the onset of the fall turnover in early October. DO saturation in the surface water remained above 100 percent throughout the period, and peaked again near 114 percent during the fall bloom (survey W9714, see Section 5). Both surface concentration and saturation fell substantially by the late October survey (W9715), potentially a result of vertical mixing with oxygen deficient bottom water (Figure 6-1a and b) and microbial respiration of carbon material generated by the fall bloom (Section 7.2). Surface concentration increased by the final two surveys, with saturation returning close to 100 percent.

DO in the nearfield bottom water increased slightly during February and peaked during mid-March, with an average concentration of around 10.7 mgL^{-1} (Figure 6-1a). Average concentrations declined from the March peak through mid-June (W707), reaching a concentration of around 8.8 mgL^{-1} and a saturation of around 86 percent (Figure 6-1b). Following the mid-June survey, a reversal in the decline in bottom water DO concentration was observed which resulted in an increase in concentration to around 10.1 mgL^{-1} by the mid-July survey (W9709). This reversal was even more dramatic in the saturation results (Figure 6-1b), which increased from 86 percent to almost 104 percent (the only time during the year in excess of 100 percent).

Following the mid-July survey, average bottom water DO concentration and saturation again continued to decline through the remainder of the stratified summer period. Minimum nearfield averages for DO concentration (7.2 mgL^{-1}) and saturation (77 percent) were recorded in early October (W9714, Figure 6-1). Note however the large standard deviations in averages from late October (W9715), which indicated that substantial spatial differences were evident in the nearfield bottom water. In fact, individual annual minima for DO concentration (6.38 mg/L) and saturation (68.6 percent) were reported from survey W9715 (Figure 6-2). This result can be attributed to the delayed mixing at deeper stations relative to the more shallow stations in the nearfield (Section 3.4.2), although station N04 proved to be an anomaly.

The averages for DO concentration and saturation rose by the next survey in late November (W9716), and although DO concentration continued to rise in December, there was a slight decline in saturation during the mid-December survey (Figure 6-1b). Further discussion of the 1997 results is included in the following section.

6.1.2 Interannual Comparison of DO Concentrations

The baseline DO record from the nearfield demonstrates the repetitive annual cycle typical of Massachusetts Bay (Figure 6-3). In most years, DO concentration and saturation increased during the first few surveys of the year, largely a result of oxygen production during the late winter bloom. Following these late winter maxima,

decreases in surface DO concentration due to rising water temperature were typical, although there were frequent short-term increases due to physical or biological factors. Surface DO typically rose after September with cooling water temperature and increased phytoplankton production. Bottom water followed a similar pattern, but declines in bottom water DO concentration and saturation continued in the stratified water column until the onset of mixing, typically in October.

In most respects, 1997 should have been the worst year on record for minimum bottom water DO in western Massachusetts Bay. In terms of "setup", maximum winter bottom concentrations were the lowest of the baseline period. Using the beginning of June as the onset of stratification for each year, 1997 was similar to 1994 (the worst year of the baseline period) and to 1995 (Figure 6-3). In fact, nearfield bottom DO concentrations in mid-June of each year (as documented by the June farfield survey) were lowest in 1997. Calm, dry weather produced little vertical mixing during the period, and the fall turnover was later in 1997 than in previous years (Section 3). Despite these conditions, average nearfield bottom water DO concentrations did not fall below 7.0 mg/L during 1997, and the year ranked third with respect to the magnitude of DO depression.

The absence of substantial DO depression in nearfield bottom water during 1997 can only be attributed to mitigation produced by the substantial increase in bottom DO concentration during July (surveys W9708 and W9709). Although there were several thunderstorms that moved through the area between late June and mid-July (i.e., between surveys W9707 and W9709, Section 3.1), there was little evidence of substantial vertical mixing during the period. Alternatively, there was continuous advection of offshore bottom water into the nearfield throughout the period (Figure 6-4) that may have displaced low DO water residing in the nearfield. The over-saturated conditions which were observed at depth (Figure 6-1) may also have been a result of substantial *in situ* productivity which was measured at the pycnocline during the period (Section 7.1, also see Cibik *et al.*, 1998b).

6.1.3 Interannual Comparison of DO Decline

Declines in nearfield bottom water DO occurred during the summer and early fall in each of the six years of monitoring, as did periodic increases in DO (Figures 6-3 and 6-5). The rate of DO decline was relatively uniform throughout the baseline period, ranging from a low of 0.020 $mgL^{-1}d^{-1}$ in 1997 to a high of 0.031 $mgL^{-1}d^{-1}$ in 1994 (Figure 6-5). Were the rate of decline from 1997 to be restricted to surveys W9710 through W9714, the rate would be similar to each of the other years except 1994, when the rate of decline was most rapid.

Figure 6-5 also reinforces that 1997 had the lowest "setup" concentration, which was approximately 0.4 mgL^{-1} lower than 1994. Had the average bottom water DO not increased during the subsequent two surveys and the typical decline rate of around 0.025 $mgL^{-1}d^{-1}$ occurred, the average nearfield DO around the first of October may well have been around 5.5 mgL^{-1} in 1997.

Although not quite as dramatic as in 1997, results from 1992 also showed increasing average bottom DO concentrations through July (Figure 6-5). In fact, similar increases were observed to varying degrees in each of the other years, even during 1994 (early August) although it did not appear to alter the seasonal trend. It may

therefore be concluded that the "setup" concentration at the beginning of the stratified period may not be as critical to seasonal DO minima as the respiration rate and the degree to which the bottom water DO decline is mitigated by events during the summer stratified period. In fact, the baseline record indicates that the magnitude of these mid-summer re-aeration events and the measured respiration rate are more important in determining the annual oxygen minima than is the setup concentration.

6.2 Annual DO Cycle in Stellwagen Basin and Other Areas

6.2.1 1997 Results

The DO pattern for surface and bottom water in Stellwagen Basin was generally similar to that observed in the nearfield region (Figure 6-6). The average surface DO concentration in the four Stellwagen Basin stations (F12, F17, F19, and F22) had a maximum value of 11.5 mgL^{-1} that occurred early in the year (Figure 6-6a). Surface concentrations then gradually fell through August, reaching an annual minimum of around 8.5 mgL^{-1}. Surface concentrations increased by the October farfield survey, and after a slight decline in late November, rose to around 9.5 mgL^{-1} in December. Survey results indicated that the surface samples exceeded saturation from late March through October (Figure 6-6b).

DO in the bottom water rose from around 10 mgL^{-1} in early February to 10.5 mgL^{-1} by late March, followed by a steady decline through the summer and early fall (Figure 6-6a). The main difference in bottom water results from Stellwagen Basin compared with those from the nearfield was that the period of the late June/July increase in nearfield bottom water DO concentration and saturation (Figure 6-1a and b) was not well documented by farfield survey coverage. An apparent decrease in the rate of decline was evident in the subsequent August farfield survey data (W9711), but there is no evidence that this was related to the July observations in the nearfield. Minimum average bottom water DO concentration and saturation in Stellwagen Basin (7.3 mgL^{-1} and 77 percent, respectively) were reported during the October farfield survey.

Annual bottom water DO results from other regions were also generally similar, with peak average concentrations reported during the late winter (Figure 6-7a). Cape Cod Bay peaked earlier than the other farfield regions, with a maximum of 11.2 mgL^{-1} reported in late February. Maxima in other regions occurred in late March/early April (range 9.9-10.5 mgL^{-1}). Regional differences were evident in average bottom DO minima, with Boston Harbor reaching its minimum concentration (8.0 mgL^{-1}) during the August survey, but reaching its minimum late-season saturation (ca. 95 percent) during December (Figures 6-7a and b). Other regions produced minimum averages for DO concentration and saturation during the October farfield survey. Both concentration and saturation minima were recorded in Cape Cod Bay (6.9 mgL^{-1} and 75 percent, respectively).

As was the case in the Stellwagen Basin results, regional sampling did not provide coverage of the late June/July period. However, Cape Cod Bay did exhibit an increase in both concentration and saturation during the August survey compared with June (Figure 6-7a and b). To a lesser degree, results from the Offshore region stations also exhibited an apparent upturn in the downward trend for average concentration and saturation. Whether these observations were also related to the re-aeration event in the nearfield is uncertain.

Not surprisingly, the range of DO concentrations measured at individual stations was larger than that of the regional averages presented above. In 1997, the minimum DO concentration (6.33 mgL^{-1}) was reported in western Cape Cod Bay off Plymouth during early October (Table 6-1). As mentioned previously, the minimum individual DO concentration in the nearfield (6.38 mgL^{-1}) was reported in late October at station N01.

6.2.2 Interannual Comparisons

The annual pattern of surface and bottom water DO concentration in Stellwagen Basin during 1997 was similar to previous years, and in general similar to that seen in the nearfield. Average surface DO concentration typically showed annual maxima in late winter, summertime declines, and increases during the fall bloom (Figure 6-8). Bottom water averages typically rose from early in the year to an annual peak between February and April (Figure 6-8). For the six years of sampling, the annual minimum concentration was recorded during the early October farfield survey. As with nearfield results, the lowest years for average bottom water DO were 1994 and 1995, with 1997 ranked third.

Regionally, the individual minimum concentrations measured during each year were as follows:

- 1992 - 7.10 mgL^{-1} at nearfield station N10;
- 1993 - 6.68 mgL^{-1} at Cape Cod Bay station F02;
- 1994 - 4.82 mgL^{-1} at nearfield station N01;
- 1995 - 5.60 mgL^{-1} at Cape Cod Bay station F02;
- 1996 - 5.48 mgL^{-1} at Cape Cod Bay station F01;
- 1997 - 6.33 mgL^{-1} at Cape Cod Bay station F03.

6.2.3 DO Decline in the Bottom Water of Stellwagen Basin

Oxygen levels within the bottom water of Stellwagen Basin showed a similar pattern of decline as those of the nearfield throughout summer and early fall (Figures 6-5 and 6-9). Oxygen dynamics within the two systems appear to be responding to similar physical and biological forcing parameters, as the interannual pattern of their oxygen minima show a clear direct relationship (Figures 6-3 and 6-8). The lowest average DO levels in both systems occurred in 1994. However, the magnitude of the DO decline was generally larger in the more inshore nearfield region of Massachusetts Bay than within Stellwagen Basin. The similarity in DO minima indicates that the effects of a shorter interval of bottom water stratification in the nearfield (due to its shallower depth and earlier mixing) is offset by the higher rates of oxygen consumption and warmer bottom water (Figure 3-4).

The effect of the deeper water on the carbon dynamics in Stellwagen Basin (both in terms of water temperature and the quality of the carbon substrate) can be seen in the lower rates of oxygen decline in the Basin versus the nearfield (1992-1997 average of 0.018 $mgL^{-1}d^{-1}$ versus 0.025 $mgL^{-1}d^{-1}$, respectively). The lower rate of decline in the Basin does not manifest itself in less DO depletion as the initial DO concentration is generally lower in the

Basin than in the nearfield (lower initial concentration + lower uptake = higher initial concentration + higher uptake; Figures 6-5 & 6-9).

It is not clear why the range of rates of DO decline in the bottom water of Stellwagen Basin between 1992-1994 (0.021-0.023 $mgL^{-1}d^{-1}$) and 1995-1997 (0.012-0.017 $mgL^{-1}d^{-1}$) are so markedly different. Based on the discussion in Section 6.1.3, the critical factors to evaluate the annual DO decline include respiration rate and the magnitude of re-aeration during the stratified period. The available data do not allow an adequate assessment of this apparent trend in the baseline data.

Table 6-1

Magnitude and Location of DO Maxima and Minima in the Bottom Waters

Event ID	Survey Minima		Survey Maxima	
	Value (mg/l)	Location	Value (mg/l)	Location
W9701	9.54	F27	10.86	F01
W9702	9.86	F27	11.30	F01
W9703	10.31	N06	11.04	N04
W9704	8.91	N07	11.55	F24
W9705	9.40	N06	11.03	N10
W9706	9.05	N10	9.98	N04
W9707	6.92	F01	10.07	N04
W9708	9.09	N10	9.78	N04
W9709	9.17	N04	10.60	N19
W9710	8.01	N11	9.85	N04
W9711	7.50	F31	8.87	N18
W9712	7.64	N11	8.77	N04
W9713	7.07	N10	7.79	N04
W9714	6.33	F03	10.01	N04
W9715	6.38	N01	8.41	N04
W9716	8.35	F12	9.42	N11
W9717	9.21	F19	9.75	F23

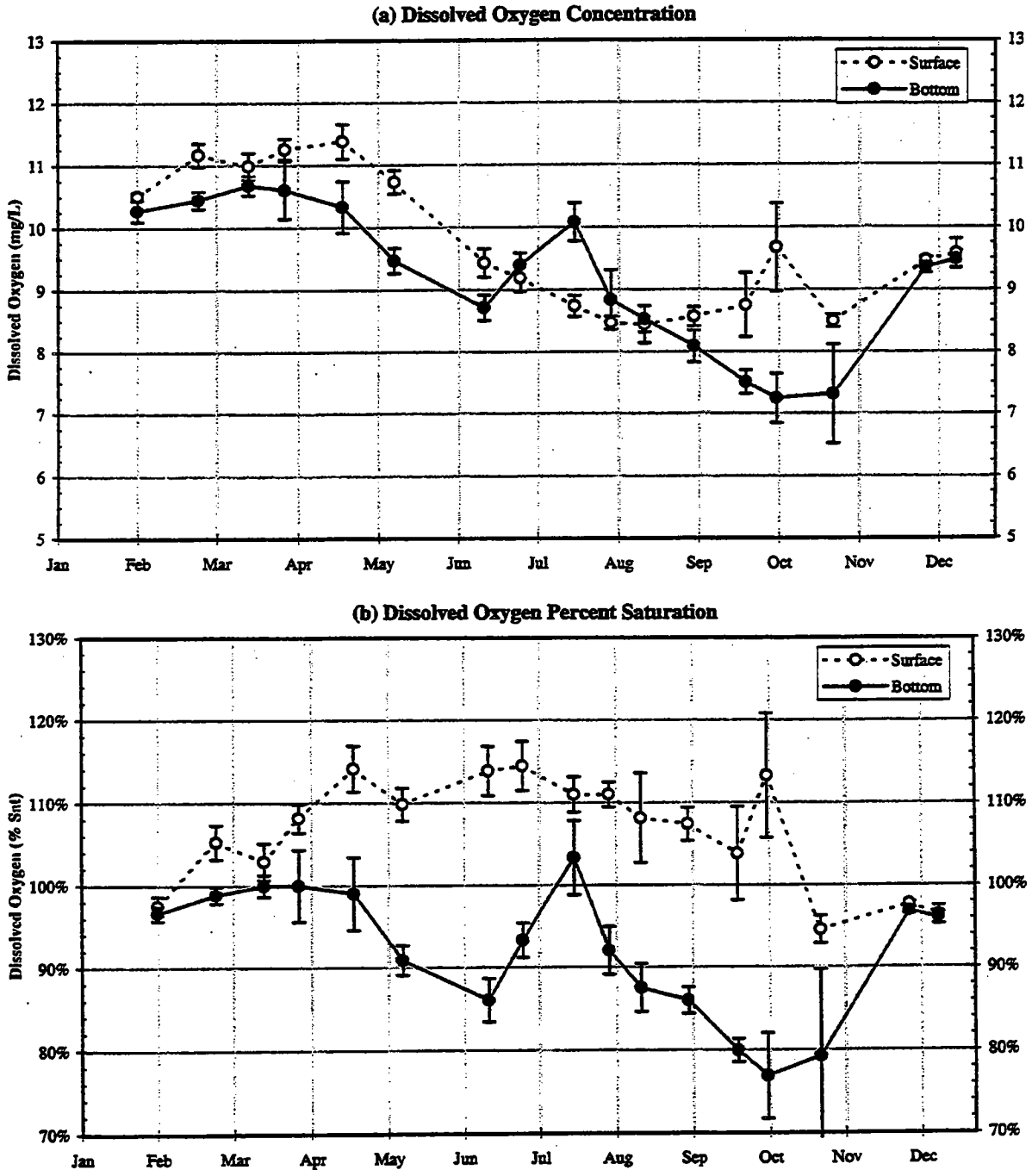

FIGURE 6-1

1997 Nearfield Dissolved Oxygen in Surface and Bottom Waters

Symbols indicate the mean of 17 nearfield stations; error bars represent +/- one standard deviation.

F6-1do.xls

a) Dissolved Oxygen (mg/L)

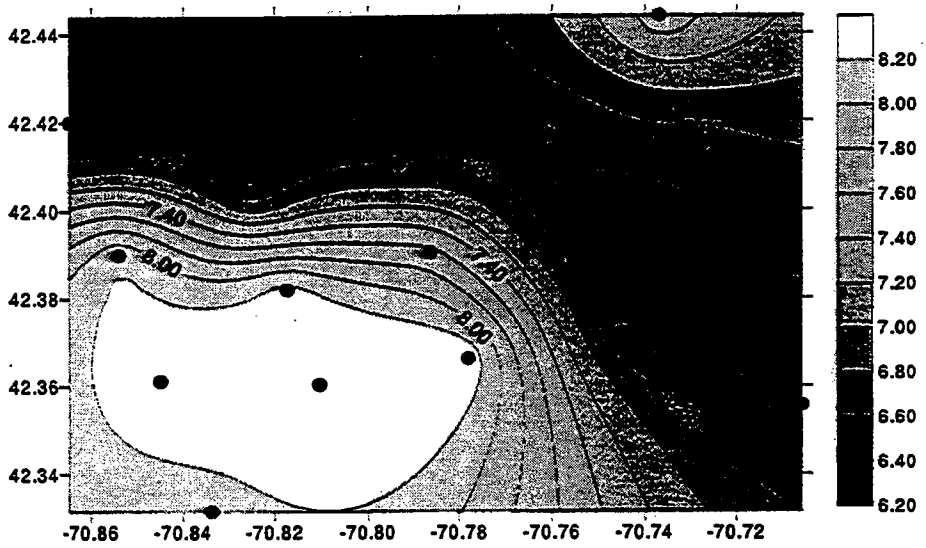

b) Percent Dissolved Oxygen Saturation (%)

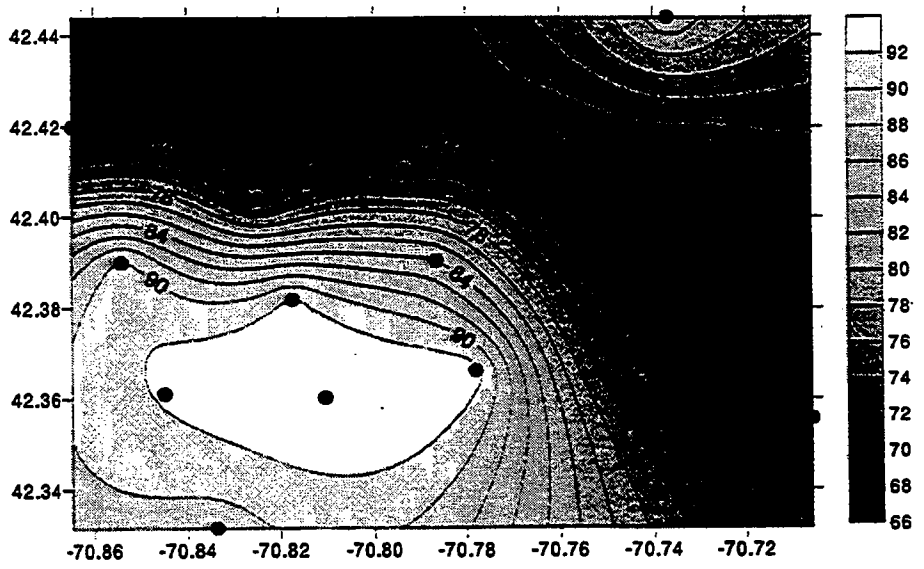

FIGURE 6-2
Nearfield Bottom Water DO Contours for Late October (W9715)

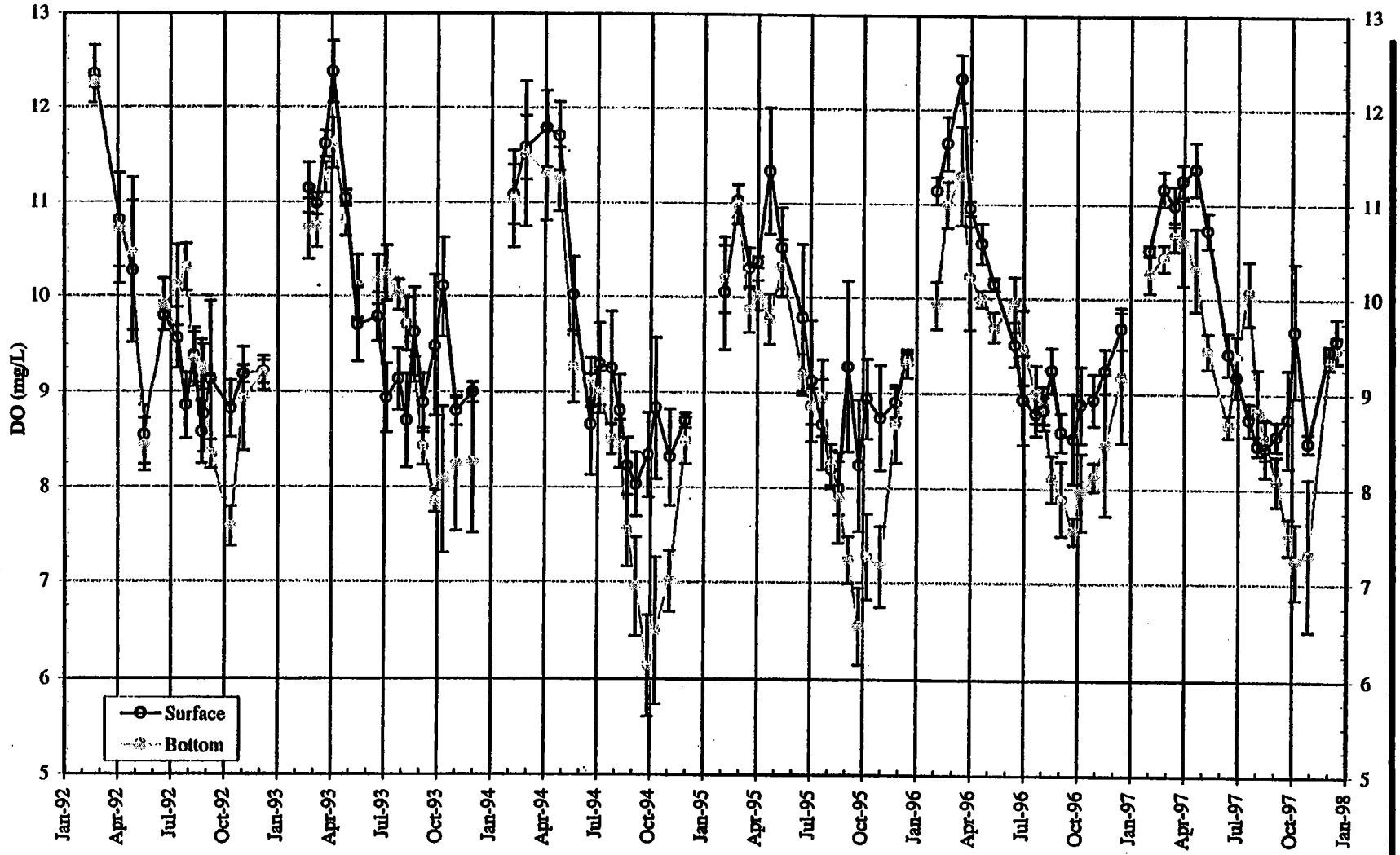

FIGURE 6-3

Interannual Nearfield Dissolved Oxygen Cycle in Surface and Bottom Waters

Symbols indicate the mean of 17 nearfield stations; error bars represent +/- one standard deviation.

newF6-3do.XLS
12/22/98

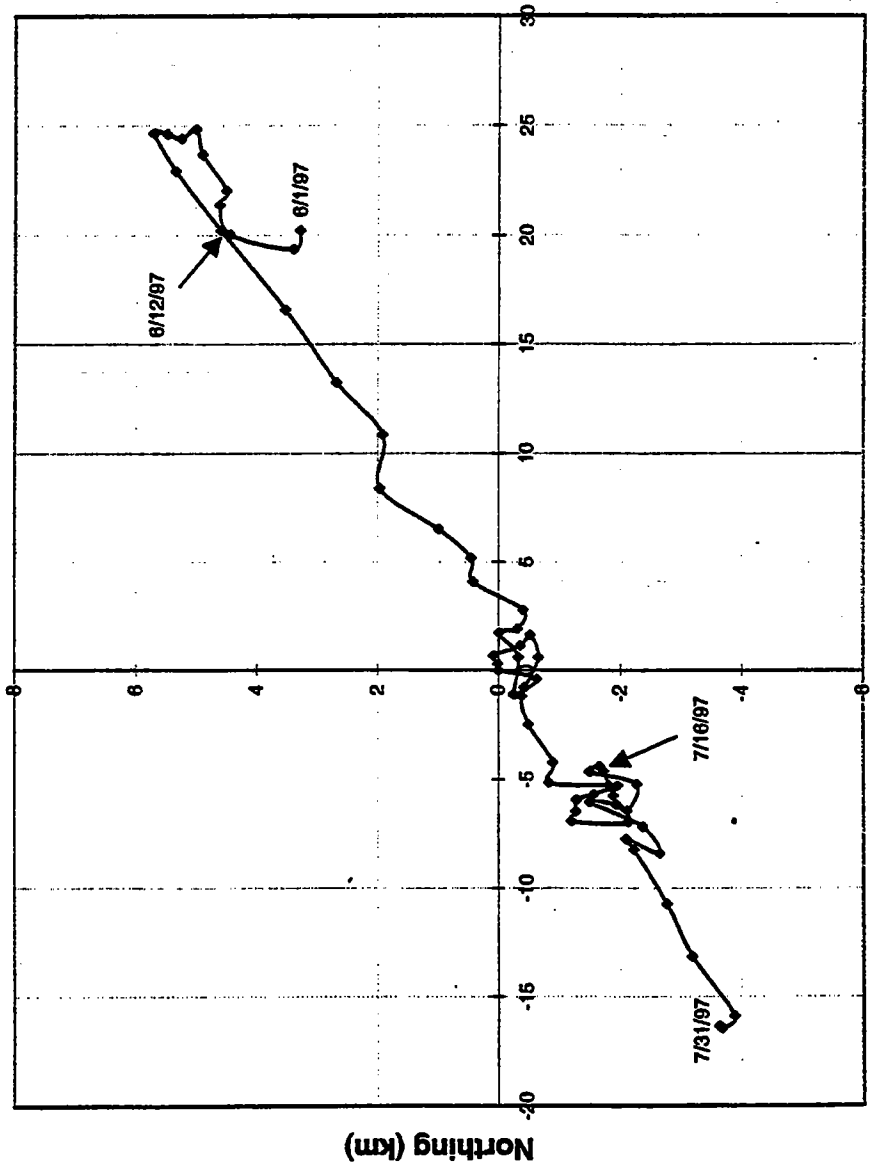

FIGURE 6-4
Progressive Vector Plot: June - July 1997
Depth = 29.2 meters (Bottom)

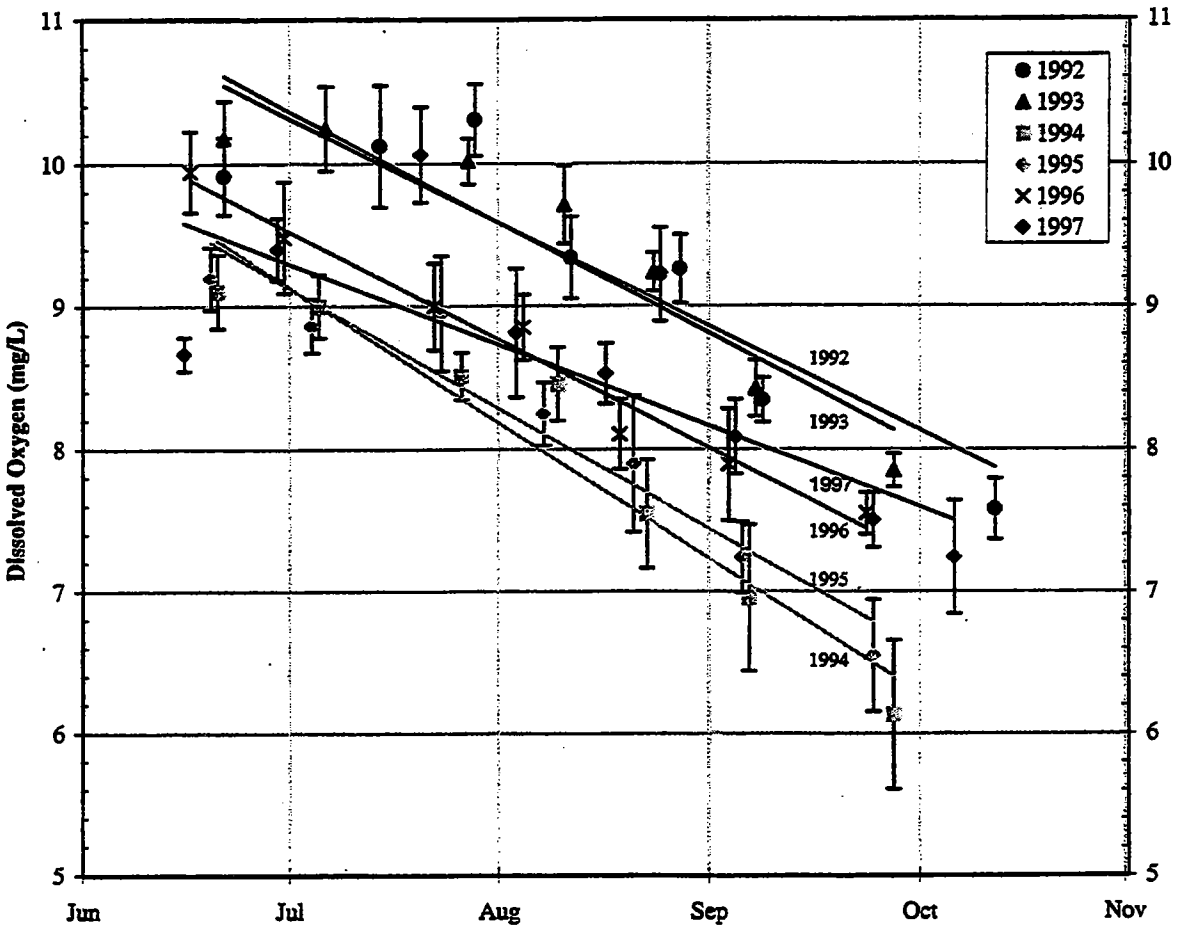

Year	Slope (mg/L/day)	Intercept* (mg/L)	R^2
1992	-0.024	11.0	0.808
1993	-0.025	11.1	0.885
1994	-0.031	10.1	0.929
1995	-0.027	9.9	0.932
1996	-0.025	10.3	0.978
1997	-0.020	9.8	0.632

FIGURE 6-5

Nearfield Dissolved Oxygen Concentrations in Bottom Waters

Symbols indicate the mean of 17 nearfield stations; error bars represent +/- one standard deviation.

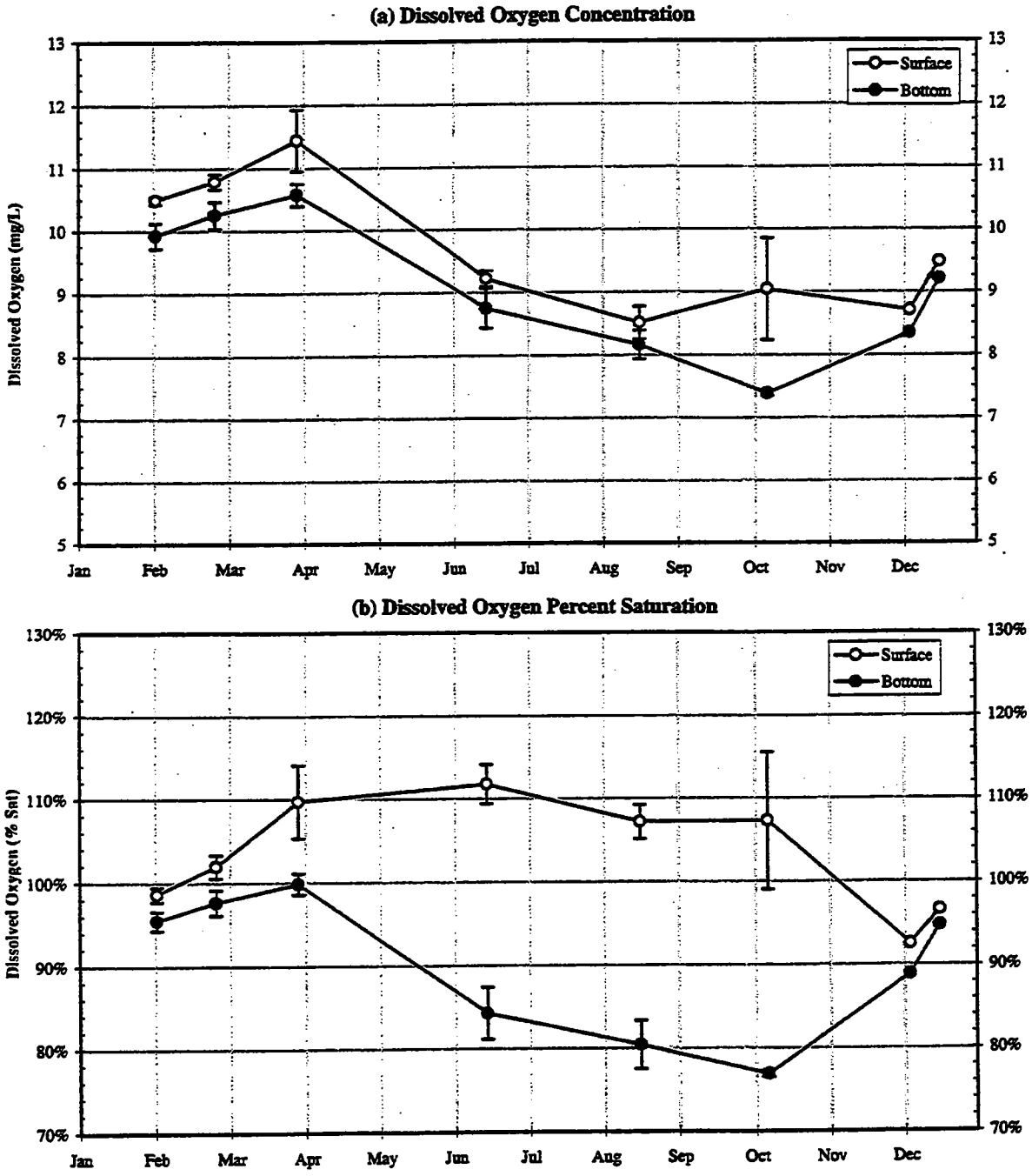

FIGURE 6-6

1997 Steilwagen Basin Dissolved Oxygen in Surface and Bottom Waters

Symbols indicate the mean of 4 Stellwagen Basin stations; error bars represent +/- one standard deviation. newF6-6DO.XLS

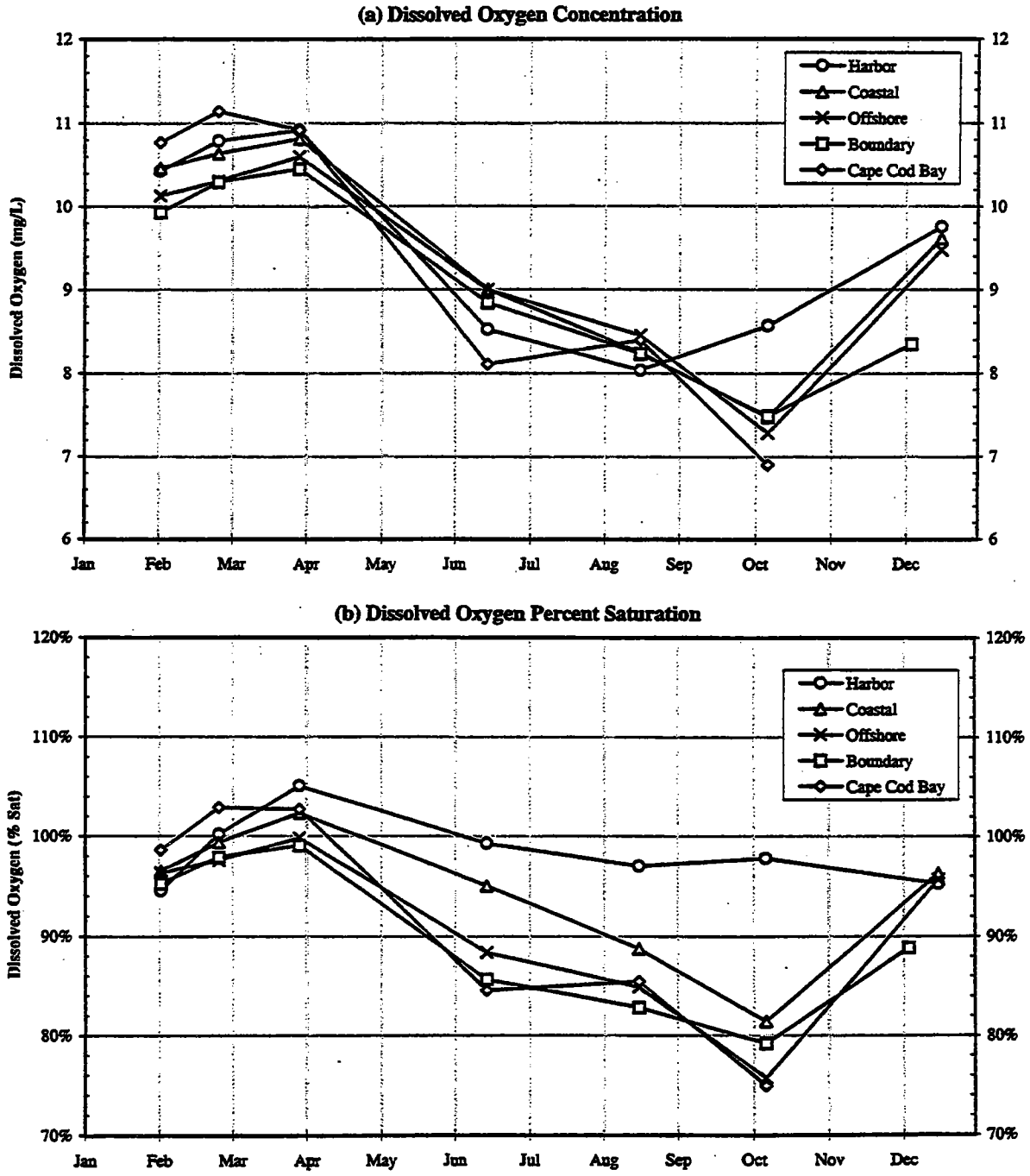

FIGURE 6-7

1997 Spatially Averaged Dissolved Oxygen in the Bottom Waters of Massachusetts and Cape Cod Bays

Symbols represent the average of all stations within each region.

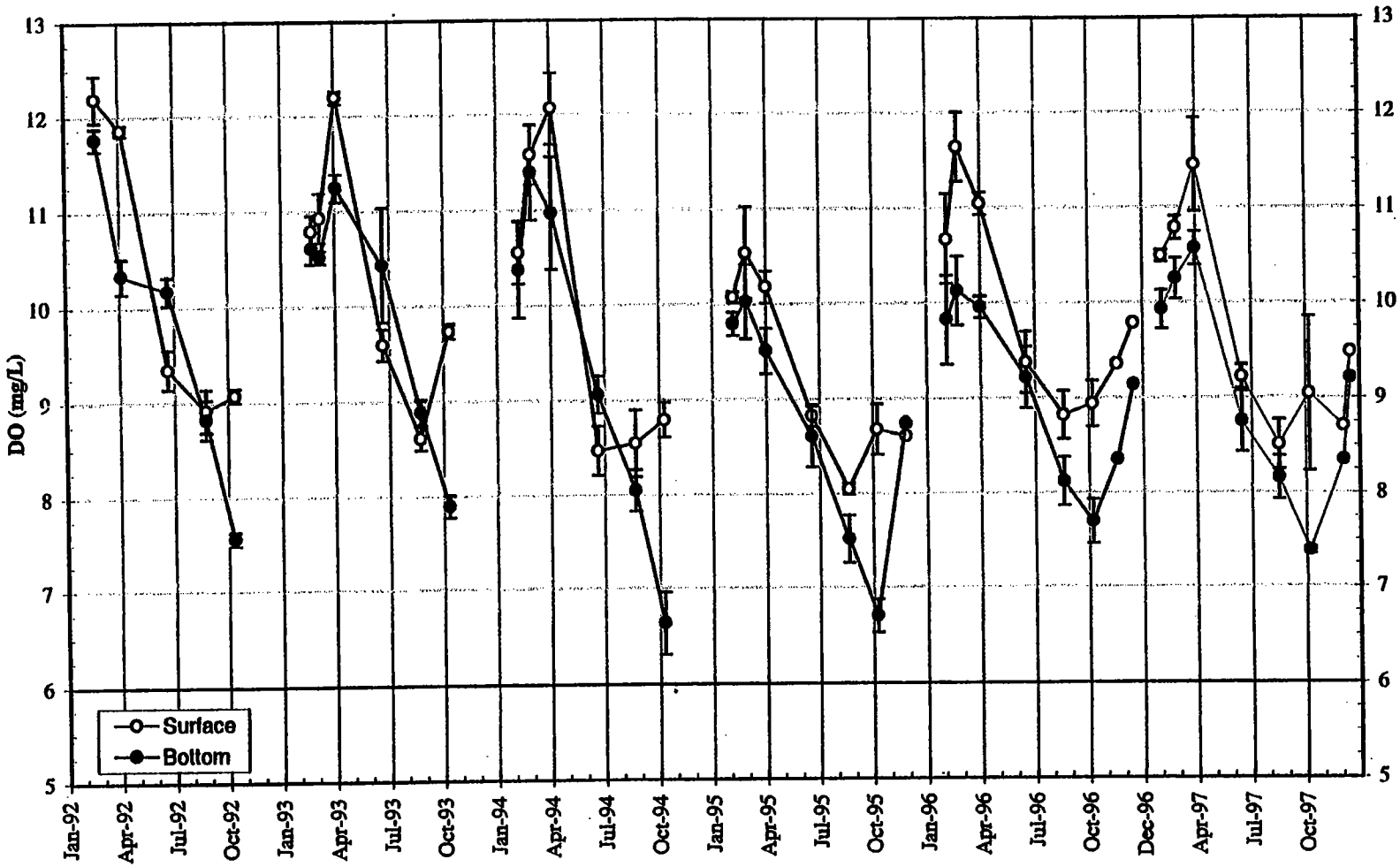

FIGURE 6-8

Interannual Stellwagen Basin Dissolved Oxygen Cycle in Surface and Bottom Waters

Symbols indicate the mean of 4 Stellwagen stations; error bars represent +/- one standard deviation.

F6-6do.XLS

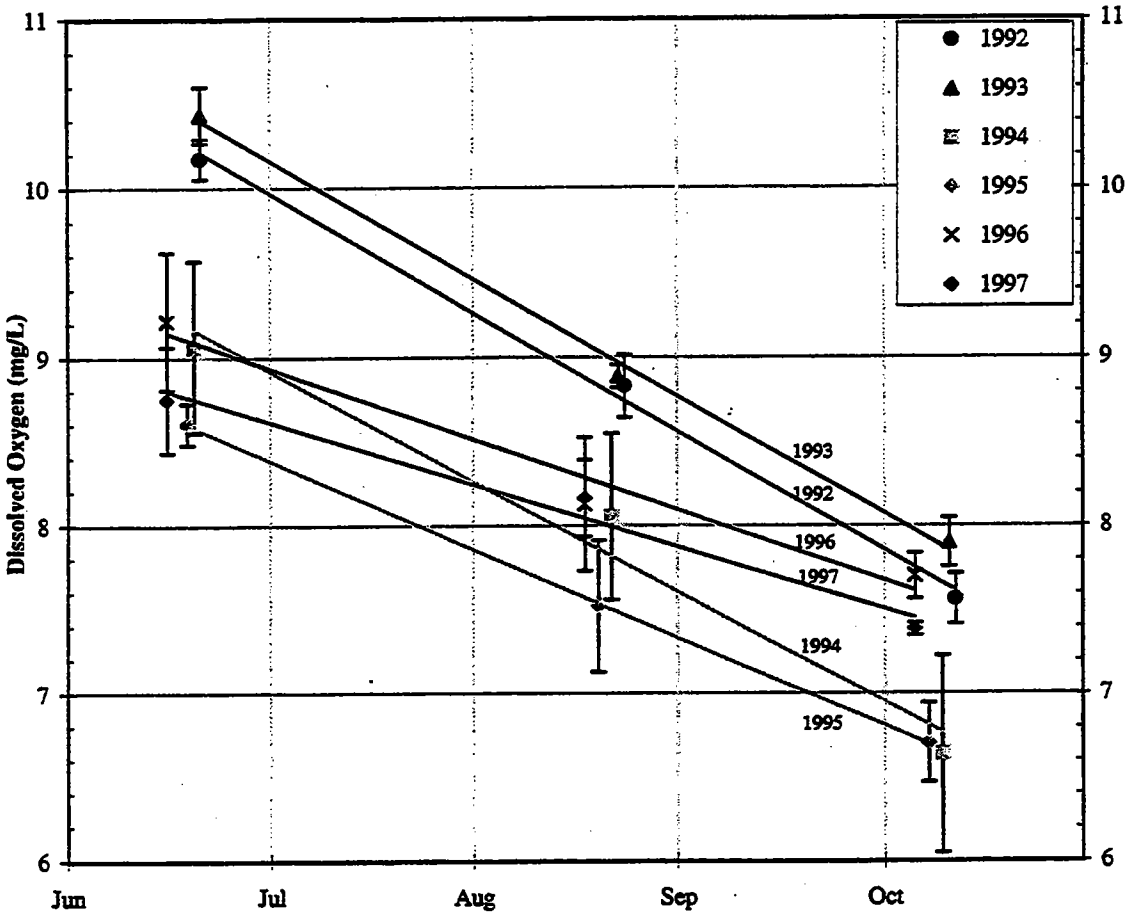

Year	Slope (mg/L/day)	Intercept* (mg/L)
1992	-0.023	10.7
1993	-0.023	10.9
1994	-0.021	9.6
1995	-0.017	8.9
1996	-0.014	9.4
1997	-0.012	11.6

* Predicted DO on June 1st based on:
DO = Slope * Date + Intercept

FIGURE 6-9

Stellwagen Basin Dissolved Oxygen Concentrations in Bottom Waters

Symbols indicate the mean of 4 Stellwagen stations; error bars represent +/- one standard deviation.

7.0 PRODUCTIVITY/RESPIRATION

7.1 Primary Production

7.1.1 Approach to Production Measurement

Phytoplankton production was measured at three stations, the Boston Harbor outer edge station F23, outer nearfield station N04 and station N18 located just south of the outfall site. Stations were visited eight (F23) or 17 (N04, N18) times throughout 1997. ^{14}C production was determined as described in the CW/QAPP (Bowen *et al.* 1997; see also Taylor, 1998). Samples were obtained at 5 depths within the euphotic zone down to the ~1-2 % light level and incubated in the presence of ^{14}C-bicarbonate in a temperature controlled incubator at light intensities ranging from approximately 5-1200 $\mu Em^{-2}s^{-1}$.

The resulting photosynthesis vs. light intensity (P-I) relationships (Cibik *et al.* 1998a; 1998b), measurements of light attenuation with depth (CTD mounted 4π sensor) and incident light time series measurements (2π scalar irradiance on the roof of the MWRA lab building at Deer Island) were used to determine hourly production ($mgCm^{-3}h^{-1}$) at 15 min intervals throughout the 12 hr day for each sampling depth. Daily depth-dependent production ($mgCm^{-3}d^{-1}$) was determined by integration of hourly production over the course of the photoperiod. Areal production ($mgCm^{-2}d^{-1}$) was determined by integration of measured activity over the depth interval of the measurements. Calibrated chlorophyll-*a* profiles were used to compute chlorophyll-specific photosynthetic parameters.

An advantage of the approach is that effects of cloud-mediated fluctuations in light intensity over the course of the day and gradual variations in light due to changes of season are automatically incorporated into production computations. Light fields on cloudless days can be used to assess potential or maximal production and variations in light intensity between days can be used to determine more "realistic" daily production rates through seasons or years.

To minimize effects of aliasing of photosynthesis measurements due to a fluctuating light field, a 2π scalar light sensor (Biospherical QSR-240) was installed on the roof of the MWRA lab building at Deer Island for the continuous measurement of incident light beginning August 1996. Data were collected every minute and the average incident light recorded at 15-minute intervals. The 15-minute interval incident light measurements collected over the photoperiod 0600 - 1800 hrs were used for primary production computations. A Microsoft Quick BASIC 4.5 program was written for computation of the following parameters for Stations N04 and N18: a) daily production ($mgCm^{-3}d^{-1}$) vs. depth (1m intervals) over the season (resolved to the day), b) areal production ($mgCm^{-2}hr^{-1}$) vs. hour of day (resolved to 15 min intervals) over the season (resolved to the day), and c) daily areal production ($mgCm^{-2}d^{-1}$) over the season (resolved to the day). The program also computed areal production in upper 5 m and upper 10 m of the water column relative to areal P_{max}* (where P_{max}* = P_{max} · [chl*a*]) over the same depth intervals vs. hour of day (resolved to 15 min intervals). This computation yielded areal

production expressed as percent saturation vs. hour of day over the above indicated depth intervals. Details of the computations are described in Taylor (1998).

7.1.2 Seasonal Phytoplankton Production

7.1.2.1 Nearfield Production

Stations N04 and N18 were chosen in 1997 for evaluation of nearfield photosynthesis. The historical station N04 was continued to provide a control measure of the photosynthetic properties of the waters entering the nearfield from the northeast boundary region and provided continuity with measurements made in other years. The position and long-term data set for N04 make it a plausible reference station for post-relocation assessments of potential outfall effects. Station N18 was a new photosynthesis station located approximately 1.5 NM south of the outfall and near a previous high frequency station N16. N18 is in a region potentially affected by effluent from the new outfall as waters move southward with the general circulation.

Areal production in 1997 (Figure 7-1) was generally characterized (as in other years) by spring and fall blooms which exhibited an average 2-4 fold greater activity than during the summer, when stratification limits the supply of nutrients to the euphotic zone. The annual pattern of average photic zone chlorophyll (Figure 7-2) for N04 and N18 generally followed the trends in areal production. The dominant features in the chlorophyll record were the spring and fall blooms, which exhibited 3-9 fold increases in chlorophyll biomass relative to other times of year. The relative magntiude of productivity during the spring and fall blooms depended upon location within the nearfield. Production within the outer regions (N04) showed a stronger spring versus fall bloom, whereas in the central nearfield (N18) the fall bloom had the greatest activity of the year. One clear difference within the nearfield was in March (W9703) where a two fold decrease in both production activity and biomass was evident at station N18.

The spring bloom in 1997 was unique relative to the two previous years, in that it was numerically dominated by *Phaeocystis* rather than diatoms (1996) or diatoms and dinoflagellates (1995, see Section 8.1). However, there was a significant biomass contribution by centric diatoms (Figures 8-5 and 8-6). The spring bloom, beginning in early February and lasting through mid April, raised production from winter values of approximately 100-200 mgCm-2d-1 to a peak in late February of approximately 2,100 and 2,600 $mgCm^{-2}d^{-1}$ for N18 and N04, respectively (Figure 7-1). The magnitude of the spring bloom in 1997 was intermediate compared with 1996 (maximum ~3,000 $mgCm^{-2}d^{-1}$) and 1995 (maximum ~500 $mgCm^{-2}d^{-1}$). The same trends were evident for chlorophyll biomass (Figure 7-2), with spring maxima of around 0.7, 5.0 and 2.0 µg chlL-1 for 1995, 1996 and 1997, respectively.

Spring bloom production occurred predominantly in the upper 10m of the water column (Figure 7-3) and resulted in modest accumulation of chlorophyll in deeper waters (around 10-30m, Figure 7-4). Bloom phytoplankton visibly influenced water column nutrients, particularly biogenic silica (Figure 4-9e; see also Figures 7-14, 7-15), indicative of the relative activity of the centric diatom component of the bloom. The spring bloom during 1997 was apparently not as heavily grazed as it appeared to be in both in 1995 and 1996 (Cibik *et al.*, 1996; 1998c).

In those years, grazing appeared to result in a greater than ten-fold reduction in production, falling to annual lows of <100 $mgCm^{-2}d^{-1}$ and a virtual clearing of water column chlorophyll just prior to the onset of summer stratification. In 1997, bloom activity and biomass gradually diminished to levels characteristic of the stratified period due to nutrient limitation. Grazing may have been hindered by the presence of *Phaeocystis* and its gelatinous colonial morphology.

During the stratified summer period, beginning in mid to late April (see Section 3), production gradually increased from ~500-700 $mgCm^{-2}d^{-1}$ to ~1,000-1,500 $mgCm^{-2}d^{-1}$ just prior to the breakdown of stratification and onset of the fall bloom. The most predominant feature during early summer stratification was a subsurface accumulation of centric diatoms in mid May (Julian Day 125-142 in Figure 7-4, also see Figure 8-4). The subsurface maximum was somewhat deeper in the outer nearfield (~18-22m depth at N04) than at station N18 (12-18m depth). The shallower depth of the chlorophyll maximum at station N18 placed it into the 7-10% light level (Figure 7-5) and resulted in a detectable subsurface productivity maximum (Figure 7-3) that was large enough to influence areal production (Figure 7-1). In the outer nearfield (N04), however, the chlorophyll maximum was at the 1-2% light level and even though biomass was higher, production was not detectable either on a volumetric or areal basis (Figures 7-3 and 7-1, respectively). A small diatom/microflagellate bloomlet occurred in the upper 5-7 m of the water column in late June-early July (JD ~175-195; Figures 7-1,7-3, and 8-3), but did not result in very significant accumulations of biomass (Figure 7-4).

In terms of chlorophyll biomass, the most intense feature of 1997 was the fall bloom of centric and pennate diatoms (see Figures 8-3 and 8-4) which peaked in the first week of October (~ JD 282). This diatom bloom resulted in an abrupt 6-14 fold increase in organic matter in approximately two weeks (Figure 7-4) and persisted for approximately one month. The bloom appeared to be fueled by nutrients released at the onset of fall mixing (Section 4). The impact of the diatom production can be seen in the depletion of silicate in the euphotic zone during this interval. The activity of the bloom (Figures 7-1 and 7-3) was more intense and lasted longer in the central nearfield (N18, peak activity ~4,200 $mgCm^{-2}d^{-1}$, duration ~1.8 months) relative to that which occurred in the outer nearfield at N04 (peak activity ~2,300 $mgCm^{-2}d^{-1}$, duration ~ 1 month). The bloom dissipated as quickly as it appeared, returning to low winter production rates in 2-3 weeks.

7.1.2.2 Harbor Edge Production

Harbor edge production during 1997 (as represented by measurements at station F23) departed from data in previous years to a greater extent than all other stations studied over the past three years. The pattern of photosynthesis typical of this station in 1995 and 1996 was a relatively smooth increase in production from winter lows of ~300-500 $mgCm^{-2}d^{-1}$ to a summer peak of ~7,000-8,000 $mgCm^{-2}d^{-1}$ in July or August, subsequently followed by a return in fall to values of ~500 $mgCm^{-2}d^{-1}$. Annual production ranged in the vicinity of 900 $gCm^{-2}y^{-1}$, at least double that of any station in the nearfield except for inner nearfield station N10 (~650 $gCm^{-2}y^{-1}$), which is heavily influenced by periodic exchanges of Harbor water. The Harbor region was generally nutrient replete and production and biomass accumulation generally tracked seasonal temperature. In contrast to the nearfield, Harbor results typically exhibited no predominant spring or fall bloom.

Production during 1997 differed from previous years, being only around a third of the 1995-1996 norm (Cibik *et al.* 1996; 1998c). Harbor edge production smoothly increased as in past years (Figure 7-1) but attained a maximum production of only ~2,200 $mgCm^{-2}d^{-1}$, leading to an annual production of ~470-640 $gCm^{-2}y^{-1}$ or roughly equivalent to annual production in the central nearfield (N18, ~450 $gCm^{-2}y^{-1}$) and only ~40% higher than the outer nearfield (N04, ~350 $gCm^{-2}y^{-1}$). As in other years, there was some influence of temporal aliasing (see potential production in Figure 7-1), but it does not change the conclusion of significantly lower production in 1997. However, during 1997 it appeared that F23 did experience high activity around the time of the fall bloom.

It is apparent that the Harbor production is characteristically different than the stratified coastal environment, and that the magnitude and duration of the summer Harbor bloom, and the timing of the survey measurements dictate the relative degree of Harbor production documented in the HOM program. It is interesting to note that the production values obtained at F23 in 1997 are commensurate with values obtained in 1994 (Kelly and Turner, 1995; Kelly, 1997), further illustrating that production at the harbor edge is subject to large scale fluctuations in activity occurring on an interannual time scale. The low stream flows characteristic of 1997 (Section 3) may have also played a role in the lower harbor production.

7.1.2.3 High Temporal Resolution Production.

As was discussed in the 1996 annual report (Cibik *et al.*, 1998c), a potentially large source of uncertainty in the computation of annual production based upon a limited number of surveys (6 to 17 per year) is the effect of light field variability which can dramatically fluctuate from day to day. Calculations of maximum potential production based solely upon cloudless day incident light fields throughout the year attempts to set an upper limit on annual production, though aliasing can exist here as well (albeit to a lesser degree, Cibik *et al.*, 1998c). True annual production will of course lie somewhere below this upper limit because of cloud cover and fog.

To begin addressing the aliasing issue the MWRA set up an incident light monitoring station on the roof at the Deer Island treatment plant, which began continuous recording of data in late July 1996. These data were incorporated into the 1996 annual report for the calculation of primary production during the onset of the fall bloom. The effect of light field aliasing on the computation of seasonal production became immediately evident in these studies as, by chance, the last six surveys in 1996 happened to fall on cloudy days. The result was an underestimation of fall production by 60-70% when production was classically calculated from the day of survey light field, relative to production obtained using the light field measured in high temporal resolution (Cibik *et al.*, 1998c). For 1997, a nearly complete annual cycle of high temporal resolution measurements of light was available for calculating effects on estimates of primary production (with only a brief gap during which the sensor was taken out of service for calibration early in the year).

The high resolution light field data for 1997 are shown in Figure 7-6. The data are presented as integrated incident light (upper panel), which is the total light exposure in $Em^{-2}d^{-1}$ over a 24-hr day, and as a contour plot of light sensor readings ($\mu Em^{-2}s^{-1}$) vs. hour of day and day of year. Two major features are evident. First, there is an approximately two-fold reduction in incident light due to the gradual shortening of day length with the onset of winter. Cloudless day incident light ranged from >80 $Em^{-2}d^{-1}$ in June-July to ~40 $Em^{-2}d^{-1}$ in the winter months.

In the summer months over half of the photoperiod was exposed to light intensities ≥ 2,000 $\mu Em^{-2}s^{-1}$, which contrasts with December where the light intensities do not exceed much beyond 1,500 $\mu Em^{-2}s^{-1}$. Secondly, the light field was highly variable, with order of magnitude weather-related changes in incident light occurring from one day to the next or persisting for a week to 10 days. These fluctuations can, as will be seen later, result in 2-4 fold changes in areal production. Intra- (e.g., cloud patches) and inter- (e.g., morning/evening fogs) diel fluctuations are seen in the lower panel of Figure 7-6 and reflect the necessity of using natural light fields for computation of daily photosynthesis.

Parameters necessary for computation of high temporal resolution primary production are illustrated in Figures 7-7 and 7-8 for stations N04 and N18, respectively. The uppermost panel depicts the incident light field obtained from Deer Island and the data in the lower three panels were gridded from 1997 photosynthesis station survey data (17 times per year). Depth-dependent light attenuation, expressed as a percent (second panel), when coupled with the incident light time series provided a quantitative measure of the *in situ* light field. Observed major changes in light penetration are associated with large biomass accumulations that occurred as a result of the spring and fall blooms (Figure 7-4, JD ~95 and 283).

High resolution photosynthesis rates were determined from the temporal and depth-dependent a) *in situ* light field and b) distributions of α^* and P_{max}^* (third and fourth panels). The parameters α^* and P_{max}^* relate to the photosynthetic capacity of a given section of the water column and when combined with *in situ* light (I_Z) permit the calculation of volumetric production [$P(I_Z)$] at that depth according to the equation $P(I_Z) = P_{max}^*(1-\exp(-\alpha^* \cdot I_Z/P_{max}^*))$. Details of the calculations are discussed in Taylor, 1998. Available incident light data permitted computation of high resolution production for the entire 1997 field season, including both the spring and fall blooms and the summer stratified period.

It should be kept in mind that the potential for aliasing may not have been completely removed in the high resolution data set. As is shown in the mooring data in Figure 5-3, tidal fluctuations in water column chlorophyll content can vary 2-4 fold at certain times of the year (e.g., late May-early June; October) and on a time scale relevant to fluctuations in the light field. This concern may be tempered to some degree, however, as the chlorophyll field at the photosynthesis stations used for the high resolution computations (Figure 7-4) are quite similar in pattern and magnitude to average nearfield water column chlorophyll distributions computed for the nearfield (Figure 4-8c). Because of the time required for collection of the data, possible high frequency tidally mediated fluctuations tend to be averaged out.

Results of the calculation are shown in Figures 7-9 and 7-10. Photosynthesis is expressed on a depth-dependent basis over the season (second panels) and on an areal basis over the course of the photoperiod and season (third panels). Depth-integrated daily production is shown in more detail in Figure 7-11. The fluctuation in depth-dependent photosynthesis in response to day to day fluctuations in light field is clearly evident by the 2-5 fold variations in production contour depth (second panel). Because aliasing did not (by chance) greatly bias the low resolution data set in 1997, most major features of high resolution depth-dependent production were similar to those derived from survey light fields (Figure 7-3).

At station N04, however, aliasing did affect the representation of the subsurface production by diatoms in early to mid-May (JD ~130-140) by the lower resolution data set. The temporal and seasonal pattern of the light field is also clearly etched into areal production expressed over the day (third panels of Figures 7-9 and 7-10), though underlying changes in photosynthetic capacity (Figures 7-7 and 7-8) dominate in controlling the longer term magnitude of production (such as the major blooms and an apparent period of senescence following the fall bloom). Notice also the decrease in α^* and P_{max}^* and resultant low production.

The contour plots (panel 4 of Figures 7-9 and 7-10) indicate between 80-90% of the photoperiod was greater than 80% of light saturation on sunny days for major portions of the year in the upper 5m of the water column. Even in late fall when incident light was significantly reduced, major portions of the photoperiod exceeded 80% of light saturation. A similar overall pattern of light saturation was observed when the depth of observation was extended into the upper 10m (panel 5) of the water column, though light limitation began to become manifest during spring and fall bloom periods when light attenuation (see also Figure 7-5) due to scattering by accumulated biomass was evident. At station N18 the brief bloom in June (JD ~175-195) also resulted in some light attenuation but also was a period when photosynthesis quantum efficiency was lower (see also Figure 7-13).

Daily areal production using the high resolution light field for stations N04 and N18 (Figure 7-11) was compared with the same parameter determined on the days of the surveys using a) survey day light fields and b) an envelope of sunny day light fields for estimating potential production. As mentioned above, the pattern and magnitude of production was reasonably well represented by survey data in 1997, unlike that which occurred in 1996 where a large fraction of surveys were conducted on cloudy days and resulted in a significant misrepresentation of the fall bloom. Annual production estimated from the high resolution data set (Table 7-1) was 348 and 428 gCm^{-2} for stations N04 and N18, respectively. The high resolution values compare reasonably well with values obtained from day of cruise data (350 and 454 gCm^{-2} for stations N04 and N18, respectively). The fidelity of this comparison is circumstantial, however, and due to compensating over and under estimation of production at different times of year by the aliased lower resolution data.

Potential still exists for large error in production estimates based on survey data only, as the envelope over which fluctuating light influences the day to day magnitude of areal production spans a range of 2-5 fold (as was also the case in 1996 when aliasing resulted in large underestimates of the fall bloom). The envelope of sunny day production (Figure 7-11; Table 7-1) yielded an estimate of potential production of 457 and 547 gCm^{-2} for stations N04 and N18, respectively. It is interesting to note that the ratio between upper limit potential production and high resolution production is remarkably consistent between stations and years. For example, potential production was 31% and 28% higher than high resolution production for stations N04 and N18 in 1997, and 31% and 30% higher for stations N04 and N10 in 1996. If this ratio is truly stable from year to year it might find useful application for the estimation of true annual production from potential production estimates derived from theoretical cloudless day light fields. It may be possible, for example, to use this ratio and potential production estimates to assess if annual production derived from day of survey measurements are significantly biased by light field aliasing.

As in past years, around one half of total annual production occurred in the spring and fall blooms (~47% and ~59% of total production occurring over ~28% and ~42% of annual cycle for stations N04 and N18, respectively, Table 7-2). Average production over the stratified period was 932 and 1,305 $mgCm^{-2}d^{-1}$ for stations N04 and N18, respectively. Higher production at N18 probably reflected the placement of similar levels of chlorophyll biomass (Figure 7-2) somewhat higher in the water column (Figure 7-4) where higher light prevailed (Figure 7-5).

The seasonal pattern for α and P_{max} (i.e., chlorophyll-specific parameters) are shown in Figures 7-12 and 7-13. The pattern was similar to other years in that values hover in the 0.02-0.06 $gC(gChla)^{-1}h^{-1}(\mu Em^{-2}s^{-1})^{-1}$ and 5-14 $gC(gChla)^{-1}h^{-1}$ for α and P_{max}, respectively, over most of the water column and year. As in other years the general trend was for α and P_{max} to be higher in the upper water column and for the two parameters to generally co-vary. Dominant features throughout the year were the >2 fold increases in α and P_{max} during the onset of the spring and fall blooms (around 10-14 days prior to activity maxima and eventual biomass accumulation). The increases in photosynthetic efficiency related by these terms reflect increasing light availability in the spring (which occurred earlier at the more seaward station at N04, Figure 7-12, than at N18, Figure 7-13). Improvement in nutrient status brought on by transient upwelling events during the stratified period and the onset of the fall turnover (Figures 7-14 and 7-15) also produced similar increases in photosynthetic efficiency.

The observed tendency for the late winter bloom to begin offshore warrants further examination. Measurements of areal production during both 1996 and 1997 provide supporting data. In each year, the bloom was initially (late February) most intense at the offshore stations, with a well-defined gradient (1996: N04>N16>N10>F23; 1997: N04>N18>F23). The repeatability of this trend between years supports the contention that a general phenomenon such as a gradient in light penetration is the underlying factor. This is consistent with the measured beam attenuation data from the Boston-Nearfield transect in late winter (Cibik *et al*, 1998a; Murray *et al.*, 1998).

The late winter productivity associated with the bloom of the centric diatom *Thalassiosira* peaked in late February (~JD 50-70) when water column photosynthetic potential (α* and P_{max}*) was greatest (Figures 7-16 and 7-17). The intensity of the bloom was tempered (and perhaps terminated) by a sustained (~10 day) cloudy period at the beginning of March, where an approximate 2.5 fold reduction in daily light (Figure 7-6) resulted in an ~2 fold reduction in areal production. A subsequent bloom, which was numerically dominated by *Phaeocystis* but dominated with respect to biomass by the centric diatom *Chaetoceros*, began to intensify around W9703 (~JD 75), and peaked during W9704 (~JD 90, see Figure 8-3 and 8-4). Both α and P_{max} decreased to a minimum during the period, when the phytoplankton had significantly depleted the major nutrients, especially silicate (Figure 7-14 and 7-15). Low α and P_{max} contributed to lower water column photosynthetic capacity (Figure 7-16 and 7-17).

The rebound in photosynthetic activity at station N18 was largely in deeper water (Figure 7-17, JD ~90-100) because of the accumulation of chlorophyll biomass evident in Figure 7-15 (comprised of both *Phaeocystis* and *Chaetoceros*, Section 8.1). Because most of the biomass was below the 5% light level, however, effect on areal production was modest relative to surface activity. Results from station N04 did not mirror this increase as the

centric diatom biomass at depth was not seen there (see Figure 8-6) nor was there a similar elevation in chlorophyll concentration (Figure 7-14).

Water column nutrient concentrations rebounded somewhat by W9705 in late April (~JD 115, Figures 7-14 and 7-15) just prior to the onset of stratification. This appeared to result in increases in α and P_{max}, particularly in N04 surface waters (Figure 7-12). There was also significant increases in deep water photosynthetic capacity by survey W9706 in mid-May (~JD 135, Figures 7-16 and 7-17), producing the only substantial subsurface activity observed during 1997 (Figure 7-14 7-15) and a deep chlorophyll maximum consisting primarily of the centric diatom *Chaetoceros*.

In late June and early July (W9708, ~JD 180-220) there were substantial increases in α and particularly P_{max} corresponding with the surface bloom of the centric diatom *Rhizosolenia fragilissma* (Section 8.1). It appeared that this event was in response to increased surface nutrient availability (particularly silicate) in late June (W9707, ~JD 180, Figure 7-15), which may have been released by water column mixing (see Figure 3-2, Section 3.2). Water column instability and resultant upwelling of nutrients into the euphotic zone in mid September to early October (W9713, Figures 7-14 and 7-15; ~JD 260-280) resulted in the sharpest increases in α and P_{max} of the year (Figure 7-12 and 7-13). The onset of the fall bloom (Figures 7-16 and 7-17) and largest accumulation of chlorophyll biomass of the year ensued (Figures 7-14 and 7-15).

Senescence in the latter half of the fall bloom resulted in dramatic decreases in α and P_{max} (Figures 7-12 and 7-13; ~JD 280-300), low α^* and P_{max}^* and ultimately the lowest productivity of the year throughout the month of November (Figures 7-16 and 7-17; ~JD 310-340). The water column was thoroughly mixed by the end of October, dissipating the bloom and initially leaving a low biomass of a relatively photosynthetically inefficient population (Figure 7-16 and 7-17). Photosynthetic efficiency rebounded with availability of nutrients, and the water column returned to typical low winter production.

7.1.3 Modeling of Phytoplankton Production.

Development of a proxy measure of photosynthesis based upon routinely determined environmental variables has been an important goal of the HOM program. The model that has been the most thoroughly investigated is based upon correlating a composite parameter, BZ_pI_o, with measured ^{14}C-phytoplankton production (Kelly and Turner, 1995; Kelly, 1997), where B is the average photic zone chlorophyll *a* concentration, Z_p is the photic zone depth (BZ_p = chlorophyll *a* content of photic zone) and I_o is the daily incident light. The model is calibrated by linear regression to yield the equation:

$$P(^{14}C) = m \cdot BZ_pI_o + C \qquad \text{Equation 1}$$

where:

$P(^{14}C)$ = ^{14}C-primary production, [$mgCm^{-2}d^{-1}$]
m = slope; (P - C)/ BZ_pI_o, [$mgCm^{-2}(mgChla)^{-1}E^{-1}$]

BZ_pI_o = composite parameter, $[(mgChla)m^{-3} \cdot m \cdot Em^{-2}d^{-1} = (mgChla)m^{-2}Em^{-2}d^{-1}]$
C = intercept (ideally = 0), $[mgCm^{-2}d^{-1}]$

with the intent of being able to estimate the equivalent of ^{14}C-primary production given the slope term m. In the 1996 Annual Report (Cibik *et al.*, 1998c) it was shown that though the model is able to track general trends in activity, it poorly described production in quantitative terms. Calibration regressions varied by distance from shore and from year to year. Bloom events were misrepresented in time and magnitude, and calculation of annual production from modeled data was subject to large error.

Incorporated within the linear BZ_pI_o model are two inherent assumptions: a) that photosynthesis is on average light limited so that a fluctuation in I_o will result in a linearly proportional change in production and b) that water column chlorophyll *a* is equally efficient for organic carbon production over the spatial and temporal scale that the regression is computed (i.e., quantum efficiency is constant). Studies in the 1996 annual report showed that the regression was affected both by degree of light saturation and by relative photosynthetic efficiency of the resident phytoplankton (Cibik *et al.*, 1998c). The exercise did suggest, however, that if means were available to account for the effects of variability in photosynthetic efficiency, the simple BZ_pI_o model might be made applicable to real world photosynthesis.

Inclusion of an empirically derived or easily measured factor into the simple equation was considered, similar to the approach wherein the empirically determined fugacity coefficient is introduced into the ideal gas law to allow its application in the real world (i.e., at pressures greater than near vacuum). Re-inspection of the idealized BZ_pI_o regression equation (Equation 1) provided a possible suggestion:

$$\mathbf{P(^{14}C) = m \cdot BZ_pI_o} \qquad \text{Equation 2}$$

When ordinarily implemented the slope term, m, is defined to be a constant. Previous analysis indicated that m is really a variable whose magnitude can change quite dramatically (Cibik *et al.*, 1998c). Inspection of the units of m, $[mgCm^{-2}(mgChla)^{-1}E^{-1}]$, indicates that they are the same as those for depth-integrated α. If a proxy measure of depth-integrated α were easily obtainable for each station at various times of the year without the necessity of conducting ^{14}C-P-I incubations, equation 2 might be applicable as a proxy measure of primary production.

Over the past decade much has been gained in the understanding of the optical properties of photosynthesis. Subcellular physiological and biophysical events during photosynthesis can be sensed fluorometrically and expressed mathematically. For example, α is the product of two parameters that can be measured, the maximum quantum yield of photosynthesis (Φ_{max}; [mol CO_2 fixed (mol Photons)$^{-1}$ and a* the chlorophyll-specific spectrally averaged *in vivo* absorption cross-section [m2 (molChla)$^{-1}$] (e.g., Cleveland *et al.*, 1989). It is theoretically possible to use a standard fluorometer and the photosynthesis inhibitor DCMU to arrive at a parameter that is proportional to Φ_{max}.

The parameter, a fluorescence ratio (Fdcmu - Fo)/Fdcmu is the maximum change in the quantum yield of fluorescence ($\Delta\Phi_{max}$), and can be used as a surrogate index of Φ_{max} (Falkowski, 1992). Fo is determined by the

measurement of *in vivo* fluorescence as quickly as possible after introduction of dark adapted samples (~30 min in dark) into the fluorometer. After the reading is made DCMU is introduced into the sample, followed by exposure for ~ 1 min to white light to close all reaction centers by preventing the reoxidation of the electron carrier Q_A (discussed in Cibik *et al.*, 1998c). The fluorescence is again measured to determine the Fdcmu. The parameter a* can be obtained via specialized spectrophotometric absorption measurements made on phytoplankton samples entrained on glass fiber filters. These measurements are somewhat involved and must be conducted carefully, but are dramatically less labor intensive than the process of conducting ^{14}C-P-I incubation studies.

During the 1997 HOM surveys it was possible (with availible personnel) to make DCMU fluorescence measurements on the photosynthesis surveys where ^{14}C-production measurements were also being made. It was not, however, possible to also measure a*. Though both terms of the equation $\alpha \approx \Delta\Phi_{max} \cdot a^*$ would not be available it was hoped that the proportionality between α and $\Delta\Phi_{max}$ would be strong enough to reflect effects of change in nutrient status and season in a manner analogous to effects upon α derived from the ^{14}C measurements.

For station N04 in 1997 this seems qualitatively to be the case (Figure 7-18, upper panels). All major events leading to large increases in 14C-derived α, namely the onset of the spring and fall blooms and the apparent nutrient rebound (Figure 7-14) leading to an increase in α at the surface (~JD 115) were paralleled by similar changes in $\Delta\Phi_{max}$. Minima in α after the spring bloom when nutrients were transiently depleted (Figure 7-14, ~JD 80-100) and in deeper waters during the stratified period generally paralleled decreases in $\Delta\Phi_{max}$. At station N18 (Figure 7-19), similarity in the overall pattern of α and $\Delta\Phi_{max}$ was also evident, though fidelity was significantly reduced. Onset of the spring and fall blooms were generally reflected by increases in $\Delta\Phi_{max}$ but not nearly as well as at station N04. At the harbor edge station F23 correlation between the two parameters was poor (Figure 7-20).

To normalize depth integrated $\Delta\Phi_{max}$ to α for implementation in Equation 2, a regression was performed implementing the equation $\alpha \approx \Delta\Phi_{max} \cdot a^*$ on the assumption that the a* is on average constant, in much the same way that the slope term, m, in Equation 1 was assumed to be a constant in the BZ_pI_o regression. Unfortunately, but not unexpectedly, there is a large scatter about the regression line indicating that a* varies substantially throughout the season (Figure 7-21, upper panel). When the regression equation was applied to depth integrated $\Delta\Phi_{max}$ for normalizing to α (a* assumed constant) the two terms tracked one another with only modest fidelity (Figures 7-18 through 7-20, lowermost panels). When the normalized $\Delta\Phi_{max}$ term was applied to Equation 2 for estimation of production (Figure 7-21, lower two panels) agreement with measured ^{14}C production was essentially no better than that obtained with the original BZ_pI_o model, which was shown as unreliable for estimating production (Cibik *et al.*, 1998c). It appears that the normal experimental error in the determination of $\Delta\Phi_{max}$, when compounded with variability in a*, did not result in the desired incremental improvement in our ability to model production with bio-optically derived parameters.

Given the fact that $\Delta\Phi_{max}$ does show qualitative and semi-quantitative correspondence with measured changes in α, at least in the nearfield, there is hope that by expanding DCMU fluorescence studies to also include

spectrophotometric measurements of filtered phytoplankton samples to assess a*, the chlorophyll-specific spectrally averaged *in vivo* absorption cross-section, one might close in upon an approach for modeling coastal primary production using ordinary laboratory equipment and the standard water column property measurements undertaken during most monitoring studies.

7.2 Water Column and Sediment Respiration

Biological processes appear to be the primary drivers controlling oxygen balance throughout much of Massachusetts Bay. Primary production appears to be the dominant source of organic matter input hence the substrate for oxygen respiration (Section 7.1). Water column and sediment respiration are the dominant sinks for oxygen in Massachusetts Bay. More recent analysis indicates the importance of air-sea exchange in the oxygen balance of the surface water (Gerath *et al.*, in preparation). However, air-sea exchange acts primarily to vent photosynthetically produced oxygen during periods of high production, and to balance the oxygen saturation gradient produced by seasonal temperature variations. This physical process therefore supports the observed depletion of oxygen within the Bay water.

In systems like Massachusetts and Cape Cod Bays, water column respiration typically accounts for the majority of carbon mineralization (on an areal basis, m^{-2}). However, during stratification when oxygen depletion is a concern, oxygen uptake in bottom waters is more equally distributed between water column and sediments (Cibik *et al.*, 1996; 1998c). The increased relative importance of sediment oxygen uptake during stratification results from 1) a major reduction in the vertical transport rate of labile organic matter to support bottom water respiration compared with periods of vertical mixing; and 2) the differential "holding" times of organic matter in the water column versus sediments (i.e., particles fall through the water but are held in the sediments).

Particle retention by sediments allows periodic organic matter deposition events (usually following blooms) to exert an oxygen demand on bottom water for extended periods (months compared to days). In order to understand the carbon and oxygen dynamics of Massachusetts Bay and the factors that control bottom water oxygen depletion, water column respiration measurements were conducted within both the nearfield and Stellwagen Basin. Sediment respiration measurements (performed as part of the HOM Program Benthic Flux Monitoring) focused on depositional environments to determine seasonal dynamics and upper limits of sediment oxygen uptake through this pathway. Measurements focused on the vertical distribution of water column uptake rates, as well as sediment uptake, during the mixed and stratified water column periods to relate the fate of photosynthetically derived organic matter to the draw-down of bottom water oxygen levels (Section 6). To support these goals, detailed vertical studies of water column respiration were conducted in 1997 to define the relationship of this oxygen sink within sub-pycnocline waters. Integration of the productivity and respiration programs also supported development of a carbon balance (see Section 9) to ascertain the potential importance of allochthonous carbon inputs; and development of an oxygen balance from which to assess the potential for increases in oxygen deficits under changing organic matter inputs.

Both water column and sediment respiration are controlled by the availability of labile organic matter and the environmental temperature. These two loci of oxygen uptake differ primarily in their ability to "store" organic

matter while it is being re-mineralized. Organic particles typically have a relatively short life span (days-weeks) within the water column, as they are freely advected or sink to the bottom sediments. In contrast, organic particles reaching the sediments remain available for decomposition for months to years, with refractory compounds often permanently accumulating in depositional areas. The result is that water column rates of respiration at fixed locations typically show larger and more frequent temporal variations compared to sediment rates, which are buffered by the more constant nature of their organic matter pool. The following sections detail the major results of the water column (7.2.1) and sediment (7.2.2) respiration measurements within Massachusetts Bay through 1997.

7.2.1 Water Column Respiration

Water column oxygen uptake is dominated by the respiration of phytoplankton, zooplankton, and heterotrophic microorganisms. In regions of high inputs of reduced inorganic nitrogen (for example NH_4^+), autotrophic processes may also be important. Within the surface water of Massachusetts Bay, phytoplankton respiration and heterotrophic respiration currently predominate. Within the Bay's bottom water, heterotrophic respiration dominates and during stratification accounts for almost all of the respiratory activity. Measurements taken during 1997 represent the combined oxygen uptake by all of these forms, whereas oxygen inputs from all sources, including photosynthesis, are excluded by the incubation methodology.

Rates of water column respiration were determined in the same time series and locations in the nearfield (stations N04 and N18) and Harbor (station F23) as the primary production measurements (Section 7.1, Figure 1-2). In addition, profiles of respiration and associated water column parameters were collected in Stellwagen Basin (station F19). Measurements were made at three depths (surface, mid and bottom). During stratification, the upper two depths were generally within the surface mixed layer (at the surface and near the pycnocline) except in Stellwagen Basin. Also, given the importance of bottom water oxygen depletion to assessing system health, respiration was measured at additional depths below the pycnocline to allow better determination of the magnitude of water column respiration during stratification. Since oxygen depletion in Stellwagen Basin is one of the main focus points of the oxygen program, but only sampled 6-7 times throughout the year by the HOM Water Column Program, additional bottom water sampling was collected in concert with the four benthic flux surveys and included in this analysis.

Water column respiration was assayed using triplicate samples collected to determine initial conditions, and parallel triplicate bottles for incubation to determine oxygen uptake at each depth. Samples were kept at *in situ* temperatures in the dark. Since in open water rates of oxygen consumption are typically low due to carbon availability, care was taken to maintain "clean" incubation bottles. Bottles were acid washed (HCl) between surveys, and periodically "digested" with potassium persulfate to remove organic films. As a result, triplicate incubations typically had a C.V. of around 10%. Analysis of DO concentration was performed by Winkler reaction and potentiometric titration (Oudot *et al.*, 1988). Both respiration (in units of $uMO_2\ hr^{-1}$) and carbon-specific respiration ($uMO_2uMC^{-1}\ hr^{-1}$) rates at each of the sampling depths are presented below. Carbon-specific respiration was calculated by normalizing respiration rates to the total particulate organic carbon concentration (POC) measured in parallel with respiration in each sample. Carbon-specific respiration provides an indicator of how biologically available (labile) the POC substrate material is for microbial breakdown.

7.2.1.1 Vertical Distribution of Water Column Respiration

Respiration ranged from showing a weak (ca. two-fold) vertical gradient within the water column to a very strong gradient (>10 fold) from surface to bottom waters in both the nearfield (Figures 7-22 and 7-23) and Stellwagen Basin (Figure 7-24). Not surprisingly, the magnitude of the vertical gradient appeared to be controlled primarily by the degree of vertical mixing of the water column (see Figures 3-10 and 3-11). Temperature and organic matter production also clearly play an important role in the large differentials in respiration during stratification (Figure 3.1, Section 7.1). In general, the dramatic differential between respiration in surface versus bottom waters at all sites from spring through fall was the result of increased respiration in surface waters simultaneous with a small and variable decline in bottom water activity.

Water column respiration was not always uniform within the nearfield (Figure 7-23). Differences observed between stations were not consistent, but rather tended to follow the distribution of the rates of organic matter input through primary production (see Sect. 7.1 above, Figure 7-23). In general, the westernmost nearfield station (N18) showed slightly higher rates of oxygen uptake and photosynthesis than N04. This effect was most evident within the surface water during stratification, although about three quarters of the bottom water measurements also showed a similar relationship. However, these inter-station differences were not sustained throughout 1997, which is consistent with the general pattern in productivity (Figure 7-1).

The lack of a sustained difference between two stations that have potentially widely different relationships with the new outfall may support future analysis to assess post-relocation influences. Directly comparing water column respiration rates at these two stations throughout the year suggests a high degree of similarity (Figure 7-25). Since N04 has the best-documented photosynthesis and respiration rates within the current database, it may serve as a potential reference station for the central nearfield region. Obviously, a wider analysis is needed and several stations should be investigated, but the finding of similar rates of photosynthesis and respiration at two stations that nearly represent the extremes in potential effluent exposure within the nearfield suggests some opportunities for assessement.

Neither nearfield station typically showed higher surface respiration rates compared with the surface waters of Stellwagen Basin. However, respiration in the bottom waters during the stratified interval were generally slightly lower in the Basin than in the nearfield, most likely due to their greater depth (Figure 2-1) and lower temperatures (Figure 3-3). Greater depth allows for greater decay of organic particles as they transit the water column and supports lower temperatures that suppress decompositionl activity on the particles at depth. The most striking spatial difference was the clear difference in the nearfield versus Stellwagen Basin respiration data from the mid-depth samples. This apparent trend is not ecologically significant as it results fully from the fact that the mid depth samples in the Basin were collected below the pycnocline and represent the bottom water system (Figure 7-24), while the nearfield mid-water stations were collected above or at the pycnocline and thus are more indicative of the surface mixed layer (Figure 7-22).

During winter and early spring when the water column was unstratified, vertical structure in respiration rates depended primarily upon the ability of mixing to create a vertically homogeneous distribution of organic matter.

Although the water column is relatively isothermal during the mixed periods (Figures 3-1 and 3-3), it is clear that significant vertical heterogeneity exists in the particulate field. This vertical structure is evident in both the nearfield and Stellwagen Basin in key respiration-related parameters such as photosynthesis, chlorophyll *a* and POC (Figures 7-3, 7-4, and 7-26). In fact, POC levels were consistently higher in surface versus bottom waters all along the harbor to outer nearfield transect (Figure 7-26). It also appears that vertical differences in these organic matter source parameters are generally proportional to the observed vertical differences in oxygen uptake (Figures 7-22 and 7-24).

In the nearfield stations (N04 and N18), surface and bottom water respiration rates were relatively similar due to mixing, and increased during the late winter surveys (W9702- W9703) due to increased respiration rates from biomass created by the bloom. As the bloom senesced (W9703-W9704) respiration rates became constant throughout the water column, most likely due to sinking of organic matter into bottom waters and continued production at the surface. By April a consistent differential of several fold higher activity in surface versus bottom waters had developed which continued into the fall. This strong vertical respiration gradient is most likely controlled by differential water temperature and organic matter availability (Figures 3-3 and 7-26). These results indicate that even during the mixed interval, the substrate and biological processes controlling oxygen uptake within the water column are not uniformly distributed, but tend to be concentrated in the surface waters. Surface water respiration rates showed higher rates of oxygen uptake throughout the year.

It is notable that even during the mixed period, particulate organic matter levels (most likely photosynthetically derived) remain substantially higher within the surface than bottom water. It is clear that during the mixed interval, the POC distribution is the predominant factor generating the vertical gradient in water column respiration. However, the generally low absolute rate of respiration is likely the result of the low environmental temperatures during this interval. It also appears that "biological stratification" within the study area generally persists throughout both the (physically) stratified and mixed intervals.

The effect of mixing on the respiration rates can be clearly seen when comparing mid-depth and surface samples (both mixed layer), and surface and bottom waters (Figure 7-27). During the mixed interval, bottom water respiration is generally equivalent to the surface water rates. In contrast, during stratification bottom water falls significantly away from the equivalence line. It also appears that at the higher rates of surface water respiration which are in blooms, both the mid-depth and bottom water rates, tend to show lower rates than the surface. It is probable that the cause for this non-equivalence is that the higher rates result from the general concentration of blooms at the surface (see Section 7.1), with the carbon being "diluted" by mixing when the bloom senesces.

While vertical differences were evident in both the mixed (generally) and stratified (always) intervals, water column respiration rates during stratification were much more strongly depth-dependent, with mixed layer rates more than an order of magnitude higher than bottom waters. The higher rates within the upper layer appear to be the result of the higher POC levels and more than 10°C higher temperatures. In addition to the quantity of POC, the quality of the organic matter also favors higher respiration within the surface waters. By correcting the *in situ* rates for the variable POC levels (i.e., the carbon-specific respiration rate), it is possible to gain insight into variations in organic matter quality (i.e., lability) with depth (Figures 7-28 and 7-24).

During the mixed period, the water column is generally isothermal so that similarity in carbon specific rates over depth can only be the result of similar substrate quality. At these times it appears that accelerated delivery of POC to bottom water results in similar substrate quality (though not quantity) throughout the water column. During the mixed interval, bottom water carbon-specific respiration can exceed surface water rates (W9701-W9703 in Figure 7-28). However, during the stratified period, differences in substrate quality, in addition to substrate quantity and temperature, appear to be a primary factor supporting higher surface versus bottom water rates. In fact, the surface to bottom difference in carbon-specific respiration during the stratified interval is a factor of 2-3 higher than is typically due to temperature effects alone.

Additional support for the importance of organic matter quality/delivery is demonstrated by the spike in bottom water carbon-specific respiration during the August storms (see Section 3, Figure 3-2). The August (and subsequent) samplings of the nearfield showed elevated carbon-specific respiration at depth. This shift can be seen as an increase between surveys W9711 and W9712 in the carbon-specific rates of the bottom water. These results suggest that physical down mixing of substrate with increased lability may have been associated with the storm events. This may have taken the form of down mixing of surface waters or particles entrained near the pycnocline. The pycnocline showed a continuous deepening beginning with W9711 through de-stratification in late October.

It is possible to determine the relative importance of temperature versus organic matter quantity and quality effects on water column respiration by evaluating the relationship of carbon-specific respiration to environmental temperature. Nearfield and Stellwagen Basin stations exhibited a direct relationship between the rate of oxygen uptake per unit carbon and the environmental temperature (Figures 7-29 and 7-30), although the relationship is not equally apparent within each of the two regions. In the nearfield, a positive relationship appears only at the higher temperatures (ca. 8-20°C), which are predominantly data from the stratified interval and early fall. The reasons for this is currently unclear, but is likely related to the wide variation in carbon quality associated with the winter and early spring blooms, which obscures the effect of temperature at the lower range. In contrast, during the stratified interval, carbon quality may be relatively more constant and temperature effects therefore more apparent.

The results from Stellwagen Basin show a much clearer picture of the temperature effects. When the mixed layer data are analyzed, a clear linear relationship with temperature is seen with a calculated Q10 (over the temperture range 5 to 15°C) of 2.2 (compared to 2.9 for the combined 1995 and 1996 data alone). The lack of a relationship in the bottom water respiration in both the Basin and Nearfield is almost certainly due to large seasonal differences in organic matter quality (high during mixed period versus low during stratification), which again obscures the temperature effect. The results indicate that both temperature and substrate quality are responsible for the vertical structure in oxygen uptake in this system. The 10-fold differences in carbon-specific respiration in the bottom water within the same temperature regime (compared to the 2-3 fold temperature effect) is testament to the limitation of respiration by the quality of organic substrate. Therefore, during the interval when input of oxygen from surface waters is restricted, factors that increase either the delivery of labile organic matter to bottom water or bottom water temperature should serve to increase respiratory oxygen demands.

7.2.1.2 Interannual Comparison 1992-1997

Water column respiration rates were not a focus of study during the 1992-1994 monitoring effort. As a result interannual comparisons are limited. In addition, since respiration was measured on only six surveys, seasonal comparisons between years are not supported. Sufficient data do exist from 1994 (Kelly and Doering, 1995) from which to make some general observations. However, no bottom water respiration data were collected during 1994. The first year of comprehensive water column respiration measurements was 1995, so that most of the discussion will involve only 1995-1997 results.

Water column respiration within both the nearfield (stations N04 and N18) and Stellwagen Basin (F19) during 1997 showed similar patterns and rates at comparable stations in 1995 and 1996 (Figures 7-31 and 7-32). A single-event spike during the spring of 1995, attributed to a localized centric diatom bloom at Station N16, yielded the single-highest measurement during the three year period. While the rates in the nearfield varied throughout the year, respiration rates during 1997 were generally similar throughout the water column to those in 1996. During the stratified period, distinctly higher rates occurred in surface and mid-water versus bottom water as discussed previously, but the pattern again was repeated in each year of sampling. Similarly, Stellwagen Basin respiration rates were consistent between years, except for slightly higher rates in surface water in 1997. It is difficult to evaluate the significance of these potentially higher 1997 rates given the low frequency of the sampling.

While the data vary, surface water respiration rates within the nearfield in 1994, 1995, 1996 and 1997 were generally higher than offshore, consistent with the lower levels of chlorophyll a at the offshore stations (Figures 5-11 and 5-12). The relative constancy of overall water column respiration rates over the past three years agrees well with the pattern of measured organic matter pools (Figure 7-33). In addition, the general trend of significantly higher respiration rates in surface versus deeper waters was observed in all years. However, the vertical distribution of respiration rates was not as obvious in 1994 between nearfield and offshore stations (e.g., Figure 19 in Kelly and Doering, 1995). Unfortunately, the limited sampling does not allow a rigorous comparison of rates in mixed versus stratified water column. Specific problems with the earlier model-projected bottom water respiration in 1994 (Kelly and Doering, 1995) have been discussed elsewhere (Cibik *et al.* 1998c). In short, data support for the model was insufficient and underlying assumptions not supported as indicated by the additional data from the more detailed program.

While the individual respiration measurements are temporally variable, the rates of bottom water respiration during the stratified interval are relatively constant within both the nearfield and Stellwagen Basin over the three high frequency monitoring years. Similarly, surface and mid-water respiration rates show similar ranges and seasonal patterns between years. Since respiration is a key process being related to both photosynthesis and oxygen depletion and since it appears to be relatively consistent between years, it may represent a relatively robust indicator of organic matter enrichment in this system. The difficulty will be that seasonal measurements will need to be compared rather than individual measures.

7.2.2 Sediment Respiration

Annual oxygen uptake by benthic sediments is a measure of total community metabolism which controls organic matter turnover within the benthos. Total community metabolism includes the respiration of benthic animals and plants as well as carbon remineralization by heterotrophic microorganisms. Sediment respiration is similar to water column respiration in that it is controlled primarily by the availability of respirable organic matter and *in situ* temperature. However, it differs in three major aspects. First, sediments can accumulate organic matter inputs over relatively long periods and therefore allow cumulative increases in oxygen demand as organic matter is deposited over periods of weeks to months. Organic particles within the water column typically have relatively short residence times, especially in the non-turbulent waters below the pycnocline. Therefore, deposition into sediments represents the mechanism for potential carryover of fall or spring bloom material into the stratified period.

Second, the water column throughout the nearfield and Stellwagen Basin appears to be fully oxygenated, whereas oxygen penetration into the sediments of these systems is relatively shallow (centimeters). The result is that in the sediments, unlike the water column, a fraction of the organic matter decay is through anaerobic microbial processes such as denitrification and sulfate reduction. Denitrification, although at present not a major pathway for carbon mineralization, represents an important potential sink for fixed nitrogen, particularly if concentrations of nitrate in the overlying water increase (Section 4). Within deeper sediments, sulfate reduction produces sulfide as an end-product, some of which is permanently stored within the sediments as metal sulfides but most of which is re-oxidized to sulfate on an annual basis. However, due to the time-lag between sulfide formation in the deeper anoxic layer and oxidation of sulfide by surface exchanged oxygen, single time-point estimates of the rate of surface oxygen uptake can either over- or underestimate the rate of carbon mineralization taking place. In most systems, an amount equivalent to the mass of sulfide produced over the course of a year is oxidized each year (except for that permanently buried), thus the annual oxygen uptake rate reflects the annual carbon remineralization rate.

Furthermore, in systems like Massachusetts Bay, carbon flow through sulfate reduction is almost certainly small relative to aerobic processes and therefore errors due to the sulfide oxidation time-lag are likely very small even on single time-point samples. Increases in the mass of total reduced sulfur and/or non-pyritic reduced sulfur over several years has been suggested as an indicator of an increase in the rate of organic matter loading to sediments. While reduced sulfur pools can reflect loading rates, they represent the residue of the much larger reduction-oxidation cycle. In contrast, annual sediment oxygen uptake rates represent the total carbon remineralization rate, which should be a direct indicator of the annual loading of decomposable organic matter to the benthos.

Third, while both water column and sediment oxygen uptake affect bottom water oxygen levels, water column uptake is distributed throughout the hypolimnion, whereas sediment uptake is concentrated at the sediment-water interface. Only through mixing, diffusion, etc. does sediment oxygen uptake interact with the full hypolimnion. The result is that the deepest waters of a system typically contain the lowest concentrations of oxygen on an annual basis (see Section 6). The increased distance from the oxygen "source" in the overlying mixed layer further influences this phenomenon. In addition, sediment oxygen dynamics are important on an ecological basis

in that where low oxygen or high sulfide levels occur, infaunal populations, hence food chain dynamics are affected.

For these reasons, and the fact that sediments can be reliably re-sampled over a prolonged interval, sediment oxygen and nutrient dynamics have been measured over several years in the monitoring program. In 1995, 1996 and 1997 in concert with the detailed water column respiration and photosynthesis measurements, sediment respiration was assayed at four stations during five events (1995 & 1996) or three stations during four events (1997). Issues to be addressed involve the role of sediments (along with water column respiration) in system carbon/nutrient mineralization and bottom water oxygen depletion, and their sensitivity as an indicator of organic matter loading rates.

Sediment oxygen uptake within the sediments of the western nearfield and Stellwagen Basin show a seasonal cycle linked to temperature and organic matter availability. All sites showed increasing oxygen uptake with initially increasing bottom temperatures (Figure 7-34). However, the overall pattern of respiration differed in some major respects between the years. Although in the nearfield the rates of oxygen uptake during the stratified interval compared well between 1995 and 1996, different rates were evident during the mixed interval. In 1996, during winter and early spring the sediments were about two times as active as during 1995. In contrast, during the late fall mixed interval, all of the stations showed a decline in rates not seen in 1995, even under steadily increasing temperatures.

The bottom water temperature cycle was very different from that of the surface waters (see Section 3). Maximum temperatures in surface water occur during late summer during stratification while maximum temperatures in bottom water occur after stratification as warmer surface water mixes downward. 1997 temperature maxima were observed in late October and early December in the nearfield and Stellwagen Basin respectively (Figure 3-4). The significantly higher rates of respiration at these sites in 1997 may have been associated with settling and storage of the large subsurface *Chaetoceros* bloom documented in mid-May (and perhaps remnants of the *Phaeocystis* bloom as well). The higher peak rates (at temperatures comparable to previous years) suggest an increase in organic matter availablity enhanced sediment heterotrophic activity (Figure 7-34).

It is the interplay of organic matter delivery and temperature that generates the seasonality in sediment respiration. The effect of the temperature cycle is to produce the highest rates of respiration during the stratified period and fall and lower rates during the winter and early spring prior to stratification. The effect of the colder pre-stratification water should be to help to "preserve" freshly deposited spring bloom material until waters warm. This warming occurs following stratification. This would be the likely process supporting the enhanced rates in 1997 driven by the very large *Chaetoceros* and *Phaeocystis* blooms. The effect of the warmer sediments during the fall bloom should be to promote the degradation of freshly deposited bloom material. Given the temporal sequence, much of the fall bloom is likely degraded prior to the onset of stratification during the following spring and summer.

Since water column mixing occurs at the fall bloom (and is intimately associated with it, Sections 4 and 7.1), the effect of the fall bloom on the bottom water oxygen deficit is unclear. The data suggest that the significantly

larger spring blooms in 1996 and 1997 may have been responsible for the higher rates of sediment remineralization during the first half of the year in 1996 and during the stratified interval in 1997, compared to the same period in 1995. These high rates of decay appear to have consumed much of the deposited labile pool from the spring bloom by the end of the stratified period as evidenced by the slowing or declining respiration even as temperatures continued to rise. Modeling of oxygen within the nearfield indicates that the effects of oxygen uptake by sediments and the water column are distributed throughout the sub-pycnocline waters. Therefore, the effect of these higher rates of sediment respiration on bottom water oxygen depletion will tend to be "diluted" by through the bottom water volume (Gerath *et al.*, in preparation).

Given the significance of benthic respiration to the overall bottom water oxygen balance during stratification, as well as the seasonal distribution of rates, it appears likely that the spring bloom plays a more important role in oxygen deficits than the fall bloom. As stated for water column respiration (section 7.2.1.2), factors that increase delivery of organic matter through the pycnocline during stratification should result in increased levels of annual oxygen depletion in bottom water in both the nearfield and Stellwagen Basin. Before it is possible to determine the proportional increase in oxygen deficit per unit carbon deposited, an evaluation of the potential lability of the organic matter delivered must be evaluated.

7.2.3 Cycles of Carbon Fixation, Remineralization and Oxygen

While water column mixing and stratification play the major role in mediating the vertical distribution of respiration rates through temperature and organic matter delivery, the ultimate factors controlling respiration is the timing and mass delivery of labile organic matter input from both photosynthesis and allochthonous sources. While the role of allochthonous sources requires further examination, it is clear that respiration within the euphotic zone generally parallels the measured rate of carbon fixation (Figure 7-31). Departures from this trend typically are related to bloom events where production typically exceeds respiration (and sinking), which allows biomass to increase (Figure 7-35). However, major photosynthetic events do show increases in respiration rates due to both increased plant respiration and heterotrophic respiration associated with the increased size and lability of the organic matter pool. This bloom effect is typically strongest in the fall bloom, most likely due the warmer temperatures (ca. >10°C) under which it occurs. But it is during the summer stratified interval, when organic matter pools are low (Figure 7-33), that the closest coupling is seen between respiration and photosynthesis (Figure 7-31).

It is clear that water column respiration tracks phytoplankton production, supporting the contention that *in situ* production is the primary source of substrate for oxygen demand in this system. While the source of substrate is undoubtedly similar between water column and sediments, the ability of sediments to store organic matter produces a temporal "disconnect" between production and remineralization. The "excess" production over respiration in the water column (Figure 7-35) is the likely source of the sediment organic matter. It is notable that at the highest rates of production, the "excess" carbon is proportionally the greatest, again supporting the contention that the spring (and possibly fall) bloom is the major organic matter source for sediment respiration during stratification.

Given the variability in daily photosynthesis with light field (Section 7.1) relative to the greater temporal averaging which occurs in the factors controlling respiration rates, the photosynthesis/respiration relationship observed within the euphotic zone is reasonable. Although variable, it appears that carbon fixation exceeds respiration within the euphotic zone throughout the year, but also that *in situ* respiration remineralizes an amount nearly equivalent to fixation. As noted in the previous section, since almost all of the carbon fixed by photosynthesis occurs within the mixed layer, both organic matter quantity and quality are always highest within this zone (Section 7.1).

The near equivalence in organic matter production and remineralization within the euphotic zone (predominantly within the mixed layer), serves as a "biofilter", reducing organic matter transport to bottom waters during stratification. The lower bottom water respiration rates found throughout the nearfield and offshore stations during stratification are consistent with a low delivery of organic matter (Figures 7-22 and 7-24). However, as stated above, factors that increase organic matter delivery can increase oxygen uptake from bottom waters. Such events have been seen in previous years in association with diatom blooms or short-term breakdown of stratification, which provides a mechanism for increased vertical transport. However, it is also possible that the high zooplankton grazing can also facilitate vertical transport through fecal pellet formation to the extent to affect respiration (Cibik *et al.*, 1996).

Under existing conditions, seasonal variations in bottom water oxygen uptake appear to be dominated by the availability of organic matter (with secondary temperature effects). High rates of bottom water respiration occur during the unstratified intervals, when vertical transport of POC is uninhibited and carbon fixation from the high productivity periods (i.e., late winter and fall blooms) is greatest. In contrast, during the stratified period, bottom water respiration remains low. During stratification, the vertical transport of organic matter to deeper water is restricted both by the strong pycnocline and by the significantly increased respiratory capacity of the surface waters due to the warmer summer temperatures (Q10=2-3). However, it is becoming clear that during the stratified interval, there is a highly labile organic matter pool within the surface mixed layer and that large increases in bottom water respiration result when physical processes enhance the vertical transport of this pool. This conclusion is supported by the observed stimulation of bottom water respiration associated with short-term mixing and advection events, and the onset of fall de-stratification. Support for this conclusion has been seen in each year, with the increased respiration associated with the August storms in 1997 being the most recent example. This response is consistent with strong vertical gradients in both the quality (Figure 7-28) and quantity (Figure 7-26) of organic matter within the water column. It appears that oxygen dynamics within the nearfield during stratification, while controlled in part by the onset and duration of stratification are also strongly influenced by the timing and extent of organic matter delivery to the bottom waters and sediments.

Another gauge of the influence of water column respiration on POC transport can be derived by analyzing vertical profiles (Figure 7-36a-c). It is notable that water column respiration tracks temperature more than POC even within a single profile (Figure 7-36a and b). In addition, these data indicate for the first time that water column respiration is relatively uniformly distributed below the pycnocline. Until these measurements, a linear interpolation was sometimes used between mid and bottom measurements to calculate water column production.

It now appears that this approach will result in an overestimate of water column respiration and that a more accurate approach would be to use the bottom water values to represent the sub-pycnocline region.

Estimates of the time required to remineralize all of the water column POC pool at various depths can be derived from the measured pool and respiration data (Figure 7-37). While this approach is almost certainly an underestimate of the turnover time, it provides a good indicator of the fate of organic matter in this system. It appears that within the surface mixed layer that respiration is active enough to consume most of the organic matter before it is lost from this layer. In contrast, organic matter below the pycnocline is relatively "stable" with turnover times of more than 2 weeks, a seemingly excessive time to expect a particle to remain suspended at depth.

It appears that since about 90% of the POC is generated near the surface that mixing and respiration are sufficient to prevent it from reaching the sediments. However, POC which is produced *in situ* or penetrates the pycnocline will not be remineralized within the water column but will likely enter the sediment carbon cycle. This observation appears to be independent of station, which would be expected given the common source of the POC. Entry of additional organic particles with properties similar to those present within the sub-pycnocline region may also be expected to enter the sediments. Stimulation of sub-pycnocline photosynthesis represents such input. In addition, given the small amount of existing primary production to enter the sediments, a relatively small increase in sub-pycnocline production may have a disproportionate influence on the oxygen cycle.

While the major site of organic matter decay throughout the year is in the water column, particularly in the mixed layer, the sediments become relatively more important during stratification due to the "starvation" of bottom water by reduced organic matter transport through the pycnocline (Figure 7-36). The importance of the sediments to the stratified interval DO decline varies inversely with the depth of the water column. In the nearfield, sediments account for approximately half of the oxygen uptake in the bottom water during stratification (Cibik *et al.* 1998c, table 7-3). The relative contribution of SOD to bottom water oxygen declines in Stellwagen Basin is lower than the nearfield (approximately one-third of observed uptake). In the nearfield region in 1995 and 1996 measured respiration rates were only moderately higher (22%-58%) than the observed oxygen depletion rate during stratification. This is expected since (a) there is ventilation of bottom waters (Gerath *et al.*, in preparation) and (b) sediment respiration for depositional areas is used as the average benthic oxygen uptake rate.

However, in 1997 respiration was 2.4 fold higher than the observed oxygen decline. The most likely cause of his mismatch is that there appeared to be a major intrusion of DO-rich water during the stratified interval (see Section 6). This event can be seen in the large increase in measured DO in July. This event was critical to maintaining oxygen levels as both the bottom water and sediment respiration rates were the highest of the past three years, which if 1995 or 1996 conditions had occurred would have resulted in one of the lowest oxygen minima on record. It is likely that the higher rates of respiration resulted from the settling of the *Chaetoceros* and *Phaeocystis* bloom, possibly supported by sustained production during summer.

7.2.4 Nutrient Recycling

Given the concerns about potential trophic change due to altered nutrient loading with the outfall relocation, further examination of the existing nutrient budget is warranted to fully elucidate baseline conditions. The baseline monitoring record has provided increased understanding into the relative roles of *in situ* production and respiration, as well as the important role played by physical forcing (stratification, mixing, and advection). Building on this knowledge, an examination of the relative role of in situ nutrient regeneration to primary production in the nearfield was undertaken.

If it is assumed that the removal of nutrients in the nearfield from the winter high to the spring low is due to primary production, then the net water column primary production rates for the period can be calculated. This approach can be used for each phytoplankton nutrient DIN, DIP, and Si04). The reliability of this approach is maximized if the selected time frame is constrained to a period of active productivity (when nutrients are being rapidly utilized), and where sufficient temporal data coverage is available. For evaluations of the nearfield region of Massachusetts Bay, the optimal period is the late winter/spring bloom.

Table 7-4 summarizes the nutrient removal rates (uptake rates) during the late winter/spring bloom period during 1997. Also shown are the calculated average daily carbon fixation rates (primary production) based on estimated nutrient ratio of C:N:P:Si of 106:16:1:16. The C:N:P ratios are the traditional Redfield ratios (Redfield *et al.*, 1963), while the N:Si of 1:1 is based on previous observations that the distribution of DIN and silicate concentrations fall on a 1:1 ratio line during the spring bloom (Cibik *et al.* 1998c). Calculations were done for the interval between each of the four surveys conducted during the bloom period, as well as for the changes occurring between surveys 1 and 4. All data were taken from the nearfield-averaged data set as used in Figures 4-1 to 4-3. The surface estimates were based on an average of the surface concentrations and the depth above the mid-depth sample. Bottom estimates were based on an average of the bottom values and the depth below the mid-depth sample to a depth of 35m (the approximate average depth of the nearfield area).

Although removal rates were usually similar in the surface and bottom layers during the 1997 late winter/spring bloom, there were sufficient differences to warrant that separate surface and bottom layer rates be used to calculate the water column integrated averages for production (mg $Cm^{-2}d^{-1}$) listed in Table 7-4. This was accomplished by multiplying the estimated primary production rates based on volume ($mgCm^{-3}d^{-1}$) times the average water depth (m) for each layer and adding the surface and bottom results. The near parallel removal in surface and bottom water of nitrate + nitrite (165 $mgCm^{-2}d^{-1}$ vs. 163 $mgCm^{-2}d^{-1}$) and silicate (181 $mgCm^{-2}d^{-1}$ vs. 192 $mgCm^{-2}d^{-1}$) is typical of a diatom-dominated spring bloom in this region. The overall total water column daily production rate based on an average of individually calculated rates for DIN, phosphate and silicate was 356±15 $mgCm^{-2}d^{-1}$, or a total of approximately 20.8 g Cm^{-2} for the 57 day spring bloom period.

The importance of nutrient regeneration and recycling within the water column to photosynthetic production is underscored by comparison of productivity based on nutrient uptake during the spring bloom (Table 7-4) with the direct measurements of primary production (Section 7.1). Again, results in Table 7-4 estimated the amount of carbon fixed based upon the rate of uptake of DIN, phosphate and silicate from the water column surveys,

assuming proportionality with the Redfield ratios and that declining nutrient levels resulted solely from photosynthetic uptake. The average production estimated for this 57 day interval (~21 gCm^{-2}) is around one-fifth of the measured rate of primary production during this interval (ca. 100 gCm^{-2}), and around 15 percent of the potential production (ca. 135 gCm^{-2}, Figure 7-11). The reason for this apparent discrepancy is that the static Redfield approach does not account for recycling of nutrients within the system. Assuming that a substantial portion of the "missing" nutrients is not being imported, this analysis indicates that nutrients regenerated by water column respiration would account for most of the nutrients required to support photosynthesis during the spring bloom. This is consistent with the directly measured respiration rates which are sufficient to account for more than half of the missing nutrients required to support the measured photosynthesis.

A further example of the importance of nutrient recycling is in the stratified summertime water column. Nutrient regeneration during the mixed interval is relatively uniformly distributed throughout the water column (Section 7.2). The strong nutrient depletion in surface waters at the onset of stratification is a result of nutrient uptake by phytoplankton. Replenishment of surface water nutrients occurs through either horizontal or vertical transport (with the latter including atmospheric deposition), or through recycling. It is reasonable to assume that replenishment via transport would be similar to that during the early season bloom period. However, the relative absence of nitrogen and other dissolved nutrients in the surface layer, the sustained productivity levels (ca. 1,000 $mgCm^{-2}d^{-1}$, Figure 7-11), and the increasing zooplankton abundance throughout the period (Section 8.2) all attest to a very dominant role for nutrient recycling during stratification. For example, based on water column respiration and production rates in the surface layer during the stratified periods of 1995-1997, generally more than two-thirds of the carbon fixed was respired in the surface layer. This process yields an equivalent amount of dissolved nitrogen and phosphorus for continued in situ production in the surface layer.

Finally, Table 7-5 summarizes the nutrient loss or removal rates (uptake rates) during the spring bloom period for the years 1992 to 1997 calculated in a similar manner. Although there is significant scatter in these averaged uptake rates, during three of the years shown (1992, 1995, and 1997), the rates were lower and were less variable than during the other three years. Interestingly, large spring blooms of *Phaeocystis pouchetii* (1992 and 1997, Section 8.1) characterized two of these years. The inherent annual variability in nutrient uptake (and associated production), coupled with the apparently dominant role of nutrient recycling in the water column, emphasizes the need for integrated analyses of water chemistry and biological rate measurements.

Table 7-1. Areal production ($gCm^{-2}y^{-1}$) in 1997.

Measurement	Station N18	Station N04
Production on Day of Cruise	454	350
Potential Production Envelope	547	457
High Resolution Production	***428***	***348***

Table 7-2. Relative contribution of seasonal events to annual production.

Station	Event	Julian Days	Production	Percent
N04	Spring Bloom	41-90	97	28
	Stratified Period	~91-262	162.7	47
	Fall Bloom	263-318	68.1	19
	Winter	1-41; 319-365	~20.2	6
N18	Spring Bloom	41-114	93.3	22
	Stratified Period	~115-235	159.1	37
	Fall Bloom	236-318	157.1	37
	Winter	1-41; 319-365	~18.5	4

TABLE 7-3

Massachusetts Bay Oxygen Dynamics: Stratified Interval

Year	Observed Btm Water D.O. Decline (mg/L/d)	Watercolumn Respiration Potential Decline (mg/L/d)	Sediment Respiration Potential Decline (mg/L/d)	Ratio Potential/Observed
1992	0.024			
1993	0.025			
1994	0.031			
1995	0.027	0.0168	0.0161	1.22
1996	0.025	0.0182	0.0213	1.58
1997	0.020*	0.0226	0.0262	2.44

* D.O. "intrusion" year

TABLE 7-4

Spring bloom primary production rate estimates based on different nutrient removal rates during Surveys 1-4 for all nearfield stations, 1997. See text for calculation details.

Survey #	Julian Date	• Days	Aver. N+N (μM)	• N+N (μM)	• N+N per day (μM/d)	Est Prim Prod (mg C/m^3/d)	Avg Dep (M)	Est Prim Prod (mg C/m^2/d)	Total Water Col Prod(mg C/m^2/d)
Surf 1	33		9.00				16.6		
Surf 2	57	24	5.68	-3.32	-0.138	11.0	16.3	180	
Surf 3	76	19	4.50	-1.18	-0.062	4.9	15.6	77	
Surf 4	90	14	1.72	-2.79	-0.199	15.8	16.2	257	
			Ave. for whole spring bloom period:	-7.28	-0.128	10.2	16.2	165	
Bot 1	33		8.89				18.4		Surf + Bottom
Bot 2	57	24	6.93	-1.96	-0.082	6.5	18.7	121	301
Bot 3	76	19	4.70	-2.22	-0.117	9.3	19.4	181	258
Bot 4	90	14	2.67	-2.03	-0.145	11.6	18.8	217	474
			Ave. for whole spring bloom period:	-6.22	-0.109	8.7	18.8	163	
								Ave prod for whole period	328
Survey #	Date	• Days	Aver. DIN (μM)	• DIN (μM)	• DIN per day (μM/d)	Est Prim Prod (mg C/m^3/d)	Avg Dep (M)	Est Prim Prod (mg C/m^2/d)	Total Water Col Prod(mg C/m^2/d)
Surf 1	33		10.59				16.6		
Surf 2	57	24	6.17	-4.43	-0.184	14.7	16.3	240	
Surf 3	76	19	6.00	-0.16	-0.009	0.7	15.6	11	
Surf 4	90	14	2.17	-3.83	-0.274	21.8	16.2	353	
			Ave. for whole spring bloom period:	-8.42	-0.148	11.8	16.2	190	
Bot 1	33		9.79				18.4		Surf + Bottom
Bot 2	57	24	7.39	-2.39	-0.100	7.9	18.7	148	388
Bot 3	76	19	6.28	-1.12	-0.059	4.7	19.4	91	101
Bot 4	90	14	3.59	-2.69	-0.192	15.3	18.8	287	641
			Ave. for whole spring bloom period:	-6.20	-0.109	8.7	18.8	163	
								Ave prod for whole period	353
Survey #	Date	• Days	Aver. PO_4 (μM)	• PO_4 (μM)	• PO_4 per day (μM/d)	Est Prim Prod (mg C/m^3/d)	Avg Dep (M)	Est Prim Prod (mg C/m^2/d)	Total Water Col Prod(mg C/m^2/d)
Surf 1	33		0.92				16.6		
Surf 2	57	24	0.70	-0.22	-0.009	11.9	16.3	195	
Surf 3	76	19	0.66	-0.04	-0.002	2.4	15.6	37	
Surf 4	90	14	0.42	-0.24	-0.017	21.4	16.2	348	
			Ave. for whole spring bloom period:	-0.50	-0.009	11.1	16.2	179	
Bot 1	33		0.91				18.4		Surf + Bottom
Bot 2	57	24	0.79	-0.12	-0.005	6.1	18.7	114	308
Bot 3	76	19	0.68	-0.12	-0.006	8.0	19.4	155	192
Bot 4	90	14	0.52	-0.15	-0.011	14.0	18.8	263	612
			Ave. for whole spring bloom period:	-0.39	-0.007	8.7	18.8	163	
								Ave prod for whole period	343
Survey #	Date	• Days	Aver. SiO_4 (μM)	• SiO_4 (μM)	• SiO_4 per day (μM/d)	Est Prim Prod (mg C/m^3/d)	Avg Dep (M)	Est Prim Prod (mg C/m^2/d)	Total Water Col Prod(mg C/m^2/d)
Surf 1	33		9.45				16.6		
Surf 2	57	24	4.26	-5.19	-0.216	17.2	16.3	281	
Surf 3	76	19	3.30	-0.96	-0.051	4.0	15.6	63	
Surf 4	90	14	1.45	-1.85	-0.132	10.5	16.2	171	
			Ave. for whole spring bloom period:	-8.00	-0.140	11.2	16.2	181	
Bot 1	33		8.98				18.4		Surf + Bottom
Bot 2	57	24	5.60	-3.38	-0.141	11.2	18.7	209	490
Bot 3	76	19	3.48	-2.12	-0.112	8.9	19.4	173	235
Bot 4	90	14	1.67	-1.81	-0.130	10.3	18.8	193	364
			Ave. for whole spring bloom period:	-7.32	-0.128	10.2	18.8	192	
								Ave prod for whole period	373

TABLE 7-5

Average Nutrient Uptake Rates for 1992-1997 Spring Bloom Periods

All uptake Rates are in µmoles liter^{-1}d^{-1}

	Year	Julian Day Start	End	Days	DIN	NH4	N+N	PO4	SiO4
#	1997	33	90	57	0.128	0.01	0.118	0.007	0.139
*	1996	40	79	39	0.232	-0.001	0.233	0.016	0.344
#	1995	99	136	37	0.153	0.005	0.148	0.01	0.094
*	1994	66	83	17	0.385	-0.002	0.387	0.024	0.308
*	1993	84	100	16	0.298	0.034	0.264	0.02	0.355
#	1992	57	102	45	0.137	0.008	0.129	0.004	-0.105
	***Rapid** growth yrs. Average:*				0.305	0.01	0.295	0.02	0.336
	***#Slow** growth yrs. Average:*				0.14	0.008	0.132	0.007	0.041

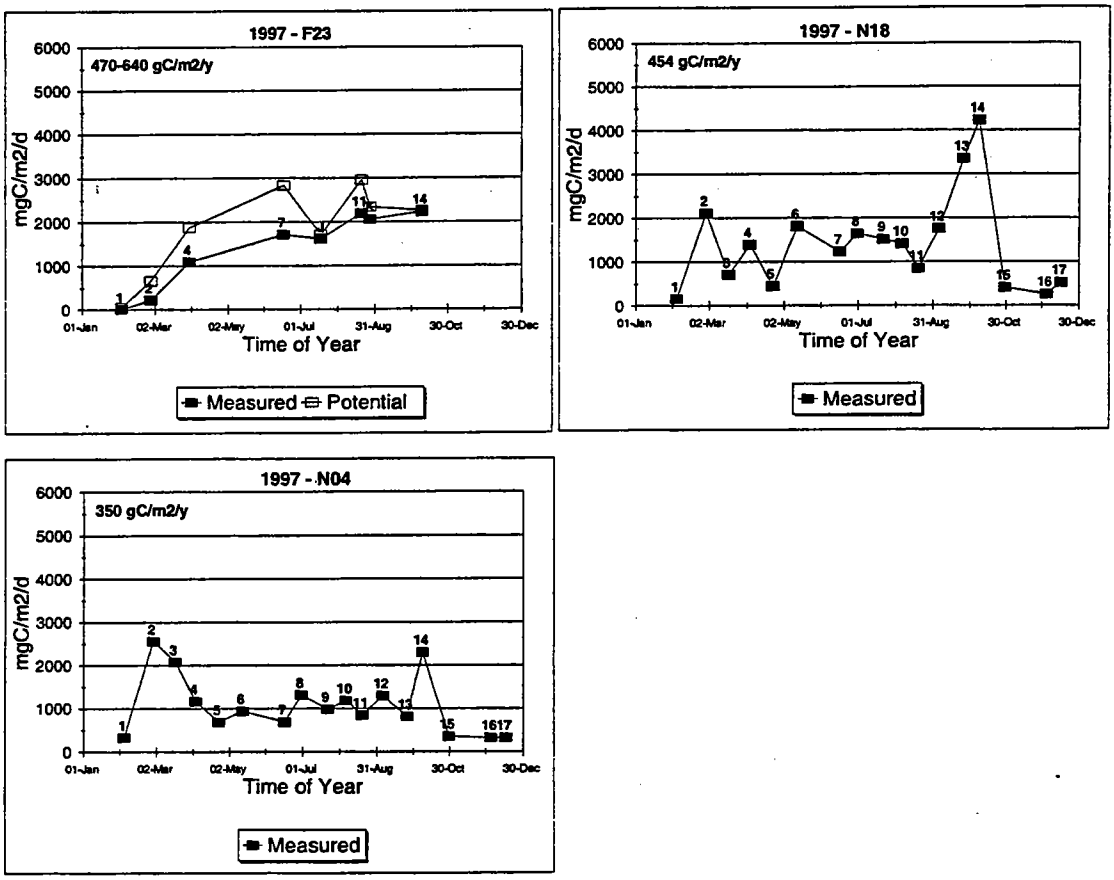

Figure 7-1

Areal production over the 1997 season. Closed symbols, production calculated using the incident light regime on the day of the cruise. Open symbols, potential production using cloudless day light fields for the indicated time of year. Potential production for N04 and N18 shown later in Figure 7-11. Cruise numbers are indicated by the numbers above each datum point. Annual production for indicated station is shown in the inset of each panel.

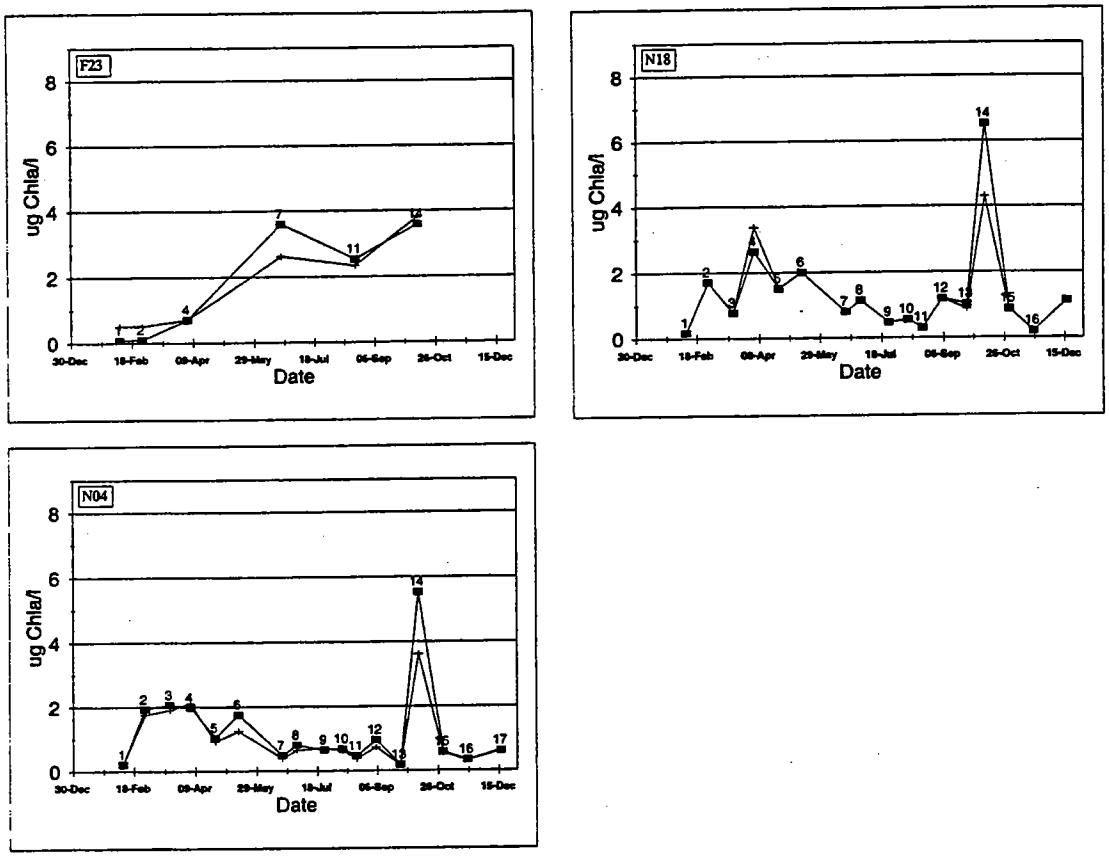

Figure 7-2

Chlorophyll-a distribution at the harbor edge and nearfield in 1997. Squares, average chlorophyll-a concentration in the photic zone above the 0.5% light level. Crosses, average chlorophyll-a concentration in the entire sampled water column.

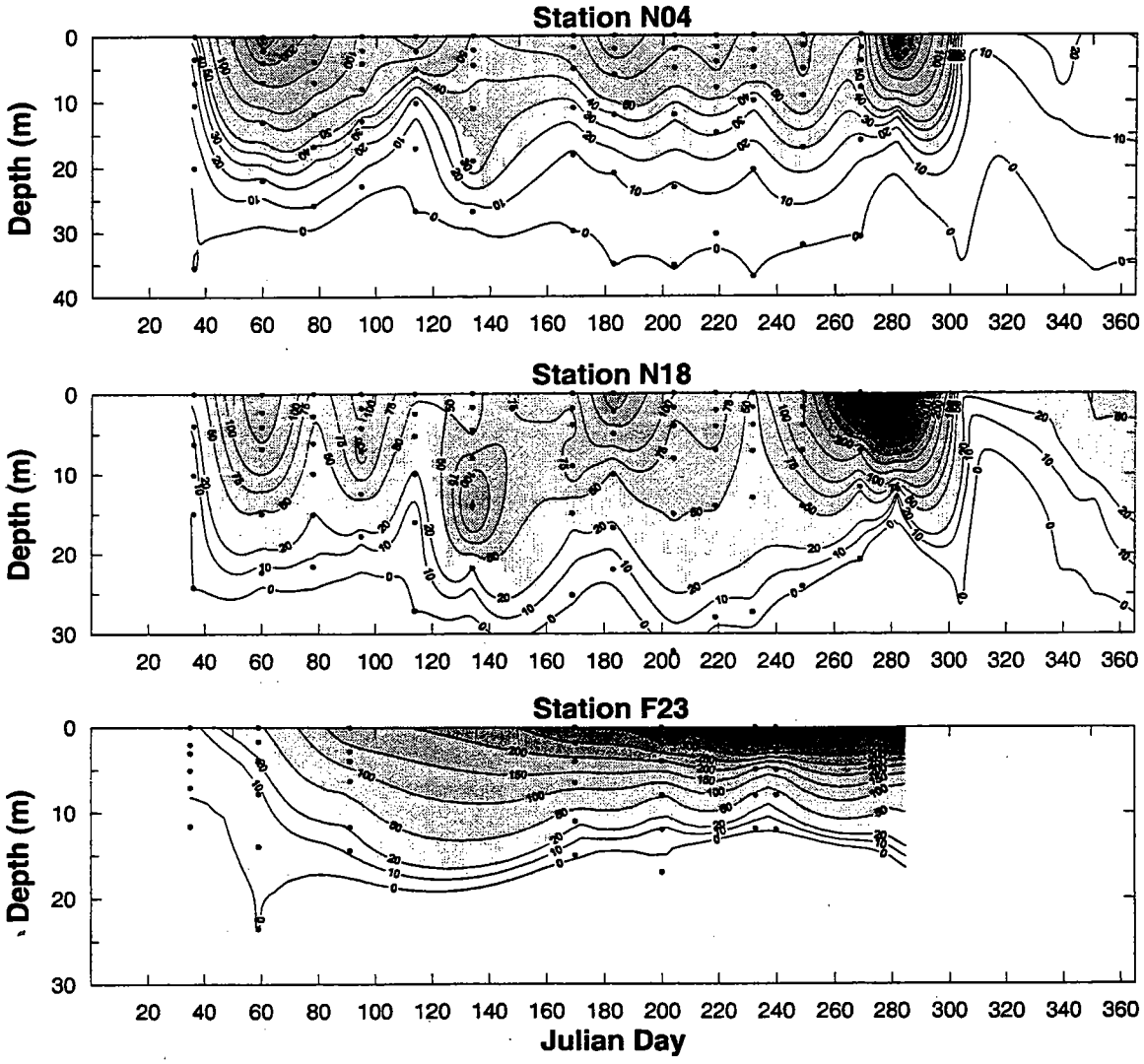

Figure 7-3

Daily Production. Contour values expressed in mgC/m3/d.

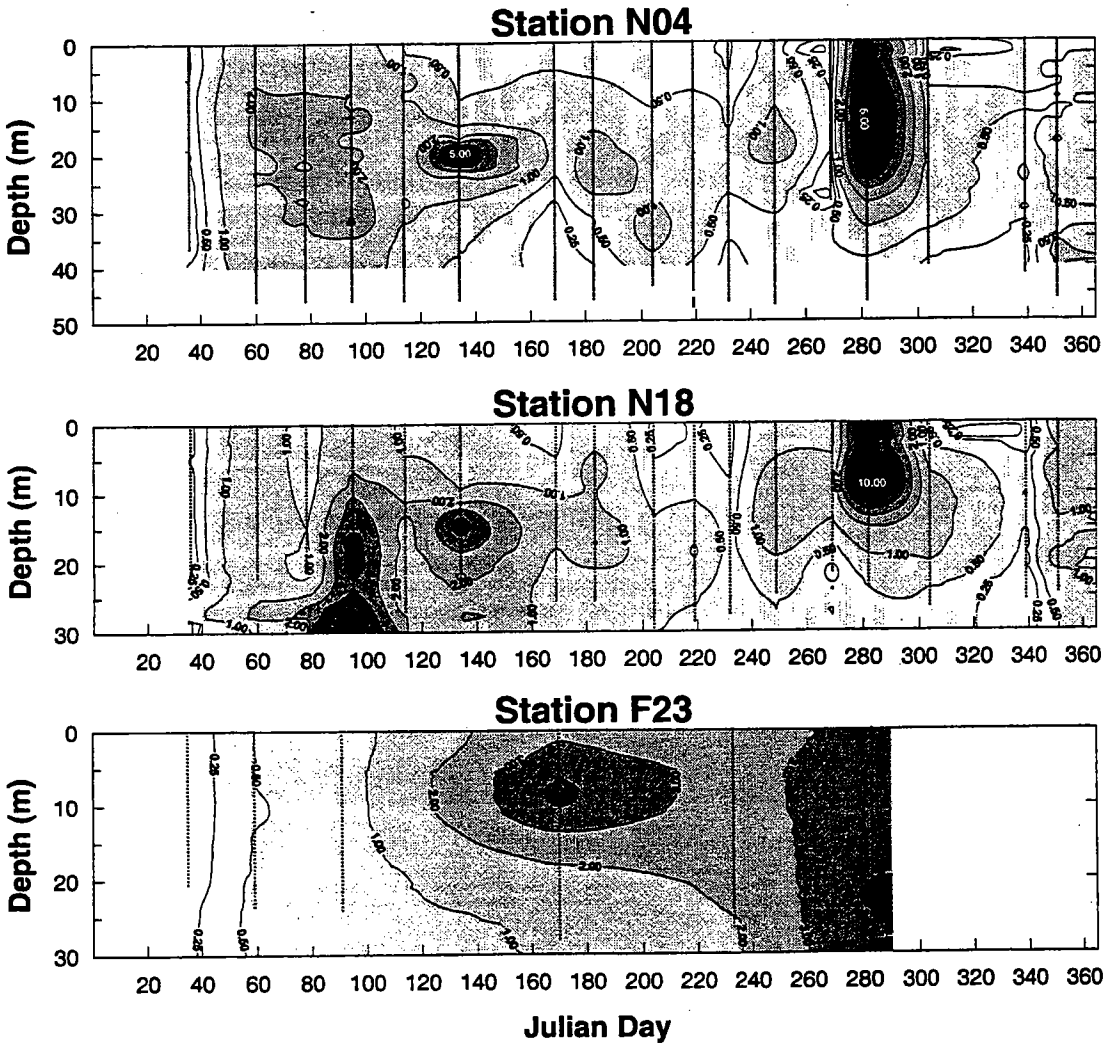

Figure 7-4

Chlorophyll-a distribution in the water column of the harbor edge and nearfield region in 1997. Dotted vertical lines represent date and depth of fluorescence measurement.

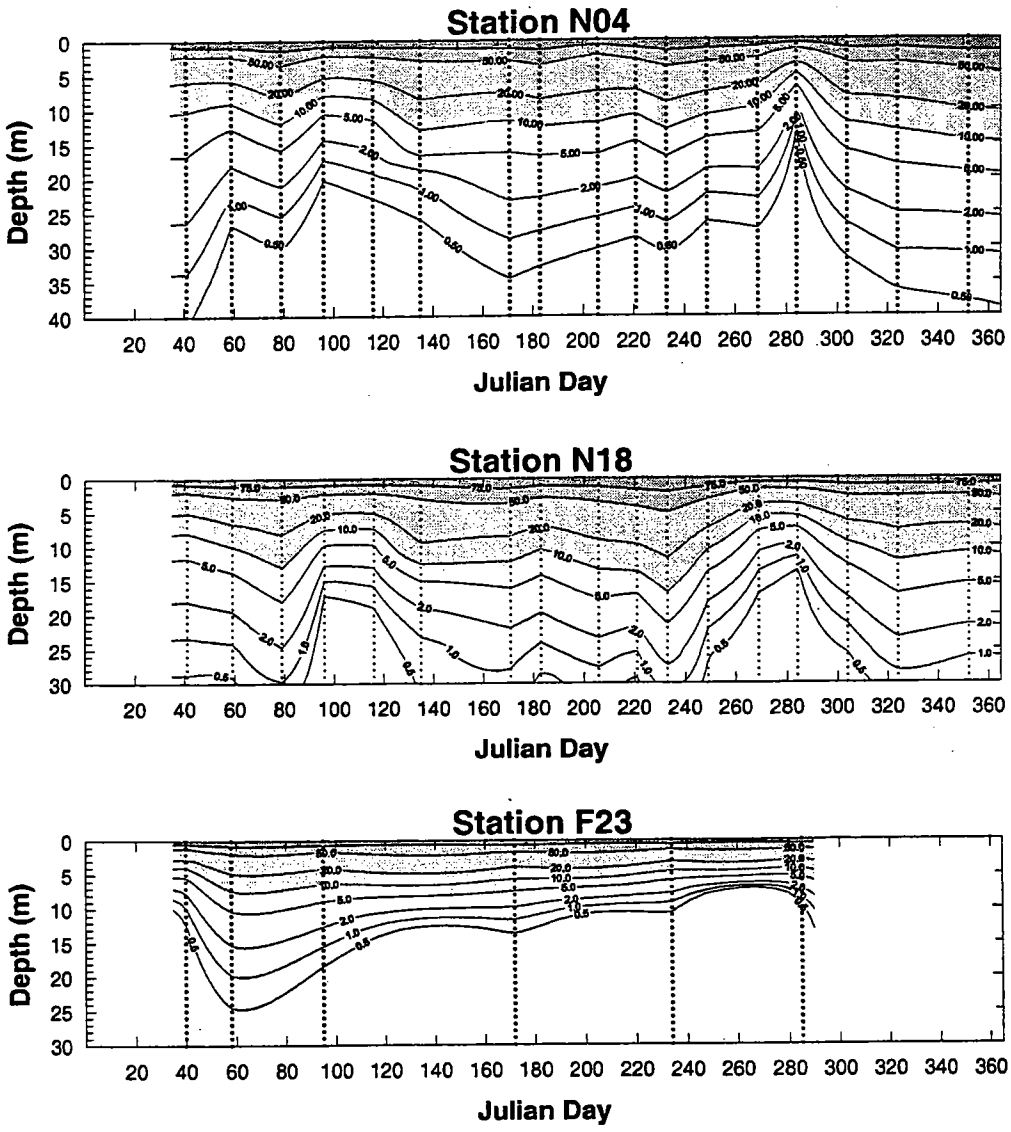

Figure 7-5

Percent subsurface light.

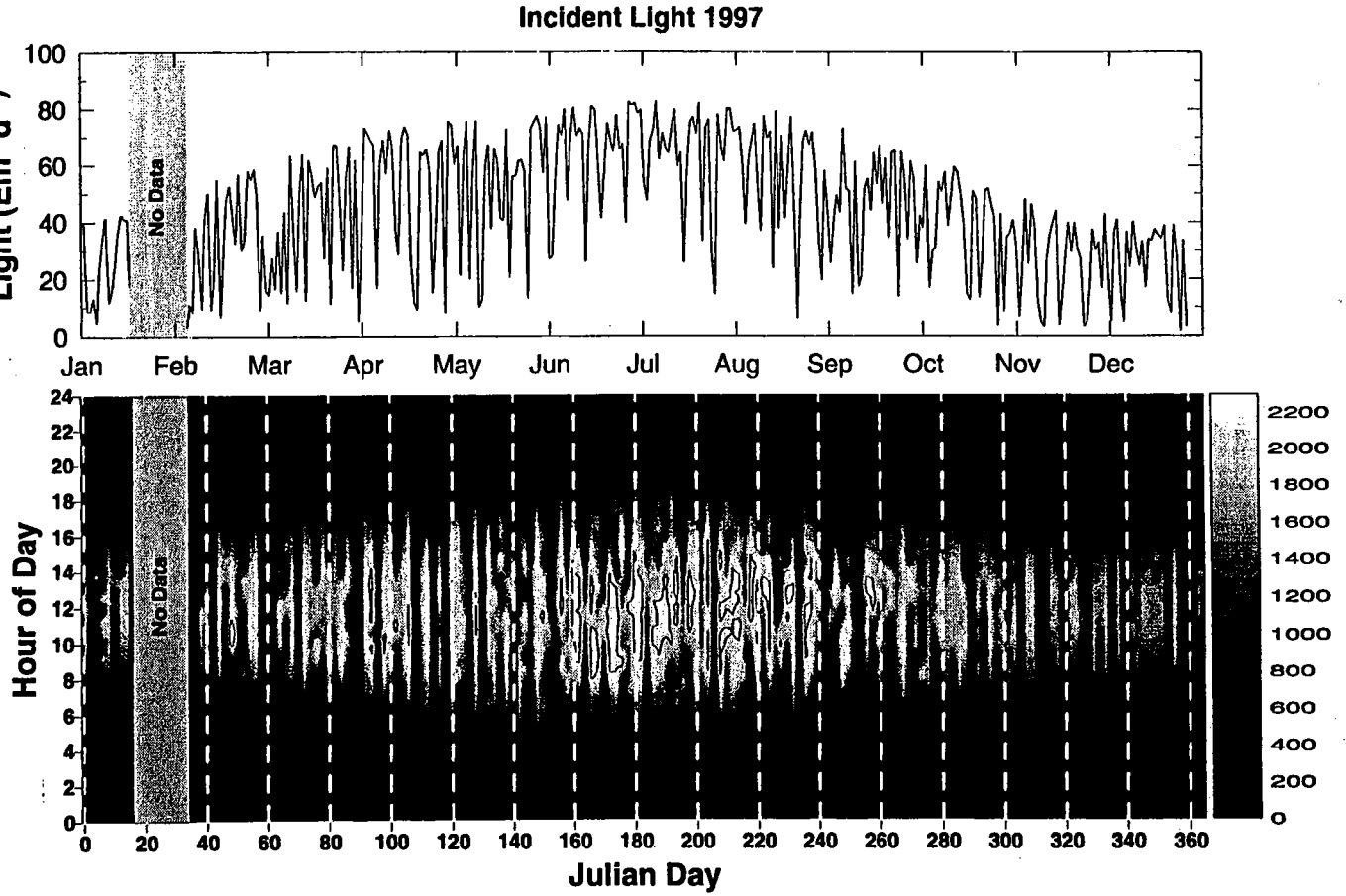

Figure 7-6.

1997 Incident light field. Upper panel, integrated incident light obtained by summation (BASIC program) of the 15 min sensor readings (uEm-2s-1) multiplied by 900 sec (sample)-1 and by 10-6 E uE-1 to yield total incident light exposure over the 24 hr diel cycle (Em-2d-1). Lower panel, contour plot of light sensor readings vs. hour of the day (resolved to 15 min intervals) and daily time interval during the year.

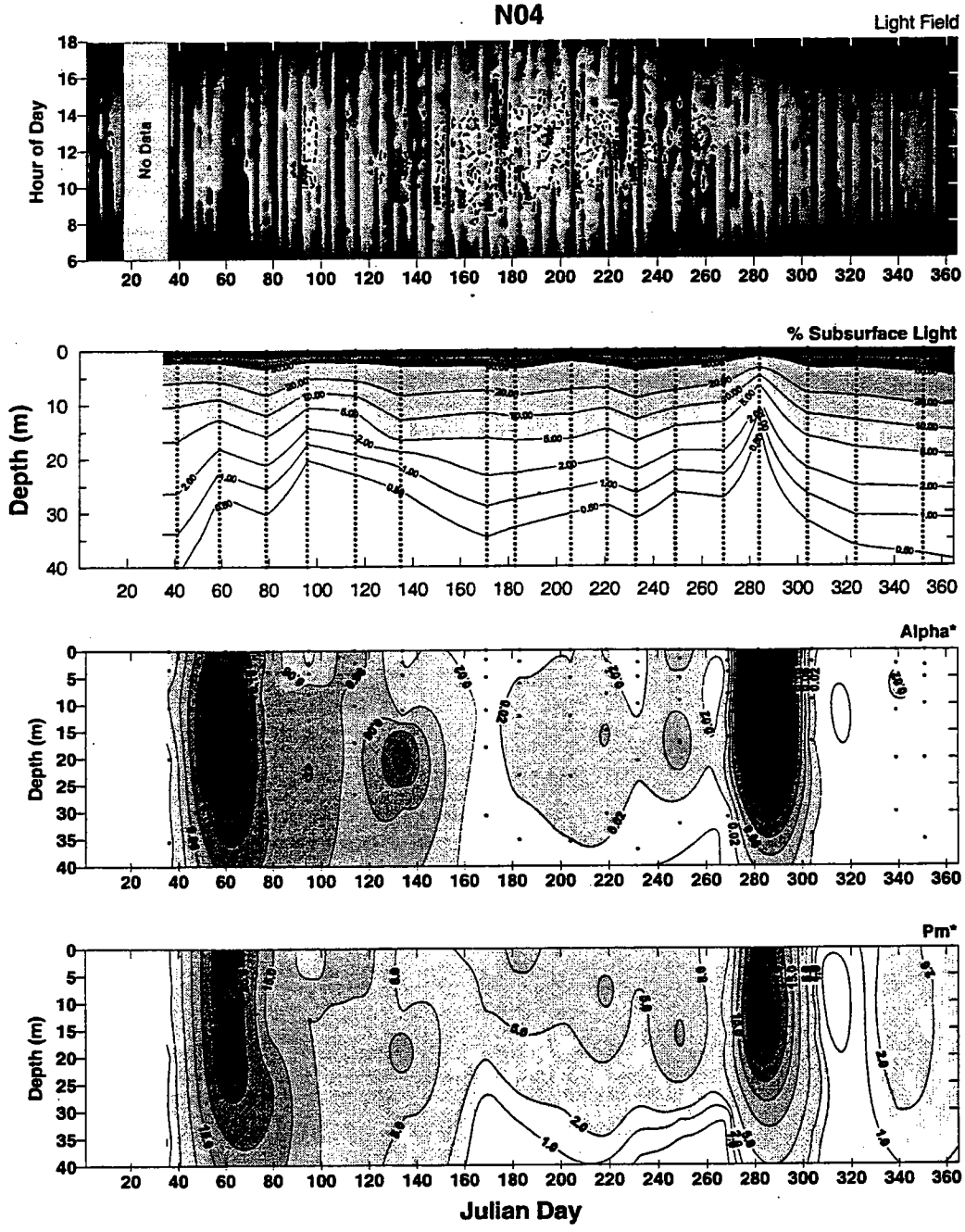

Figure 7-7
Parameters used for computation of high temporal resolution primary production at Station N04. Panel 1, Deer Island incident light measurements at 15 min intervals from 0600 to 1800 hrs, standard time. Panel 2, percent subsurface light (Iz/Iz=0*100) vs. depth over the season, where Iz is the 4pi light field at depth z recorded by the CTD, Iz=0 is the 4pi light field just under the sea surface at depth zero. Panel 3, alpha* vs. depth over the season. Panel 4, Pmax* vs. depth over the season.

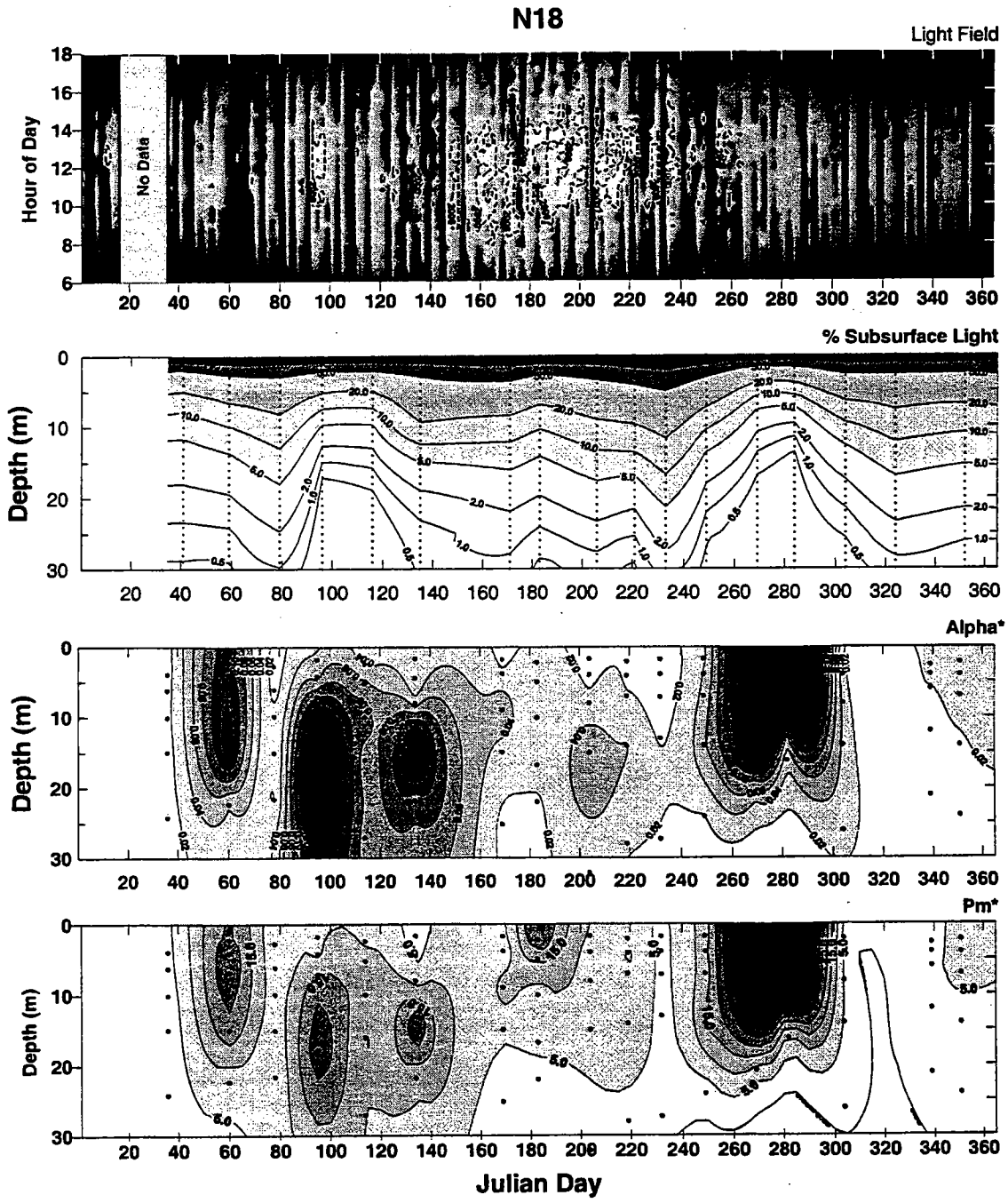

Figure 7-8
Parameters used for computation of high temporal resolution primary production at Station N18. Identification of panel contents are as described in the legend of Figure 7-7.

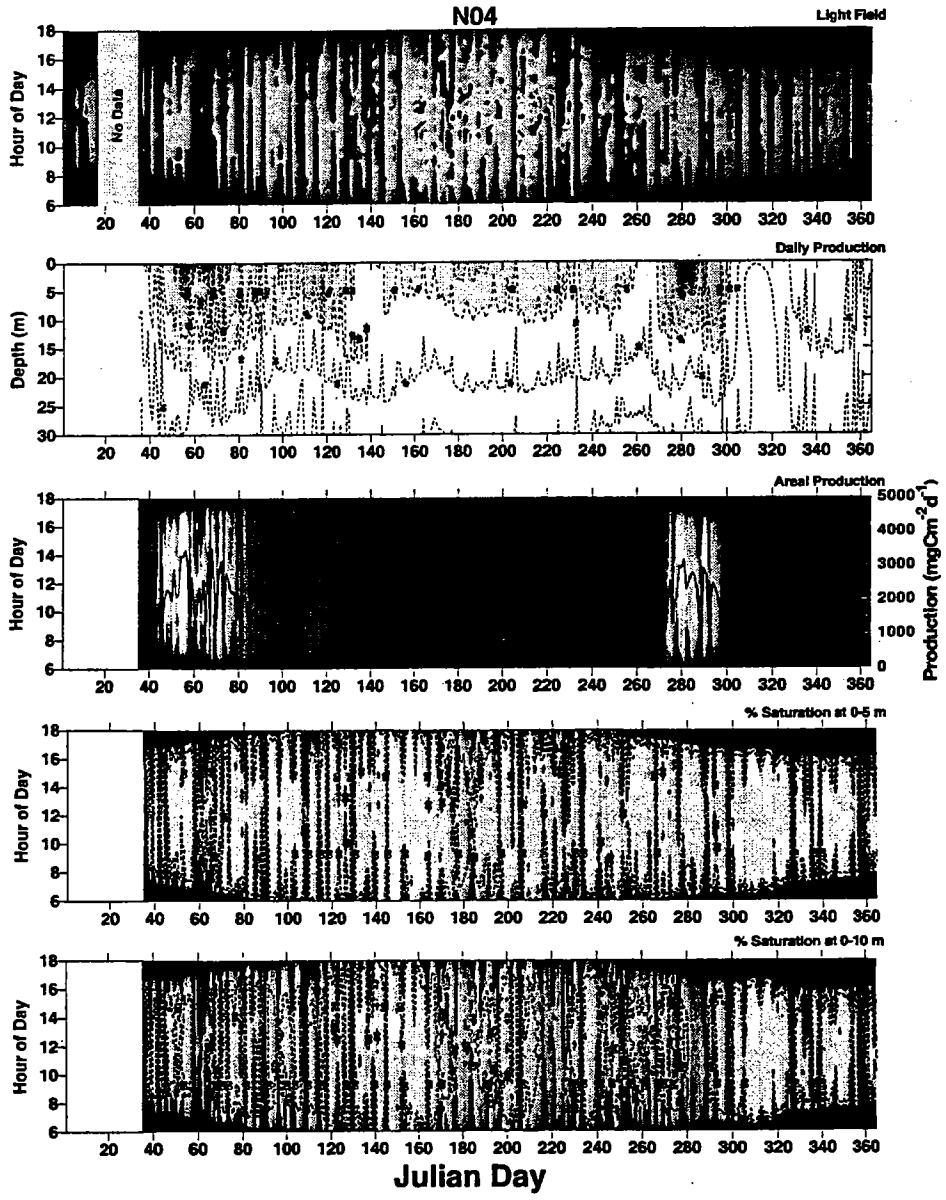

Figure 7-9
High temporal resolution production at Station N04 during 1997. Data in Figure 7-7 were used for computations using a BASIC program as described in Methods. Panel 1, light field expressed in uEm-2s-1. Panel 2, daily production (mgC m-3d-1) vs. depth (1 m intervals) over the season (resolved to the day). Panel 3, areal production down to 40 m (mgCm-2hr-1) vs. hour of day (resolved to 15 min intervals) over the season (resolved to the day). Panels 4 and 5, area photosynthesis percent saturation from 0-5 m and 0-10 m depth vs. hour of day (resolved to 15 min intervals) over the season (resolved to the day), respectively. Percent saturation was computed as areal production in upper 5 m and upper 10 m of the water column relative to areal Pmax* over the same depth intervals vs. hour of day. Pmax* was computed as the product Pmax[chla].

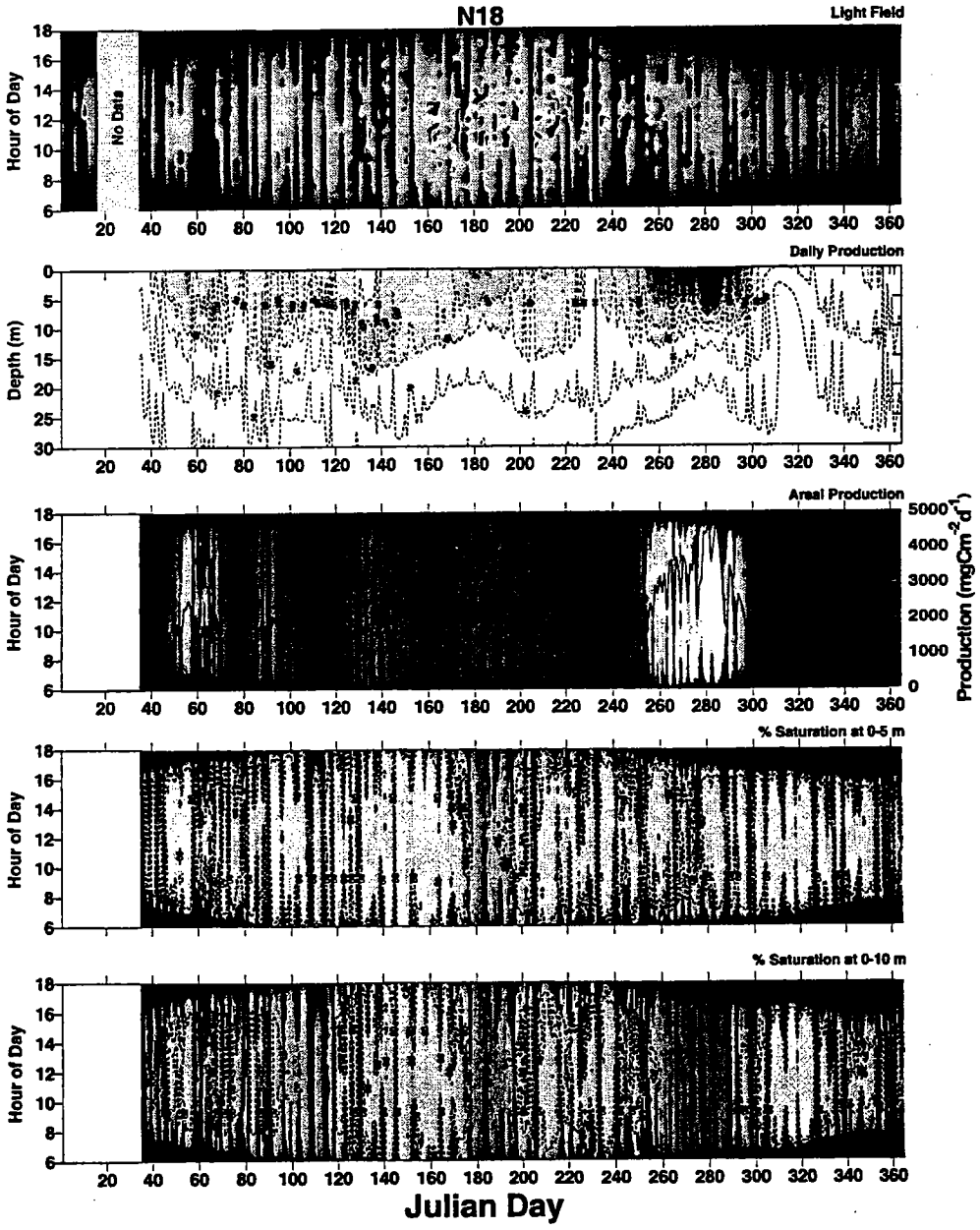

Figure 7-10
High temporal resolution production at Station N18 during 1997. Panel contents are as described in the legend of Figure 7-9 except that production is determined to a depth of 30 m.

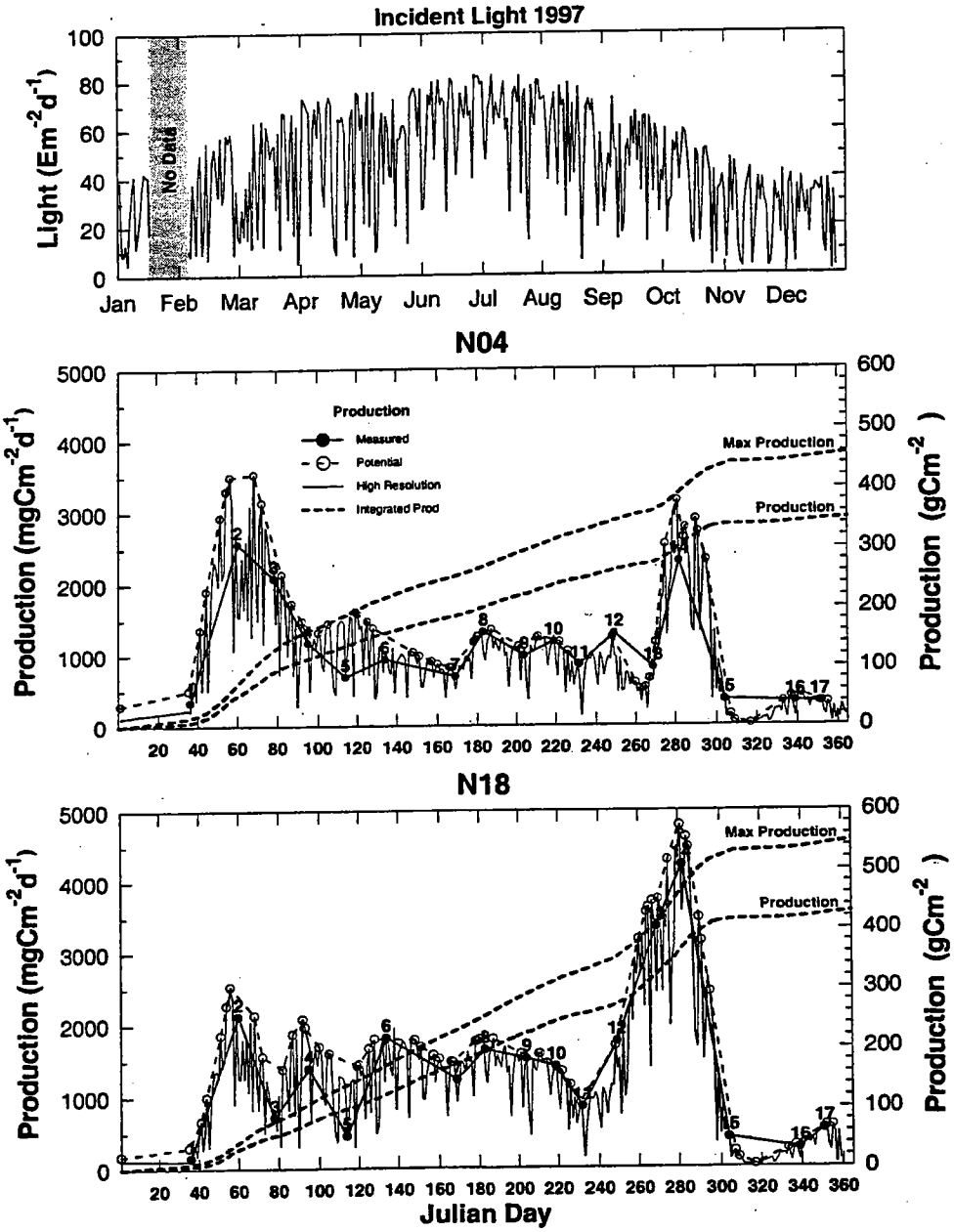

Figure 7-11

High temporal resolution areal production at Stations N04 and N18 during 1997. Panel 1, incident light field as described in the legend of Figure 7-6. Panels 2 and 3, areal production for Stations N04 and N18, respectively. Closed circles-solid line, areal production (mgCm-2d-1) determined on the survey day indicated by the number using the incident light field that occurred on that day. Open circles-dashed line, potential areal production determined using a cloudless day incident light field that would occur at the indicated time of year. Thin solid line, high resolution areal production computed using the Deer Island incident light time series and gridded photosynthesis parameters as described in Methods. Thick dashed lines, integrated seasonal production (gCm-2) obtained by summation of daily areal production or potential areal production.

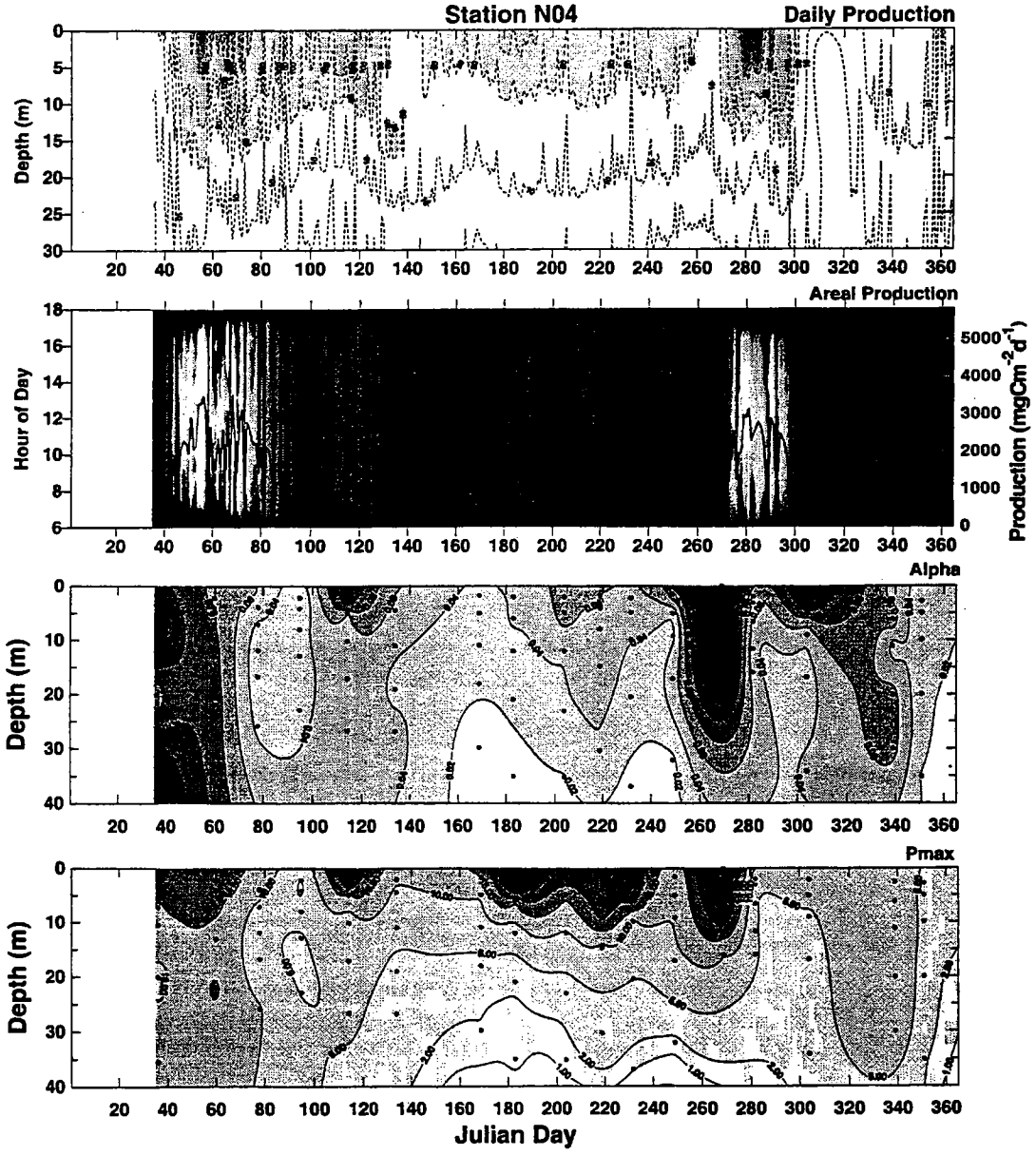

Figure 7-12
Comparison of Alpha and Pmax with depth-dependent and areal production at Station N04 in 1997. Panel 1, production (mgCm-3d-1) vs. depth througout season. Panel 2, areal production (mgCm-2h-1) vs. time of day. Panels 3 and 4, Alpha and Pmax vs. depth throughout season.

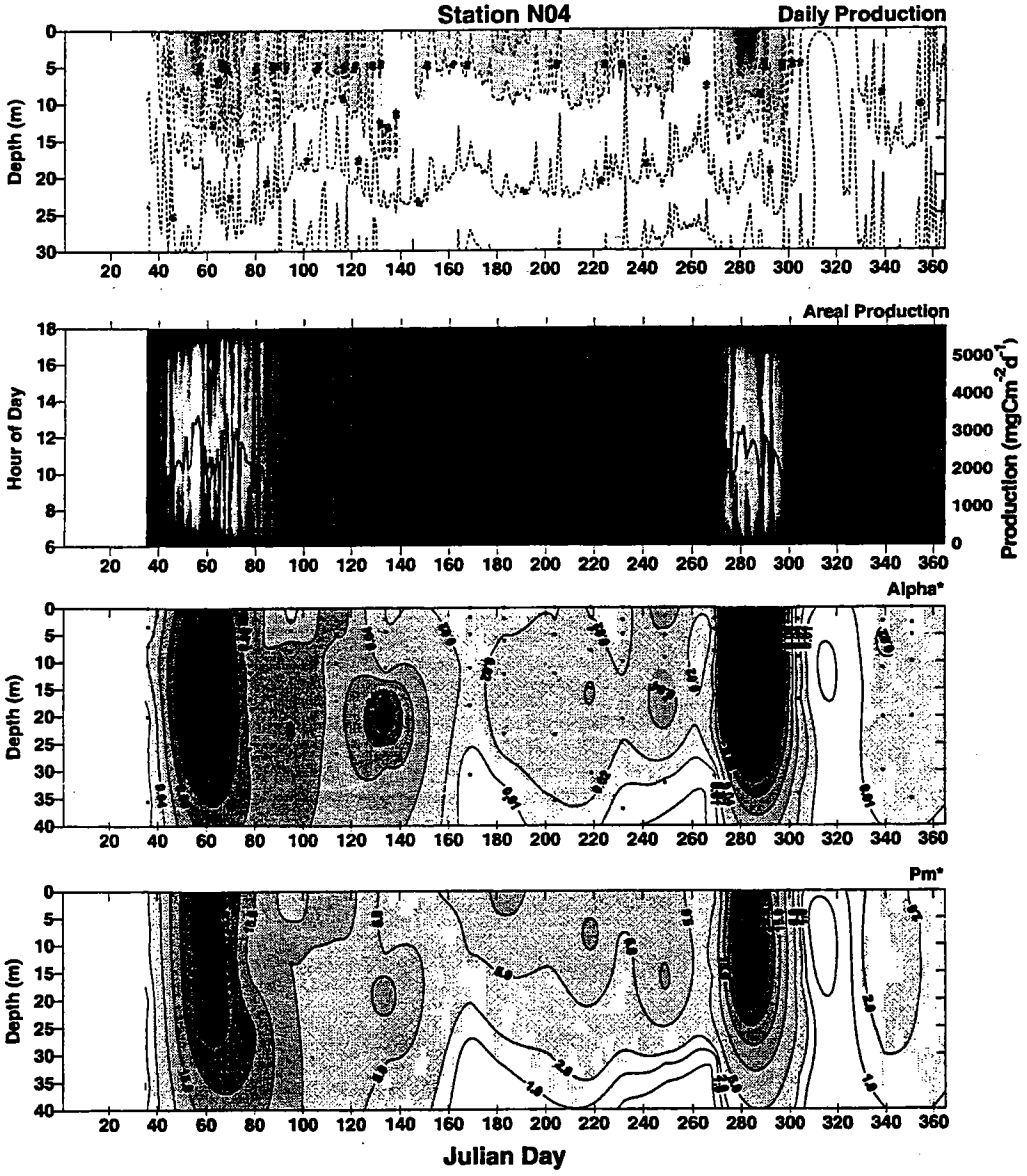

Figure 7-13
Comparison of Alpha and Pmax with depth-dependent and areal production at Station N18 in 1997. Panel 1, production (mgCm-3d-1) vs. depth througout season. Panel 2, areal production (mgCm-2h-1) vs. time of day. Panels 3 and 4, Alpha and Pmax vs. depth throughout season.

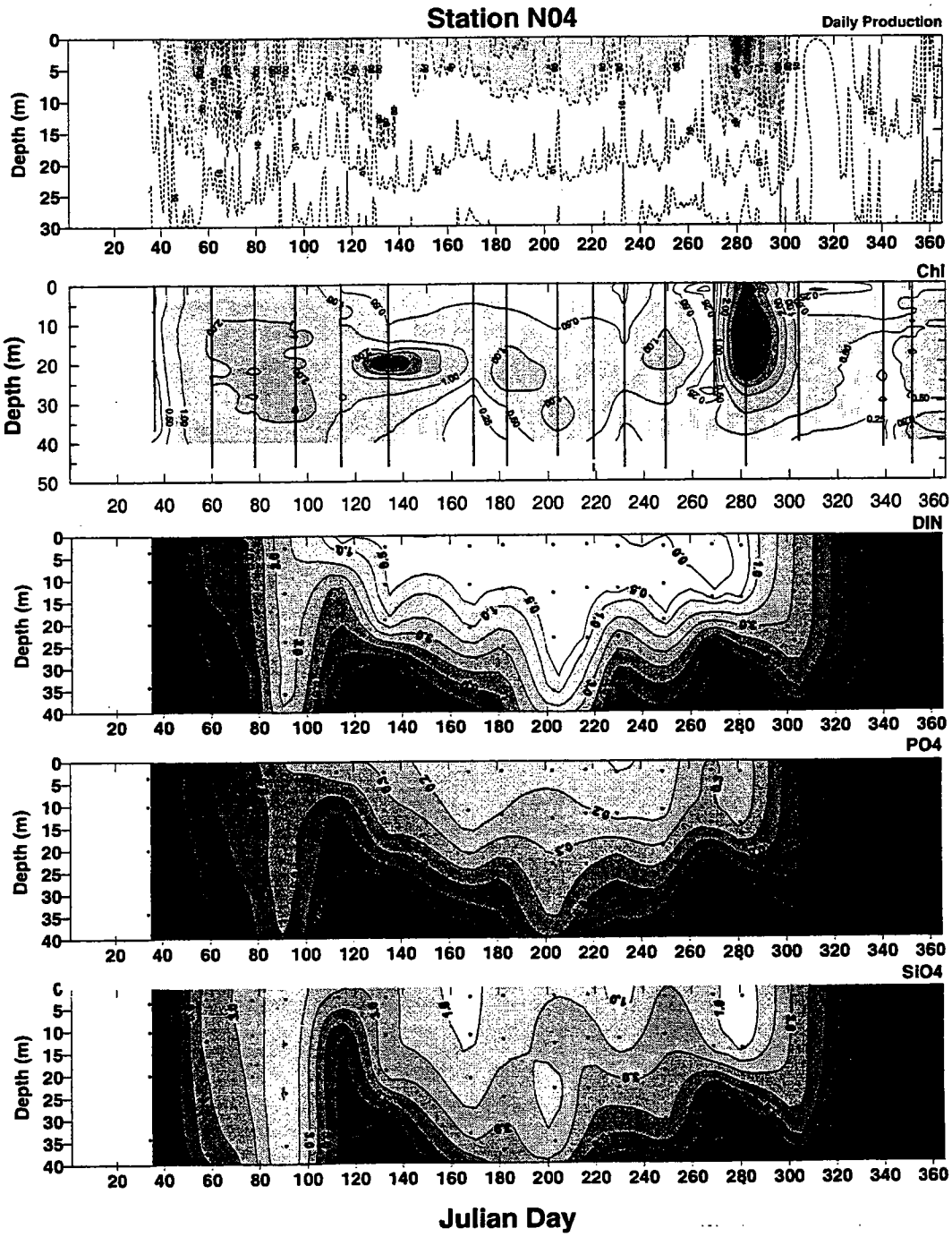

Figure 7-14
Comparison of nutrient field with daily production and water column chlorophyll at Station N04 in 1997. Panel 1, production (mgCm-3d-1) vs. depth througout season. Panels 2, 3 and 4, DIN, phosphate and silicate (ugl-1).

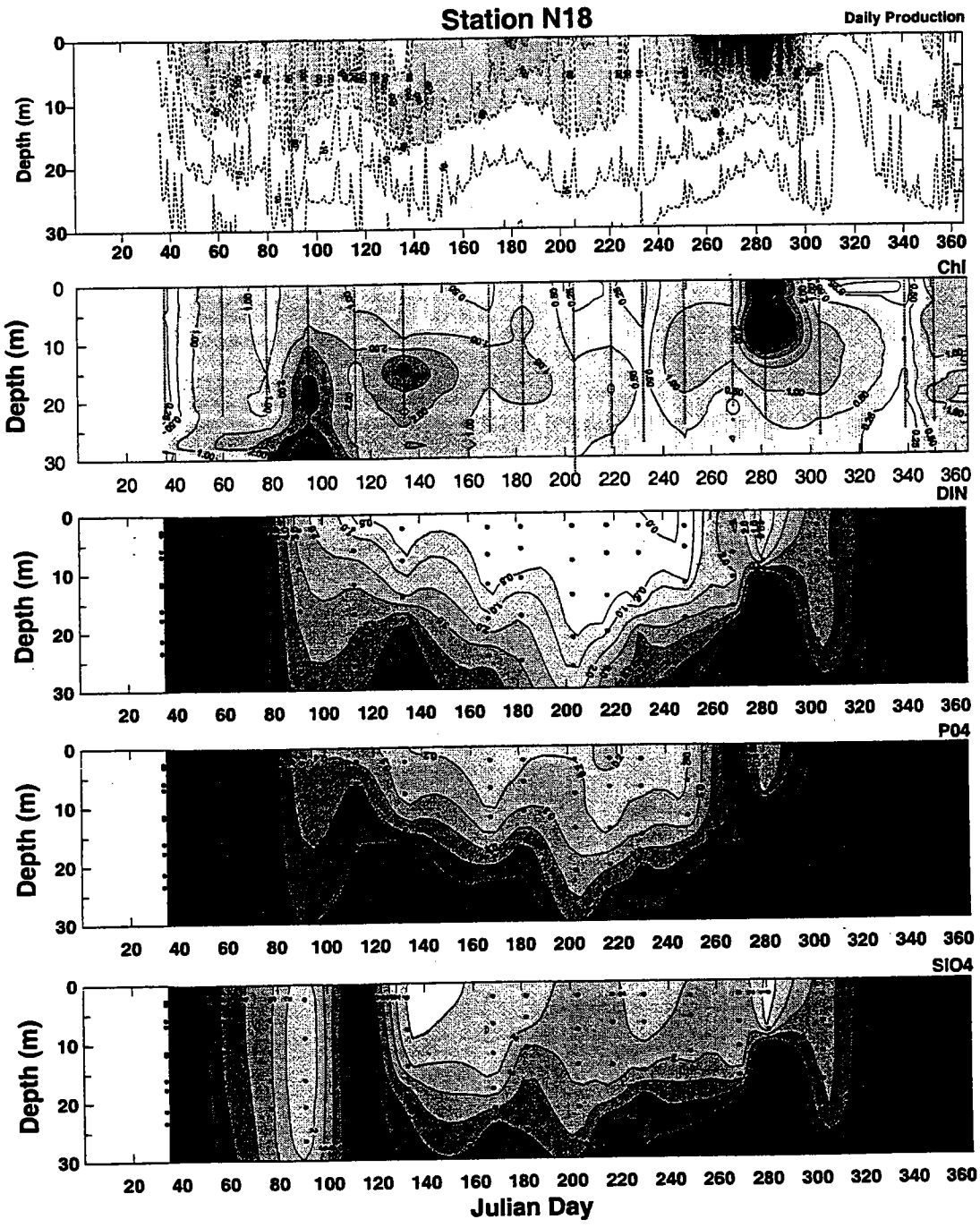

Figure 7-15
Comparison of nutrient field with daily production and water column chlorophyll at Station N18 in 1997. Panel 1, production (mgCm-3d-1) vs. depth througout season. Panels 2, 3 and 4, DIN, phosphate and silicate (ugl-1).

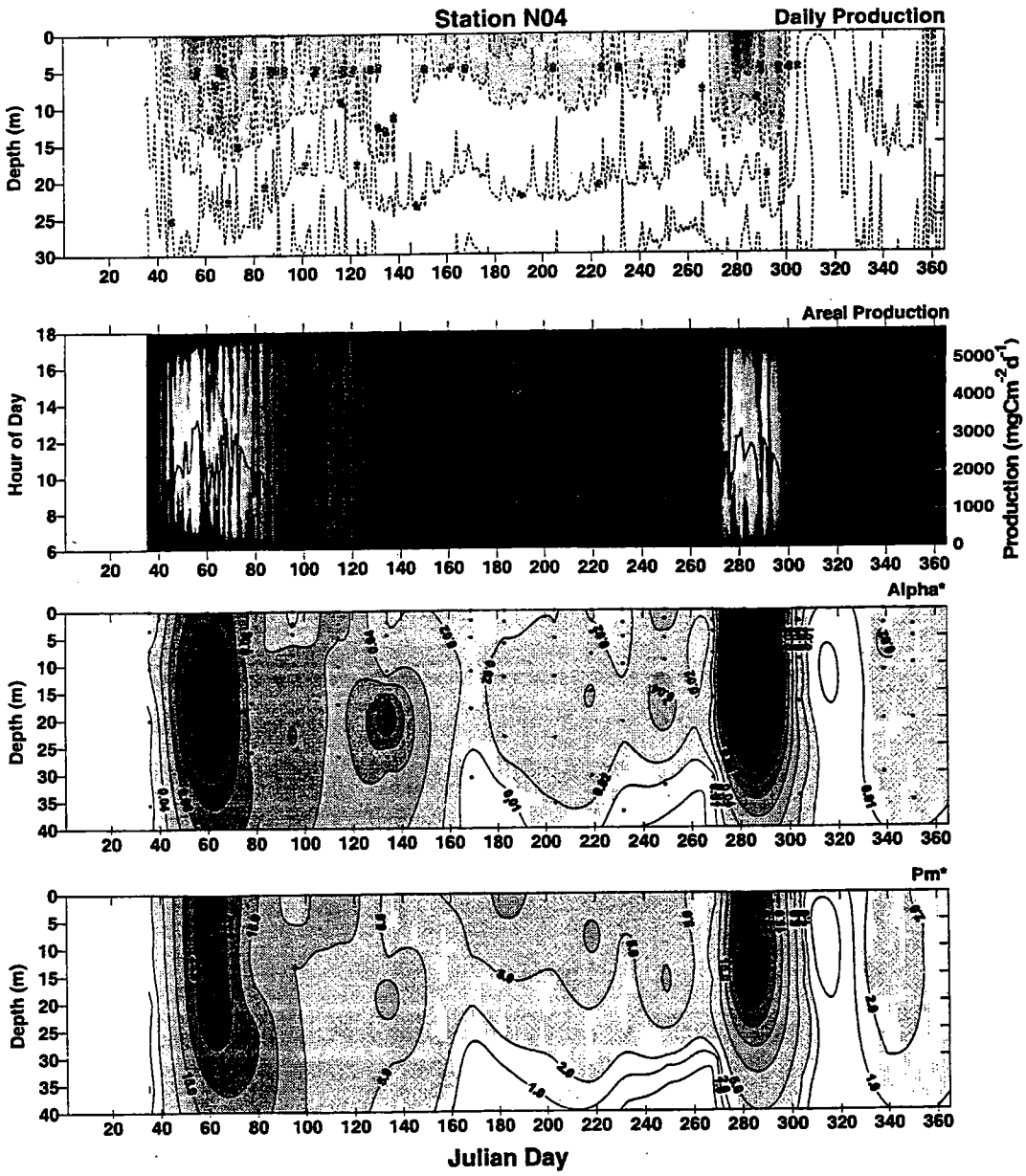

Figure 7-16
Comparison of Alpha* and Pmax* with daily and areal production at Station N04 in 1997. Panel 1, production (mgCm-3d-1) vs. depth througout season. Panel 2, areal production (mgCm-2h-1) vs. time of day. Panels 3 and 4, Alpha* and Pmax* vs. depth throughout season.

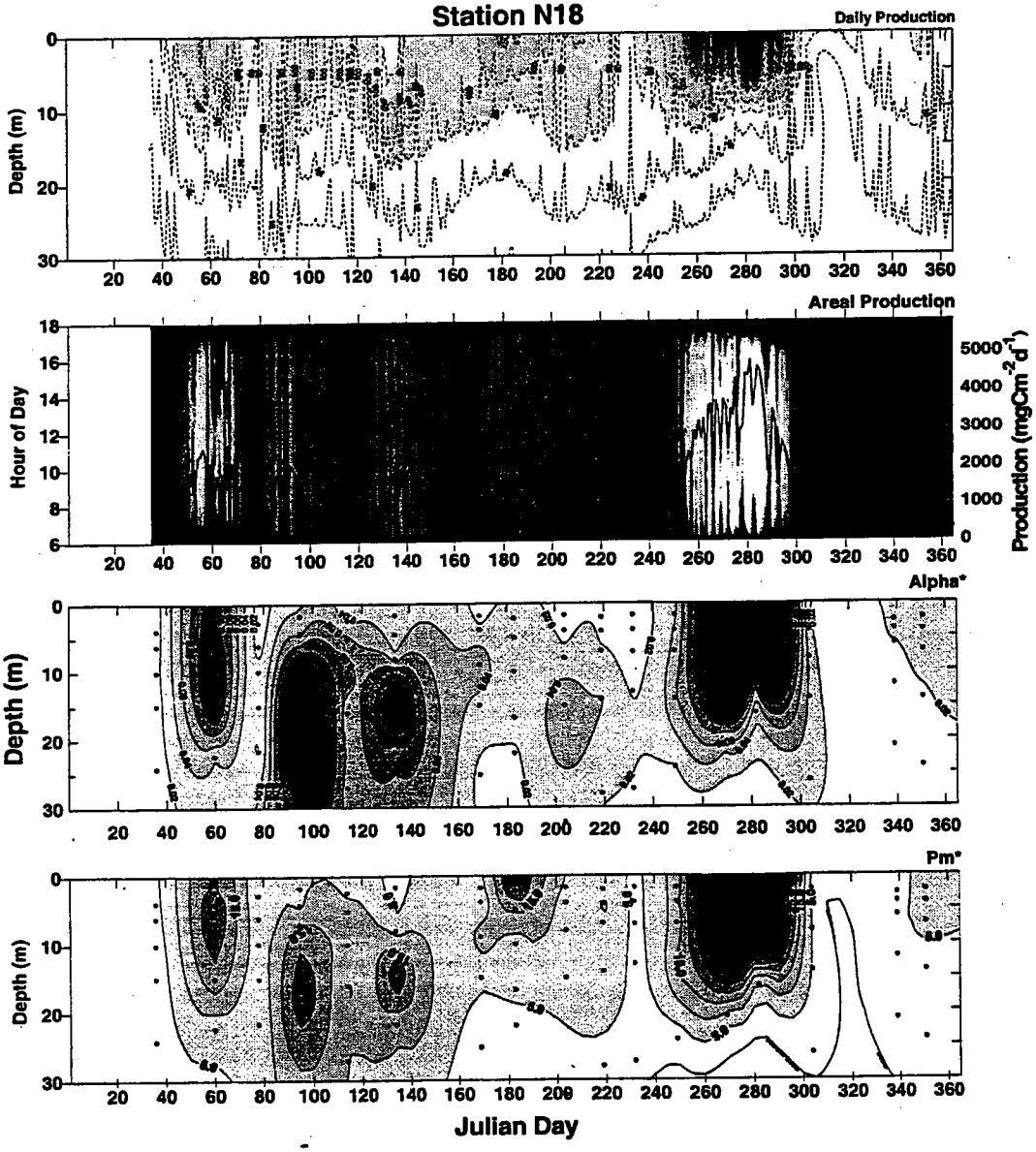

Figure 7-17
Comparison of Alpha* and Pmax* with daily and areal production at Station N18 in 1997. Panel 1, production (mgCm-3d-1) vs. depth througout season. Panel 2, areal production (mgCm-2h-1) vs. time of day. Panels 3 and 4, Alpha* and Pmax* vs. depth throughout season.

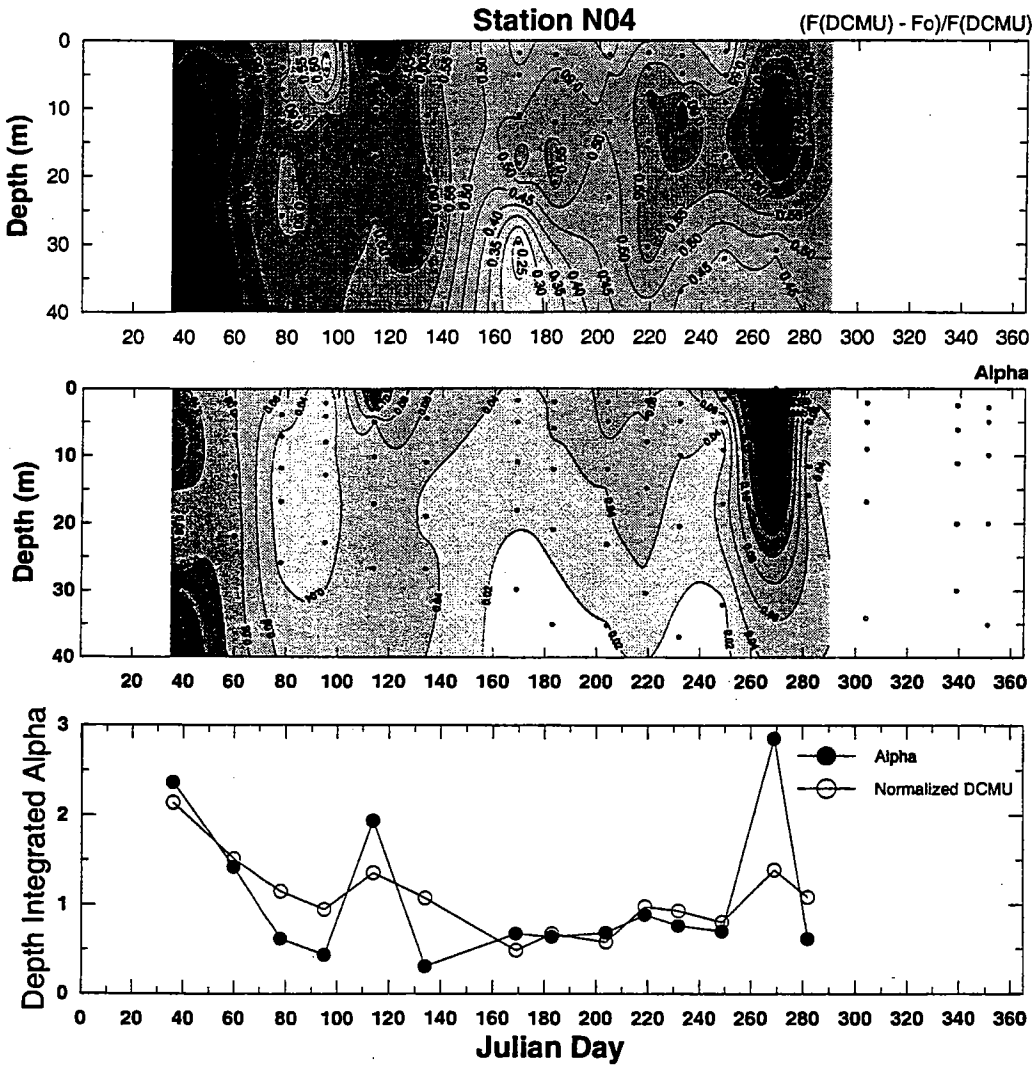

Figure 7-18

Comparison of maximum change in the quantum yield of fluorescence and alpha at station N04 in 1997. Panel 1, maximum change in the quantum yield of fluorescence [(Fdcmu - Fo)/Fdcmu) vs. depth and day of year. Fo is determined by the measurement of in vivo fluorescence as quickly as possible after introduction of dark adapted samples (30 min in dark) into the fluorometer. After the reading is made, the inhibitor DCMU is introduced into the sample, followed by exposure for ~ 1 min to white light to close all reaction centers by prevention of the reoxidation of the electron carrier QA (discussed in Cibik, et al., 1998). Fluorescence in the presence of the inhibitor (Fdcmu) is then measured. Panel 2, Alpha [gCgchl-1h-1(uEm-2s-1)-1] vs. depth and day of year. Panel 3, comparison of depth integrated Alpha (gCm2gchl-1E-1) and normalized depth integrated (Fdcmu - Fo)/Fdcmu. A linear regression of a plot of depth integrated (Fdcmu - Fo)/Fdcmu vs. depth integrated Alpha was performed and the slope term used to normalize depth integrated (Fdcmu - Fo)/Fdcmu. Explanation in text.

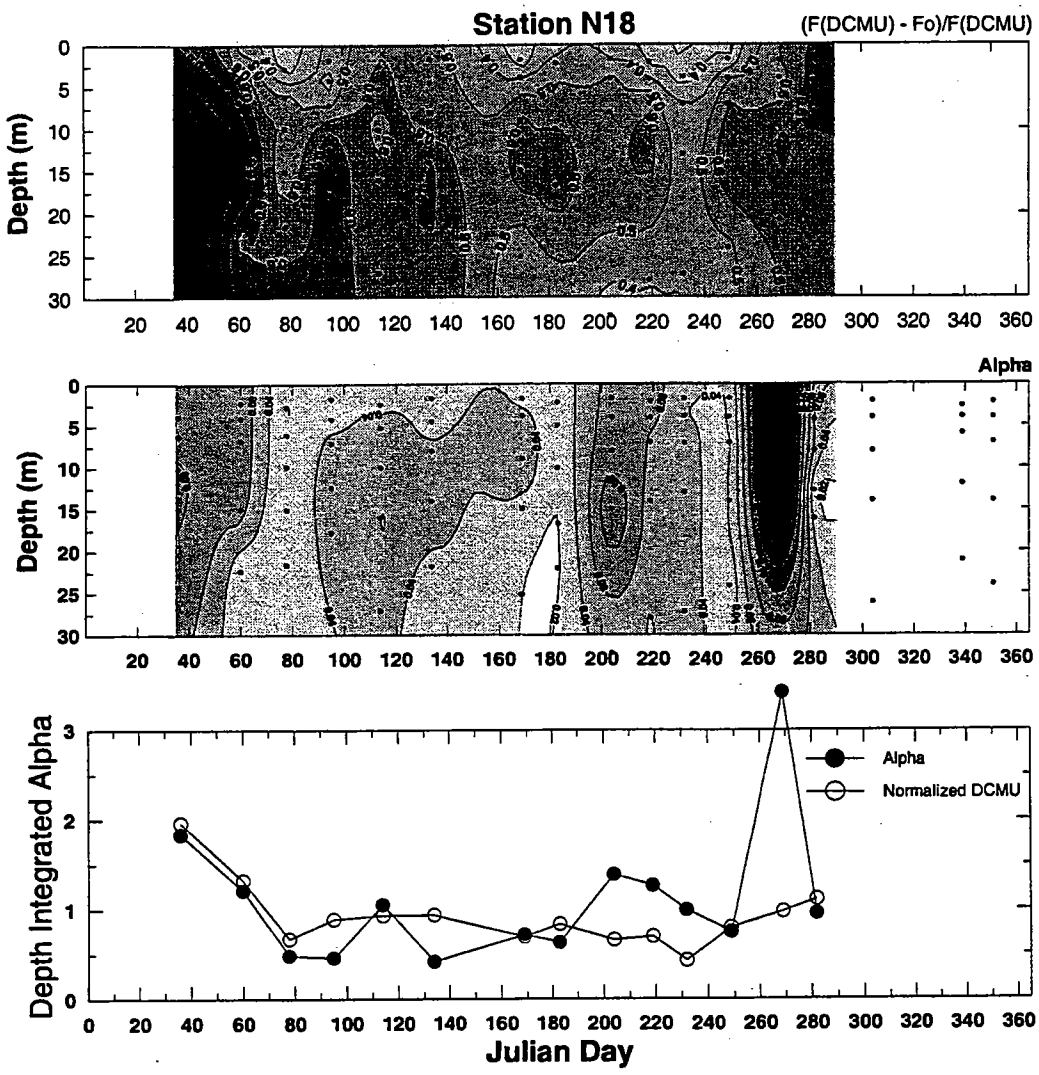

Figure 7-19
Comparison of maximum change in the quantum yield of fluorescence and alpha at station N18 in 1997. Panel contents are as described in Figure 7-18,

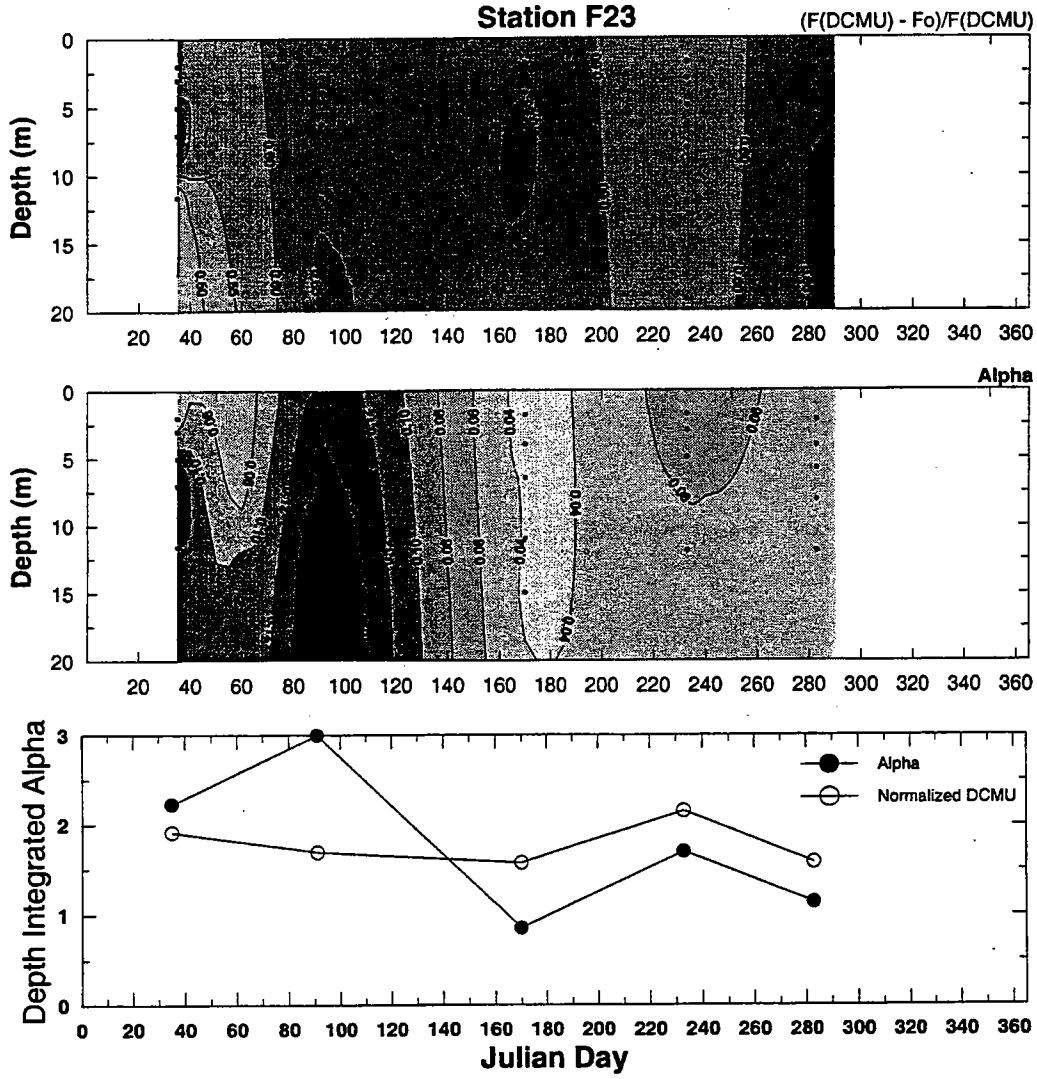

Figure 7-20
Comparison of maximum change in the quantum yield of fluorescence and alpha at station F23 in 1997. Panel contents are as described in Figure 7-18,

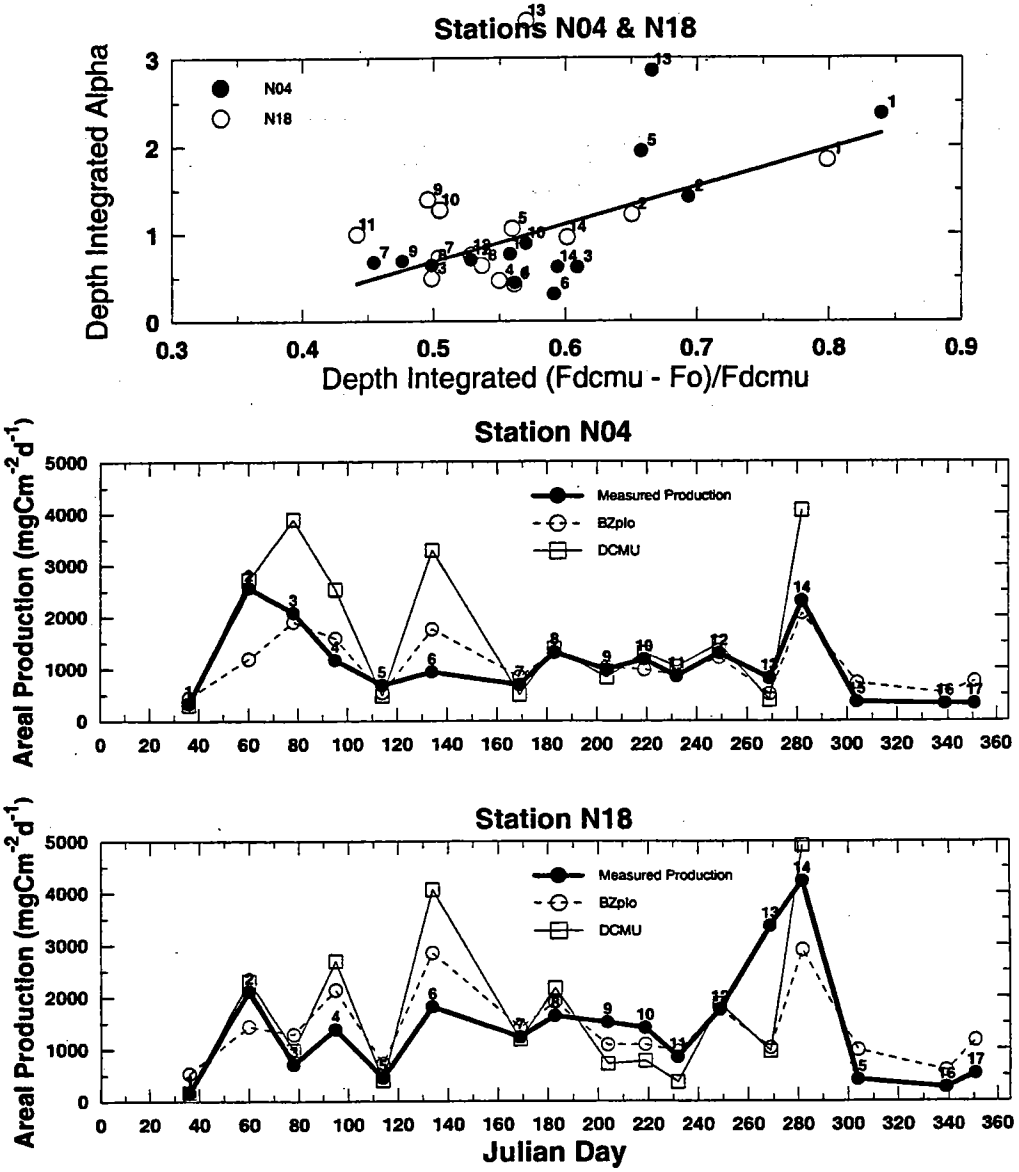

Figure 7-21
Comparison of Stations N04 & N18 areal production measured in 1997 with production estimates based upon BZplo and DCMU regressions. Panel 1, regression of depth integrated Alpha vs. depth integrated (Fdcmu - Fo)/Fdcmu. Panels 2 & 3, 14C-areal production in comparison with modeled production.

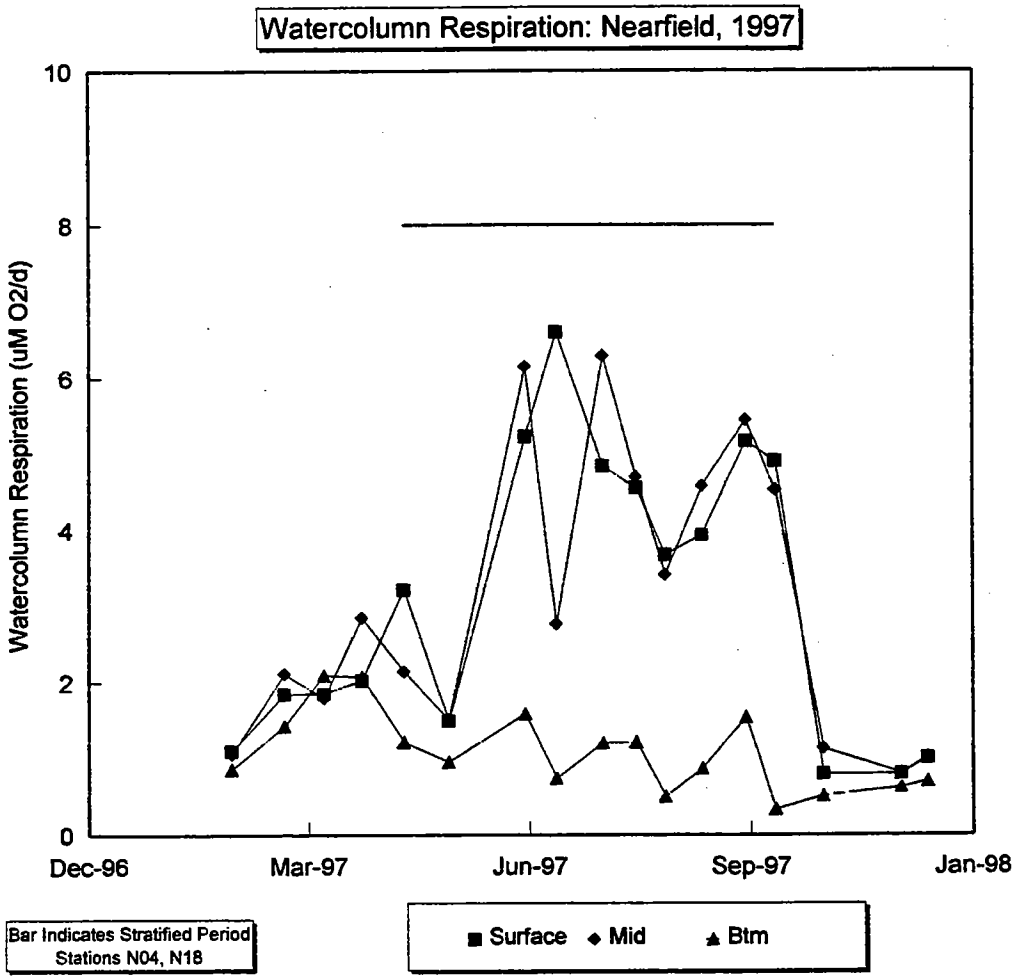

FIGURE 7-22
Vertical distribution of water column respiration averaged over nearfield stations N04 and N18, throughout 1997. Horizontal bar represents the stratified interval.

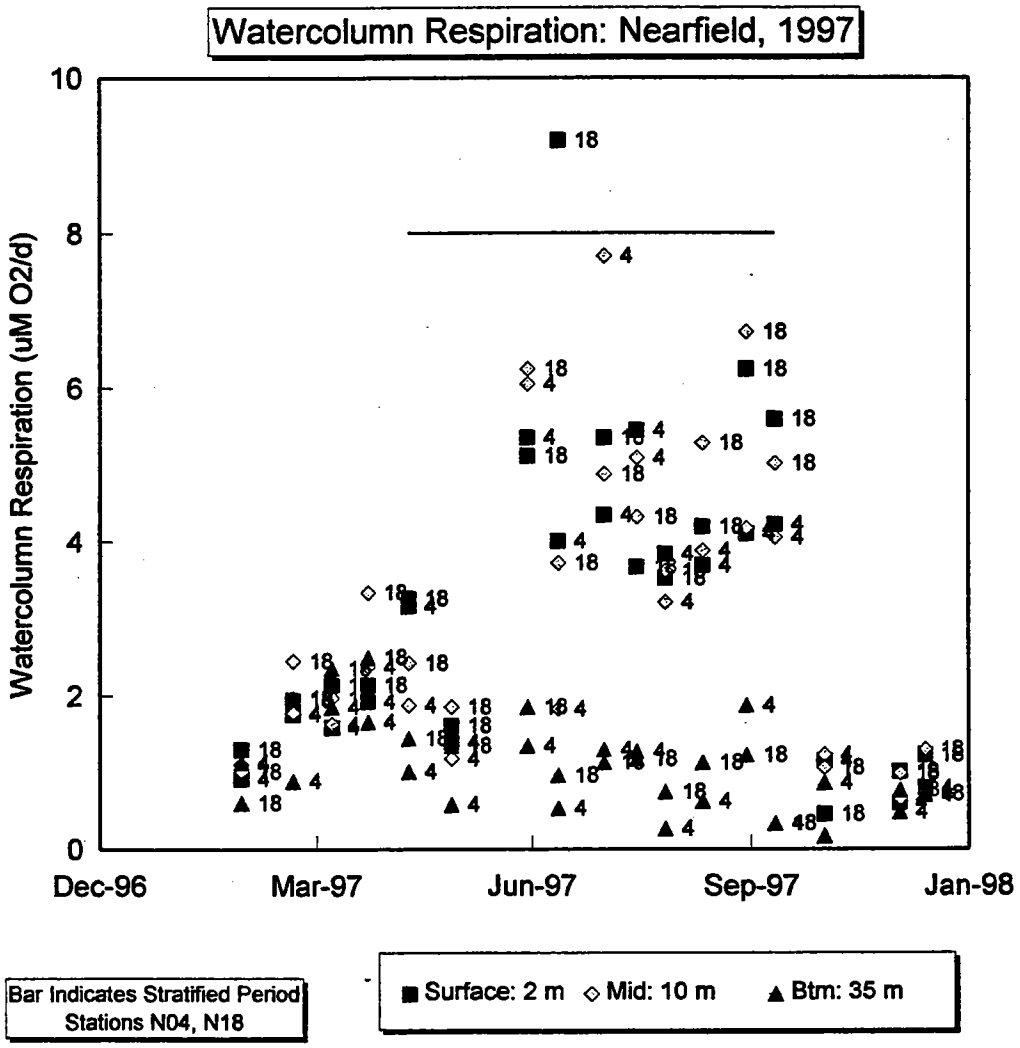

FIGURE 7-23
Vertical distribution of water column respiration at nearfield stations N04 and N18, throughout 1997. Horizontal bar represents the stratified interval. Numbers to the right of symbols represent station i.d.'s.

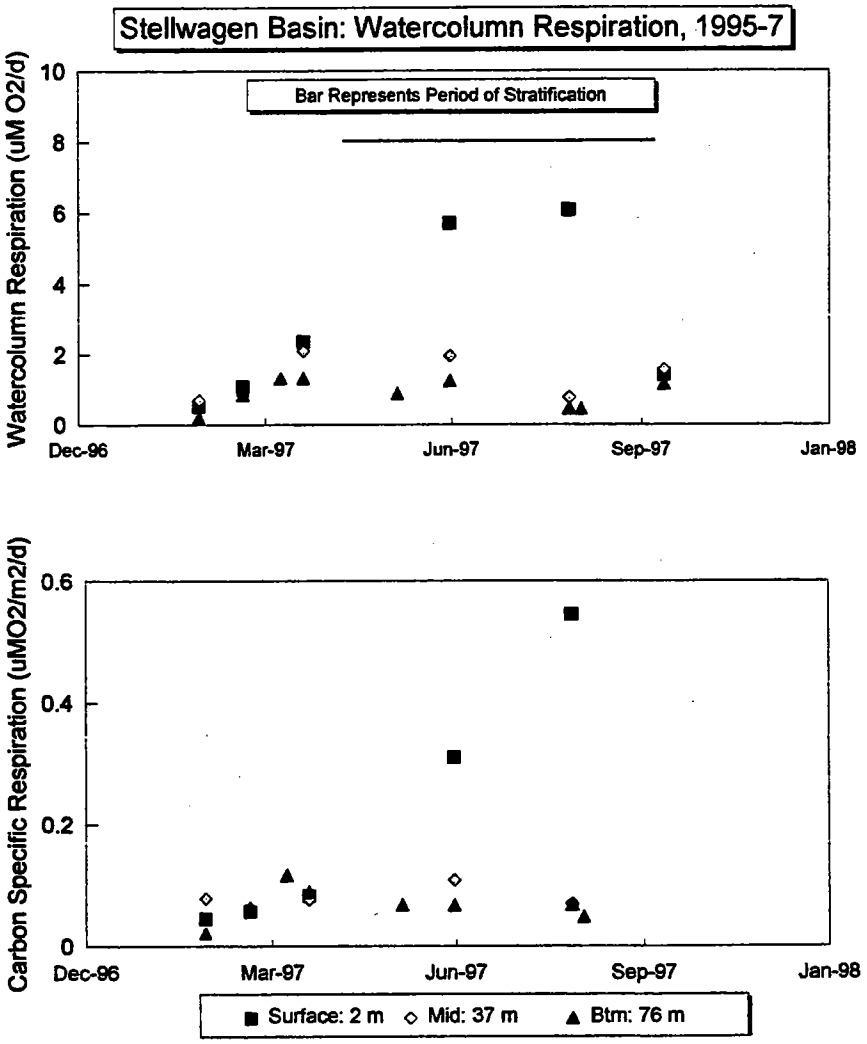

FIGURE 7-24

Vertical distribution of water column respiration at Stellwagen Basin Station F19, measured during water column surveys and benthic flux surveys throughout 1997. Horizontal bar represents the stratified interval. Top: water column respiration, Btm: carbon specific respiration or water column respiration normalized to the measured pool of POC.

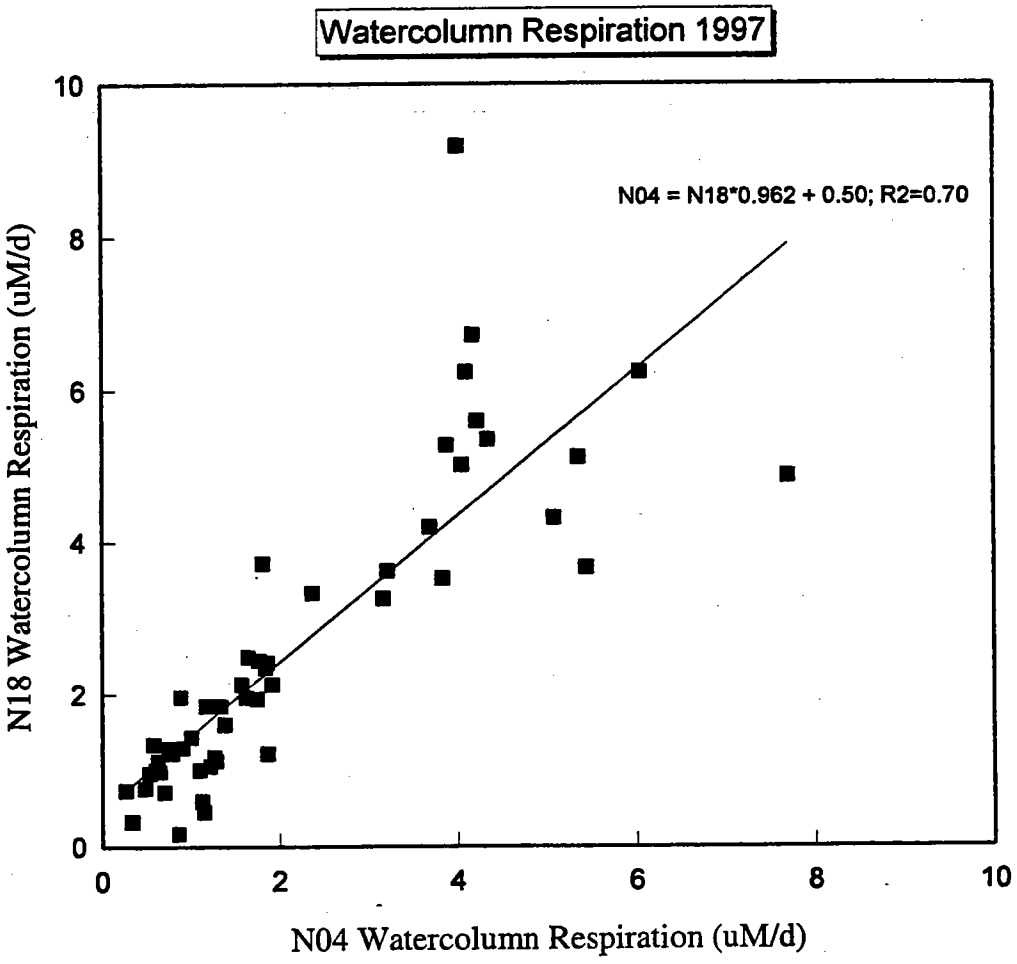

FIGURE 7-25
Comparison of nearfield stations N04 and N18 water column respiration rates from all depths during 1997. The line is a linear regression of the points, the slope is not significantly different from 1 ($p<0.05$).

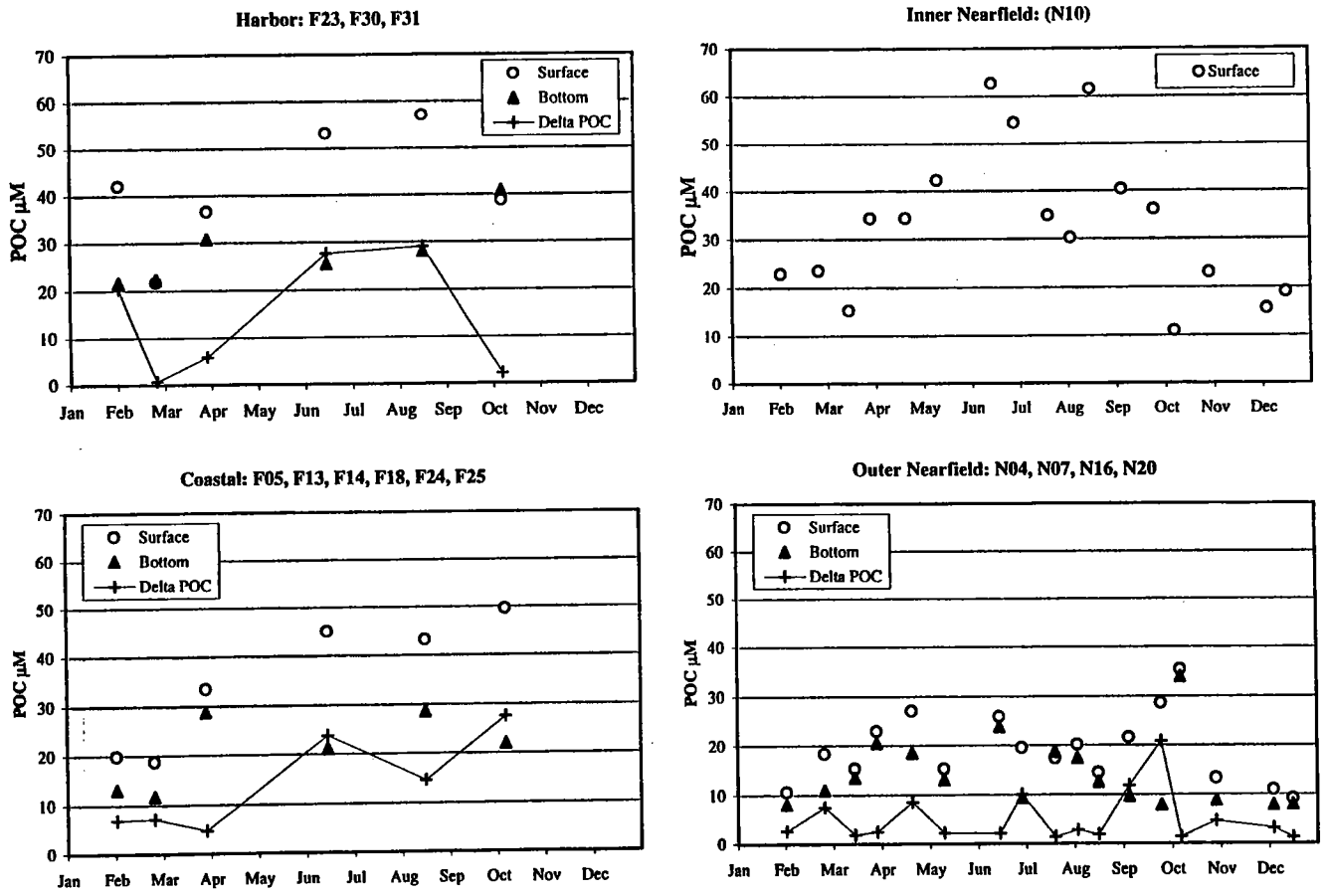

Note: N10 only sampled at the surface and mid-depth

FIGURE 7-26

1997 Regional Particulate Organic Carbon (POC) Concentration Averages

Surface, Bottom, and Delta (Surface-Bottom) Survey Averages

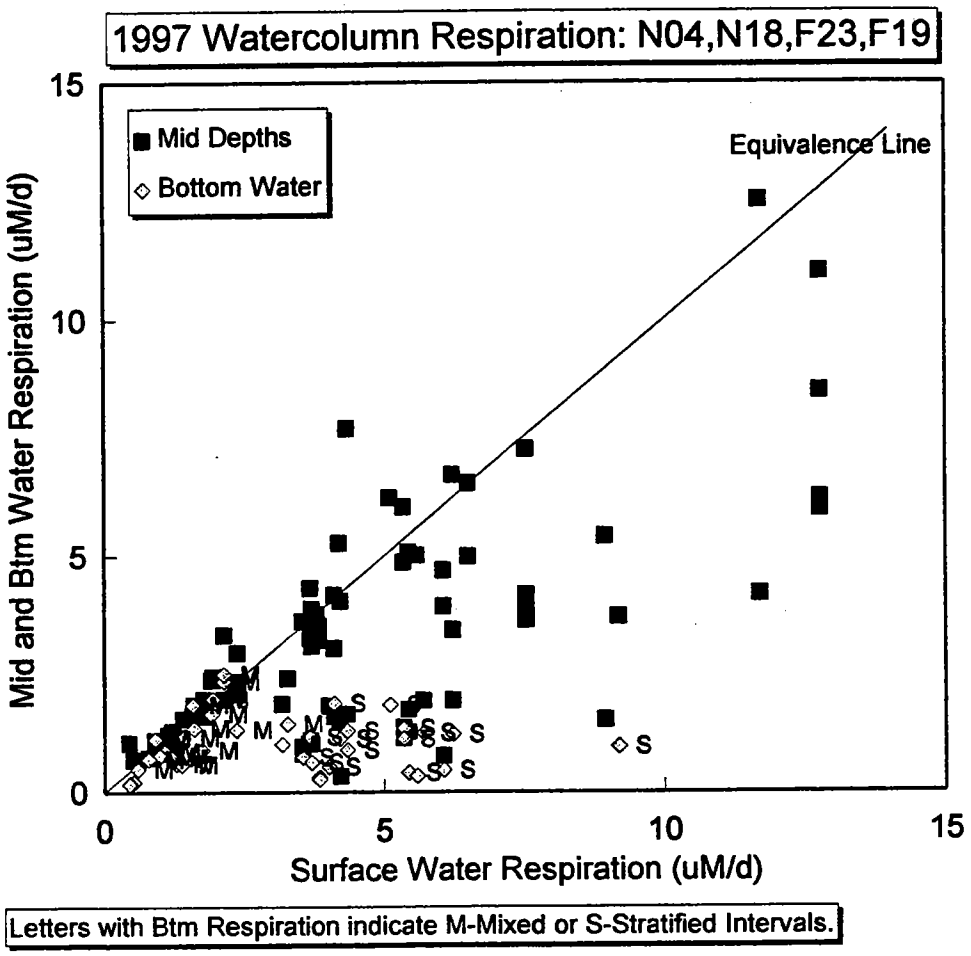

FIGURE 7-27
Relationship of mid and bottom water respiration rates compared to surface water values throughout 1997. Letters to the right of symbols represent mixed interval (M) and stratified interval (S).

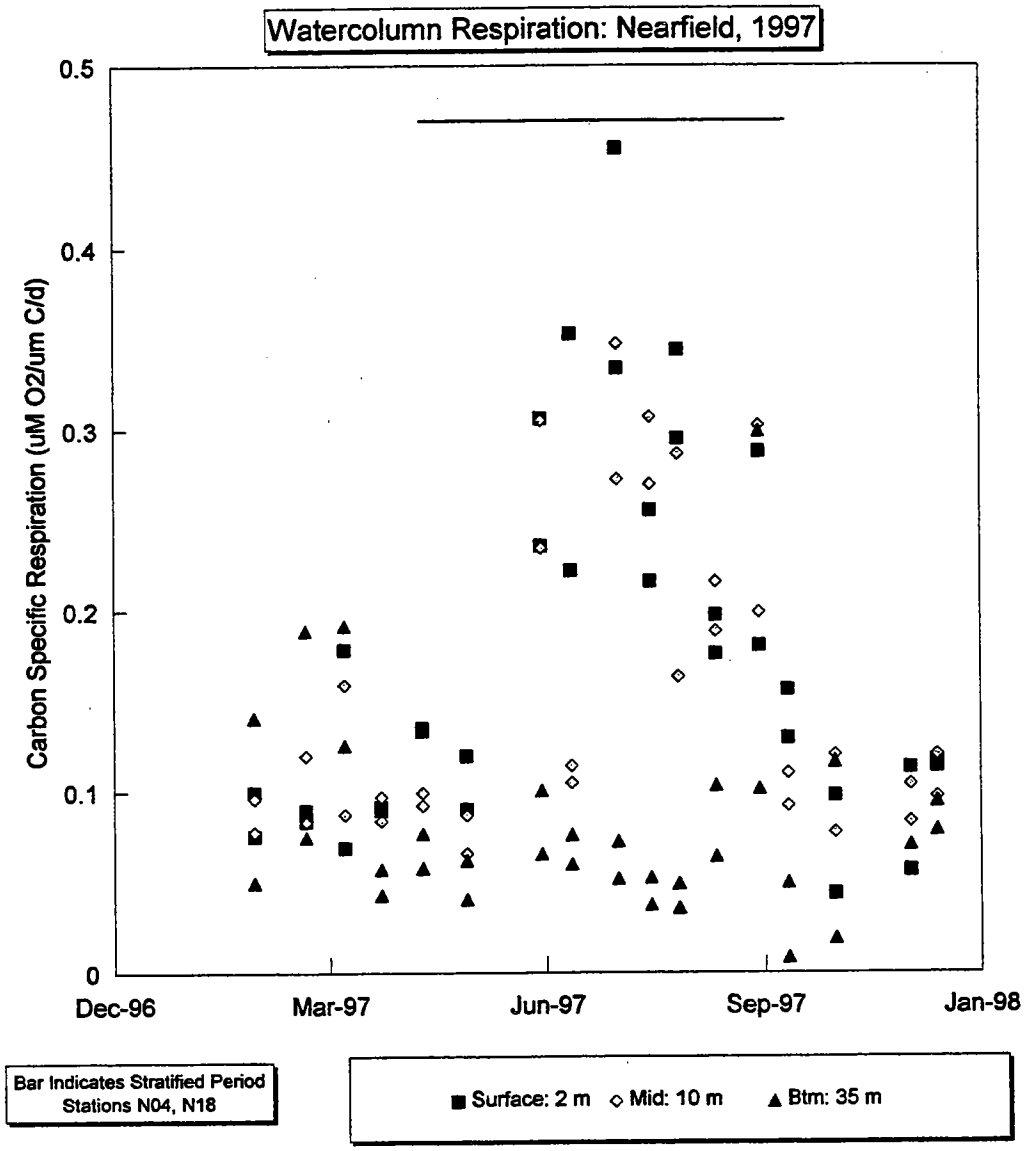

FIGURE 7-28
Vertical distribution of carbon specific respiration within the nearfield (N04 and N18) throughout 1997. Bars represents the approximate stratified interval.

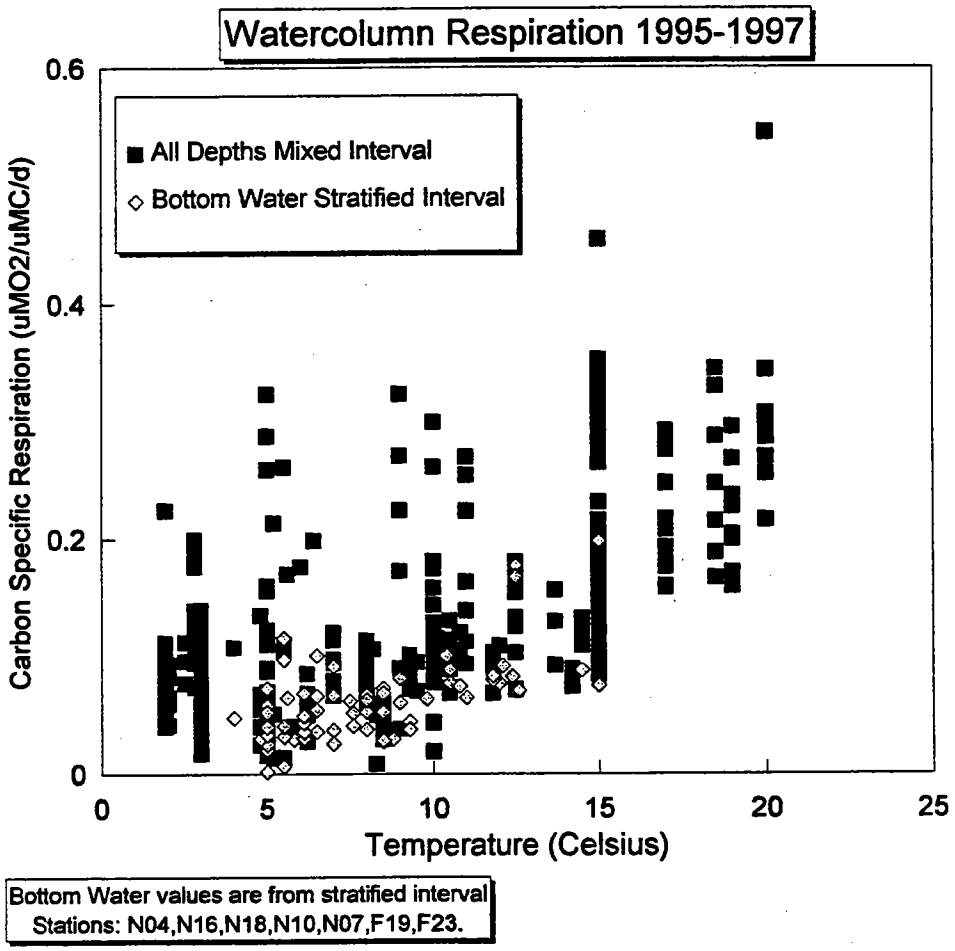

FIGURE 7-29
Carbon specific respiration in the nearfield stations, N04 and N18, versus temperature from all HOM surveys 1995-1997. Values are separated into all depths during mixed layer plus surface and mid depths during stratification and bottom water respiration during stratification.

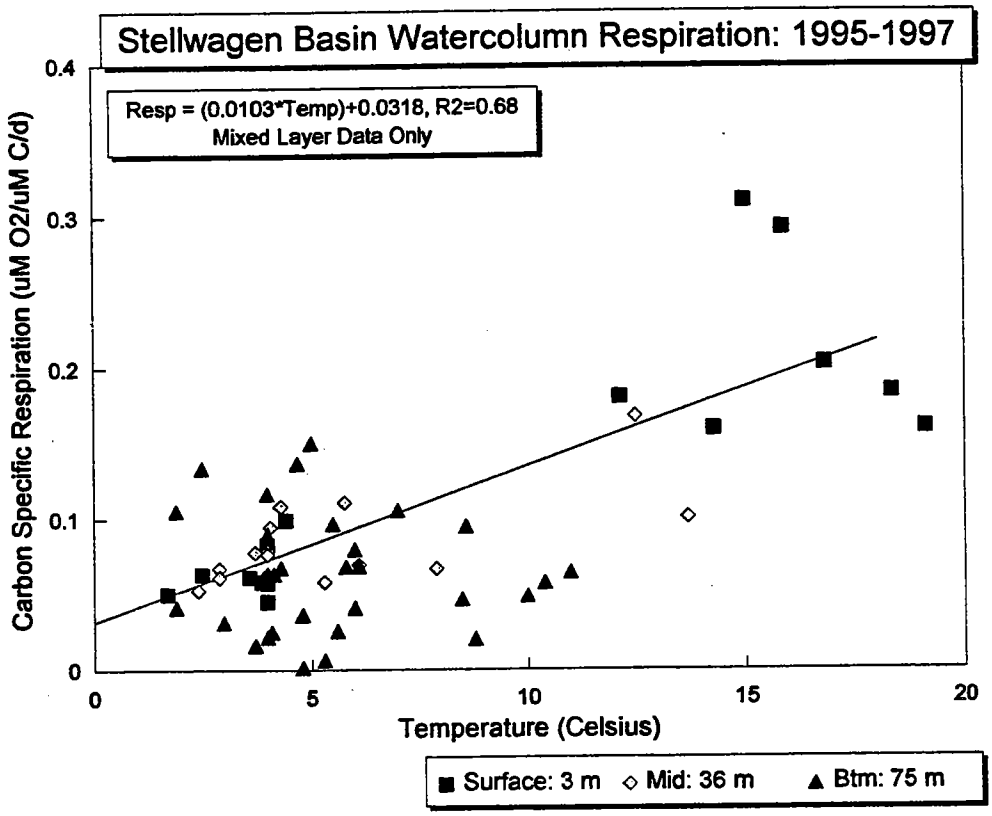

FIGURE 7-30
Carbon specific respiration for Stellwagen Basin (F19) versus temperature from all HOM surveys 1995-1997. Only surface and mid-water samples are used in regression.

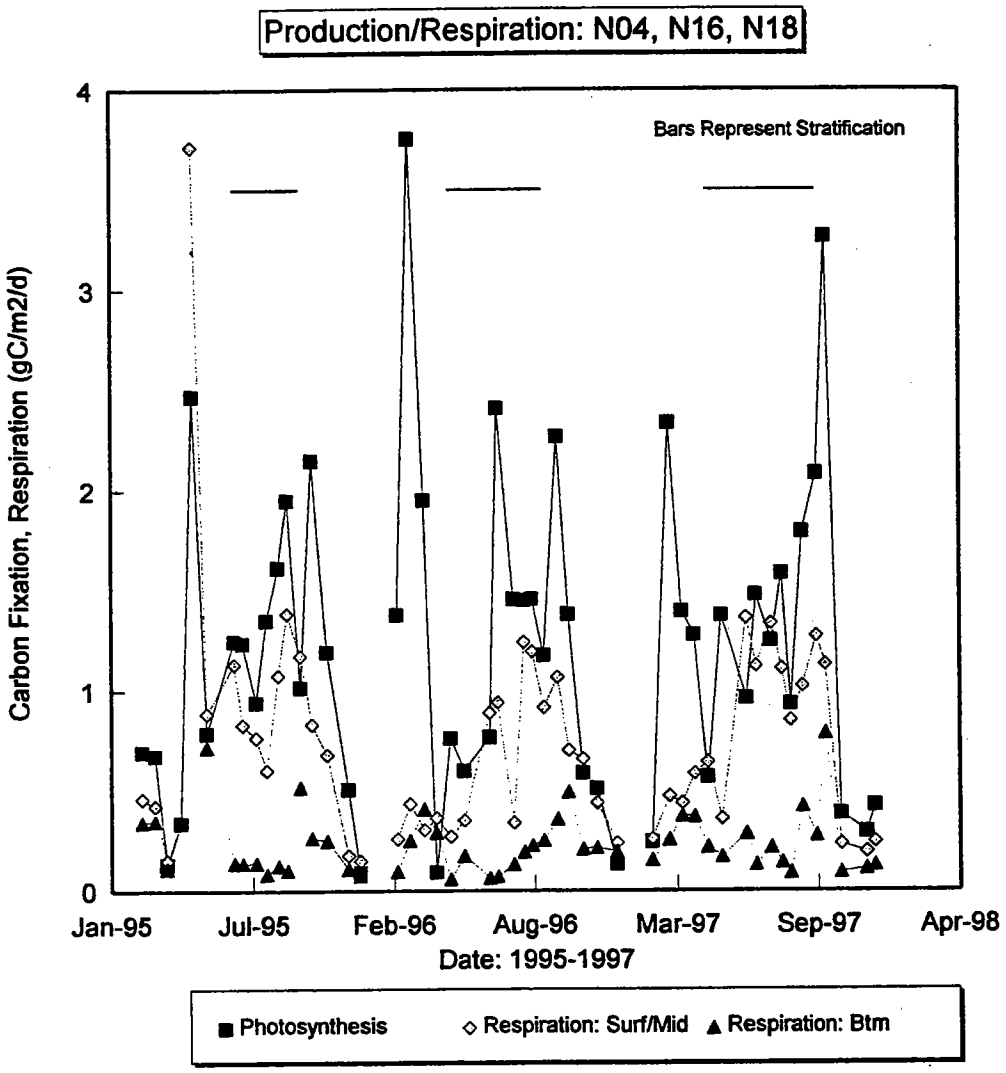

FIGURE 7-31

Nearfield surface and mid water average and bottom water respiration rates and photosynthesis from all HOM surveys 1995-1997. All values are as carbon equivalents (RQ assumed equal to one). Bars represent approximate stratified interval.

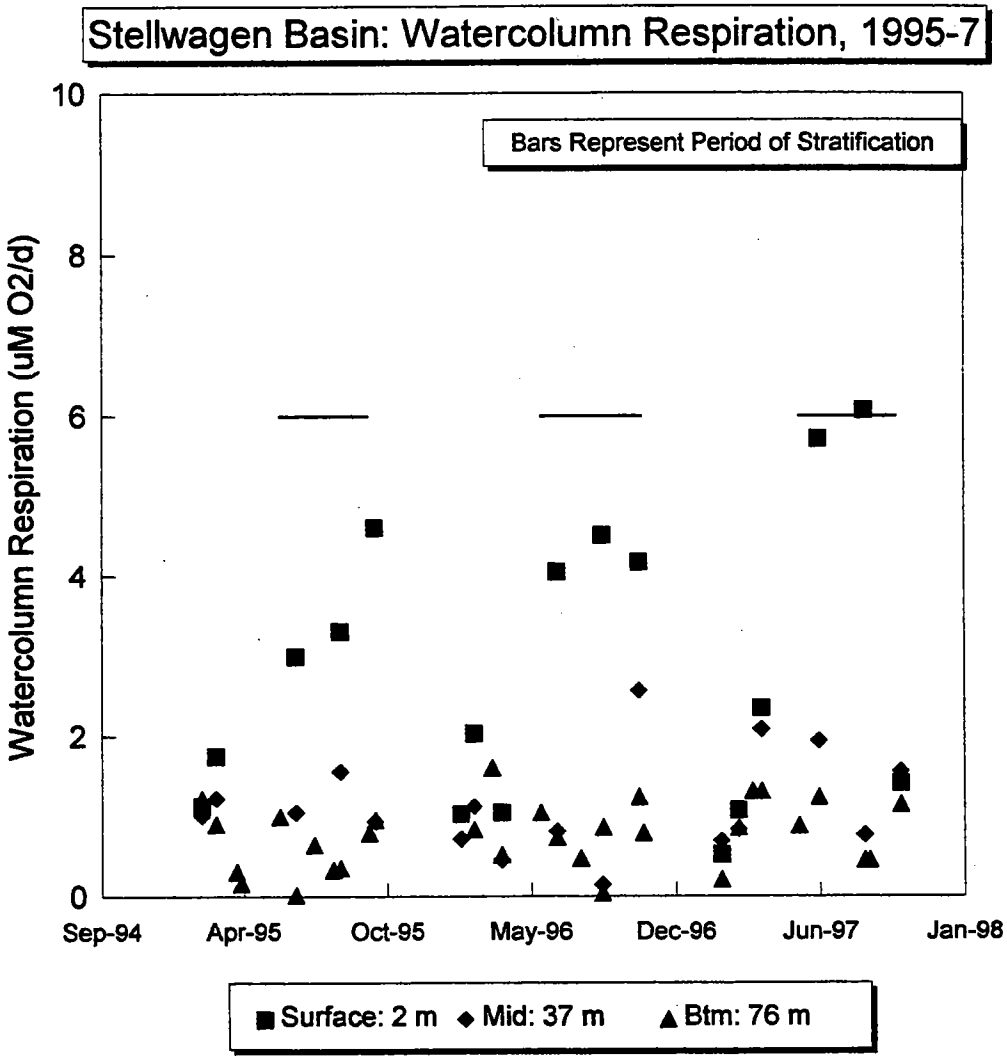

FIGURE 7-32
Stellwagen Basin surface, mid and bottom water respiration rates from all HOM surveys 1995-1997. Bars represent approximate stratified interval.

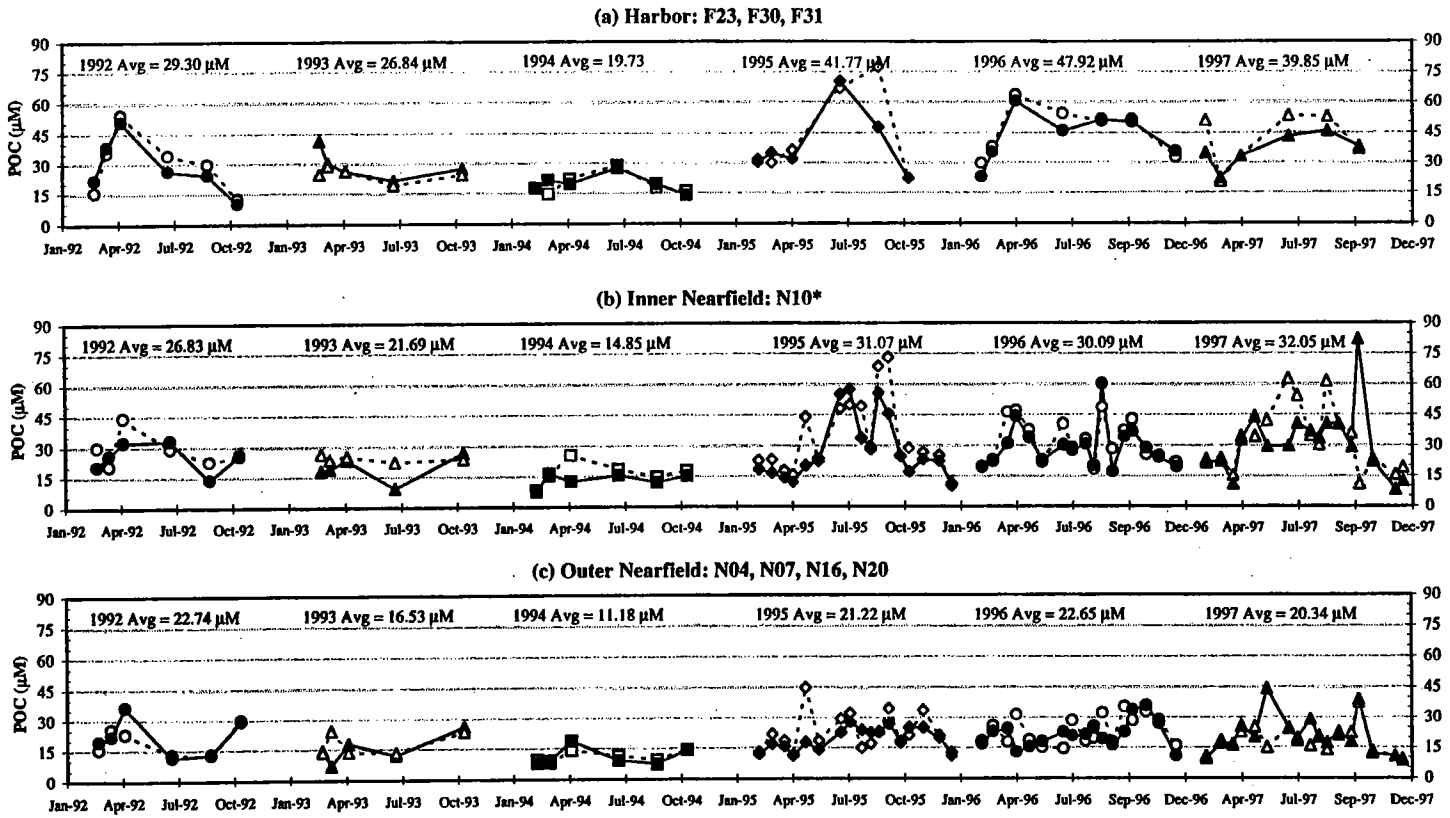

* Please note that in 1996 and 1997, Inner Nearfield is represented by stations N10 and N11

FIGURE 7-33

Interannual POC Concentration Survey Averages for Selected Areas in the Harbor and Nearfield Regions

Open symbols indicate surface average. Closed symbols indicate chla max average.

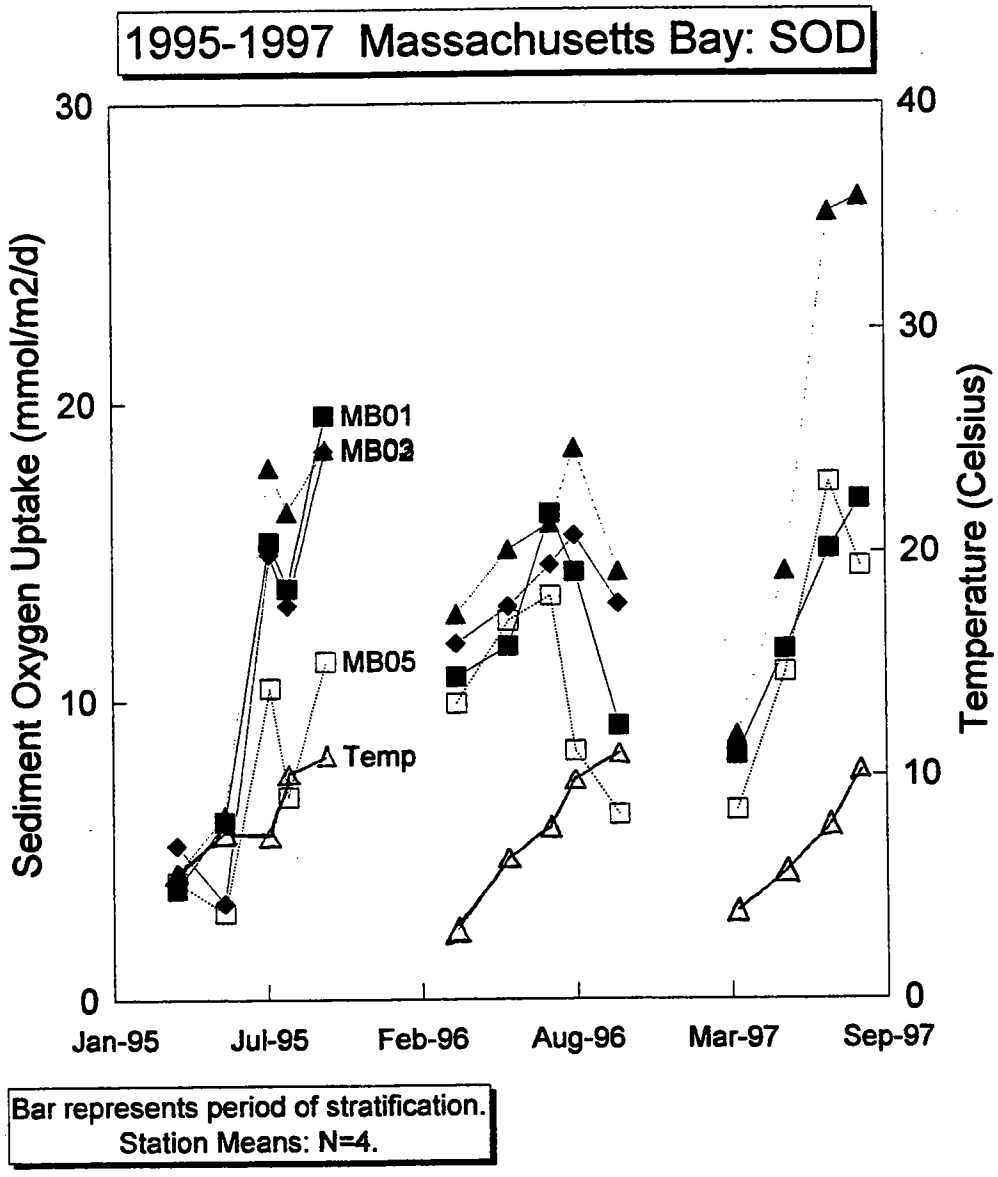

FIGURE 7-34
Sediment respiration in the nearfield (MB01, MB02, MB03) and Stellwagen Basin (MB05) and temperature from 1995-1997. Temperature represents average of all stations.

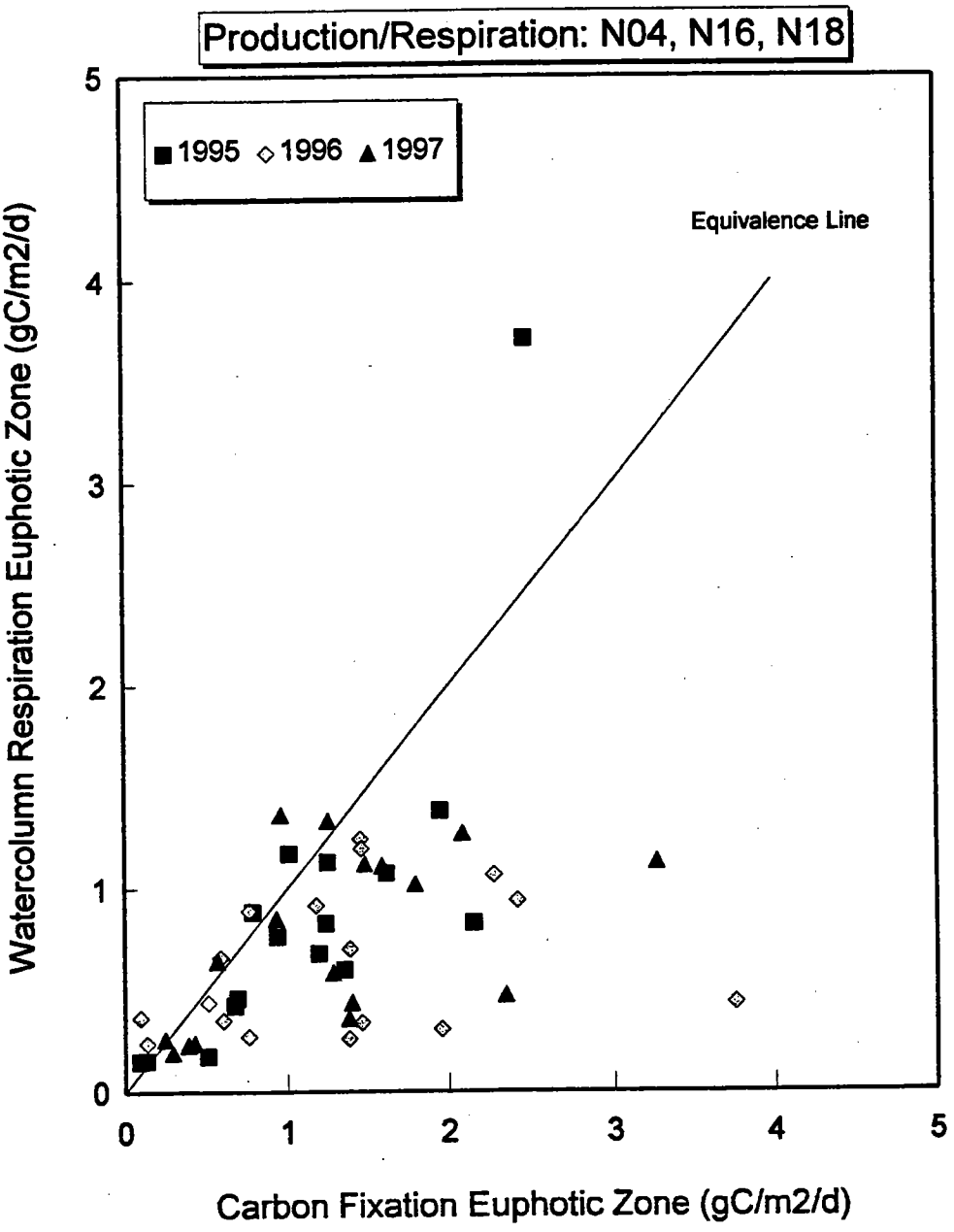

FIGURE 7-35
Relationship of water column carbon fixation to respiration in the outer nearfield, 1995-1997. Values below the line indicate organic matter accumulation.

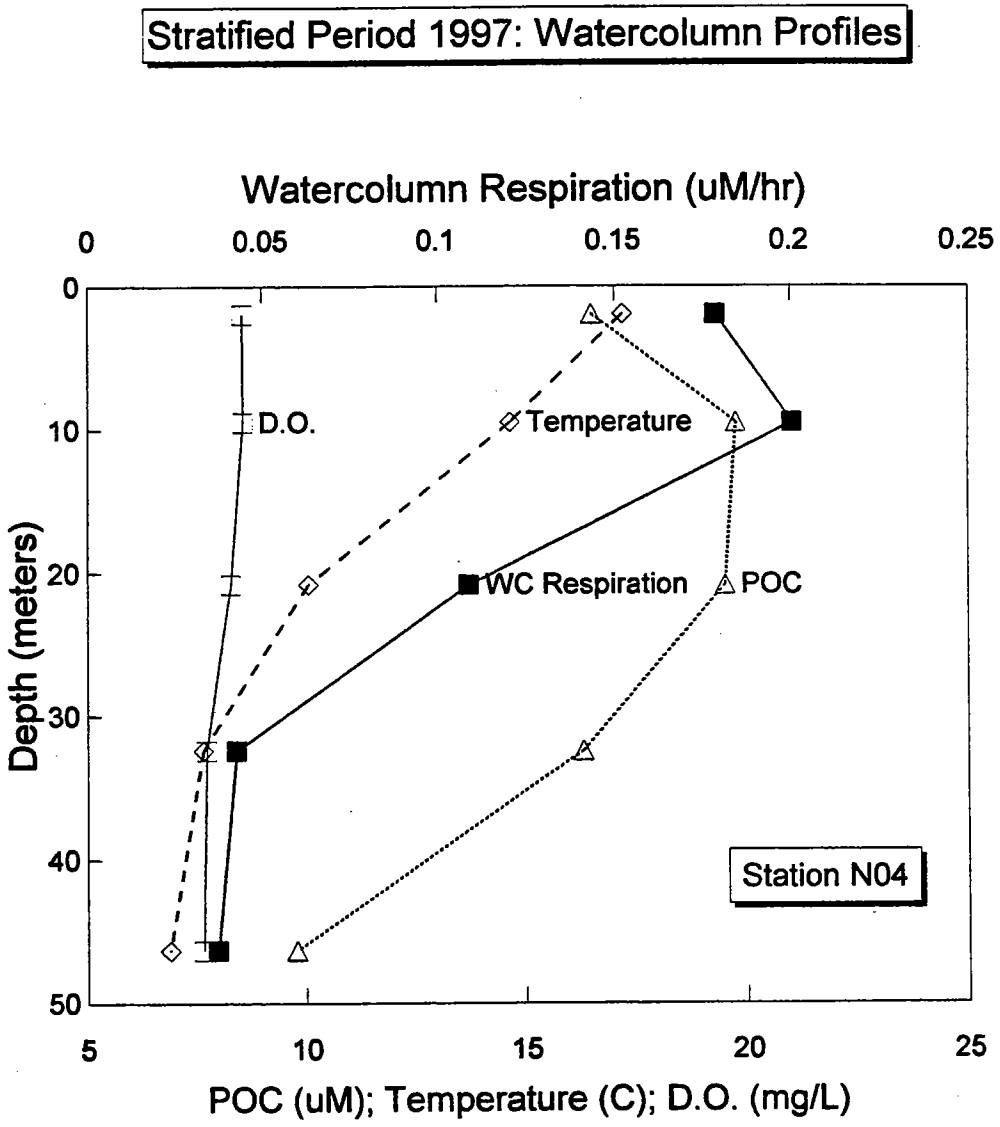

FIGURE 7-36a

Profiles of water column respiration (uMO2/hr), particulate organic carbon (POC), temperature and dissolved oxygen during the stratified interval in 1997: Station N04.

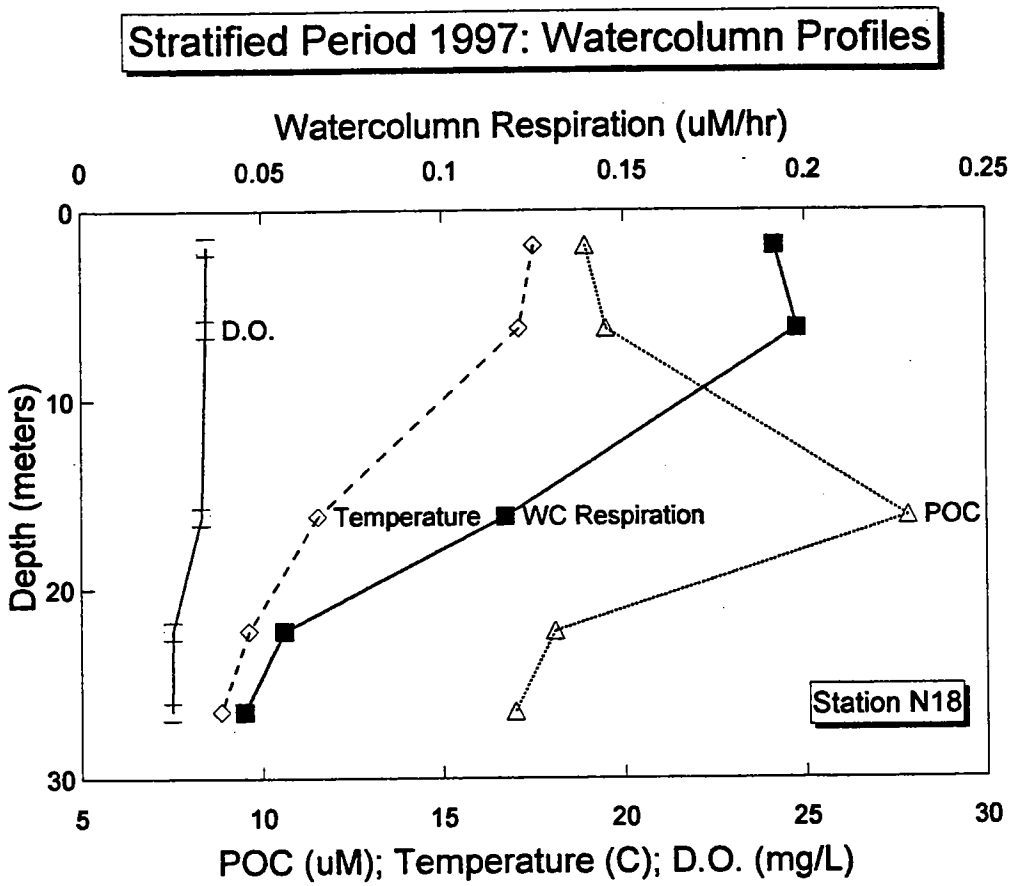

FIGURE 7-36b
Profiles of water column respiration, particulate organic carbon (POC), temperature and dissolved oxygen during the stratified interval in 1997: Station N18.

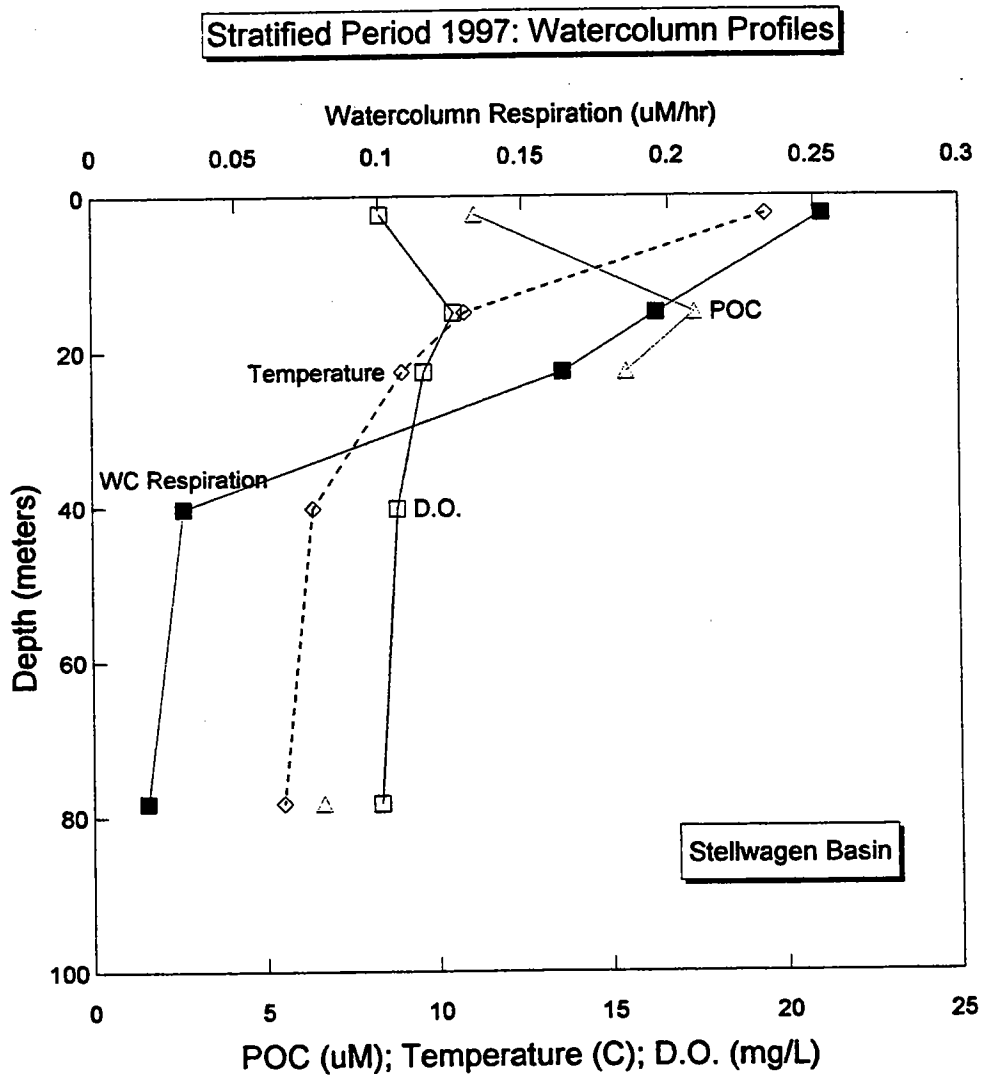

FIGURE 7-36c
Profiles of water column respiration, particulate organic carbon (POC), temperature and dissolved oxygen during the stratified interval in 1997: c) Stellwagen Basin.

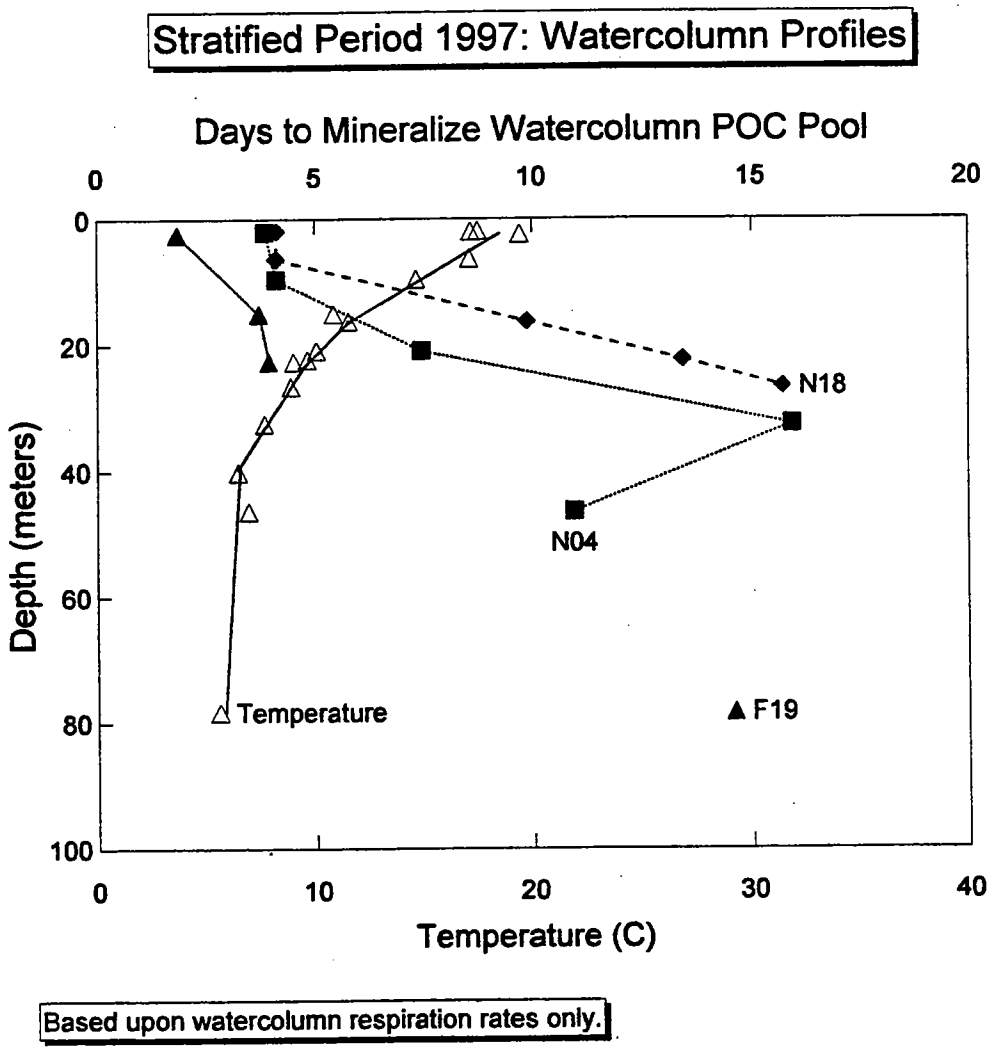

FIGURE 7-37
Estimated time required to remineralize the particulate carbon (POC) pool throughout the water column of the nearfield (N04, N18) and Stellwagen Basin (F19). The temperature profile is a composite of all sites.

8.0 PLANKTON

The 1997 HOM Program included analysis of the plankton community in Boston Harbor, Massachusetts Bay, and Cape Cod Bay during 11 nearfield and six combined nearfield/farfield surveys conducted from February to December. Two stations were occupied in the nearfield surveys, with an additional eleven locations sampled during the combined events (Figure 8-1). Sampling included whole-water phytoplankton collections at the surface (<2.5m) and at the water column mid-depth, which we operationally refer to in this report as the chlorophyll maximum (chl_{max}), as determined from *in situ* fluorescence profiles. Additional samples were taken at these two depths and screened through 20µm Nitex mesh to retain and concentrate larger dinoflagellate species. Oblique zooplankton tows were performed at each of the stations. Details regarding sampling and analysis can be found in the CW/QAPP for water column monitoring (Bowen *et al.*, 1997).

Quantitative taxonomic analyses were performed during 1997, continuing the monitoring record begun in 1992. For 1997, carbon equivalence estimates were made for both phytoplankton and zooplankton communities using species-specific carbon data from the literature. The objective of these analyses is to provide the baseline from which to evaluate the potential effects of the relocation of the Deer Island discharge to its 1999 discharge site in Massachusetts Bay. This evaluation focuses on the potential alteration in biomass or community structure that may result from the stimulatory effects of nutrient enrichment, or alternatively from inhibitory effects due to potential toxicity. Additionally, these data can support assessments of the phytoplankton community's effect on water clarity or color.

In this section, the 1997 plankton record is presented with a discussion of spatial and temporal trends. Comparisons are made with previous baseline data collected from 1992 to 1996.

8.1 Phytoplankton

8.1.1 1997 Abundance and Species Succession in the Nearfield

Whole-water phytoplankton results from the more frequently sampled stations in 1997 (nearfield stations N18 and N04) as well as nearfield station N16, are illustrated in Figure 8-2. Total phytoplankton abundance in the nearfield generally increased through March, with cell densities at mid-depth exceeding those at the surface by several-fold beginning of April. This early season peak was followed by a steady decline into June, although a secondary peak was seen at N04 during mid-May (Figure 8-2a). The less frequently sampled N16 displayed a similar trend and produced the highest phytoplankton densities during the spring of around 10 million (10M) cellsL^{-1} at mid-depth, Figure 8-2b).

Following a seasonal minimum in June, cell densities slowly increased in the nearfield into August to around 1M cellsL^{-1}. Both stations N04 and N18 showed a brief downturn during mid-August, followed by a rapid increase in density during early September. With the exception of much lower densities at mid-depth during W9713 (Figure 8-2a), phytoplankton densities continued to climb through September to reach peak densities for the year

in early October. Both surface and mid-depth samples yielded densities ≥10M cellsL^{-1} at stations N16 and N18 (Figure 8-2b and c), with results from station N04 only slightly lower (Figure 8-2a). Densities declined to around 1M cellsL^{-1} by the late October survey W9715 and continued to decline slightly thereafter.

In terms of phytoplankton community composition, the late winter bloom exhibited a noticeably small contribution from centric diatoms (Figures 8-3 and 8-4), whereas high densities of centric diatoms such as *Thalassiosira* and *Chaetoceros* typically characterize this event (see Section 7.1.3). During 1997, however, the early dominant in the year, *Thalassiosira* spp., reached densities of only around 0.2M cellsL^{-1} and its typical successor, *Chaetoceros* spp., only reached around 0.5M cellsL^{-1} during April (Cibik *et al.*, 1998b). *Chaetoceros* densities did finally bloom during May, with mid-depth results at station N04 and N18 ≥ 2M cellsL^{-1} (Figure 8-4a and c).

The main feature of the late winter/spring bloom was an extensive bloom of *Phaeocystis pouchetii*, considered to be a nuisance algal species in the HOM Program (see Section 5.3.1.4). *Phaeocystis* was the numerical dominant during March and April, reaching a peak density of 7.7M cellsL^{-1} in the nearfield (mid-depth at station N16 during W9704, Figure 8-4b). However, despite the numerical dominance by *Phaeocystis* and the relatively low numeric contribution of centric diatoms, the latter dominated the autotrophic carbon pool during the late winter/spring bloom (Figures 8-5 and 8-6). In fact, *Thalassiosira* spp. contributed around half the carbon during late February, while *Chaetoceros* spp. comprised the bulk of autotrophic carbon during March and April (Cibik *et al.*, 1998b). Late in the spring bloom (W9705), the dinoflagellate *Ceratium longipes* also contributed substantially to the phytoplankton carbon pool (Figure 8-5c; Cibik *et al.*, 1998b).

Much of the summer was characterized by microflagellate dominance and low estimated phytoplankton carbon equivalence (Figures 8-3 through 8-6). A localized bloom of the centric diatom *Rhizosolenia fragilissima* was observed at the surface at N18 during late June (Figure 8-3c) which produced a large influx of autotrophic carbon (Figure 8-5c). While their densities were relatively low, the large dinoflagellate *Ceratium longipes* dominated the autotrophic carbon in mid-depth samples of the more seaward station N04 during June and July (Figure 8-6a; Cibik *et al.*, 1998b).

The phytoplankton assemblage remained dominated by microflagellates into September, with subdominants including small dinoflagellates (*Gymnodinium* spp.) and several cryptophyte species (Figures 8-3 and 8-4). However, during the two September surveys (W9712 and W9713), the centric diatoms *Rhizosolenia fragilissima* and *Cyclotella* sp., and the pennate diatom *Thalassionema nitzschoides* became co-dominant at station N18 (Cibik *et al.*, 1998a). These taxa may have been responsible for the increased productivity and respiration rates seen at this station (Section 7.1).

The fall bloom in early October yielded the highest densities of centric diatoms reported during 1997 (Figures 8-3 and 8-4). The dominant centric was *Thalassiosira*, which exceeded 4 million cellsL^{-1} at the surface, and over 7 million cellsL^{-1} at mid-depth at N18 (Cibik *et al.*, 1998a). Co-dominants included the centric diatom *Cyclotella* sp., a small (<10 μm) unidentified pennate diatom, and microflagellates. Station N16 was also co-dominated by the pennate diatom *Asterionellopsis glacialis* and *R. fragilissima*. Carbon contributions during the fall bloom

showed a similar pattern to the abundance data (Figures 8-5 and 8-6). Following the bloom in early October, nearfield phytoplankton densities decreased and again were dominated by microflagellates, cryptophytes, and *Gymnodinium* sp.

8.1.2 Regional Comparisons for 1997

Abundance plots from each station sampled during the six farfield surveys in 1997 were used to demonstrate the differences in regional successional patterns (Figures 8-7 through 8-12). Nearfield results were included to facilitate regional comparisons. During early February (W9701), the microflagellate component of the phytoplankton assemblage dominated throughout Massachusetts Bay and Cape Cod Bay (Figure 8-7). Note however the high relative distribution of centric diatoms (*Thalassiosira gravida* and *Rhizosolenia delicatula*; Cibik *et al.*, 1998b) in southern Massachusetts Bay and Cape Cod Bay stations (F06, F01, and F02).

By late February, Cape Cod Bay had a fully developed *Phaeocystis pouchetii* bloom, with densities exceeding 5M cellsL^{-1} in eastern Cape Cod Bay (station F02; Figure 8-8). Microflagellates and *T. gravida* were co-dominants there, while microflagellates remained dominant at all other stations. By early April (W9704), *P. pouchetii* dominated many other stations, including Boston Harbor and the nearfield (Figure 8-9). Nearfield station N16 had the highest surface densities of *P. pouchetii* (Figure 8-9a), while in eastern Cape Cod Bay *P. pouchetii* had risen to 15M cellsL^{-1} in mid-depth samples (Figure 8-9b). As stated in the previous section, the *Phaeocystis* bloom persisted in western Massachusetts Bay through April, but had disappeared from samples by early May (Figures 8-3 and 8-4).

By the mid-June farfield survey (W9707), microflagellates dominated most regions and had greatest densities in Boston Harbor (Figure 8-10). The centric diatoms *Chaetoceros* sp. and *Rhizosolenia fragilissima*, as well as cryptophytes, were producing a strong bloom in Boston Harbor and adjacent coastal stations. Note in the previous section that nearfield survey data from station N18 during late June also showed surface bloom activity by *R. fragilissima*. Cryptophytes were also co-dominant in Cape Cod Bay during mid-June.

Results from the late August farfield survey (W9711) documented a strong Harbor and coastal bloom event that extended into Cape Cod Bay (Figure 8-11). Boston Harbor (F23, F30, and F31) and in the adjacent coastal region (F24 and F25) were dominated by centric diatom *Skeletonema costatum* (maximum density of 1.78 million cellsL^{-1}, Cibik *et al.*, 1998a) and cryptophytes. Coastal stations to the south of the harbor and Cape Cod Bay, however, showed differences in dominant taxa among the stations. Stations F06, F13, F01, and F02 were dominated by *R. fragilissima* at both surface and mid-depths (maximum density of 1.76M cellsL^{-1}). *S. costatum* and cryptophytes, while present in the more southerly stations, were not present to the same degree. Microflagellates dominated the nearfield and Boundary stations, which showed little diatom activity during the period.

Differences in regional assemblages were also evident during the fall bloom (Figure 8-12). The centric diatom *Thalassiosira* dominated the nearfield assemblage, while microflagellates and the centric diatom *Cyclotella* were co-dominant (Cibik *et al.*, 1998a). Dominant taxa at Cape Cod Bay stations were microflagellates, *S. costatum*,

and *Cyclotella*. The Harbor assemblage was substantially different, with the pennate diatom *Asterionellopsis glacialis* and the centric diatoms *Leptocylindrus danicus* and *L. minimus* reported as dominant forms. The dinoflagellate flora in the late season farfield samples exhibited dominant taxa similar to those reported for the nearfield stations.

8.1.3 Toxic and Nuisance Species

The HOM program includes monitoring for toxic and nuisance species, particularly *Alexandrium tamarense*, *Phaeocystis pouchetii*, and *Pseudo-nitzschia multiseries*. *A. tamarense* is a dinoflagellate that can cause paralytic shellfish poisoning (PSP) when shellfish that have concentrated the toxin are consumed. *Phaeocystis pouchetii* is considered a nuisance species due to its tendency to form mucilaginous colonies that can clog nets and produce large amounts of foam on beaches. *Pseudo-nitzschia multiseries* is a pennate diatom with toxic strains that can produce amnesic shellfish poisoning (ASP) in humans who consume shellfish that have concentrated the organism. For convenience, results for nuisance taxa from previous years of monitoring are included in the discussion below.

Alexandrium in the Massachusetts Bay region may arise from two sources: locally from benthic cysts and from advective transport of cells arising from riverine discharges in southern Maine, usually during the period April to June (Anderson and Keafer, 1992; Franks and Anderson, 1992). Once established, abundance and distribution are governed by nutrient availability, wind patterns and coastal currents. These physical controlling factors may alternatively disperse the population offshore or lead to conditions of increased residence time which allow localized blooms (Anderson and Keafer, 1995).

During most years of baseline monitoring, there were typically three surveys in the nearfield during the period when *Alexandrium* might be encountered and only one (mid-June) in the farfield. Over the baseline period, *A. tamarense* was detected in HOM samples primarily in 1993, only sporadically in 1992 and 1994, and not during 1995-1997 (Figure 8-13). Results from 1993 were consistent with Massachusetts Division of Marine Fisheries shellfish toxicity monitoring results which indicate that 1993 was the only year in this decade with significant occurrences of shellfish toxicity (see Anderson and Keafer, 1995; Cibik *et al.*, 1996). Low densities of *A. tamarense* during subsequent years have been confirmed by separate surveys conducted by D.M. Anderson (Anderson, 1997), and include recent studies using immuno-fluorescent techniques which documented peak densities of only around 30 cells/L during 1997, a level considered insufficient to produce detectable levels of dioxin in shellfish (D.M. Anderson, personal communication).

As stated in the previous sections, *Phaeocystis* was reported throughout Massachusetts and Cape Cod Bays in the late winter and spring 1997 HOM plankton monitoring. The 1997 bloom initiated in Cape Cod Bay in late February and progressed northward into Massachusetts Bay during March. The maximum density reported from 1997 samples was 14.94M cellsL^{-1} in the mid-depth sample from station F02 during W9704. Over the baseline period, *P. pouchetii* has been sporadically detected in most years, but 1992 and 1997 were the two years that produced significant blooms (Figure 8-14).

The toxin-producing strains of *Pseudo-nitzschia* cannot be differentiated from non-toxic species under the light microscope. The potential presence of toxic *Pseudo-nitzschia multiseries* in Massachusetts and Cape Cod Bays was examined by plotting all reported results for the morphologically similar species *Pseudo-nitzschia pungens*. This approach should be viewed as a conservative indicator of whether a toxic species may be present.

The 1997 record indicated that *P. pungens* occurred primarily in the summer and fall, with maximum densities at station F01 during W9711 (188,480 cells^{-1}). This was the only year within the six-year baseline where concentrations of this indicator species exceeded 100,000 cells/L (Figure 8-15), a threshold tentatively adopted by the MWRA based on literature values for domoic acid concentrations associated with ASP outbreaks (Bates, 1997).

8.1.4 1992-1997 Interannual Comparisons

While the previous (1992 to 1994) HOM sampling included six sampling stations within the nearfield, the 1995-1997 sample coverage in the nearfield included 2-3 stations. Interannual comparisons were therefore restricted to two stations to avoid confounding averaging schemes. Station N16 was selected for interannual comparisons as it was sampled throughout the baseline period (1992-1997), with the exception of W9701. Station N10 had been used in previous annual reports to provide an inshore station and thus illustrate potential responses to the horizontal (inshore-offshore) nutrient gradient. Plankton sampling at station N10 was discontinued during 1997 and the effort was reallocated to station N18. For convenience, station N18 was used in the interannual plots for comparison with the more seaward station N16.

The general baseline trend in total phytoplankton abundance includes peaks representing the spring and fall blooms, and a general increase in densities through the summer period (Figure 8-16). Centric diatoms (Figure 8-17) typically dominate the spring and fall blooms, and pennate diatoms often fuel the fall bloom as well (Figure 8-18). The general increase in densities observed over the summer and into the fall is largely produced by microflagellates, although other flagellates such as cryptophytes and dinoflagellates also generally increase throughout this period. The spring *Phaeocystis* bloom during 1997 accentuated the early season peak in total cell densities (Figure 8-16), which was also the case in 1992 (see discussion in preceding section).

The interannual pattern for centric diatoms revealed that their degree of dominance of the 1997 fall bloom throughout the nearfield was largely unprecedented over the baseline period (Figure 8-17). Other features include the large, prolonged spring bloom during 1996, which produced the highest seasonal spring chlorophyll average on record (see Table 5-2). Likewise, the predominant seasonal fall chlorophyll average during 1993 was a result of the prolonged pennate diatom bloom during that year (Figure 8-18). The overarching theme demonstrated in the HOM phytoplankton data is the considerable spatial and temporal variability that is characteristic of the nearfield.

8.2 Zooplankton

8.2.1 Annual Cycle of Total Zooplankton and Major Groups

Total zooplankton abundance in the nearfield during 1997 generally increased through June, producing the peak annual results at stations N04 and N16 (Figure 8-19). Zooplankon abundance generally declined thereafter, but reached an annual peak at station N18 during late October. The highest density for the year was observed at this time, yielding over 140,000 m^{-3}. Peak abundance in June (approximately 110,000 m^{-3}) was also observed at station N18. After the late season peak, abundances fell to low levels in November (< 40,000 m^{-3}) and remained low through December.

Zooplankton abundance was dominated by copepods and copepod nauplii, which constituted about 80 percent of the total zooplankton (Figure 8-20). Barnacle nauplii were observed during late winter in the nearfield, contributing up to 25 percent of the total (Station N16, Figure 8-21). Other groups of zooplankton combined typically constituted only a small fraction of the total zooplankton abundance, although periodic peaks in molluscan larvae (station N18, W9704) and bivalve larvae (station N04, W9715) occasionally yielded up to 60% of the total zooplankton abundance (Figure 8-21c and 8-21a, respectively).

About 40% of the copepods collected were naupliar stages, the other 60% being copepodite stages, which includes the adults. There appeared to be a relatively greater proportion of naupliar stages during the first half of the year, particularly at station N04 (Figure 8-21a). Naupliar stages made up about half of the copepods collected during the late winter and spring but less than half during the summer and fall. Given the higher abundance of total copepods during the latter half of the year, this relative shift in life stage composition reflects the relative seasonal increase in copepodite versus naupliar life stages in the samples collected.

The lower abundance of nauplii relative to copepodites is largely a result of extrusion of the smaller nauplier stages through the meshes of the net, though the somewhat shorter duration of naupliar life stages is a factor. But the higher mortality of later life stages should make those stages even less abundant relative to nauplii.

8.2.2 Regional Patterns of Dominant Taxa

The dominant zooplankton taxa were observed to have particular geographic affinities, as was observed in prior years. Taxa usually had either nearshore or offshore affinities, although a few dominant taxa were equally abundant everywhere.

Typical taxa having an offshore affinity include *Calanus finmarchicus, Centropages typicus*, and *Oikopleura dioica* (Figures 8-22 through 8-24). Abundance of these species is highest at the boundary stations and decreases markedly at the inshore stations especially near Boston Harbor. These species maintain large populations in the Gulf of Maine, and their presence in the bay is in large part due to advective input from that region. *C. finmarchicus* and *O. dioica* are primarily abundant during spring and early summer, while *Centropages typicus* is

a dominant late summer/fall species. Although *Oikopleura* and *Calanus* are primarily spring dominants, peaks were observed in Cape Cod Bay during August.

Two dominant taxa are known to be abundant offshore but are also plentiful near shore: *Oithona similis* and *Pseudocalanus* spp. (Figure 8-22 and 8-23). Peak *Oithona* abundance occurred during the latter half of the year (W9712) while *Pseudocalanus* were most abundant during late spring/early summer (W9707). Both species had lower abundances in the harbor.

Several taxa have affinities for nearshore regions (Figure 8-23 through 8-26). These taxa include the copepods *Acartia tonsa* and *A. hudsonica*, copepods that lay bottom resting eggs (*Centropages hamatus* and *Temora longicornis*), the estuarine copepod *Eurytemora herdmani*, meroplanktonic larvae (polychaete and barnacle), the cladoceran *Podon* sp. and harpacticoid copepods. Several of these taxa have ties to the sea floor either through production of benthic resting eggs, parental adult populations, or through epibenthic/planktonic migration behavior. The *Acartia* spp. are thought to be restricted to nearshore environments due to some combination of food limitation and possibly salinity intolerance of their nauplii (Cibik *et al.*, 1998d). *Centropages hamatus* and *Temora longicornis* are restricted to shallow regions where tidally induced resuspension of bottom sediment prevents their bottom resting eggs from becoming buried. Thus, these dominant zooplankton taxa can be grouped according to their nearshore or offshore affinities.

8.2.3 Annual Cycles of Dominant Copepod Species by Region

The dominant copepod (and zooplankton) species in terms of abundance was *Oithona similis*, while *Calanus finmarchicus* was the dominant species in terms of biomass. *Oithona similis* was numerically dominant in the nearfield, Cape Cod Bay and the boundary region. *Calanus* was the biomass dominant in the nearfield, Cape Cod Bay and the boundary region. *Calanus* reached peak biomass dominance during the spring/summer period. Note that the contribution of each species to total zooplankton biomass was approximated by multiplying numerical abundance by literature values for adult body carbon equivalence. While this method overestimates total biomass, it does provide a reasonable weighting for examining the relative proportion of biomass among species. Body weights used for the 8 species plotted (*Oithona* to *Centropages hamatus*) were 1, 10, 10, 10, 125, 15, 10, 10 µg carbon, respectively. For species where body weights were unknown, weights of similar sized species were used.

In the nearfield region (stations N04, N16, N18), numerically dominant species during spring were *Oithona*, *Pseudocalanus*, *Temora* and *Calanus* (Figure 8-27). Due to its large body size, *Calanus* overwhelmingly dominated the spring zooplankton biomass. During the second half of the year, *Oithona*, *Pseudocalanus*, *Temora* and *Centropages typicus* were numerically dominant, with *Centropages typicus* dominating the fall biomass. Peak abundance values were approximately 35,000 m^{-3} for *Oithona*, and less than 10,000 m^{-3} for each of the other species.

In Cape Cod Bay (Stations F01 and F02, Figure 8-28), abundance was highest during late summer and was dominated by variety of species including *Oithona, Pseudocalanus, Calanus* and *Acartia tonsa*. Spring

dominants included *Oithona, Pseudocalanus*, and *Temora*. Peak *Oithona* abundance was near 20,000 m^{-3}, while maximum abundance of the other species was less than 5,000 m^{-3}. In terms of biomass, *Calanus* again was overwhelmingly dominant during spring and summer.

At the boundary station F27 (Figure 8-29), *Oithona* and *Calanus* were the numerical dominants during the early spring while *Oithona* and *Pseudocalanus* dominated during summer/fall. Peak *Oithona* abundance was approximately 25,000 m^{-3}. *Calanus* dominated the biomass completely throughout the year.

At station F06 (Figure 8-30), *Pseudocalanus* dominated during the spring while *Oithona* dominated the rest of the year. Spring abundance was dominated by *Pseudocalanus, Oithona,* and *Temora*, while fall abundance was dominated by *Oithona, Pseudocalanus* and *Centropages typicus*. Spring biomass dominants included *Pseudocalanus , Calanus* and *Temora*.

In the coastal region (Stations F24, F25, F13, Figure 8-31), species composition was more equitable among the eight species. Spring abundance was dominated by *Temora, Pseudocalanus* and *Oithona*, while summer/fall abundance was dominated by *Oithona, Acartia tonsa, Pseudocalanus, Centropages hamatus, Temora,* and lesser numbers of *Acartia hudsonica, Centropages typicus,* and *Calanus*. Spring biomass was dominated by *Temora, Pseudocalanus,* and *Calanus*. At these more inshore stations, the overwhelming dominance of *Calanus* in terms of biomass no longer occurred and the smaller *Pseudocalanus, Temora* and *Acartia tonsa* became equally important.

In Boston Harbor (Stations F23, F30, F31, Figure 8-32), *Acartia hudsonica, Oithona* and *Temora* were dominant in terms of abundance in the spring while *Acartia tonsa* dominated the summer/fall season. *Pseudocalanus* was also abundant in the harbor. Peak *Acartia* abundance was 29,000 m^{-3}. *Calanus finmarchicus* and *Acartia hudsonica* dominated the spring biomass while *Acartia tonsa* dominated the fall biomass.

8.2.4 Interannual Observations of Dominant Taxa

Annual cycles in abundance of zooplankton were compared for the MWRA survey years 1992-1997 at five stations (F01, F02, F13, F23 and N16) that were sampled all years and one station (N04), which was sampled all years except 1995. In terms of total zooplankton abundance, fall abundance appeared to be lower in Cape Cod Bay and the coastal station (F13) in 1997 as compared to other years (Figure 8-33). The remaining values fell within the scatter of the 1992-1996 data.

Abundance of copepod nauplii in 1997 appeared to be slightly higher than most other years at stations F23 and N04 (Figure 8-34). Copepod nauplii abundance was also high in 1996 in the nearfield and Cape Cod Bay. Abundance at these stations was near the upper end of the six-year baseline range throughout most of the year. The lowest abundance of copepod nauplii was observed in 1992 in the nearfield (N04 and N16) and Cape Cod Bay (F01 and F02). It is not possible to attribute the high or low abundance to a particular species since the nauplii were not classified taxonomically.

Oithona abundance in 1997 was similar to the previous years (Figure 8-35). It appeared that *Oithona* abundance was elevated during the spring of 1997 at station N04. Highest abundance of *Oithona* occurred in 1992 during the fall at all stations. The abundance of this species was lowest in the harbor (F23) all years.

The abundance of *Pseudocalanus* and *Paracalanus* (combined due to taxonomic discrepancies between years) also had no apparent differences with prior survey years (Figure 8-36). The first half of the year is typically dominated by *Pseudocalanus*, which is a boreal animal, while *Paracalanus* is dominant during the second half of the year. *Paracalanus parvus* was not observed in the 1996 samples but reappeared in the 1997 samples. This species is subtropical, and its abundance can vary significantly from year to year. Its complete absence from the region in 1996 is curious and requires further investigation.

Acartia spp. (tonsa and *hudsonica* combined due to taxonomic discrepancies between years) abundance in 1997 appeared to be higher than most other years at stations F13 and N04. (Figure 8-37). Highest abundance of this genus occurred in the harbor during the fall of all years. Its abundance decreases markedly away from shore, and, in comparing inner and outer nearfield stations (N18 vs. N04), it can be seen that a strong gradient in its abundance exists across this region, particularly in the case of *A. tonsa* (Figure 8-38). *A. tonsa* is dominant in the second half of the year while *A. hudsonica* dominates the first half of the year.

Calanus finmarchicus abundance in 1997 also was similar to prior survey years (Fig. 8-39). Highest abundance occurred in the nearfield, especially in 1996 at station N04.

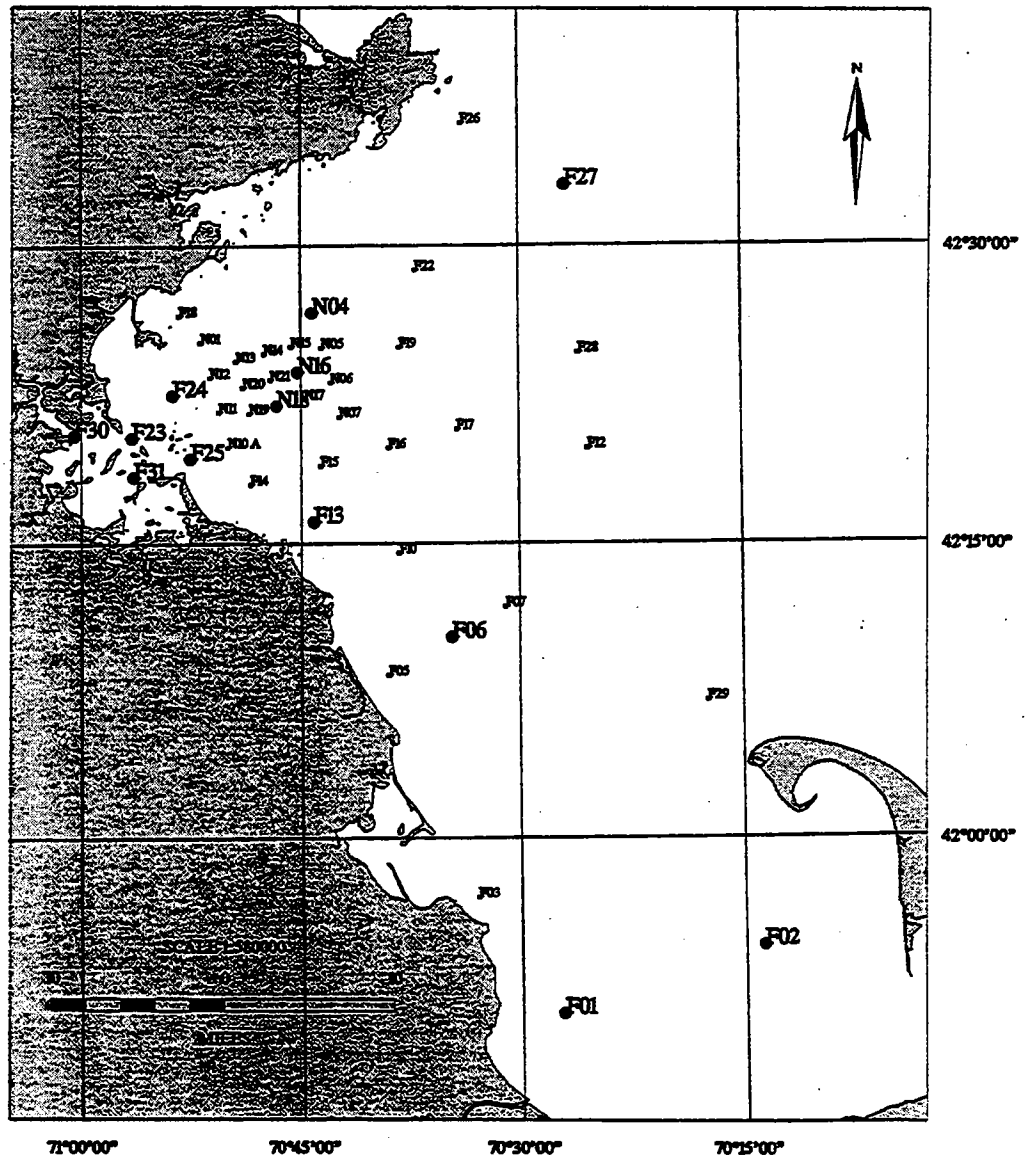

FIGURE 8-1
1997 HOM Plankton Station Locations (Enlarged Text)

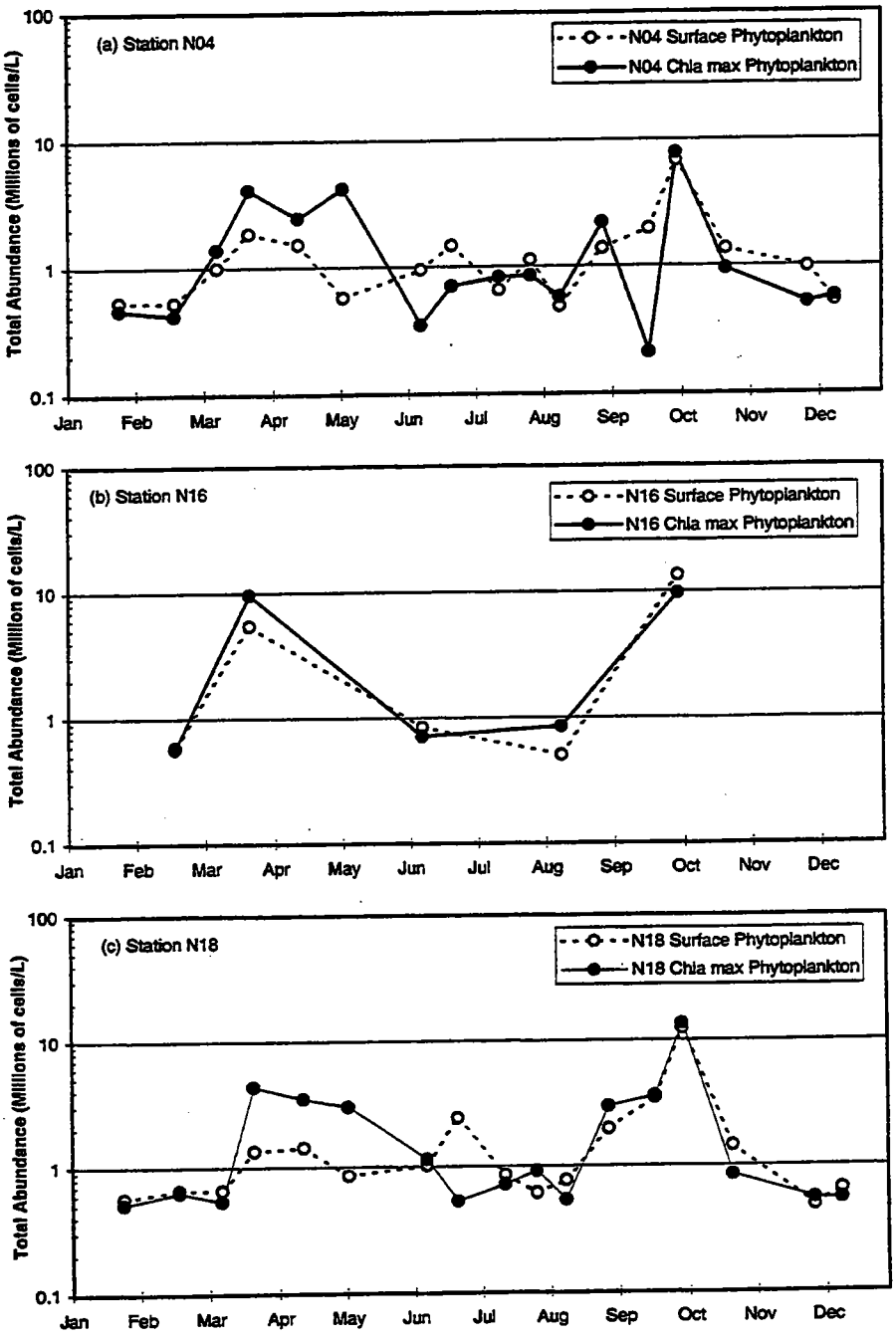

FIGURE 8-2
1997 Total Phytoplankton Abundance in Nearfield at Surface and Chlorophyll *a* Maximum Depths
Top: N04, Middle: N16, Bottom: N18

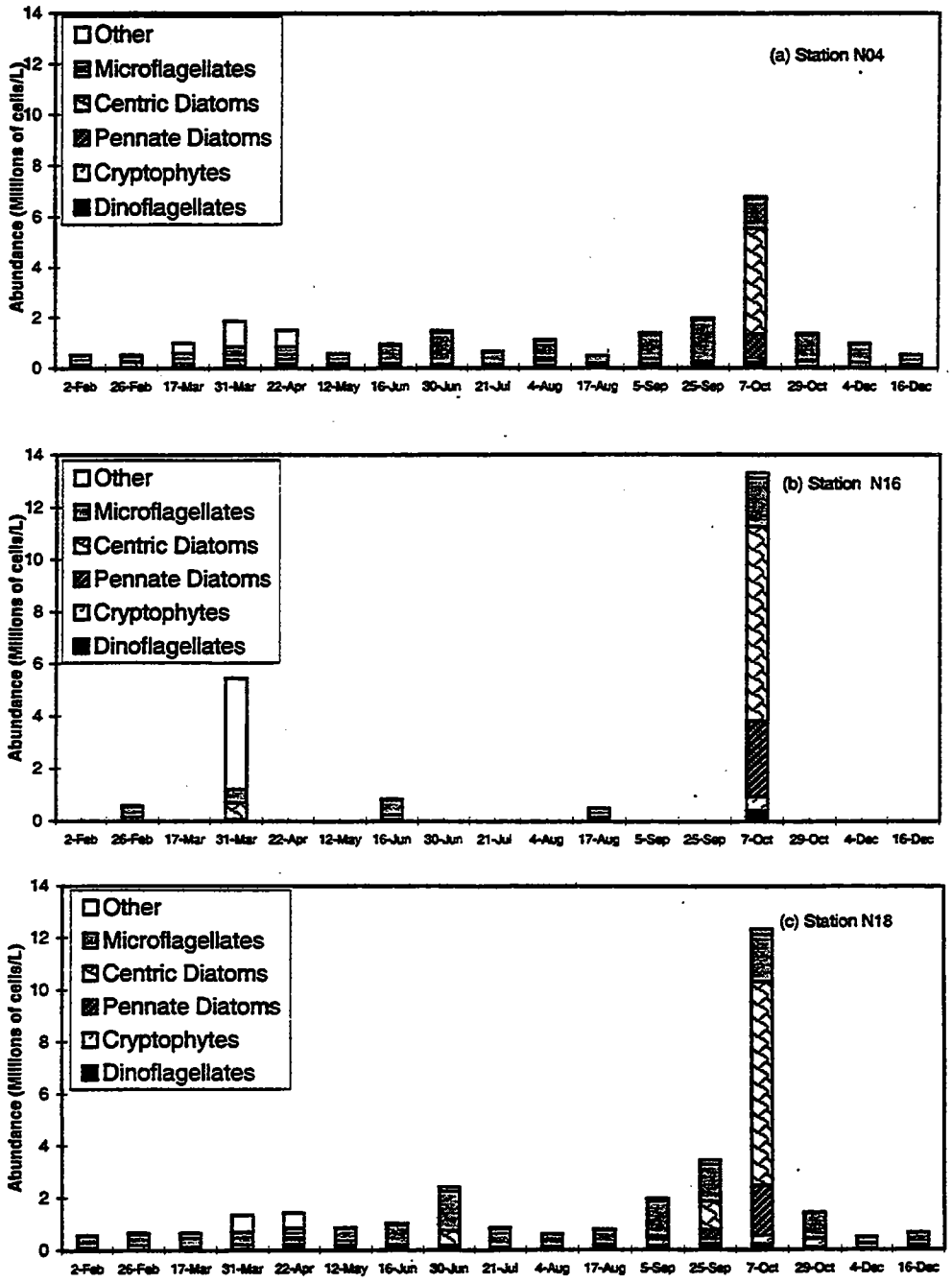

FIGURE 8-3
Distribution of Major Taxonomic Groups in 1997 Surface Samples
Nearfield Stations
Top: N04, Middle: N16, Bottom: N18

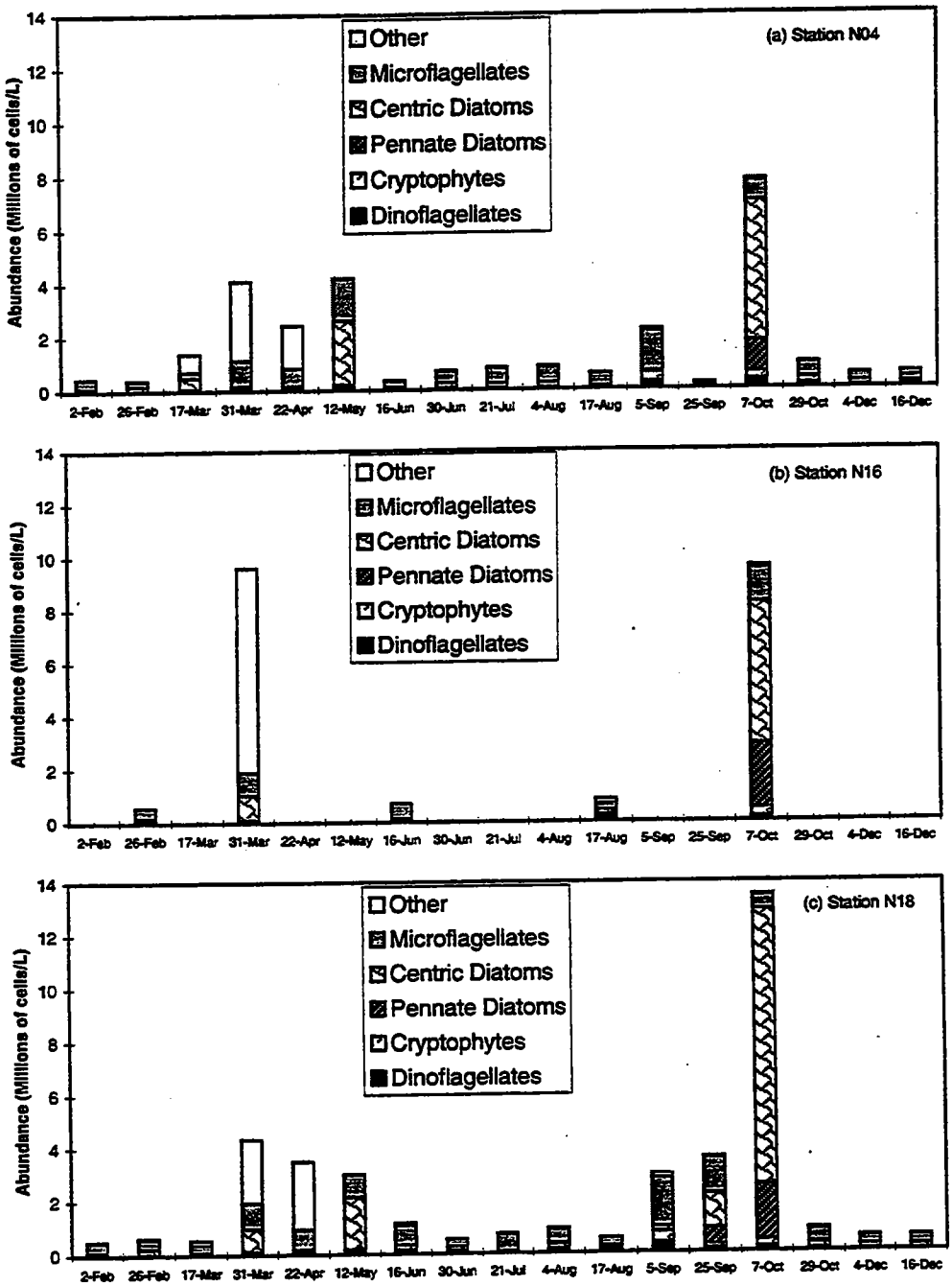

FIGURE 8-4
Distribution of Major Taxonomic Groups in 1997 Chlorophyll *a* Maximum Samples
Nearfield Stations
Top: N04, Middle: N16, Bottom: N18

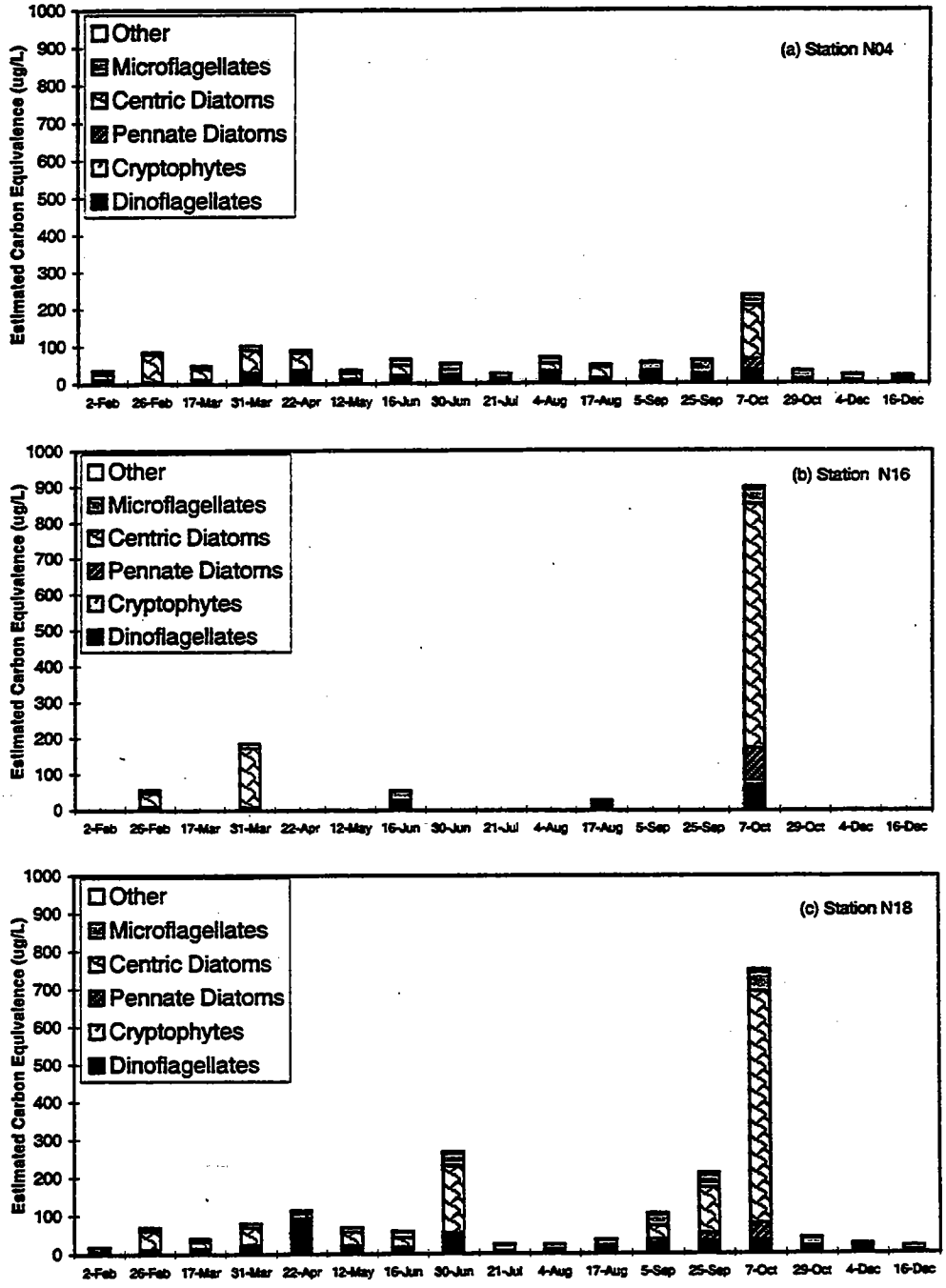

FIGURE 8-5
Distribution of Carbon by Major Taxonomic Groups in 1997 Surface Samples
Nearfield Stations
Top: N04, Middle: N16, Bottom: N18

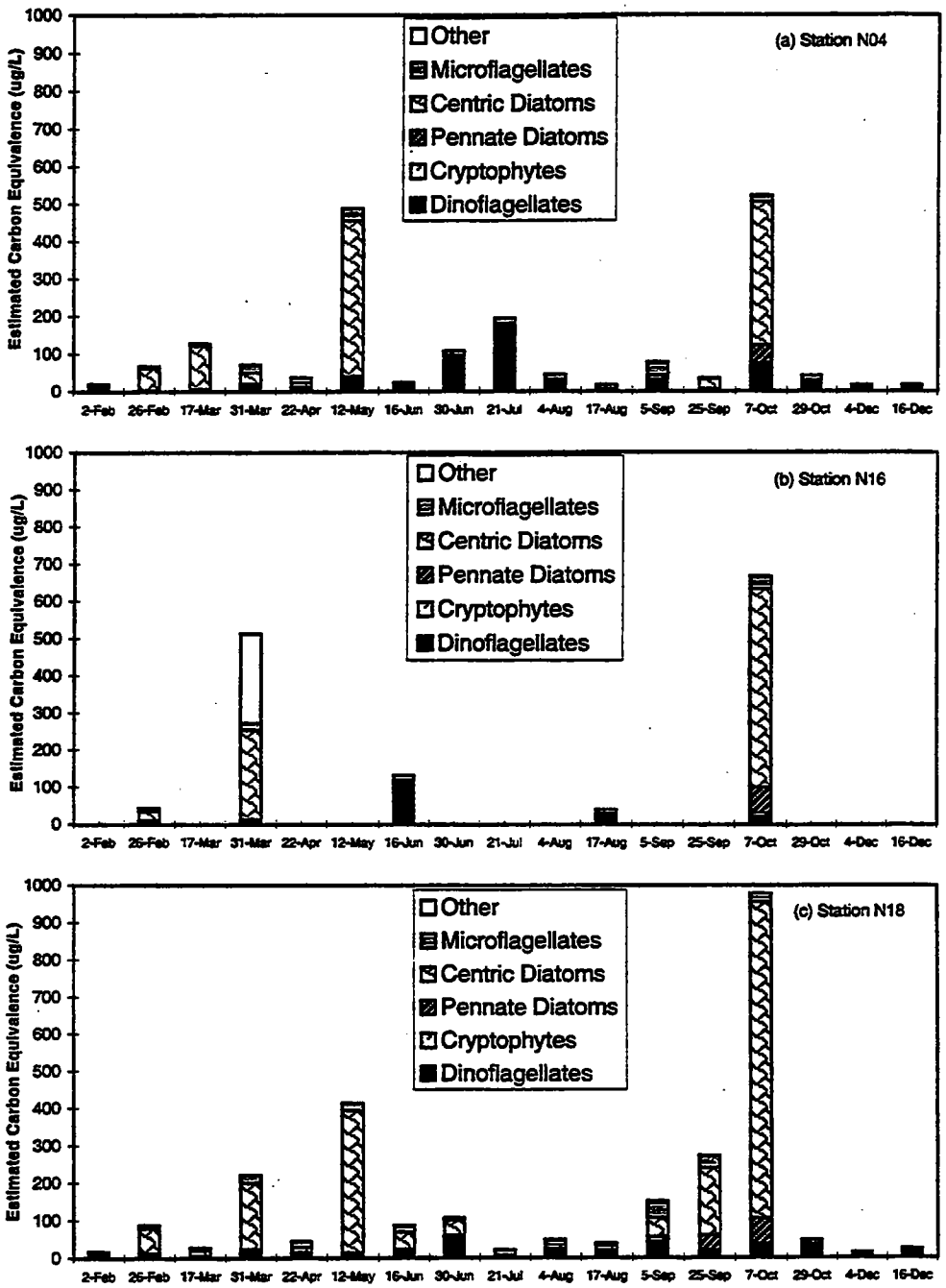

FIGURE 8-6
Distribution of Carbon by Major Taxonomic Groups in 1997 Chlorophyll a Maximum Samples
Nearfield Stations
Top: N04, Middle: N16, Bottom: N18

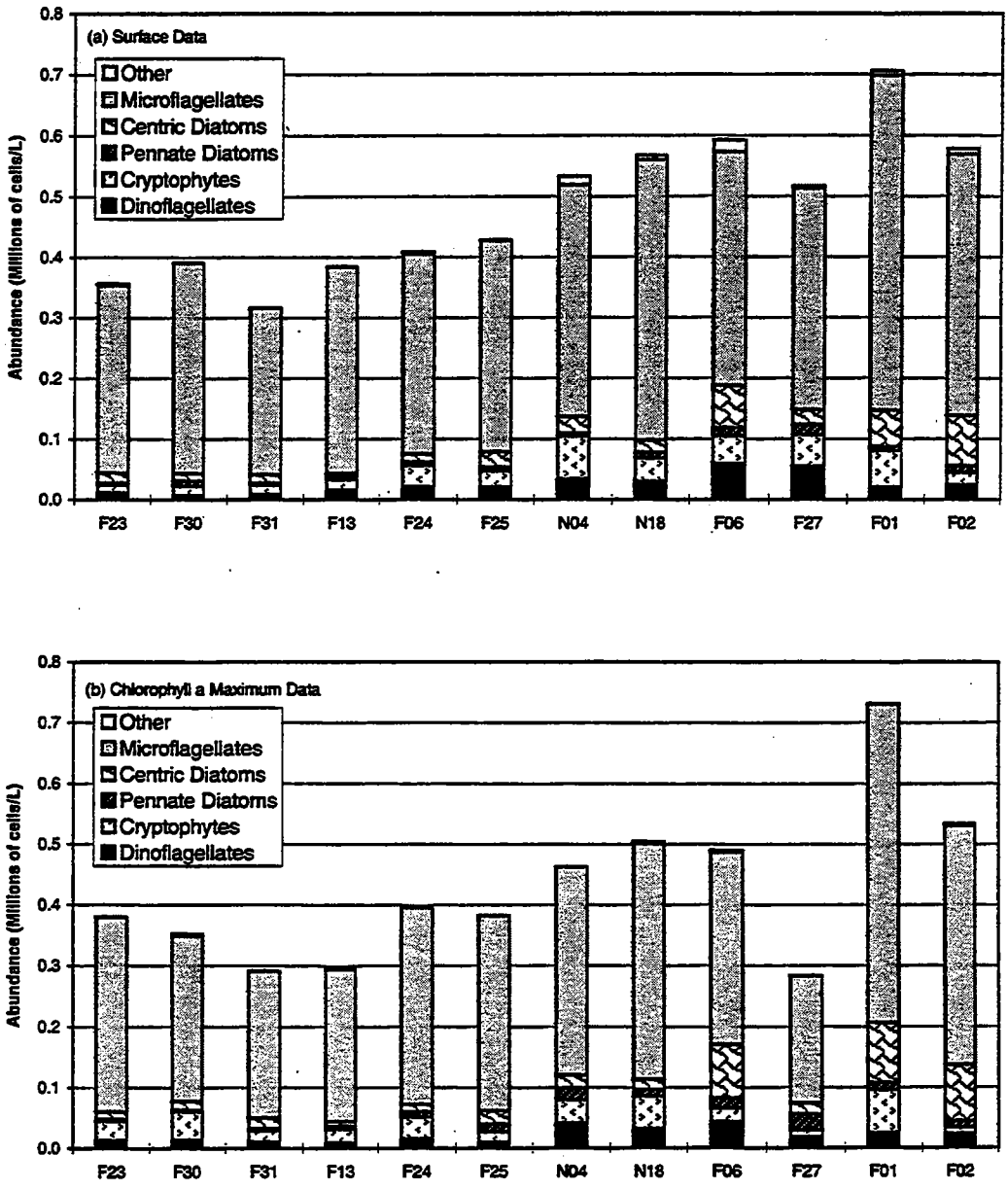

FIGURE 8-7
Phytoplankton Abundance by Major Taxonomic Group - W9701 Farfield Survey Results
February 4 - 7, 1997

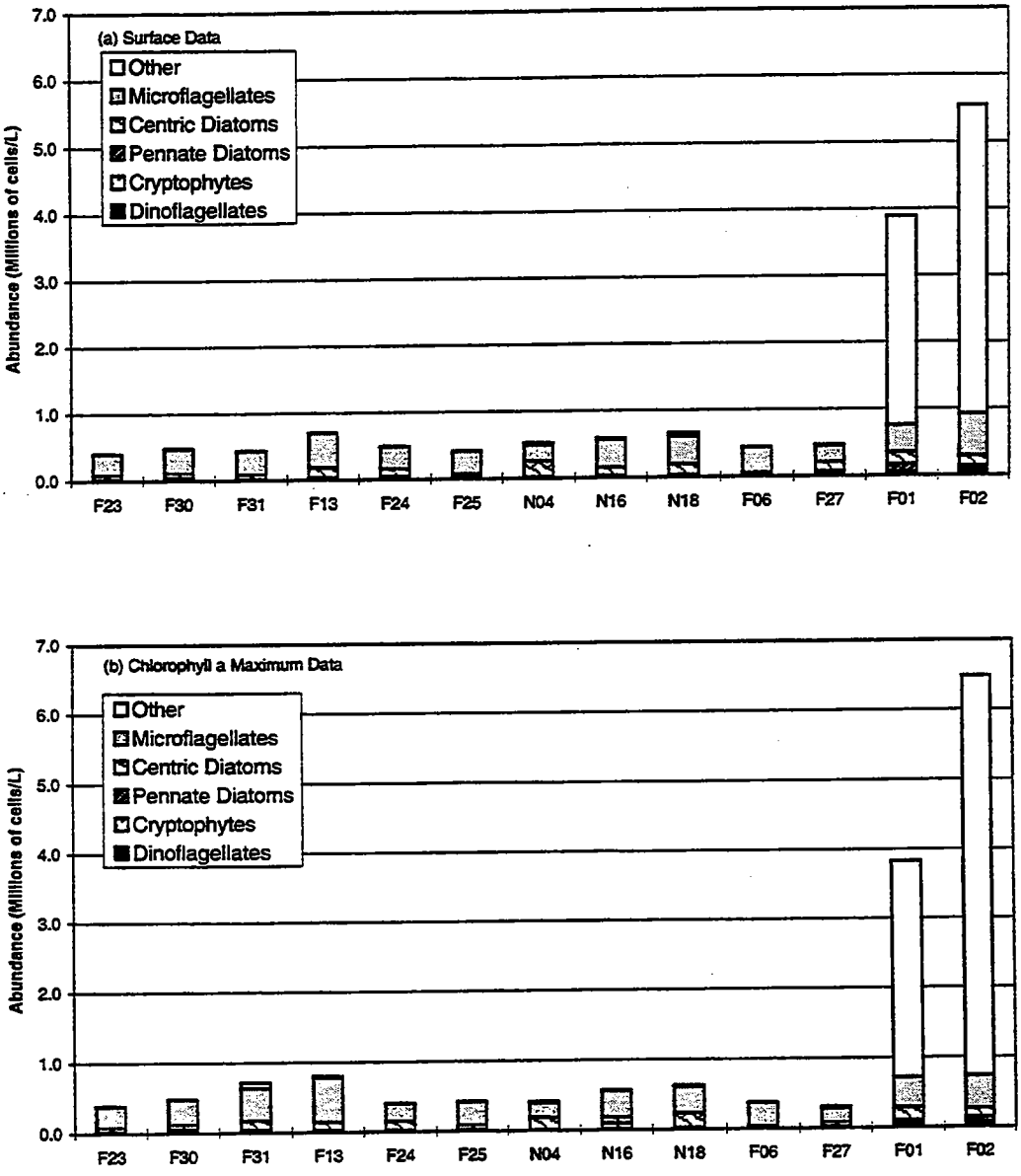

FIGURE 8-8
Phytoplankton Abundance by Major Taxonomic Group - W9702 Farfield Survey Results
February 25 - 28, 1997

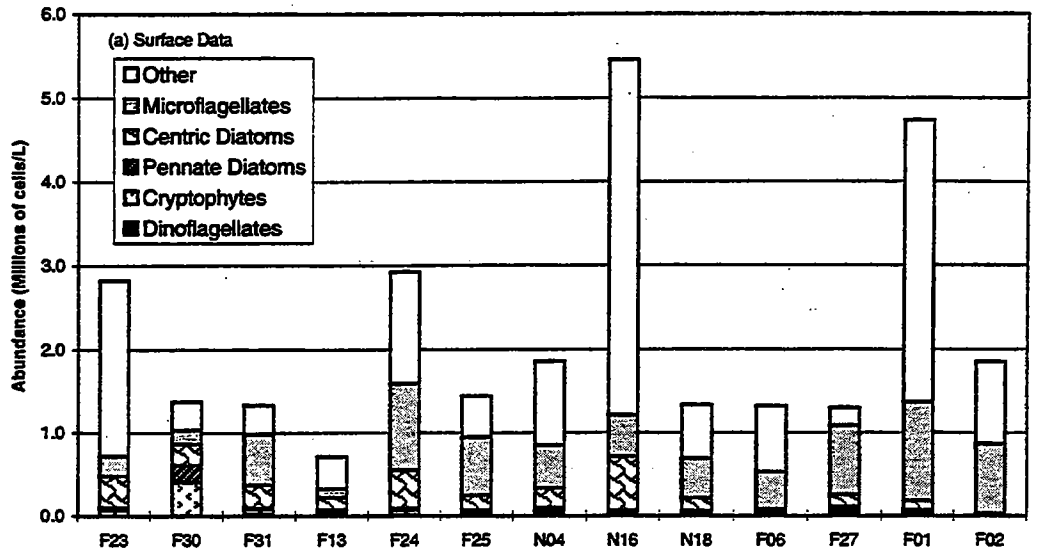

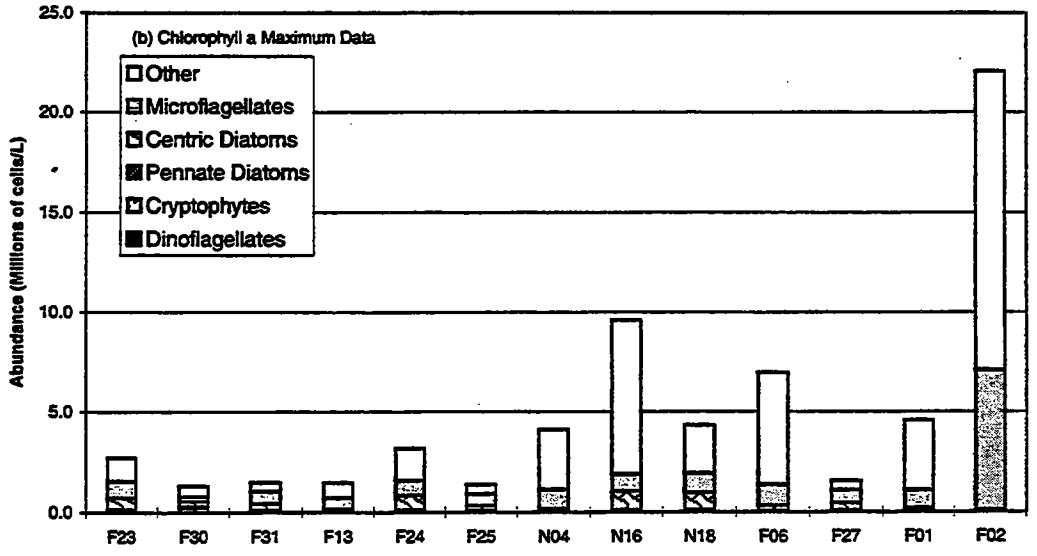

*Note difference in y-scale axis

FIGURE 8-9
Phytoplankton Abundance by Major Taxonomic Group - W9704 Farfield Survey Results
April 1 -6, 1997

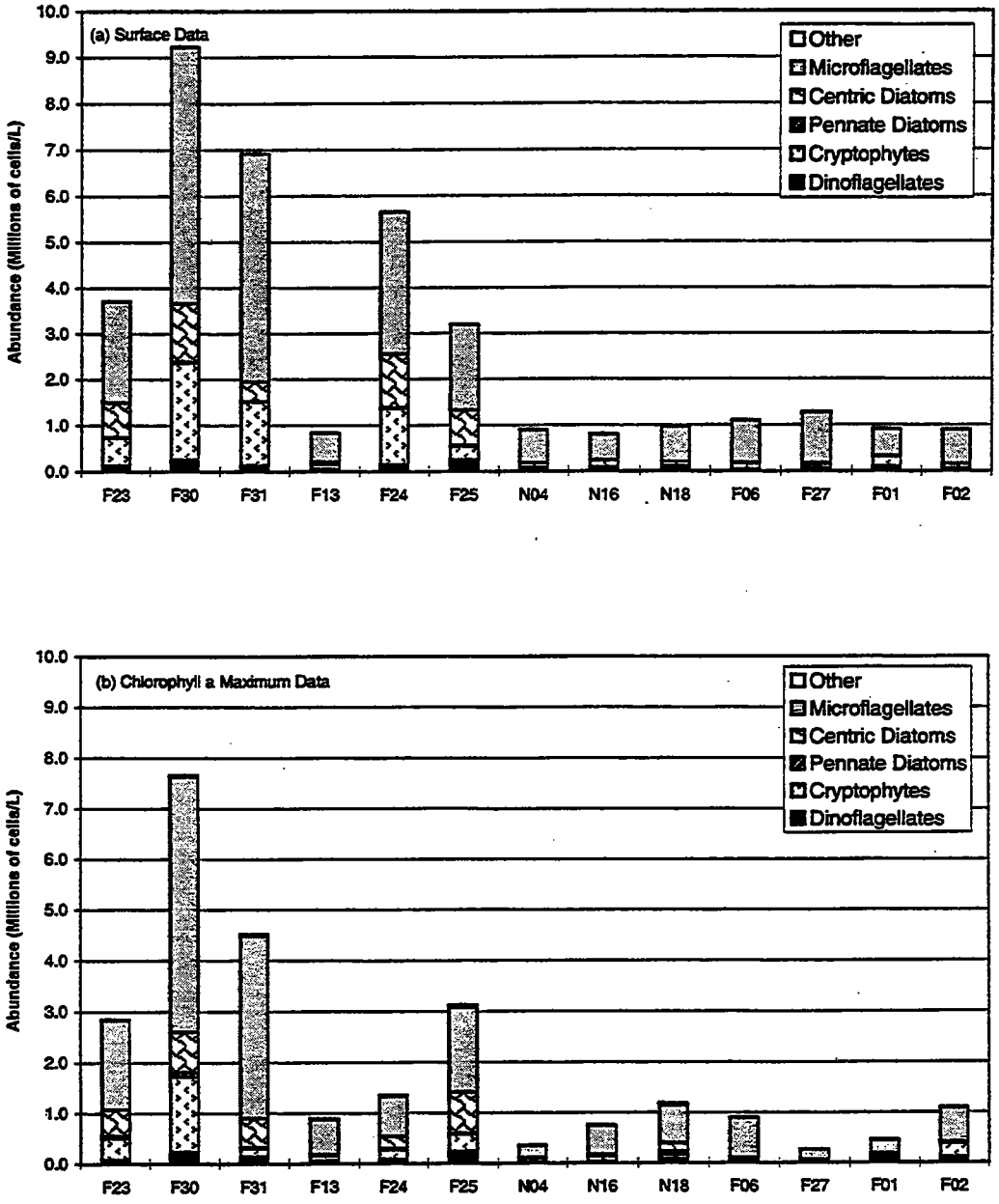

FIGURE 8-10
Phytoplankton Abundance by Major Taxonomic Group - W9707 Farfield Survey Results
June 17 - 20, 1997

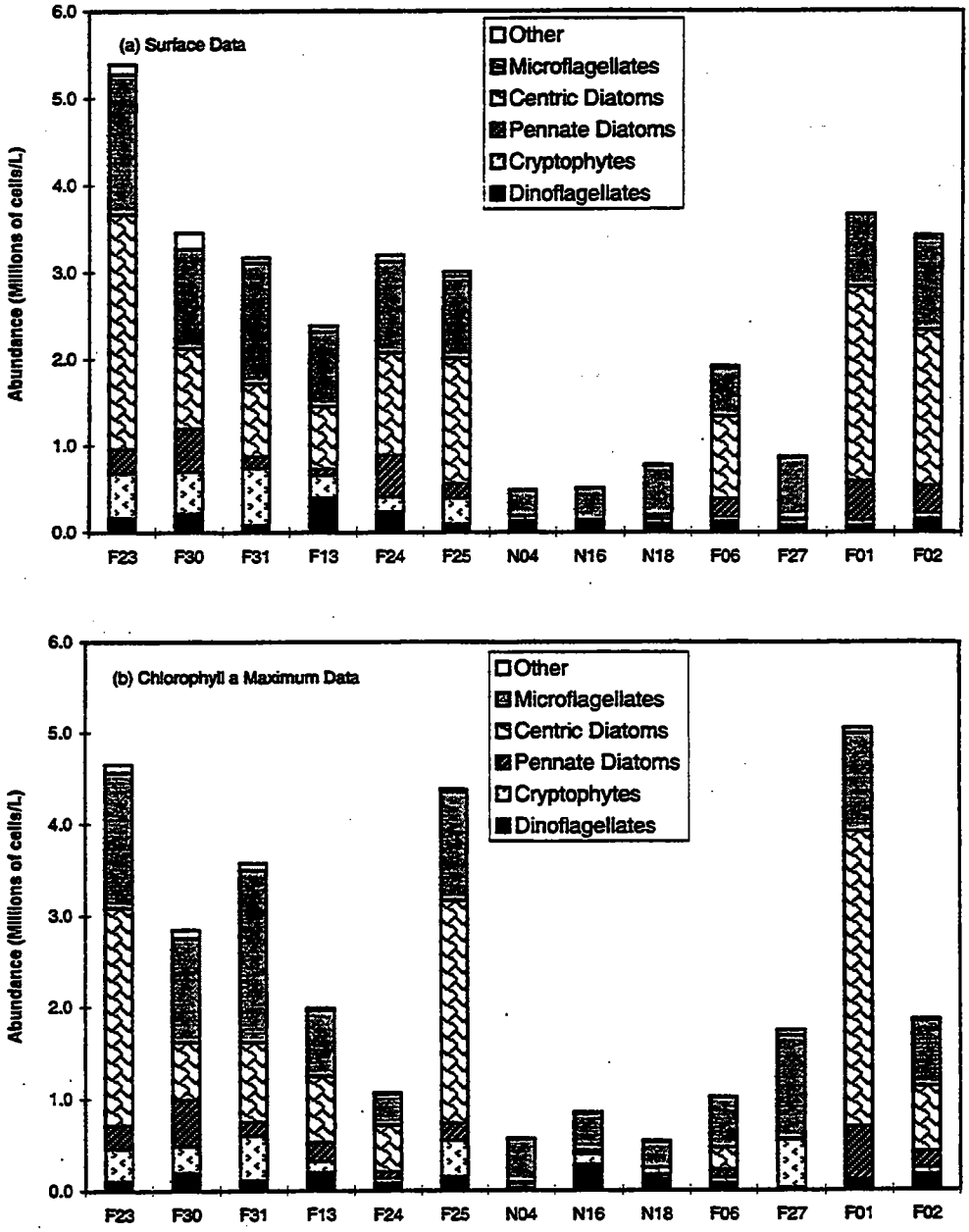

FIGURE 8-11
Phytoplankton Abundance by Major Taxonomic Group -W9711 Farfield Survey Results
August 18-20, 1997

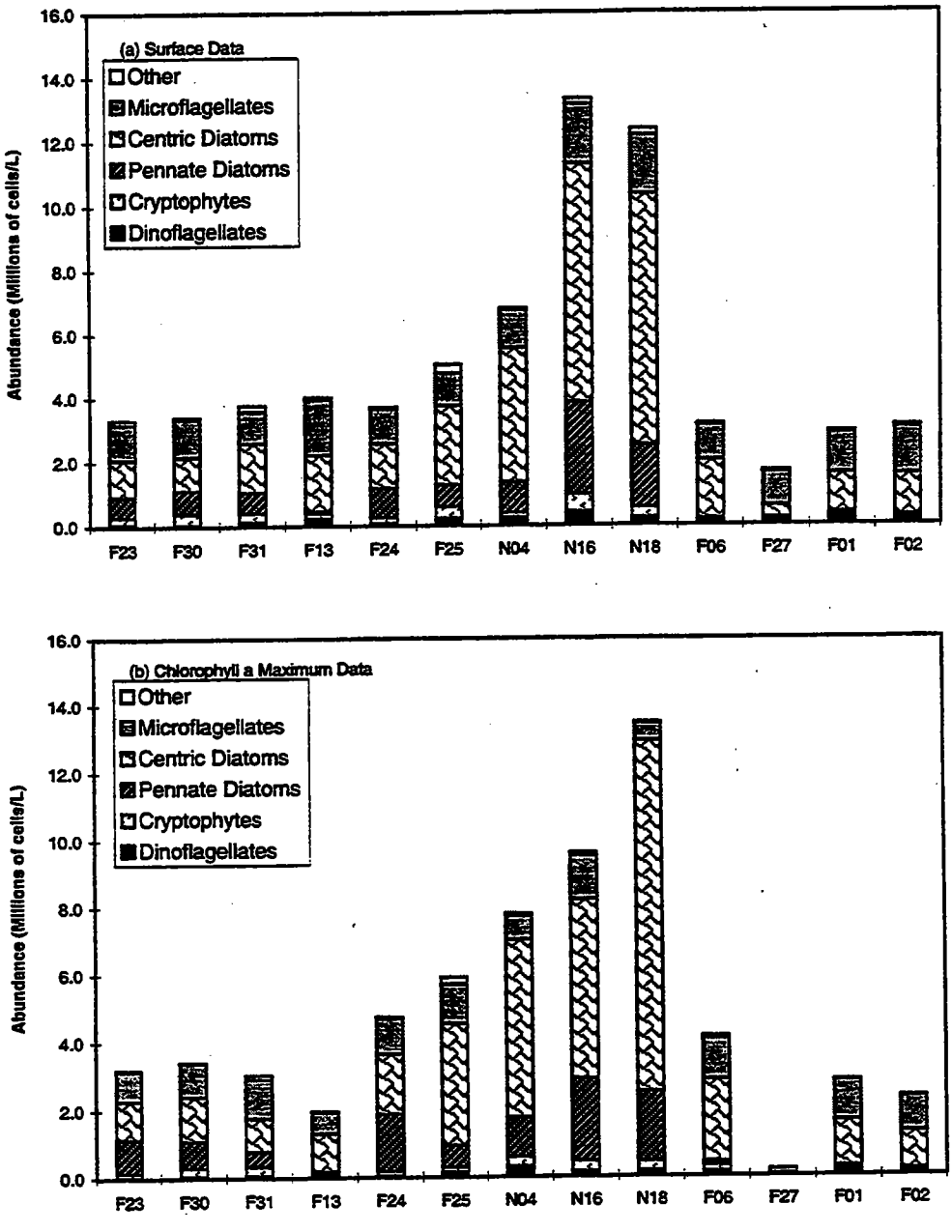

FIGURE 8-12
Phytoplankton Abundance by Major Taxonomic Group - W9714 Farfield Survey Results
October 6-8, 1997

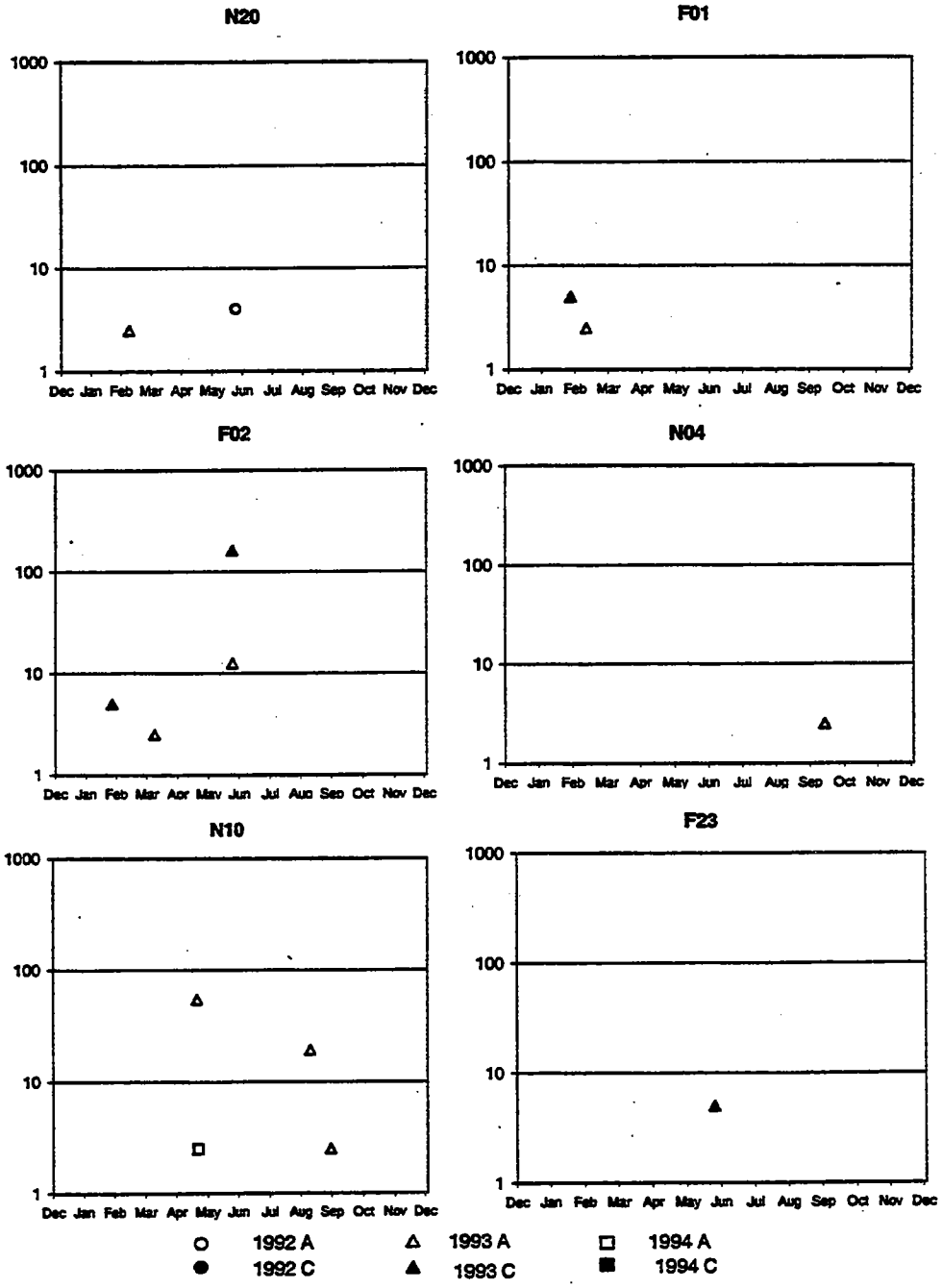

FIGURE 8-13
Interannual Distribution of *Alexandrium tamarense* (cells/L) by Region
Absent 1995-1997
(Screened Samples, All Occurrences)

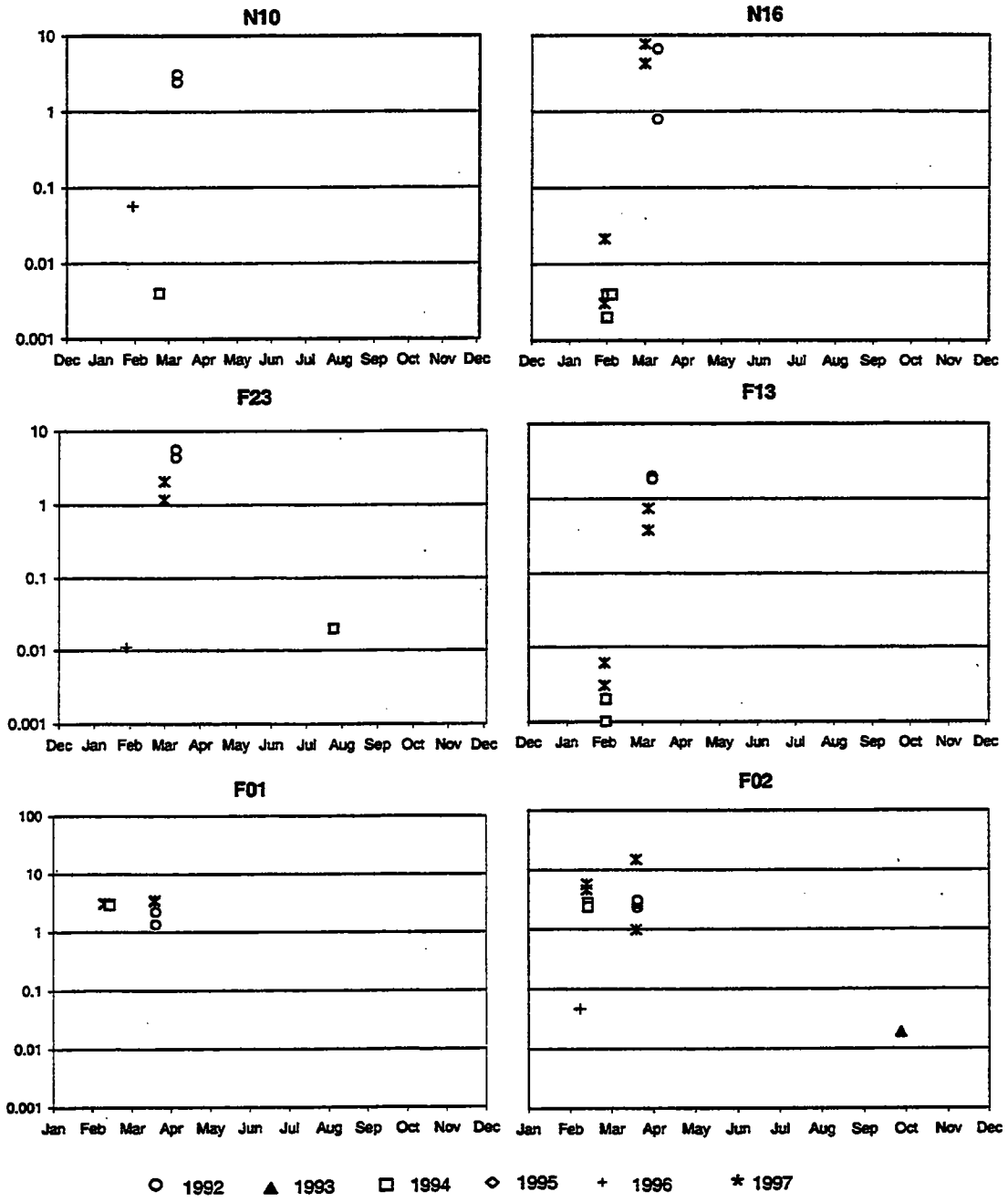

FIGURE 8-14

Interannual Distribution of *Phaeocystis pouchetii* (10^6 cells/L) by Region
(Whole Water Samples - Both Depths)

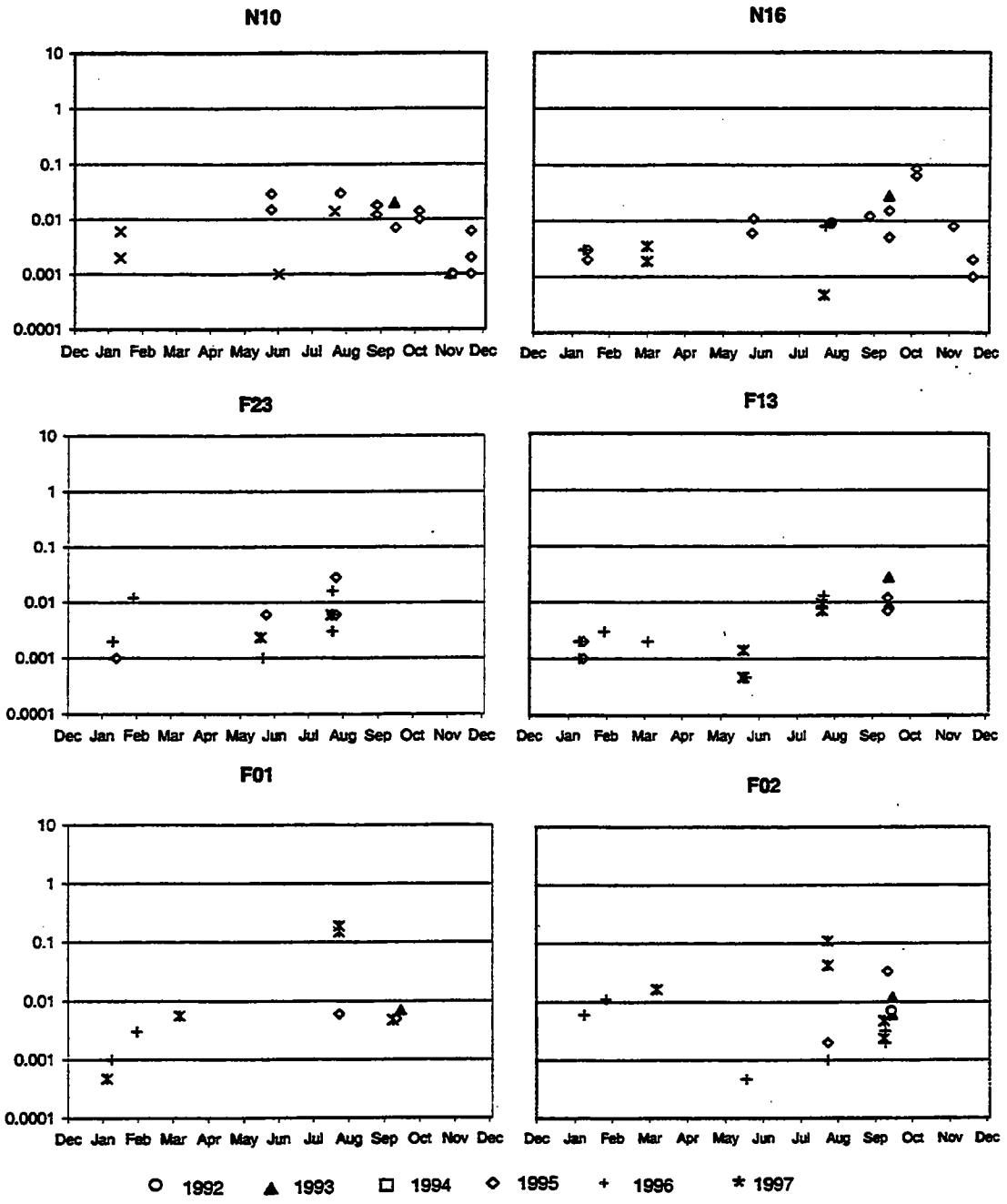

FIGURE 8-15

Interannual Distribution of *Pseudo-nitzschia pungens* (10^6 cells/L) by Region
(Whole Water Samples - Both Depths)

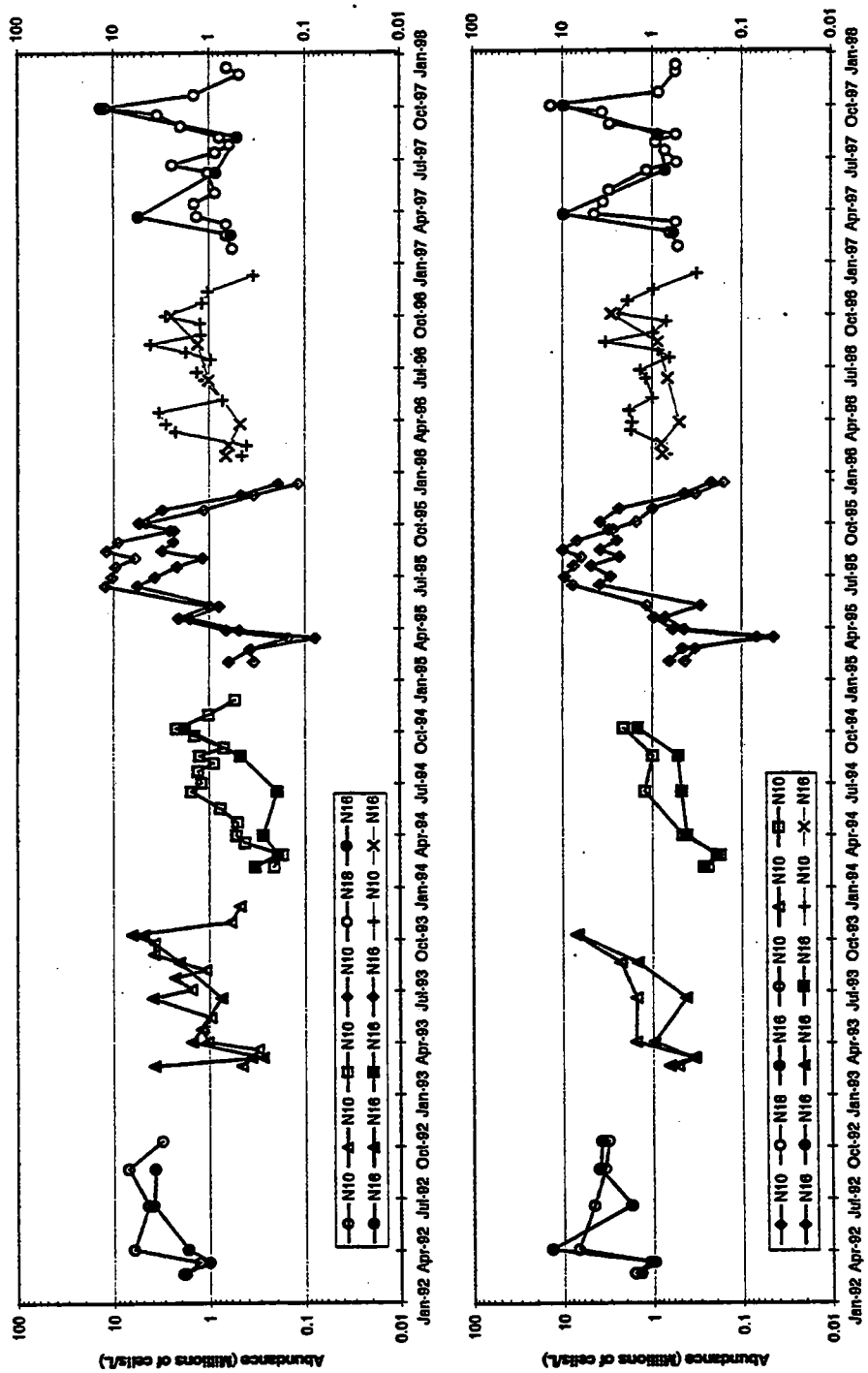

FIGURE 8-16
1992 -1997 Total Phytoplankton Abundance in Nearfield Stations N10, N16 and N18
Top: Surface Data, Bottom: Chlorophyll *a* Maximum Data

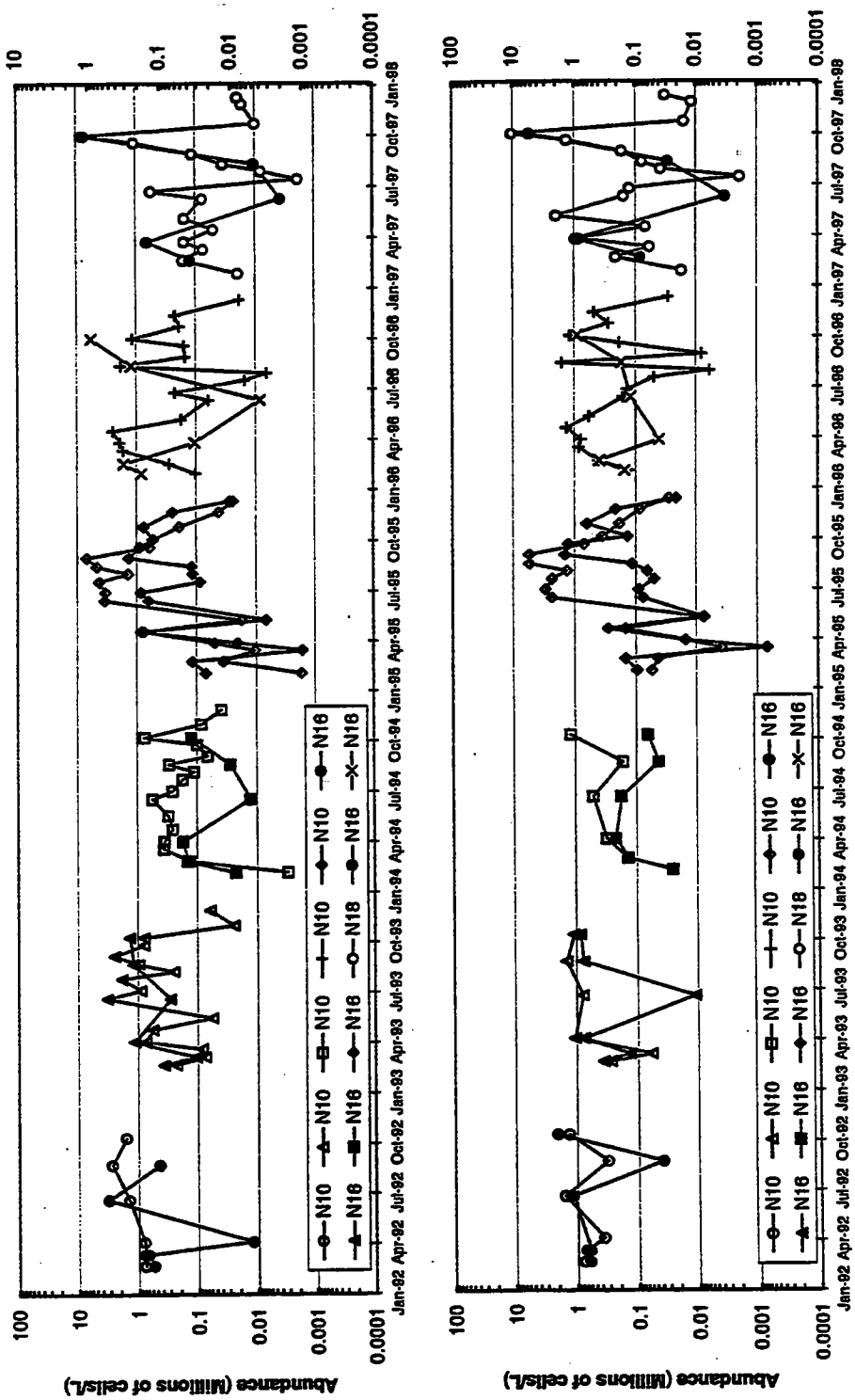

FIGURE 8-17
1992-1997 Seasonal Nearfield Pattern for Centric Diatoms in Nearfield Stations N10, N16 and N18
Top: Surface Data, Bottom: Chlorophyll a Maximum Data

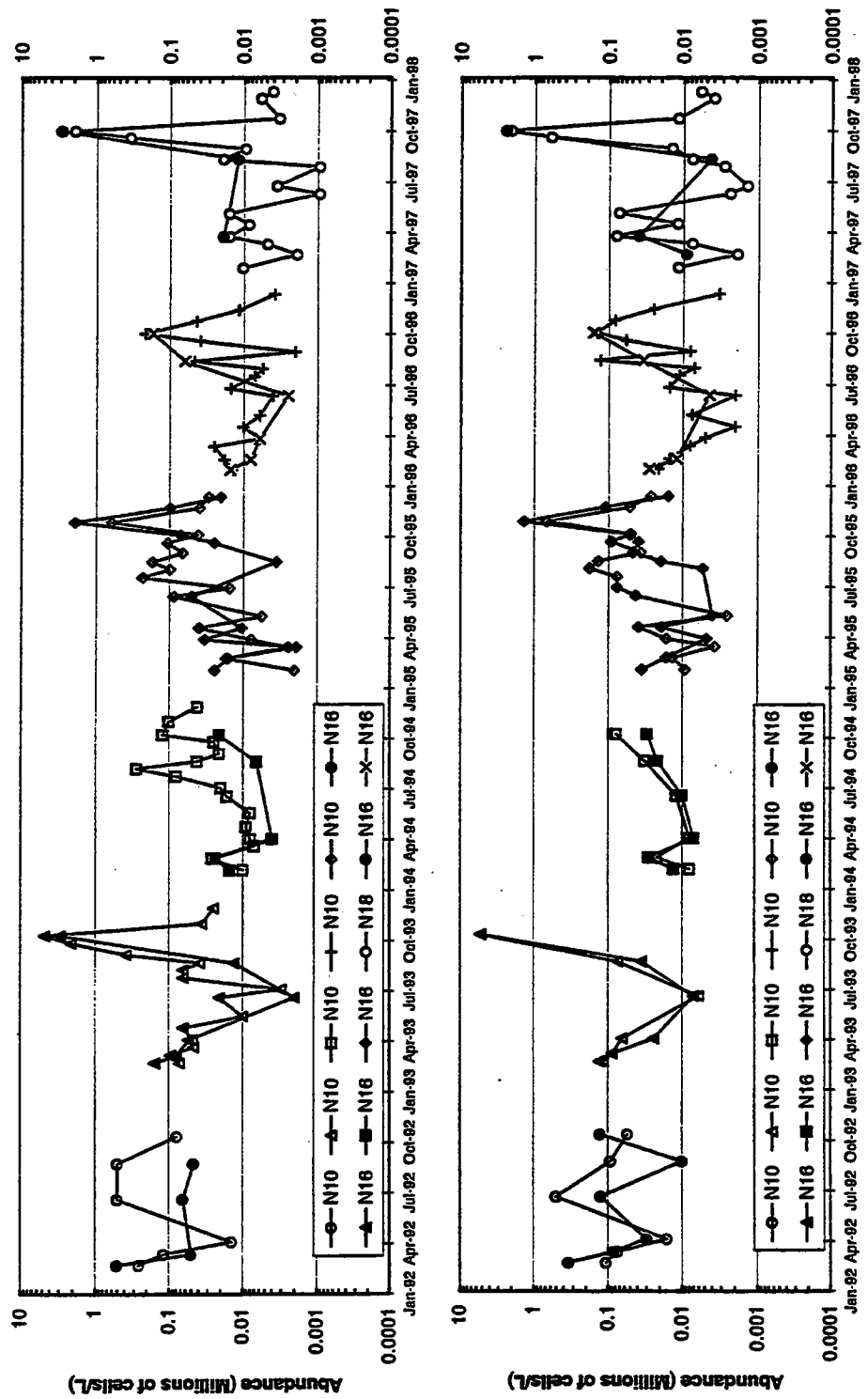

FIGURE 8-18
1992-1997 Seasonal Nearfield Pattern for Pennate Diatoms in Nearfield Stations N10, N16 and N18
Top: Surface Data, Bottom: Chlorophyll a Maximum Data

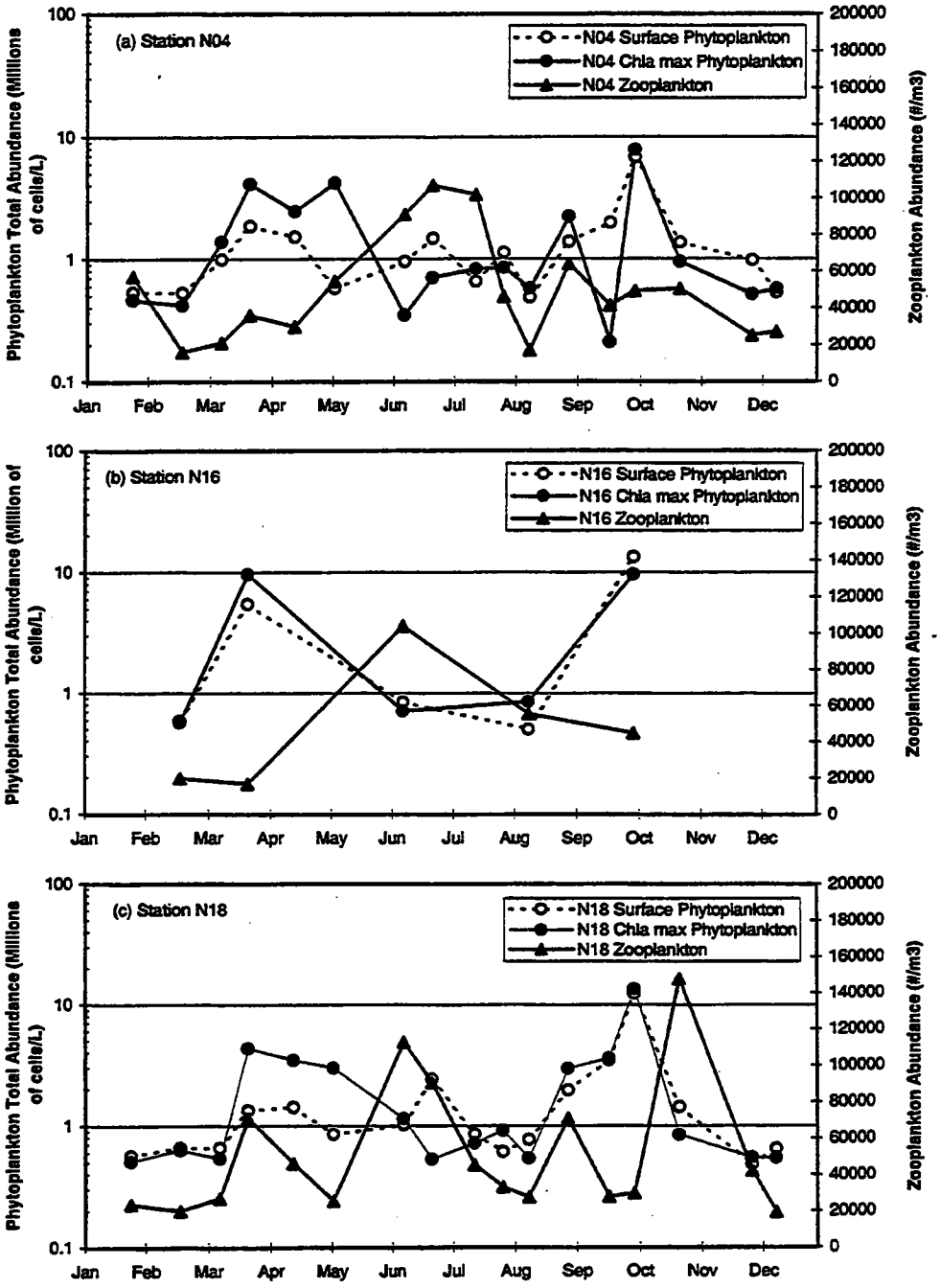

FIGURE 8-19
1997 Phytoplankton and Zooplankton Annual Cycles for Nearfield Stations
Top: N04, Middle: N16, Bottom: N18

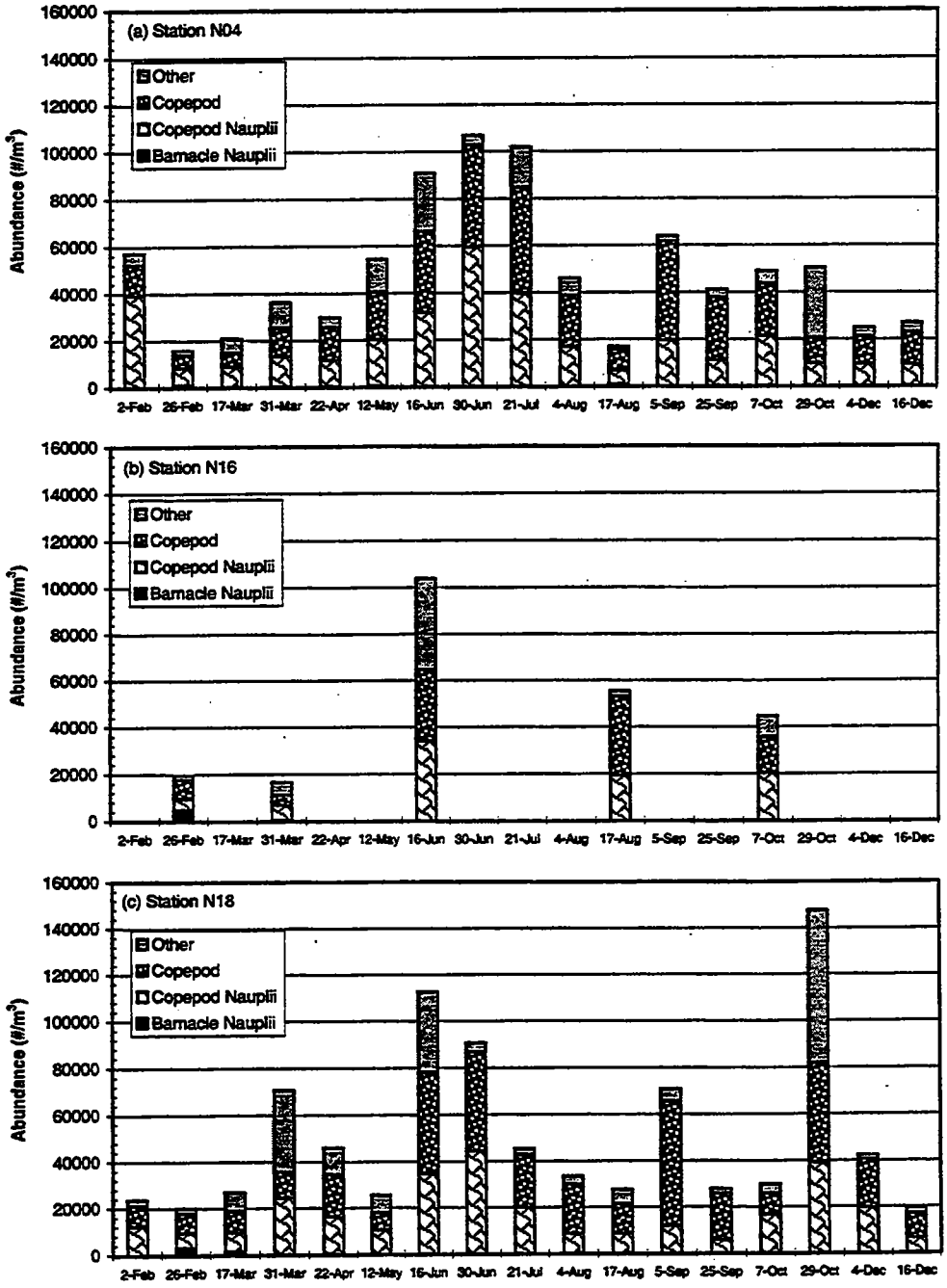

FIGURE 8-20
1997 Nearfield Zooplankton Abundance by Major Taxonomic Group
Top: N04, Middle: N16, Bottom: N18

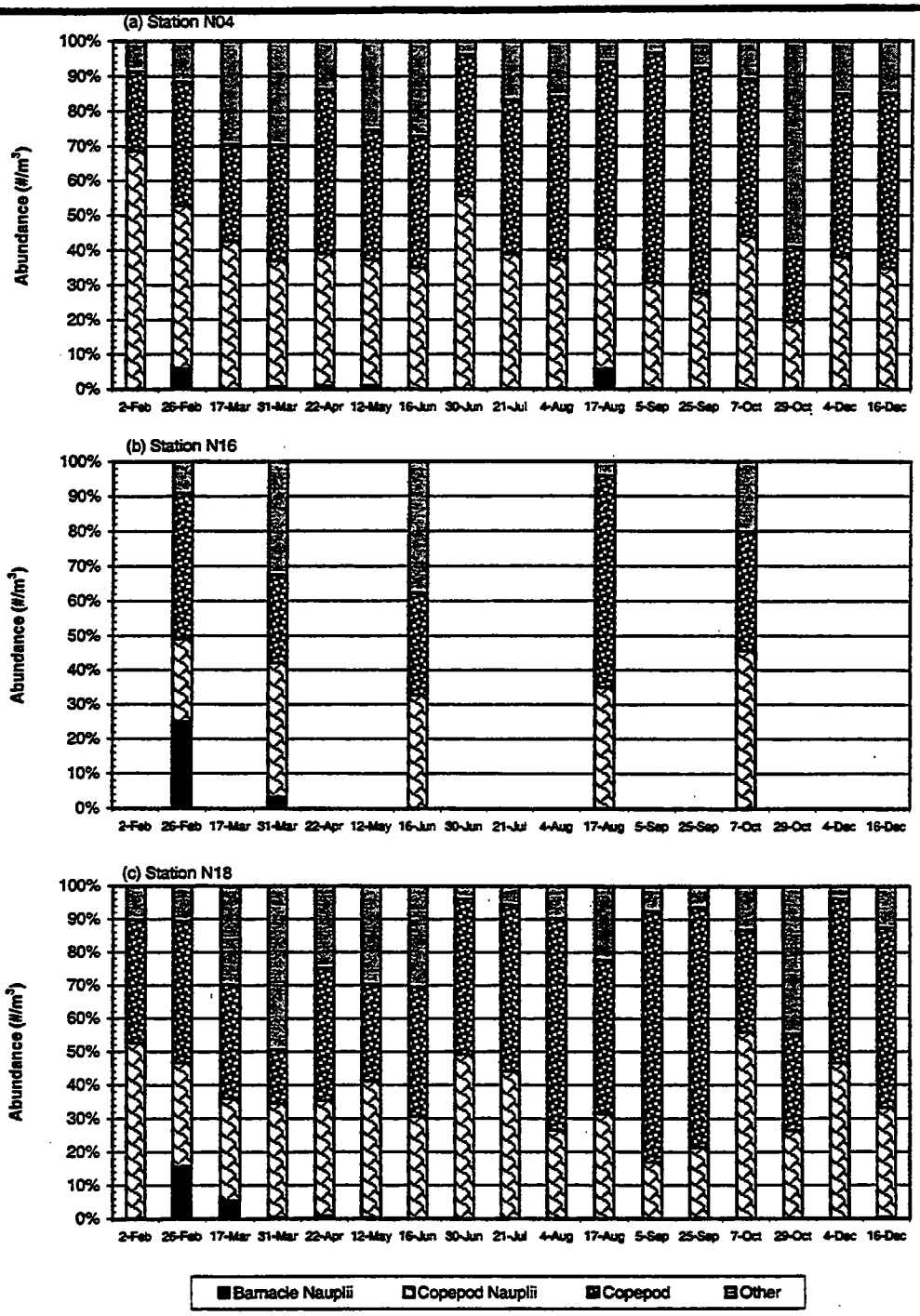

FIGURE 8-21
1997 Nearfield Percent Zooplankton Abundance by Major Taxonomic Group
Top: N04, Middle: N16, Bottom: N18

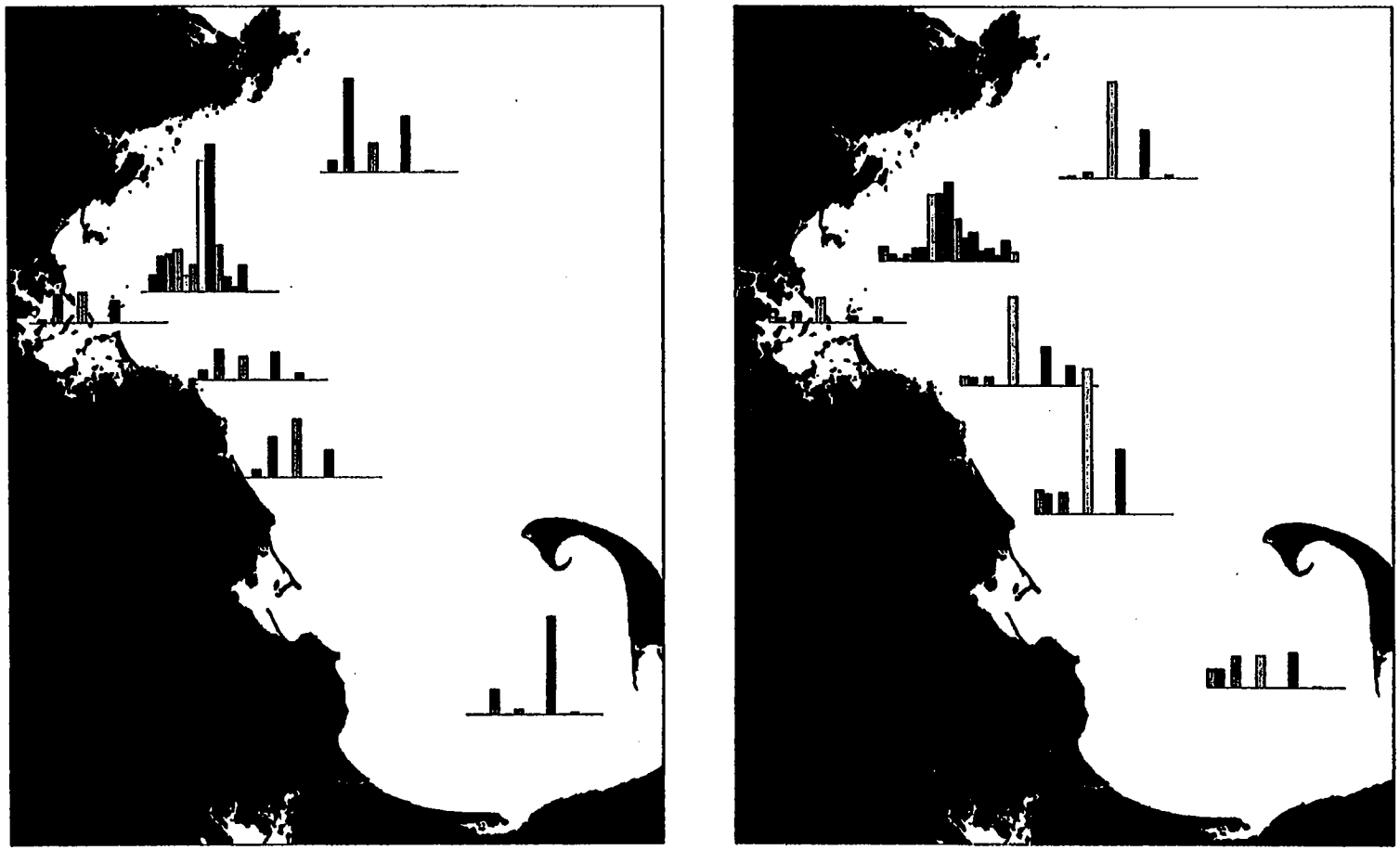

FIGURE 8-22
1997 Zooplankton Distribution
a) Calanus finmarchicus (max = 3,393/m3) and b) Pseudocalanus (max = 18,770/m3)

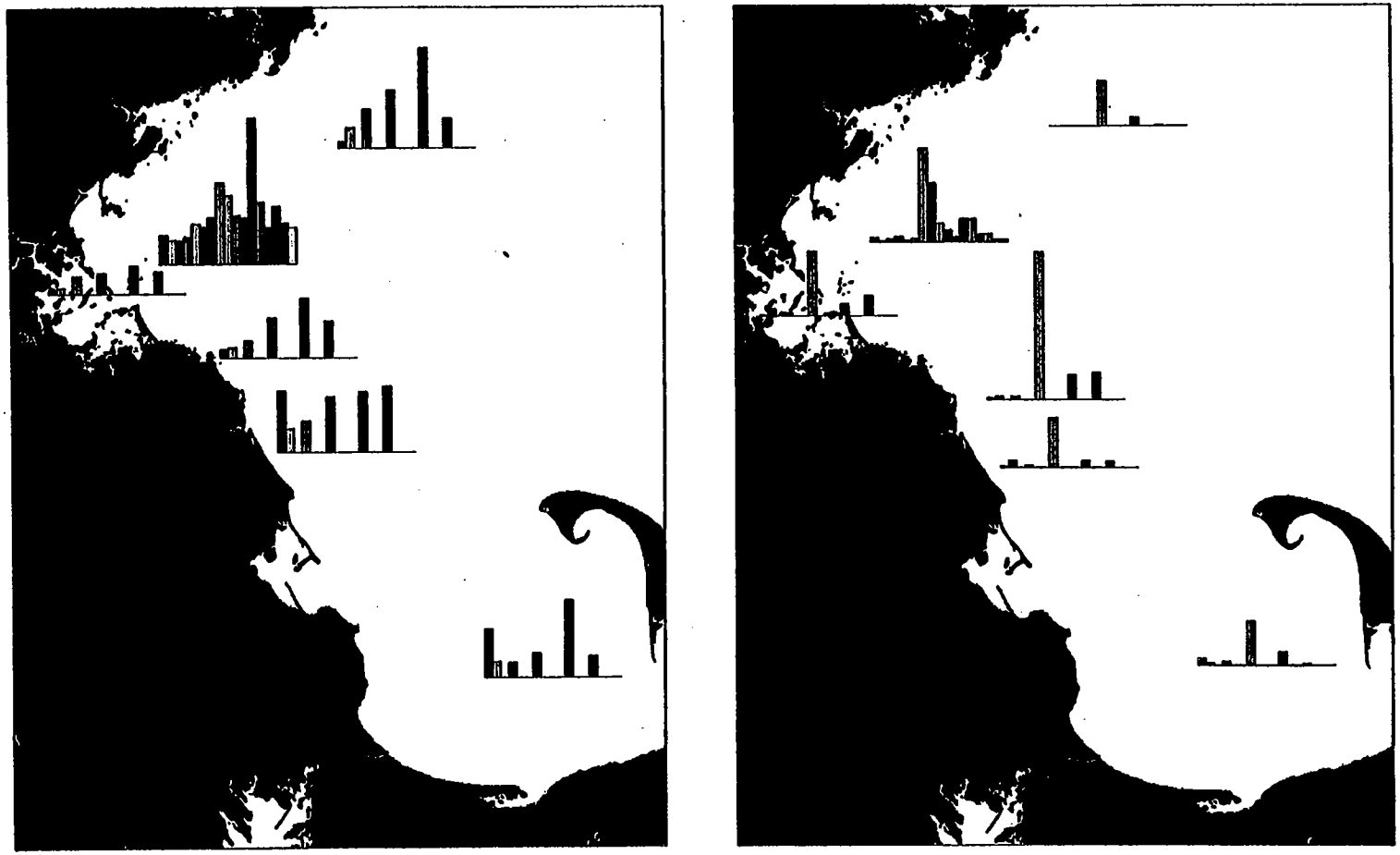

FIGURE 8-23
1997 Zooplankton Distribution
a) Oithona similis (max = 36,626/m3) and b) Temora longicornis (max = 15,174/m3)

FIGURE 8-24
1997 Zooplankton Distribution
a) Centropages typicus (max = 2,016/m3) and b) Centropages hamatus (max = 3,409/m3)

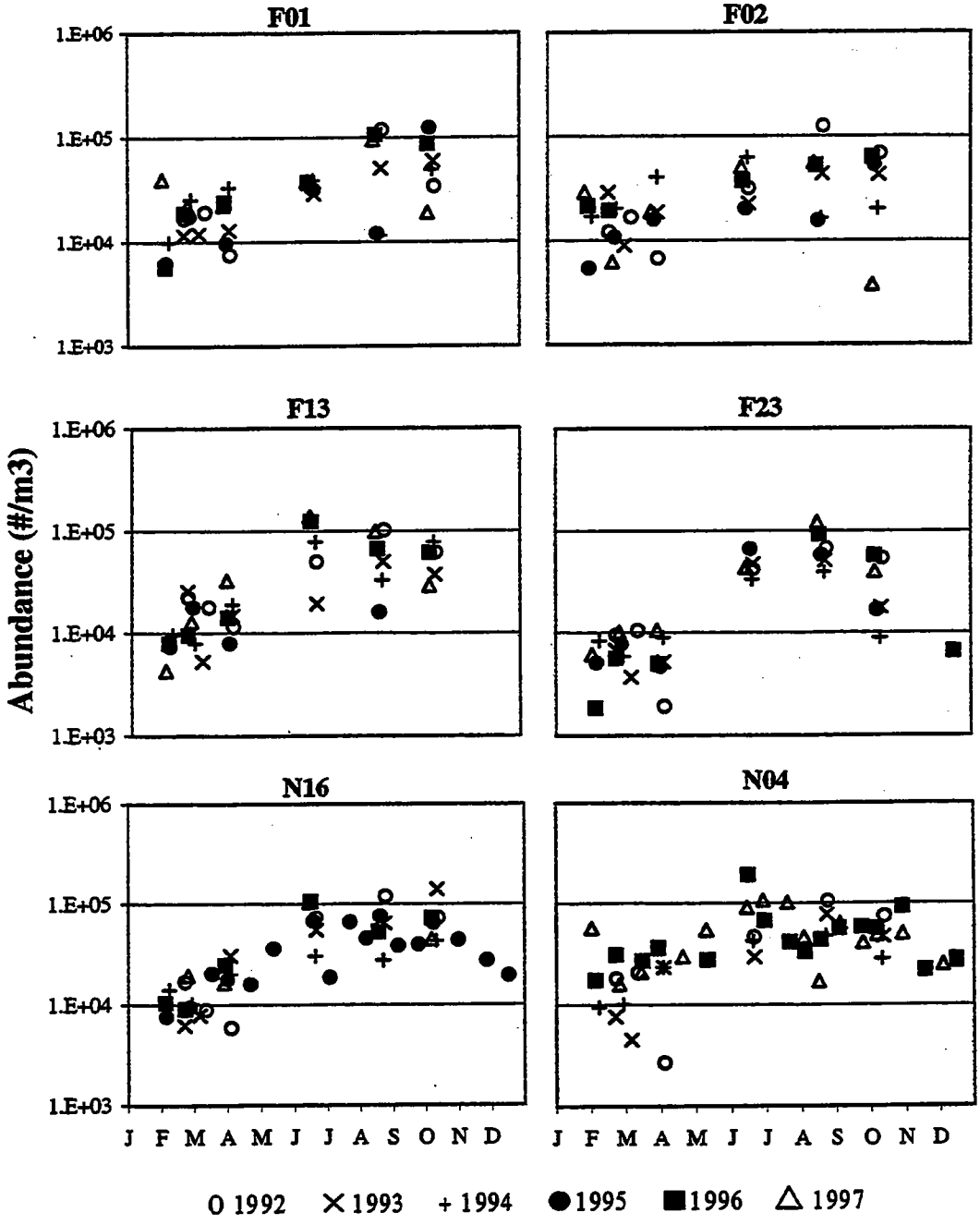

FIGURE 8-33
Interannual Distribution of Total Zooplankton by Region

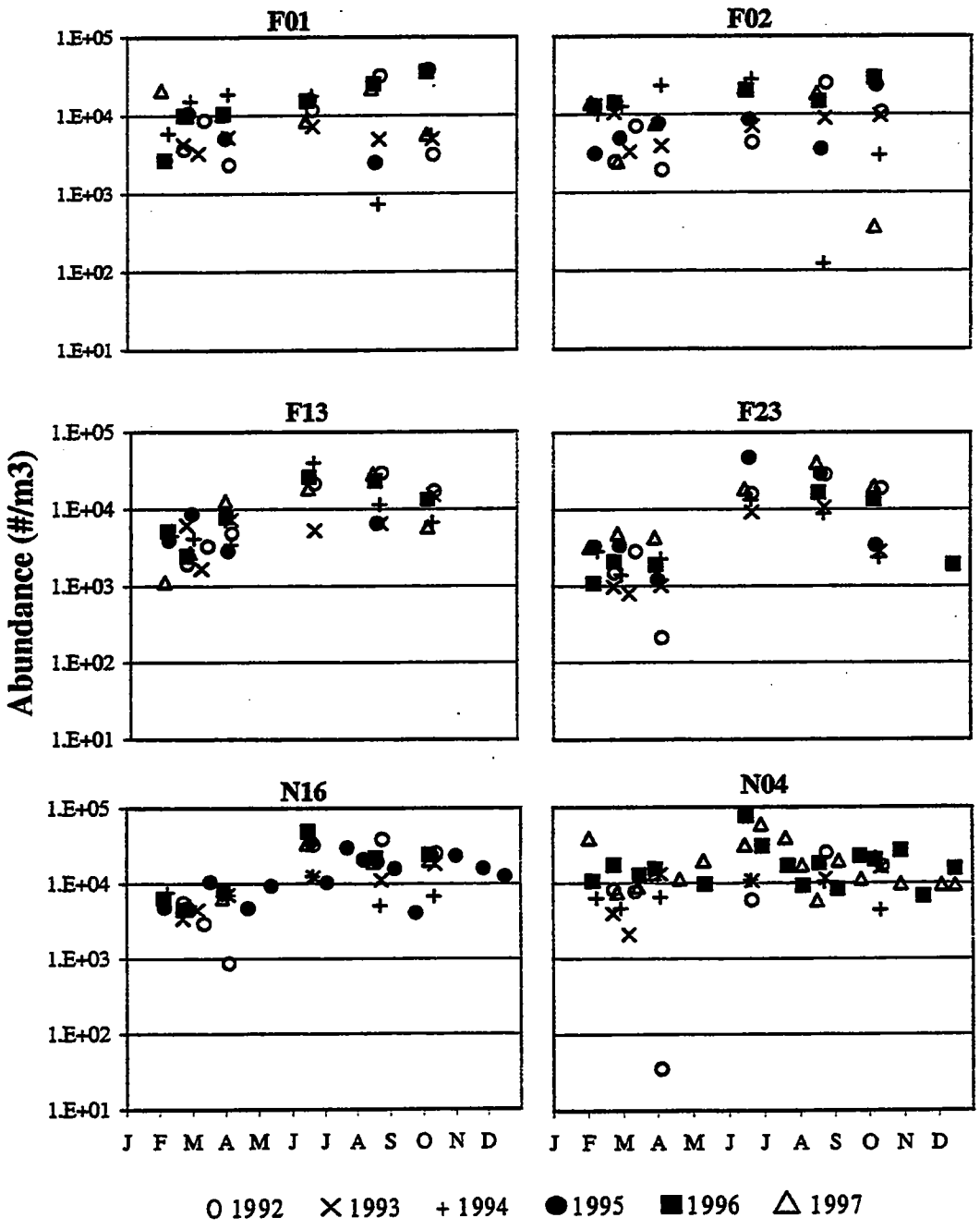

FIGURE 8-34
Interannual Distribution of Copepod Nauplii by Region

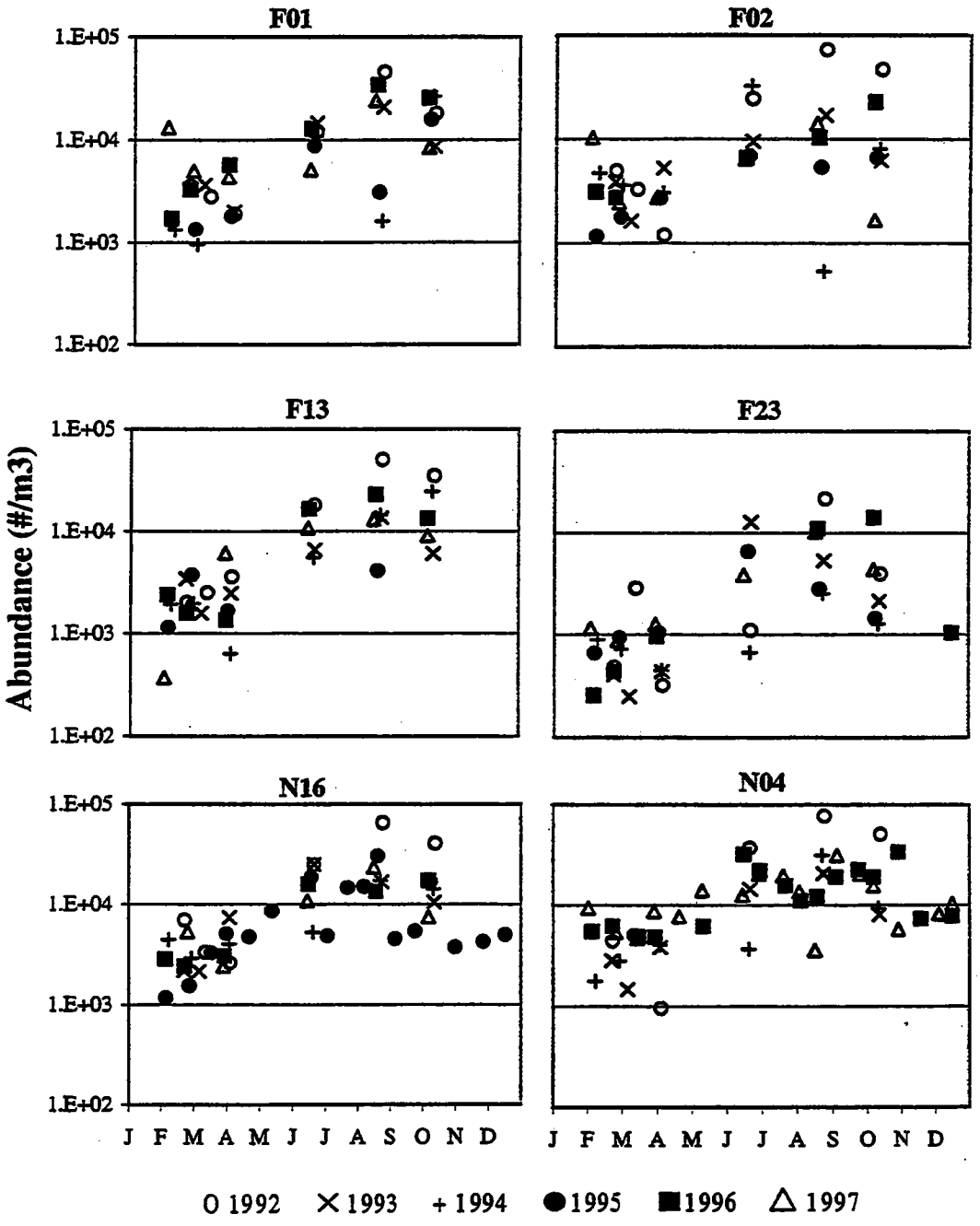

FIGURE 8-35
Interannual Distribution of *Oithona similis* by Region

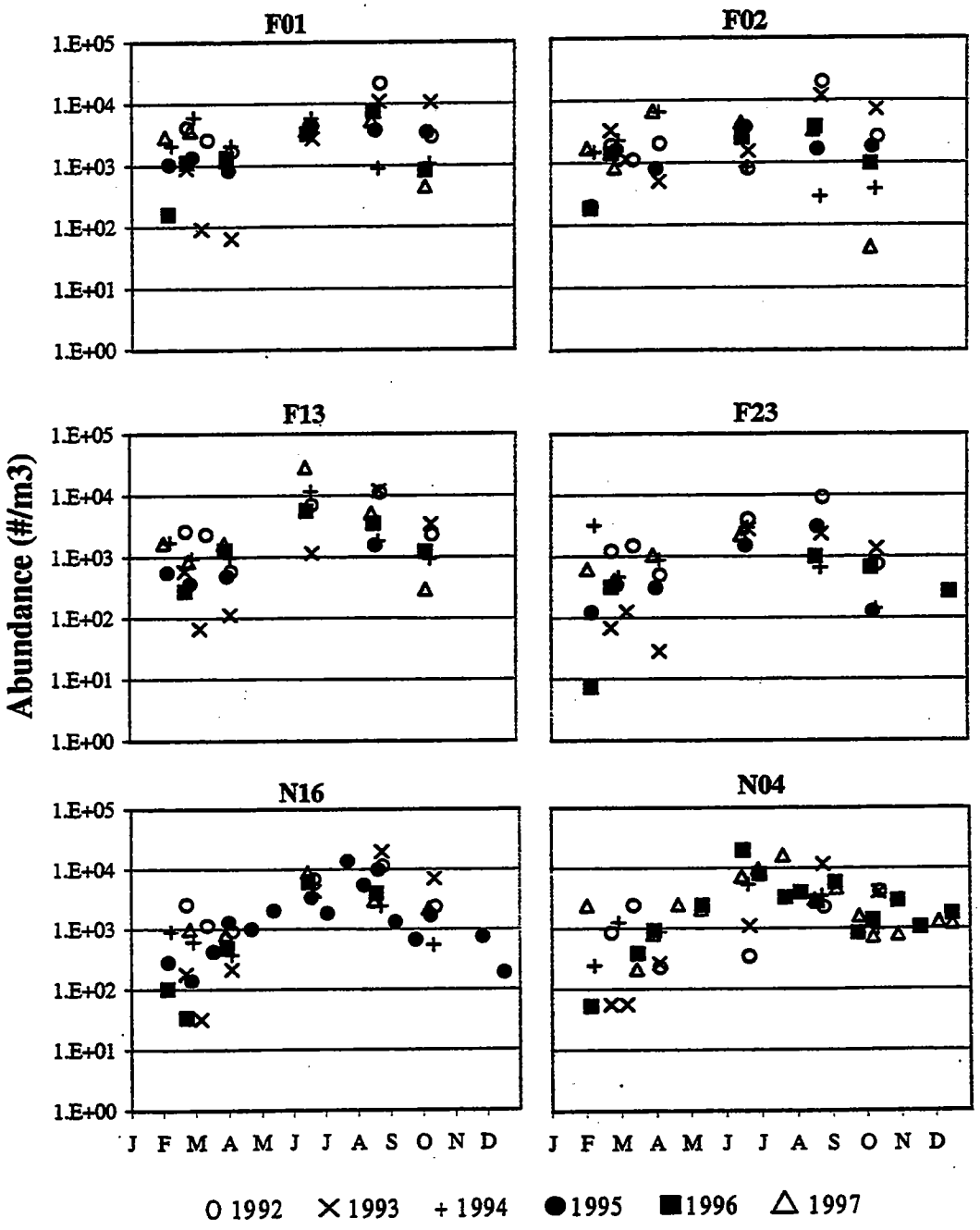

FIGURE 8-36
Interannual Distribution of *Pseudocalanus newmani* and *Paracalanus parvus* by Region

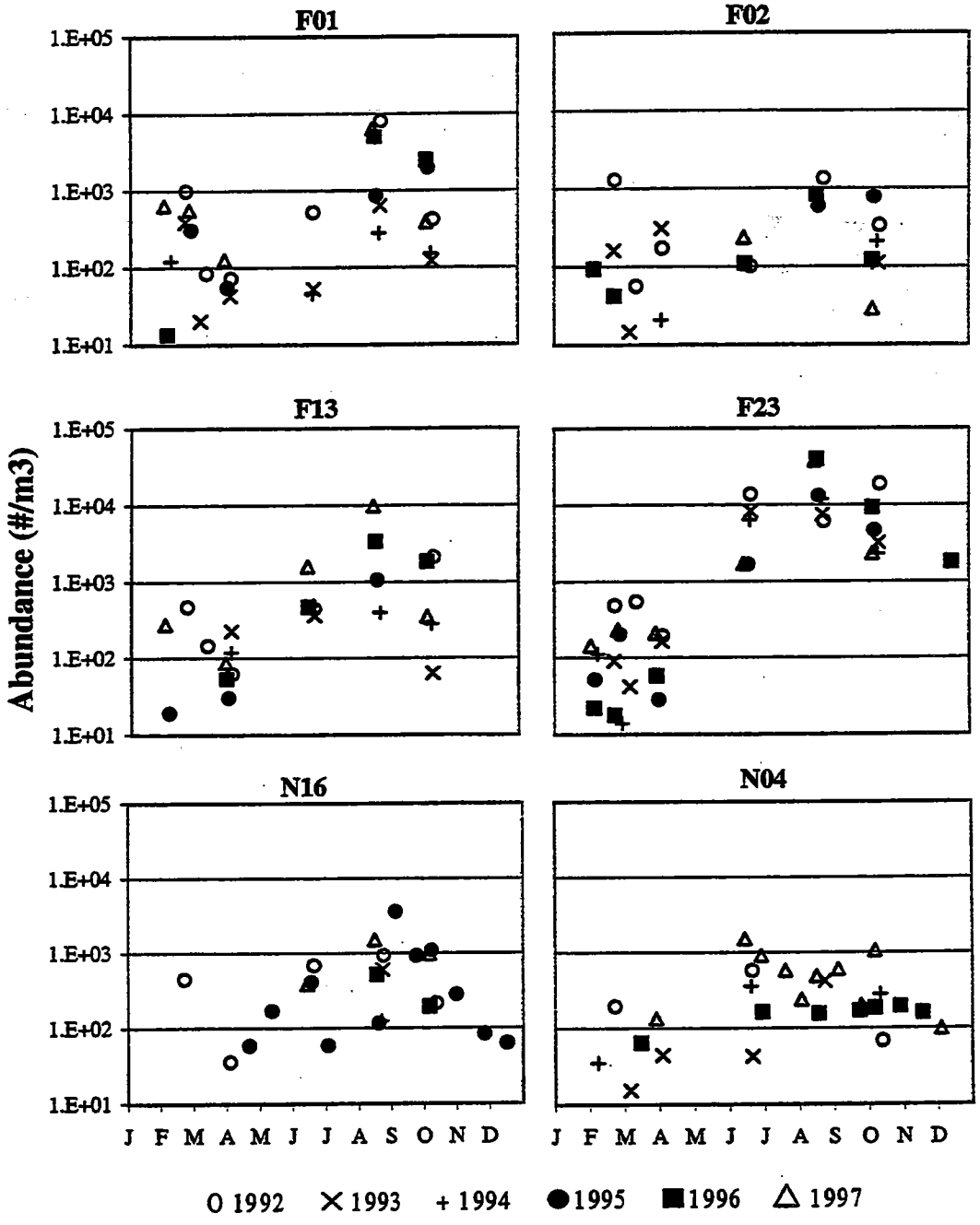

FIGURE 8-37
Interannual Distribution of *Acartia* spp. by Region

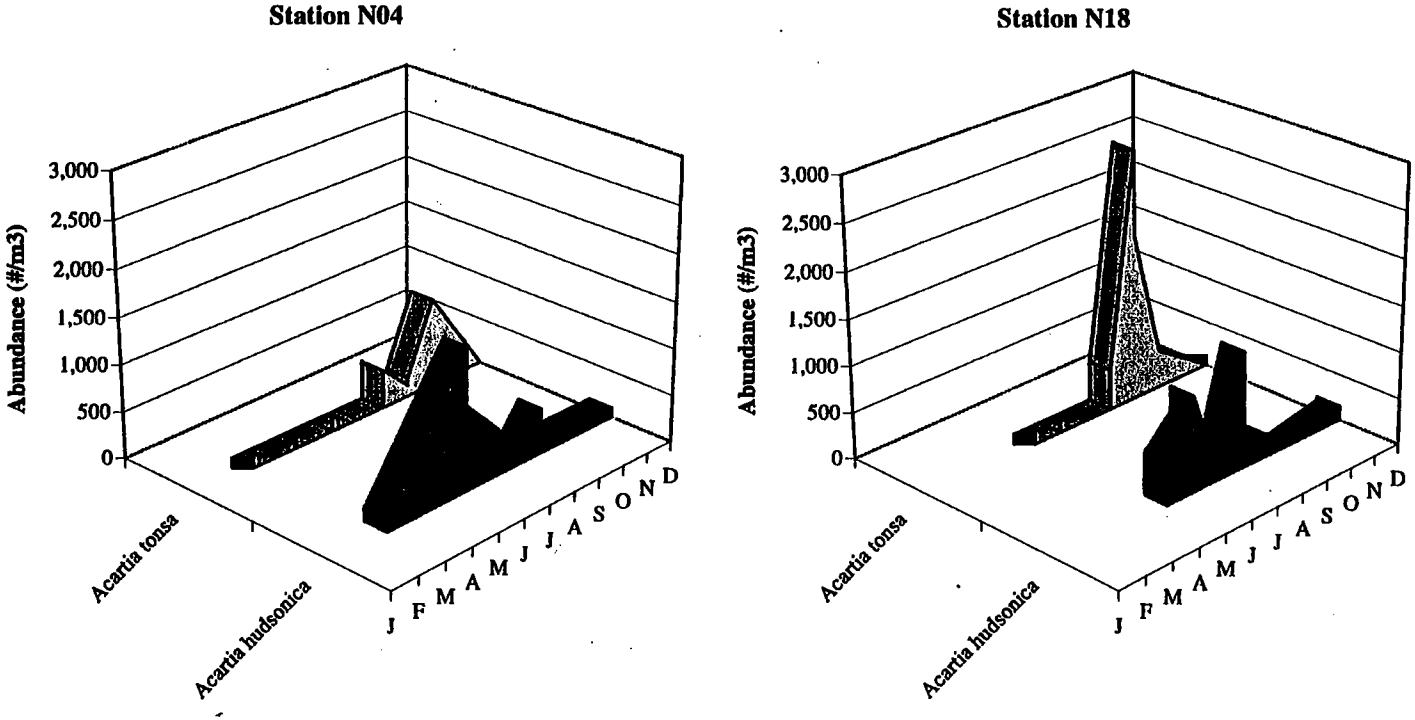

FIGURE 8-38
1997 Seasonal Abundance of *Acartia tonsa* and *Acartia hudsonica* at Nearfield Stations N04 and N18

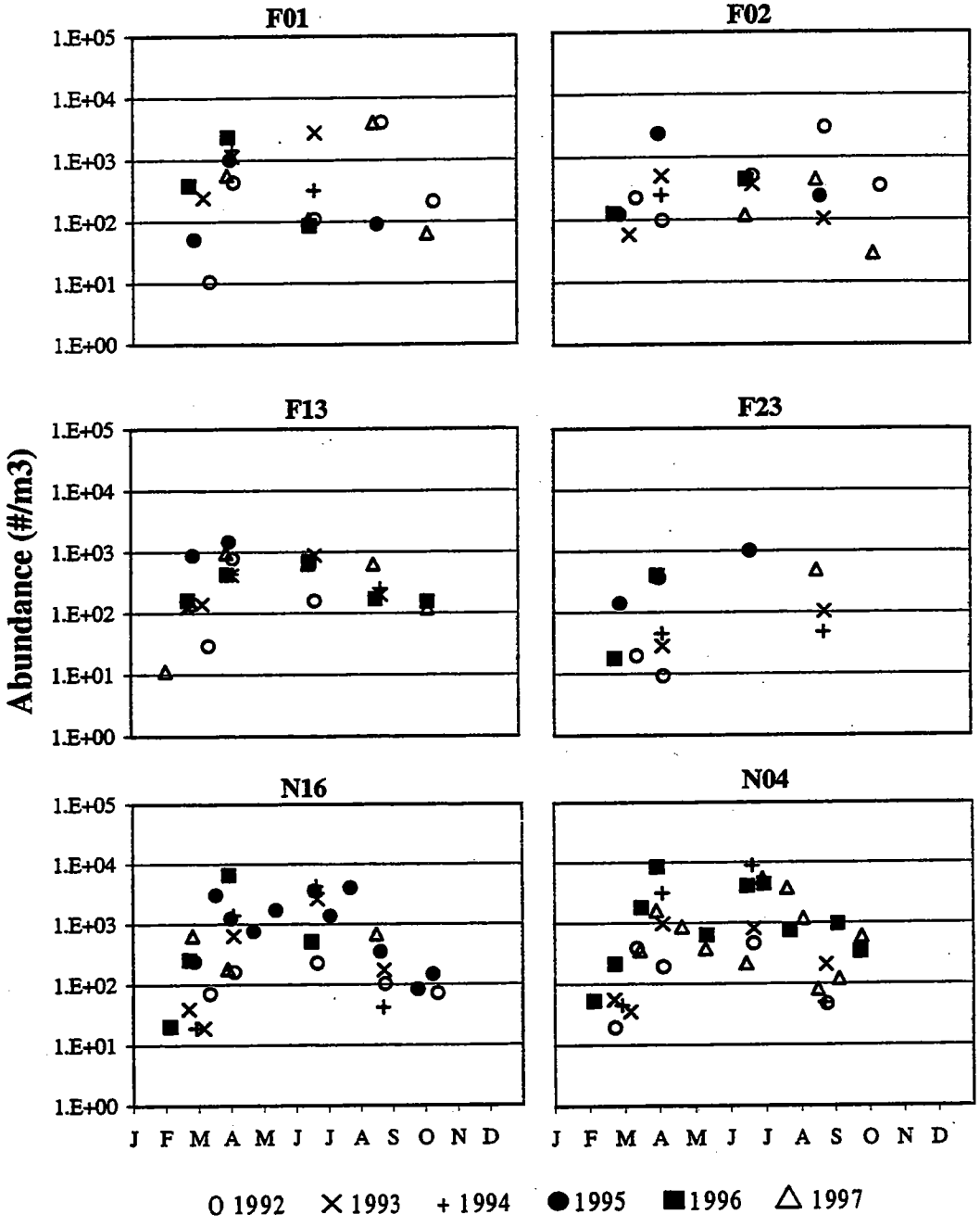

FIGURE 8-39
Interannual Distribution of *Calanus finmarchicus* by Region

9.0 DISCUSSION

This section provides an overview of the major water column events that occurred during the 1997 monitoring program. Table 9-1 provides a summary of results presented in previous sections of this report. For each area of the water column program, significant events in terms of the structure and biotic activity in the nearfield are identified, facilitating integration of the various monitoring results.

Salinity stratification was evident early in the season, with snowmelt and rainfall runoff during early April increasing its strength. Strong storms at the beginning and end of April produced vertical mixing. The onset of thermal stratification during May resulted in strong water column stratification through early October. However, partial mixing was evident during early June, late July, and late August. Advection of bottom water into the nearfield appeared to occur during late June/July, early August and late September. The August and September events showed concurrent evidence of coastal upwelling. The pycnocline at the deeper nearfield stations still showed some vertical stratification by the end of October, but complete mixing was likely early in November due to storm activity.

A phytoplankton bloom documented in late February partially stripped nutrients from the water column, however a ten-day period of cloudy weather appeared to weaken the bloom. The bloom did continue through April, resulting in depletion of surface nutrients in the nearfield through May and complete removal by early June. Mixing during late April, along with advection from the spring freshet, appeared to temporarily replenish surface nutrients, and may have contributed to a bloom at mid-depth during May. Surface nutrient concentrations also appeared to increase during early July and again briefly during August and September. Mixing during October resulted in increased nutrient concentrations by month's end.

Massachusetts Bay exhibited little phytoplankton activity during early February, but the onset of the late winter bloom was apparent in Cape Cod Bay. By the end of February, the bloom in Cape Cod Bay was fully developed, and most of Massachusetts Bay (except Boston Harbor) also was experiencing bloom conditions. Bloom activity appeared to subside during early March, but resumed by the end of the month and continued through most of April. A subsequent bloom during May was observed to occur below the developing pycnocline. During the summer, peak chlorophyll activity was seen in the Harbor and adjacent coastal stations, although a mid-June surface bloom was seen at station N04. Harbor activity continued from June through August, and even increased somewhat during the fall bloom in early October. The fall bloom appeared to initiate in late September in the shallower coastal stations, and progressed into deeper water in early October. A small chlorophyll peak was seen in December at station N10.

Nearfield bottom water DO concentration peaked during March and then began its seasonal decline. By June, the average nearfield bottom water DO concentration was the lowest on record for that period.

However, the decline in bottom water DO concentration and saturation reversed itself during late June and July, with a net increase of around 1.5 mgL^{-1} apparently averting record-setting DO minima. By the end of July, the typical decline in concentration resumed for the remainder of the stratified period. Average nearfield bottom water DO concentration and saturation reached their minima during early October, but individual minima were encountered during the late October survey.

Productivity rates in the nearfield peaked during the late winter bloom, which was followed by two small productivity peaks in April (station N18) and May (both stations N18 and N04). Meanwhile, the Harbor exhibited increasing productivity rates beginning in late March and reached a seasonal peak during June. While small periodic increases were evident in the nearfield during July and September, the Harbor showed continued high productivity during the August survey. The Harbor, nearfield, and northern Massachusetts Bay reached their annual maxima during the fall bloom in early October, however rates quickly fell to winter levels by month's end. A small increase was observed during December at nearfield station N18.

The spring bloom resulted in high water column respiration rates in the nearfield during March and April. In fact, it appeared that the spring bloom, combined with the mid-depth chlorophyll peak in May, produced some of the highest water column and sediment respiration rates seen during baseline monitoring. The high rates produced the record low oxygen concentrations reported during June. Surface respiration rates peaked in early July, declined to mid-August, and increased to a secondary peak during late September and early October. Bottom water respiration rates fluctuated through the stratified period, with peaks noted in mid-June and late July. Rates fell off until a fall peak in late September.

The late winter chlorophyll activity seen during the first survey in Cape Cod Bay appeared to be driven by the centric diatom *Rhizosolenia delicatula* and several other centric diatoms. The late winter bloom in the nearfield was initially driven by *Thalassiosira*, followed by *Phaeocystis pouchetii* and *Chaetoceros*. Following appearances in the nearfield by *Rhizosolenia fragilissima*, both this species and *Chaetoceros* then appeared to become dominant in the Harbor. The activity within the Harbor during August was predominately due to *R. fragilissima* and *Skeletonema costatum*, while *R. fragilissima* and *Cyclotella* were dominant in the nearfield. The fall bloom was driven by *Thalassiosira*, *Cyclotella*, and the pennate diatoms *Asterionellopsis glacialis* and *Thalassionema nitzschioides*.

Zooplankton abundance exhibited several peaks in the nearfield, including late March/early April, mid-June and July, late August, and October. The annual peak at N04 was during the summer, while the annual peak at N18 occurred during October. Copepod adults and nauplii typically dominated the assemblage, with *Oithona similis* and *Pseudocalanus newmani* the numerically dominant copepod taxa early in the year. As is typically the case in Massachusetts Bay, *Calanus finmarchicus* was the dominant taxon in terms of biomass. *Oithona similis* continued to be the numerical dominant later in the year, with co-dominant species including *Pseudocalanus newmani*, *Temora longicornis*, and *Centropages* spp.

Report Section	Month (10 day intervals)	February			March			April			May			June			July			August			September			October			November			December		
	Survey	1		2		3		4		5		6			7		8		9	10		11	12		13	14		15				16		17	
3.1	Meteorological Overview	Warm & Dry			Cool & Wet					Cool & Dry				Dry			Dry			Cool			Dry			Dry			Cold & Wet			Warm & Dry			
		NE		W	W	NE		NE/SS		RS/W	Hail		Calm		Calm	TS/W	TS/W	Heat Wave	TrS	RS		TS			CALM			NE	W	SS	W	SS/W			SS/W
3.2.1	Temperature													M↑					M↑	A↓	A↓	M↑		A↓	A↓ A		M↑								
3.3.1	Salinity									M↓		↑		M↓					M↓	A↑	A↑	M↓		A↑	↑ A		M↓		M↓	M↓					
3.4	Density	Weak Salinity Stratification								STRATIFIED PERIOD																	Outer NF out								
3.5	NF Currents (mid-depth)	Variable		NW		SW		SE-NW		SE		SW			N-S		E-N		SE	SE		SE	N-SE												
3.5	NF Currents (bottom depth)	SW		W		W		E-W		E-NE		W			SW		E-W		E-W	W		W-E	SW		SW	W		NW				SW-NW	SE-SW	
4.1	NF Surface Nutrients																																		
	NO_3+NO_2			↓		↓		↓		↓		↓			↓		↑		↓	↓		↑	↓		↑	↓		↑					↑	↑	
	NH_4			↓		↑		↓		↑		↓			↓		↑		↓	↓		↑	↓		↑	↓		↑					↓	↑	
	SiO_4			↓		↓		↓		↑		↓			↓		↑		↑	↓		↓	↑		↓	↓		↑					↑	↑	
	PO_4			↓		↓		↓				↓			↓		↑			↓		↑	↓		↑	↓		↑					↑	↑	
5.1	Chlorophyll a	CCB		Regional Bloom		↓		N18 Bloom				Subsurface NF Bloom			Harbor/N18							Harbor/N10					Fall Bloom							N10 Bloom	
6.3	NF Bottom Water DO					Seasonal Peak		↓		↓		↓			↓		↑		↑	↓		↓	↓		↓	↓		↑					↑	↑	
7.1	Productivity			NF Seasonal Peak		↓		N18 ↑		↓		↑			↓		↑		↓			(F13 Peak)			N18 N04	(F13 Peak)		↓					↓	N18↑	
7.2	Respiration			↑		Bottom Peak				Surface Peak					High Surface Water Respiration											Surface & Bottom		↓							
	POC-Spec Resp																	↓																	
8.1.1	Phytoplankton																																		
	Diatoms			*Thalassiosira*				*Chaetoceros*				*Chaetoceros*			*Rhizosolenia* (N04) *Chaetoceros* (F13)							*Skeletonema* (Harbor) *Rhizosolenia* (CCB)			*Rhizosolenia Cyclotella*		*Thalassiosira Cyclotella*								
	Dinoflagellates														*Ceratium*							*Gymnodinium*												
	Others			*Phaeocystis*				*Phaeocystis*							*Cryptophytes*							*Cryptophytes*					*Ceratium*							
8.2.1	Zooplankton							Seasonal Peak										Annual Peak at N04						Seasonal Peak					Annual peak at N18					

Legend

NE Northeaster W High Winds RS Rain Storm M Mixing Event A Advection NF Nearfield ↑↓ Parameter Trend

SS Snow Storm TS Thunderstorm TrS Tropical Storm GOM Gulf of Maine Intrusion ↔ Indicates temporal extent of event

TABLE 9-1
Overview of 1997 Water Column

10.0 REFERENCES

Anderson, D.M. and B.A. Keafer. 1992. Paralytic Shellfish Poisoning on Georges Bank: In-situ Growth or Advection of Established *Dinoflagellate* Populations. In: J. Wiggen, et al., (eds.), Gulf of Maine Workshop Report.

Anderson, D.M. and B.A. Keafer. 1995. Toxic Red Tides in Massachusetts and Cape Cod Bays. Final Report to the Massachusetts Water Resources Authority, January 31, 1995.

Anderson, D.M. 1997. Personal Communication with Steve Cibik.

Anderson, D.M. 1997. Toxic and Nuisance Species in Massachusetts Bay. 1996 Annual Workshop Presentation.

Bates, S.S. 1997. Personal communication with Steve Cibik, March 5, 1997. Also see: http://www.maritimes.dfo.ca/science/mesd/he/science/toxins/index.html

Becker, S. M. 1992. The seasonal distribution of nutrients in Massachusetts Bay and Cape Cod Bays [Master of Science]. Durham NH: University of New Hampshire. 127p.

Bowen, J. D., R. A. Zavistoski, S. J. Cibik, T. C. Loder, III, B. L. Howes and C. D. Taylor. 1997. Combined work/quality assurance plan for baseline water quality monitoring: 1995-1997. Boston: Massachusetts Water Resources Authority. Report ENQUAD ms-45. 93 p.

Cibik, S. J., B. L. Howes, C. D. Taylor, D. M. Anderson, C. S. Davis and T. C. Loder, III, R. D. Boudrow and J.D. Bowen. 1996. 1995 Annual water column monitoring report. Boston: Massachusetts Water Resources Authority. Report ENQUAD 96-07. 254p.

Cibik, S. J., K. B. Lemieux, J. K. Tracey, S. J. Kelly, B. L. Howes and C. D. Taylor. 1998a. Semi-annual water column monitoring report: August - December 1997. Boston: Massachusetts Water Resources Authority. Report ENQUAD 98-18. 360 p.

Cibik, S. J., K. B. Lemieux, B. L. Howes, C. S. Davis, C. D. Taylor and T. C. Loder, III. 1998b. Semi-annual water column monitoring report: February - July 1997. Boston: Massachusetts Water Resources Authority. Report ENQUAD 98-17. 442 p.

Cibik, S. J., K. B. Lemieux, B. L. Howes, C. D. Taylor, C. S. Davis, T. C. Loder, III and R. D. Boudrow. 1998c. 1996 Annual water column monitoring report. Boston: Massachusetts Water Resources Authority. Report ENQUAD 98-11. 416 p.

Cibik, S. J., K. B. Lemieux, C. S. Davis and D. M. Anderson. 1998. Massachusetts Bay plankton communities: characterization and discussion of issues relative to MWRA's outfall relocation. Boston: Massachusetts Water Resources Authority. Report ENQUAD 98-08. 140 p.

Cleveland, J.S., M.J. Perry, D.A. Kiefer and M.C. Talbot. 1989. Maximal Quantum Yield of Photosynthesis in the Northwestern Sargasso Sea. J. Mar. Res. 47, 869-886.

Falkowski, P.G. 1992. Molecular ecology of phytoplankton photosynthesis. p. 47-67. In P.G. Falkowski and A. Woodhead (eds.), Primary Productivity and Biogeochemical Cycles in the Sea. Plenum Press, New York.

Franks, P.J.S. and D.M. Anderson. 1992. Along shore Transport of a Toxic Phytoplankton Bloom in a Buoyancy Current: *Alexandrium tamarense* in the Gulf of Maine. Mar. Biol. 112:153-164.

Geyer, W.R., G.B. Gardner, W.S. Brown, J. Irish, B. Butman, T.C. Loder, and R.P. Signell. 1992. Final report: Physical Oceanographic Investigation of Massachusetts and Cape Cod Bays. August 1, 1992. 497 p.

Howes, B.L. 1998a. Sediment metabolism within Massachusetts Bay and Boston Harbor relating to sediment-water column exchanges of nutrients and oxygen in 1995. Boston: Massachusetts Water Resources Authority. Report ENQUAD 98-02. 68p.

Howes, B. L. 1998b. Sediment metabolism within Massachusetts Bay and Boston Harbor relating to system stability and sediment-water column exchanges of nutrients and oxygen in 1996. Boston: Massachusetts Water Resources Authority. Report ENQUAD 98-10. 67p.

Kelly, J. R. and P. H. Doering. 1995. Nutrient issues update 1995: metabolism in Boston Harbor, Massachusetts and Cape Cod Bays, MA (USA) during 1992-1994. Boston: Massachusetts Water Resources Authority. Report ENQUAD 95-19. 38pp.

Kelly, J. R. and J. Turner. 1995. Water column monitoring in Massachusetts and Cape Cod Bays: annual report for 1994. Boston: Massachusetts Water Resources Authority. Report ENQUAD 95-17. 163pp.

Kelly J.R. 1997. Nitrogen flow and the interaction of Boston Harbor with Massachusetts Bay throughout 1996. Estuaries, 20:365-380.

Murray, P. M., S. J. Cibik, K. B. Lemieux, R. A. Zavistoski, B. L. Howes, C. D. Taylor and T. C. Loder, III. 1998. Semi-annual water column monitoring report: February-July 1996. Boston: Massachusetts Water Resources Authority. Report ENQUAD 98-01. 397 p.

NRCC. 1998a. Climate Impacts January –December 1997. Northeast Regional Climate Center. Cornell University, New York: http://met-www.cit.cornell.edu/.

NRCC. 1998b. Precipitation Data (Logan Airport) January –December 1997. Northeast Regional Climate Center. Cornell University, New York: http://met-www.cit.cornell.edu/.

NRCC. 1998c. Climate Summaries. Northeast Regional Climate Center. Cornell University, New York: http://met-www.cit.cornell.edu/climate/Summary_Ann-96.html.

Oudot, C., R. Gerard, and P. Morin. 1988. Precise shipboard determination of dissolved oxygen (Winkler procedure) for productivity studies with a commercial system. Limnology and Oceanography 33:146-150.

Redfield, A. C., B. H. Ketchum and F. A. Richards. 1963. The influence of organisms on the composition of sea water. pp. 26-77. In M. N. Hill (ed.), The Sea, Vol.II. John Wiley, NY

Taylor, C.D. 1998. Primary Productivity Methods for MWRA HOM Program. Massachusetts Water Resources Authority

USGS, 1998a = Massachusetts Bay Long Term Monitoring Station Data Plots, http://atlantic.er.usgs.gov/fhotchki/bosatt97.gif

USGS, 1998b = Massachusetts Bay Long Term Monitoring Station Data Plots, http://atlantic.er.usgs.gov/fhotchki/bostem97.gif

USGS, 1998c = Massachusetts Bay Long Term Monitoring Station Data Plots, http://atlantic.er.usgs.gov/fhotchki/bossal97.gif

USGS, 1998d = Online current meter data, http://crusty.er.usgs.gov/epic/

USGS, 1998e - Massachusetts Bay Long Term Monitoring Station Data Plots, http://atlantic.er.usgs.gov/fhotchki/bostik97.gif

APPENDIX A

CURRENT VECTORS

			Start Time	2-Feb-97	26-Feb-97	17-Mar-97	31-Mar-97	22-Apr-97	12-May-97	16-Jun-97	30-Jun-97	21-Jul-97	4-Aug-97	17-Aug-97	5-Sep-97	25-Sep-97	7-Oct-97	29-Oct-97	4-Dec-97	16-Dec-97
			End Time	5-Feb-97	1-Mar-97	18-Mar-97	6-Apr-97	23-Apr-97	13-May-97	20-Jun-97	1-Jul-97	22-Jul-97	6-Aug-97	23-Aug-97	5-Sep-97	25-Sep-97	10-Oct-97	30-Oct-97	4-Dec-97	16-Dec-97
			Center Time	3-Feb-97	27-Feb-97	17-Mar-97	3-Apr-97	22-Apr-97	12-May-97	18-Jun-97	30-Jun-97	21-Jul-97	5-Aug-97	20-Aug-97	5-Sep-97	25-Sep-97	8-Oct-97	29-Oct-97	4-Dec-97	16-Dec-97
Start Time	End Time	Interval (min)	Depth (m)	W9701	W9702	W9703	W9704	W9705	W9706	W9707	W9708	W9709	W9710	W9711	W9712	W9713	W9714	W9715	W9716	W9717
10/1/96 17:00	1/19/97 0:00	60	5.0																	
10/1/96 18:00	2/12/97 12:59	60	21.5																	
10/1/96 18:59	2/8/97 9:59	60	26.0	X																
10/1/96 18:59	2/8/97 9:59	60	28.6																	
2/12/97 16:00	6/10/97 12:00	60	28.6		X	X	X	X	X											
2/12/97 16:00	6/10/97 12:00	60	29.2																	
2/12/97 16:59	6/10/97 12:59	60	22.4																	
6/10/97 14:59	9/23/97 9:59	60	28.6							X	X	X	X	X	X					
6/10/97 14:59	9/23/97 9:59	60	29.2																	
6/10/97 17:00	9/23/97 14:00	60	22.4																	
9/23/97 16:59	1/31/98 3:59	60	28.6													X	X	X	X	X
9/23/97 16:59	1/31/98 3:59	60	29.2																	

TABLE 1

USGS oceanographic mooring data coincident with the nearfield sampling surveys

SURVEY	DEPTH			
	Mid-depth		Bottom	
	Direction of travel	R.T.	Direction of travel	R.T.
W9701	Variable	>14	SW	>11
W9702	NW	>9	W	4
W9703	SW	>8	W	>14
W9704	SE-NW	7	E-W	8
W9705	SE	2	E-NE	4
W9706	NW	>9	W	9
W9707	N-S	>14	SW	10
W9708	E-N	>10	E-W	>14
W9709	SE	5	E-W	>13
W9710	SE	4	W	>11
W9711	SE	2	W-E	>13
W9712	N-SE	8	SW	>14
W9713	X	X	SW	8
W9714	X	X	W	13
W9715	X	X	NW	11
W9716	X	X	SW-NW	>13
W9717	X	X	SE-SW	>14

Notes:
R.T. = Residence time (reported in days)
X - mid-depth current velocity not recorded

TABLE 2
Net water movement and residence time within the nearfield

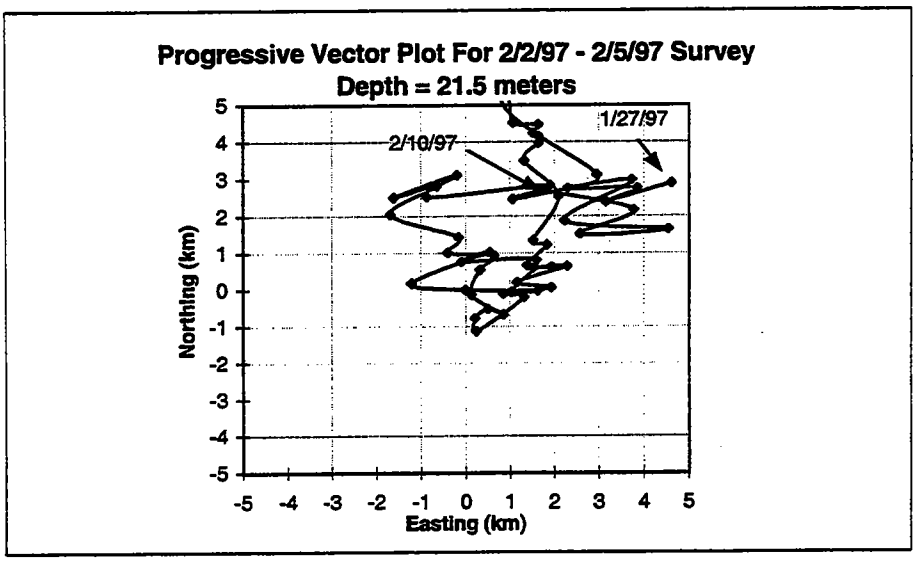

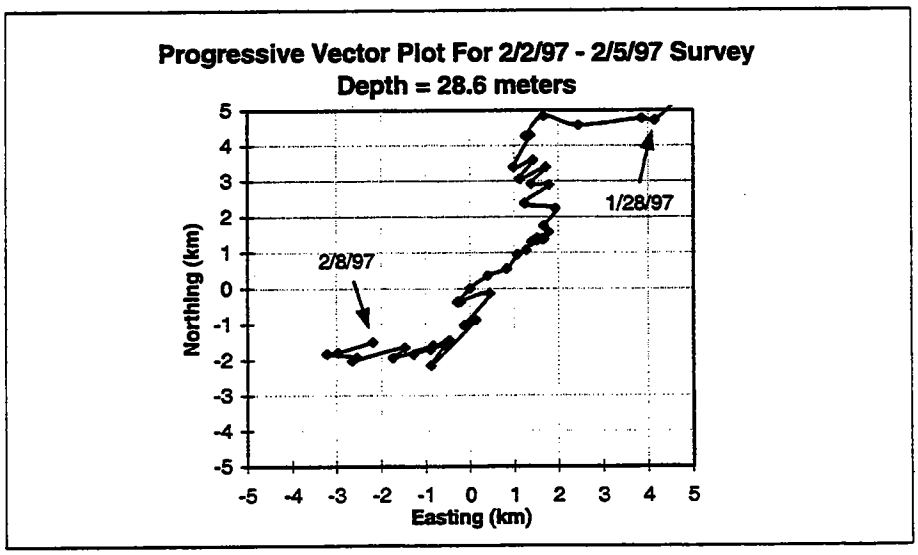

Note: The origin (0,0) is located at 42° 22.6' N latitude, 70° 47.0' W longitude.

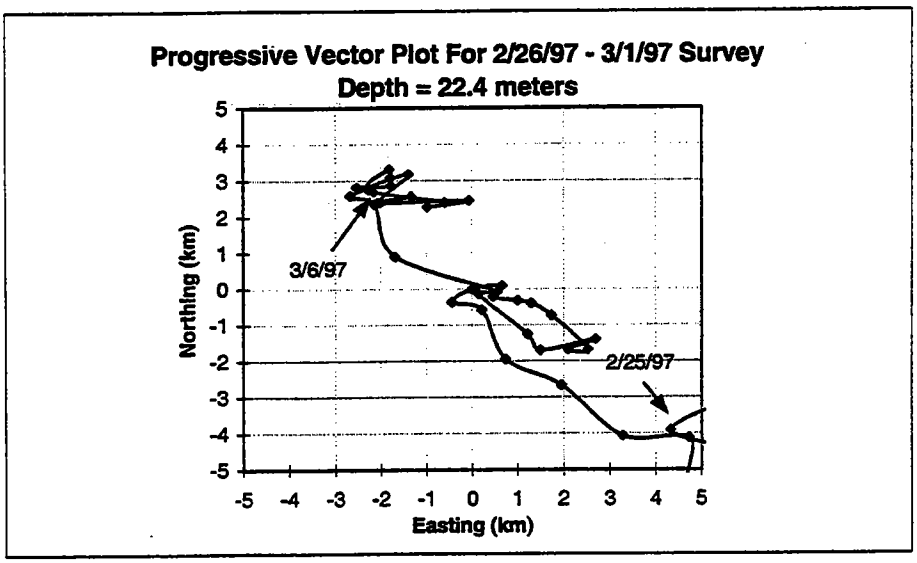

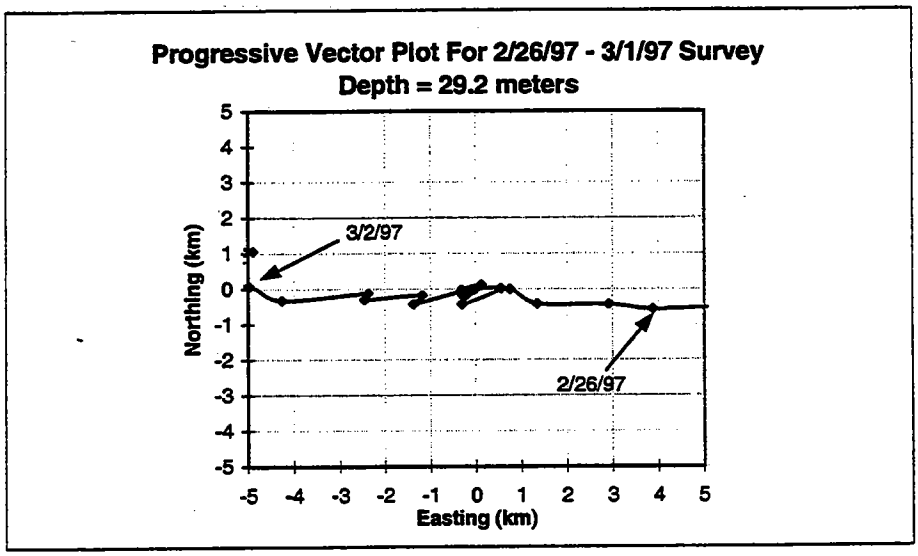

Note: The origin (0,0) is located at 42° 22.6' N latitude, 70° 47.0' W longitude.

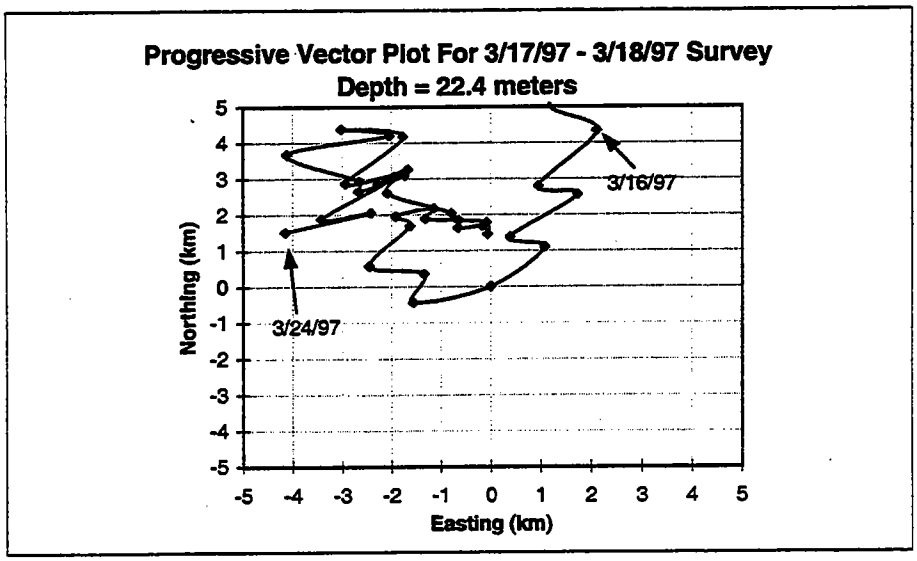

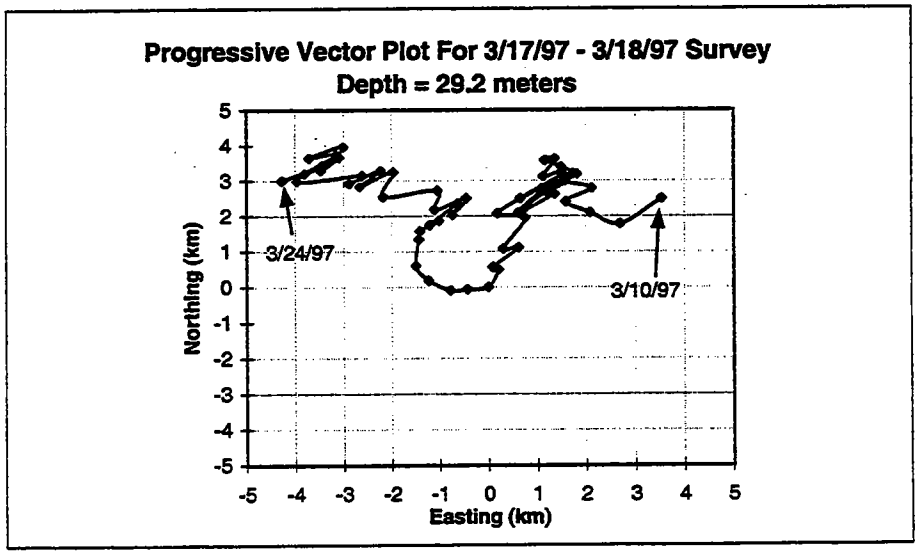

Note: The origin (0,0) is located at 42° 22.6' N latitude, 70° 47.0' W longitude.

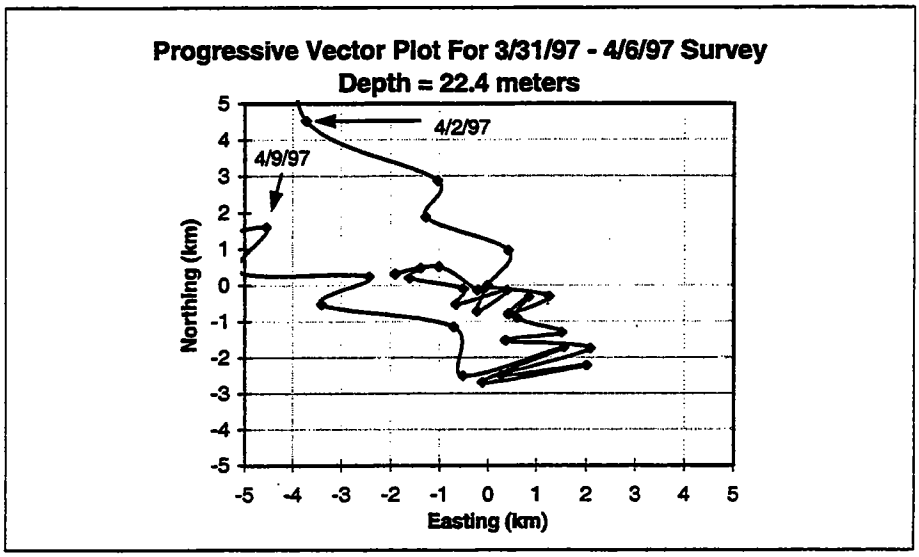

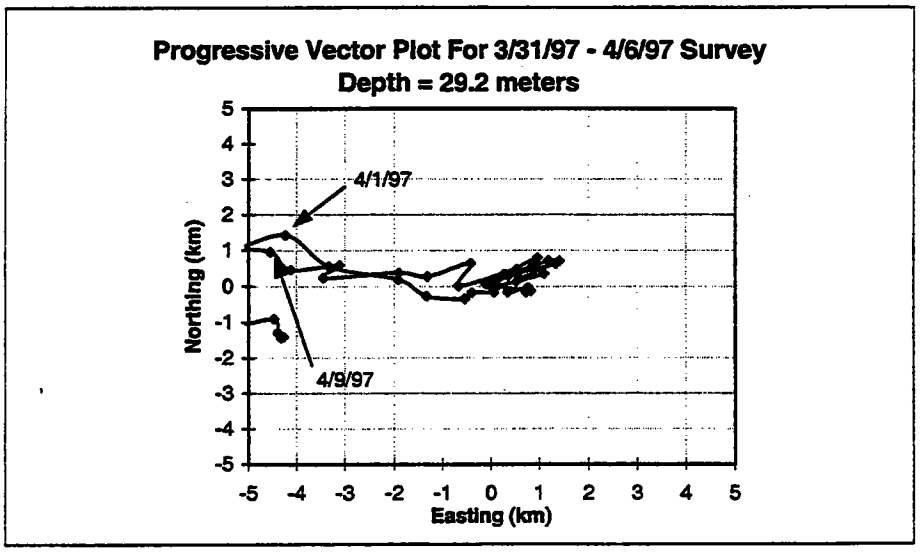

Note: The origin (0,0) is located at 42° 22.6' N latitude, 70° 47.0' W longitude.

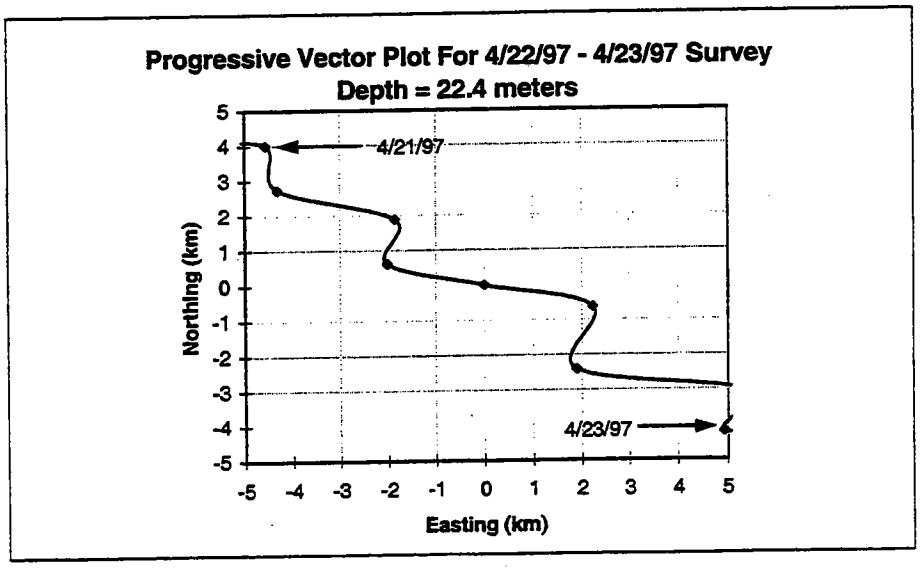

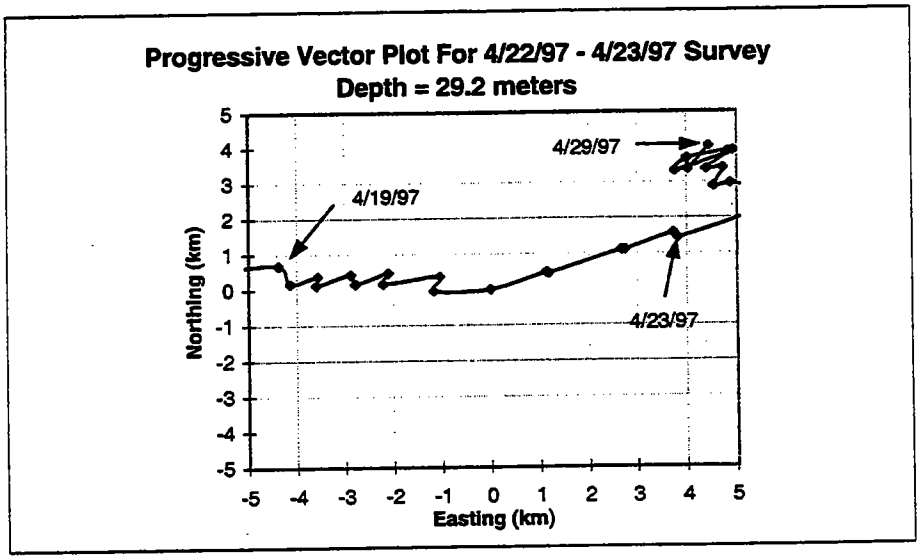

Note: The origin (0,0) is located at 42° 22.6' N latitude, 70° 47.0' W longitude.

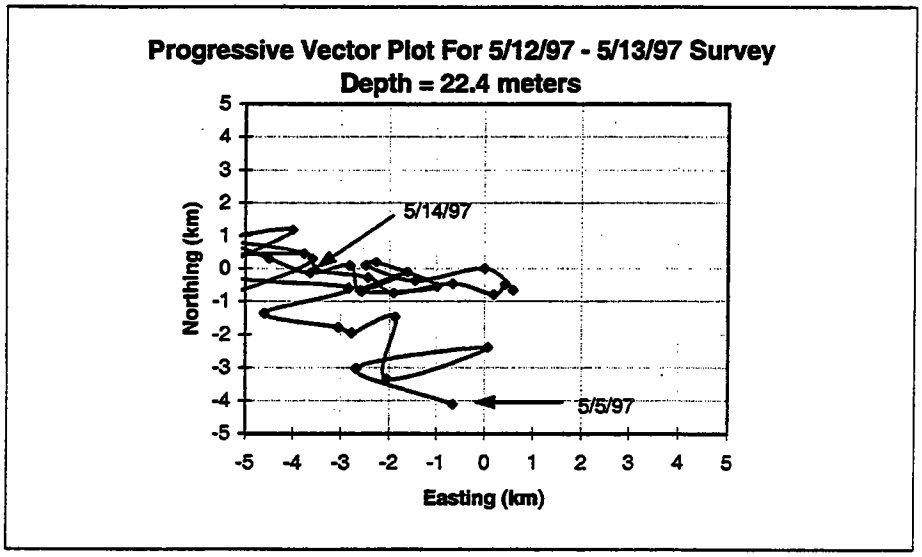

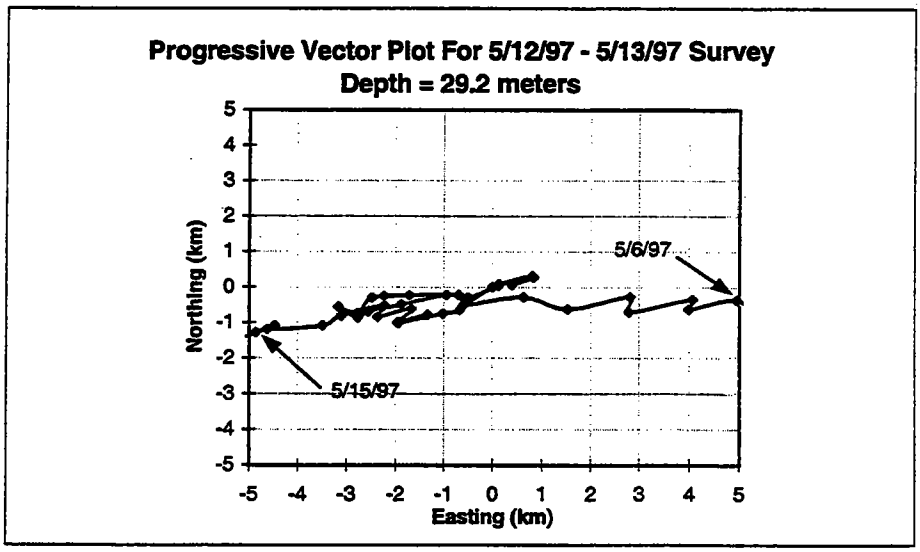

Note: The origin (0,0) is located at 42° 22.6' N latitude, 70° 47.0' W longitude.

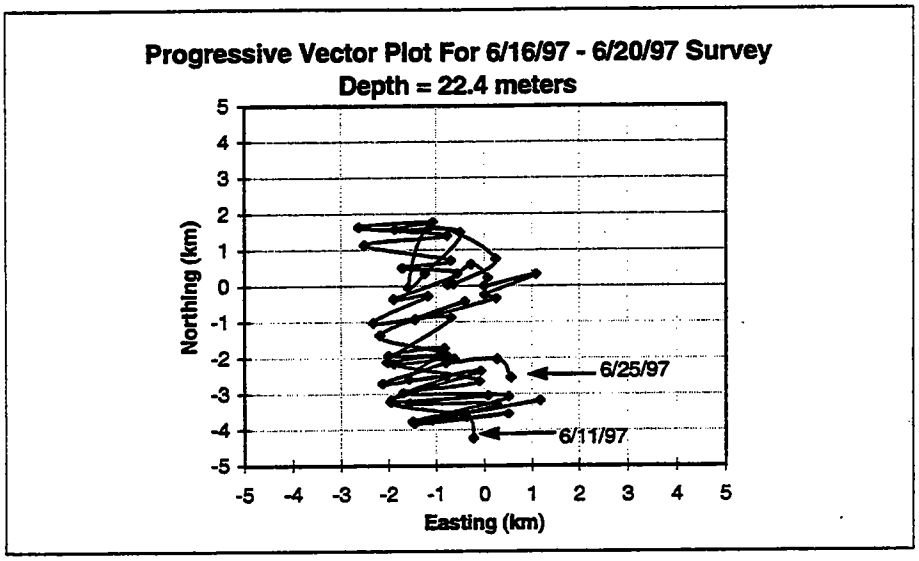

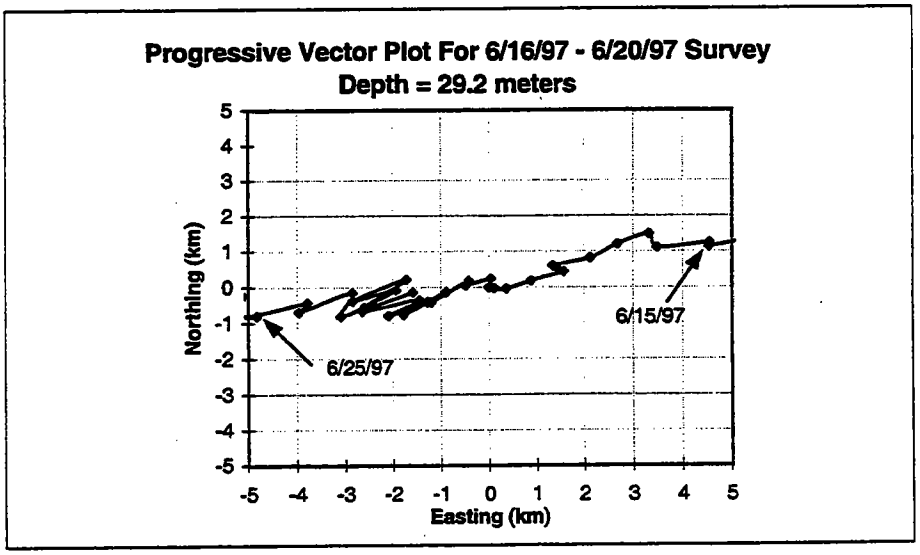

Note: The origin (0,0) is located at 42° 22.6' N latitude, 70° 47.0' W longitude.

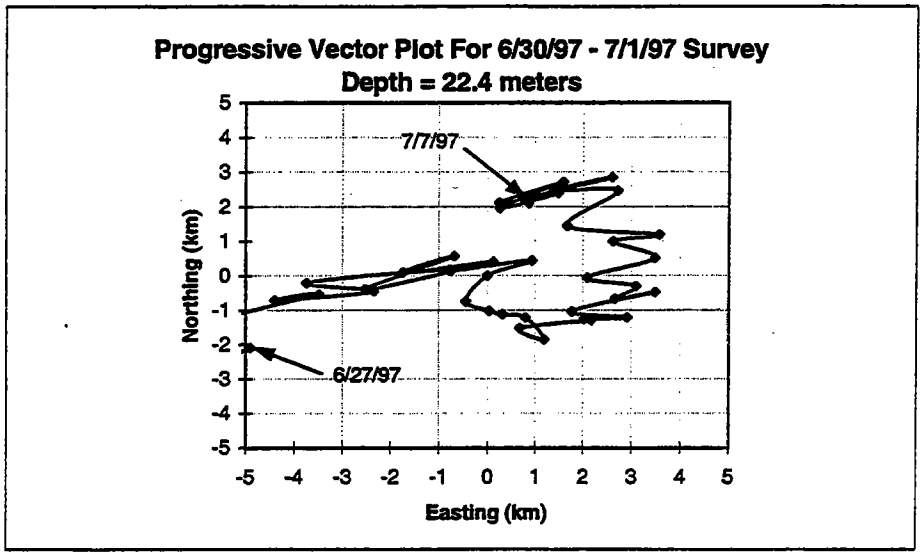

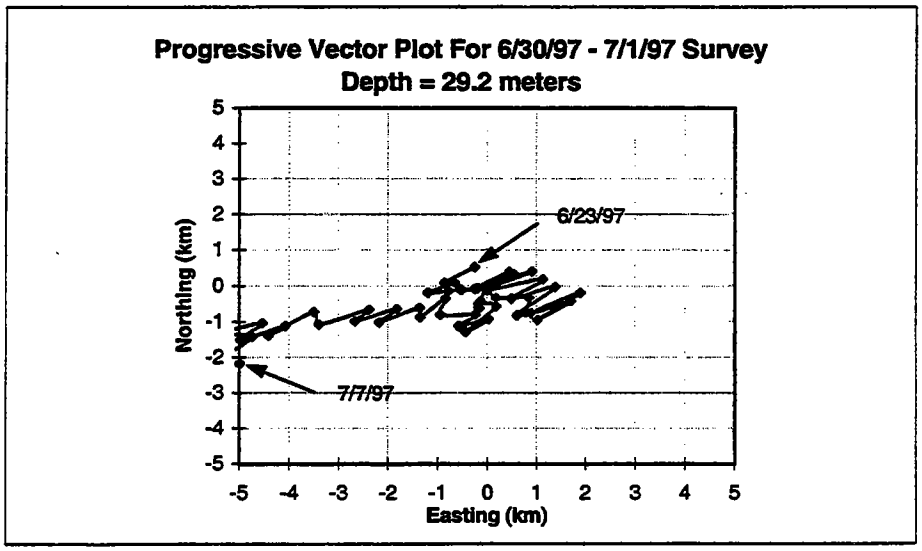

Note: The origin (0,0) is located at 42° 22.6' N latitude, 70° 47.0' W longitude.

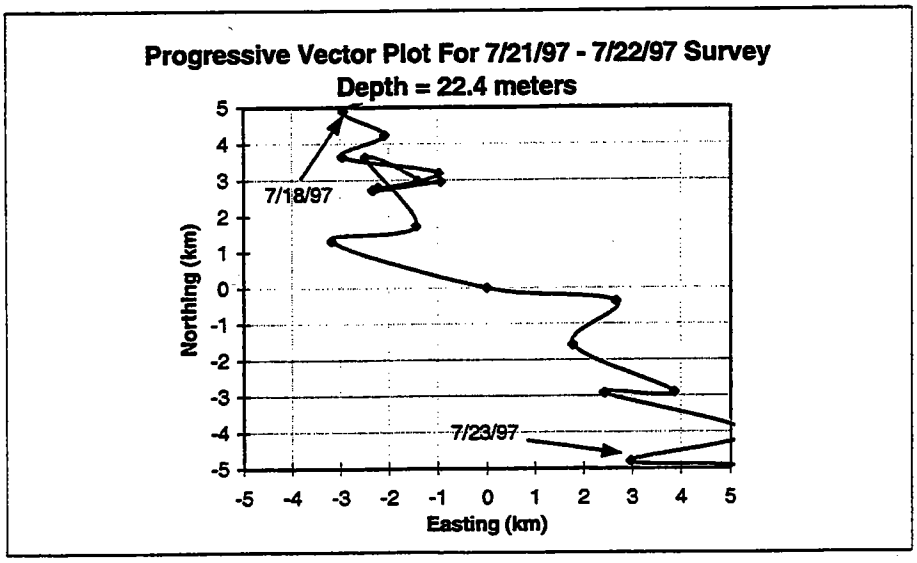

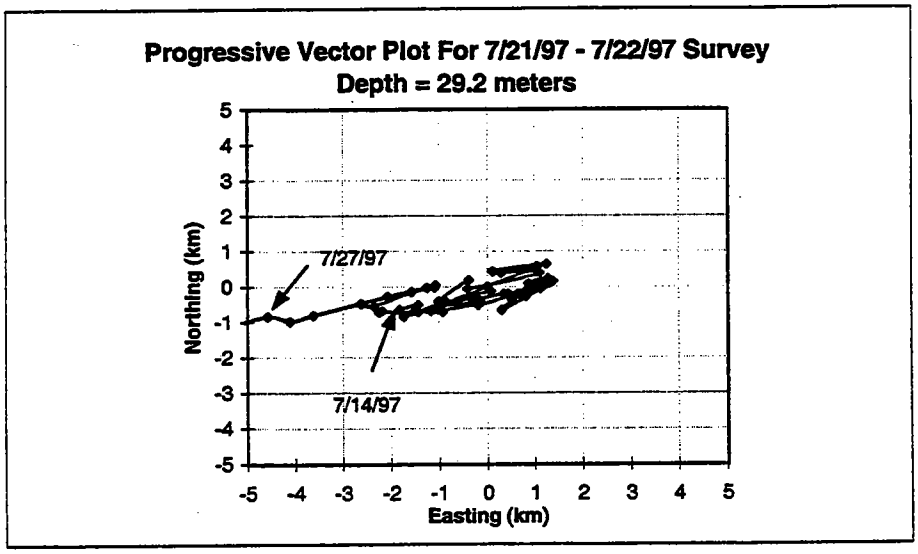

Note: The origin (0,0) is located at 42° 22.6' N latitude, 70° 47.0' W longitude.

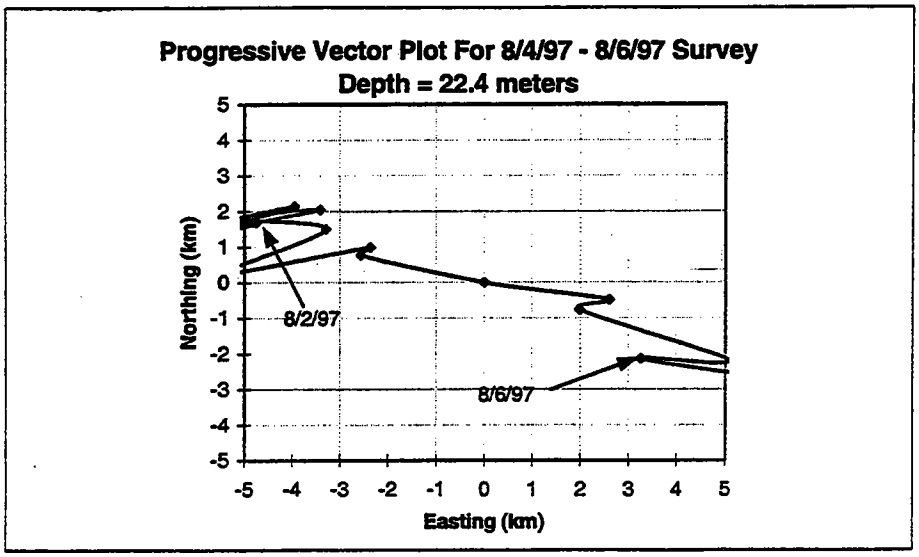

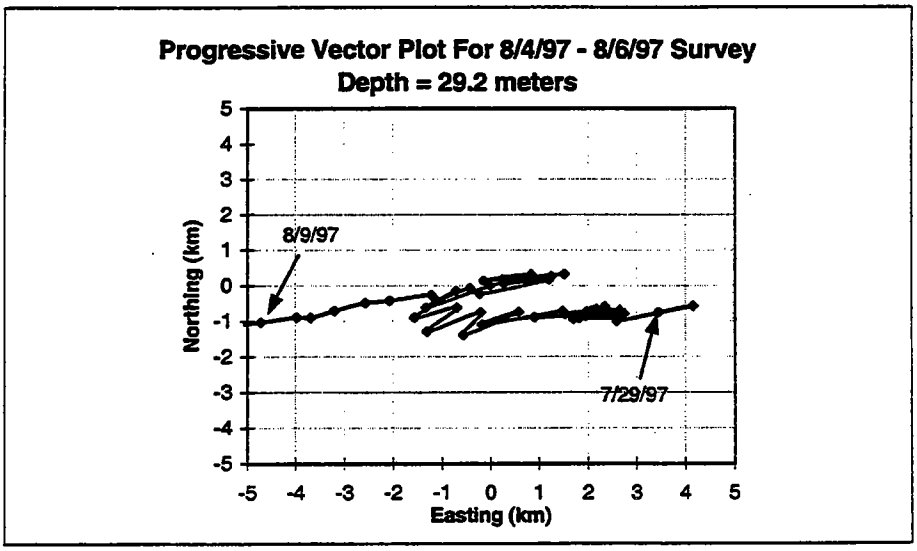

Note: The origin (0,0) is located at 42° 22.6' N latitude, 70° 47.0' W longitude.

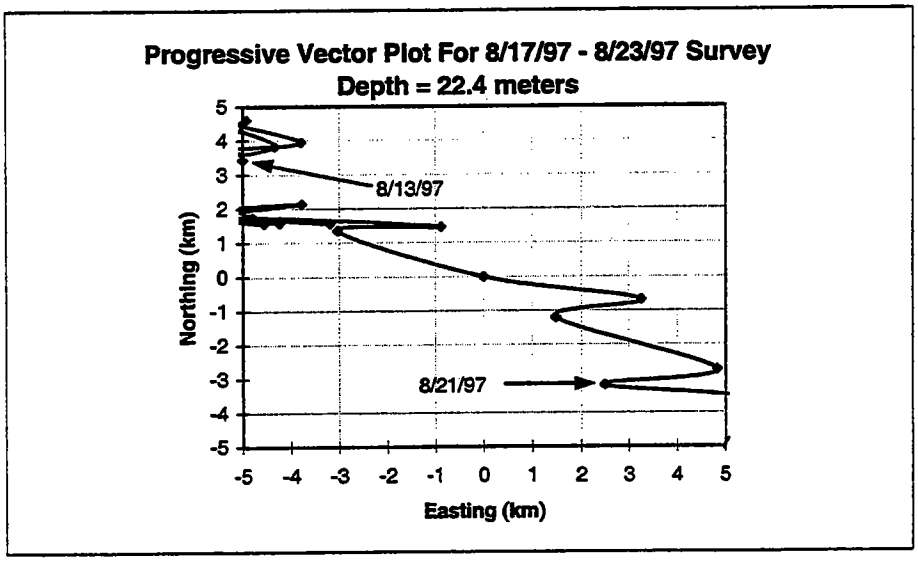

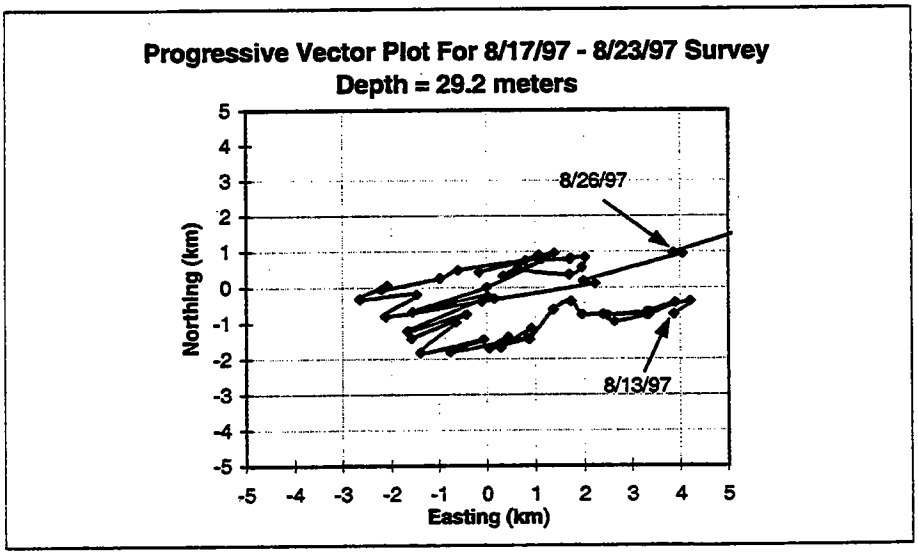

Note: The origin (0,0) is located at 42° 22.6' N latitude, 70° 47.0' W longitude.

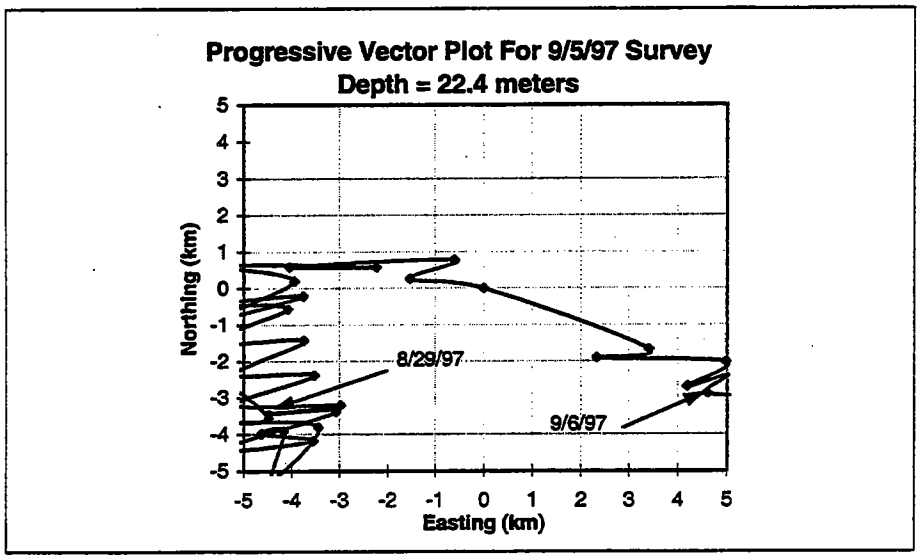

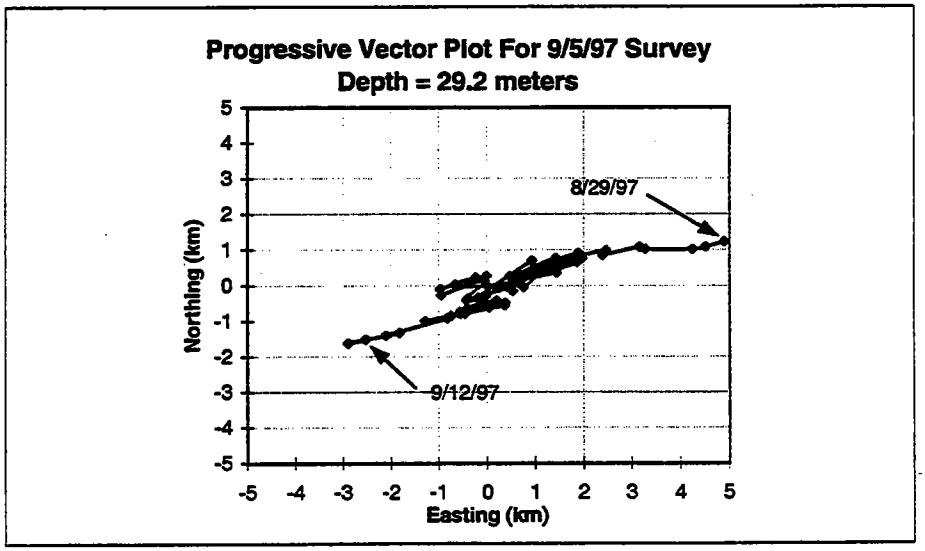

Note: The origin (0,0) is located at 42° 22.6' N latitude, 70° 47.0' W longitude.

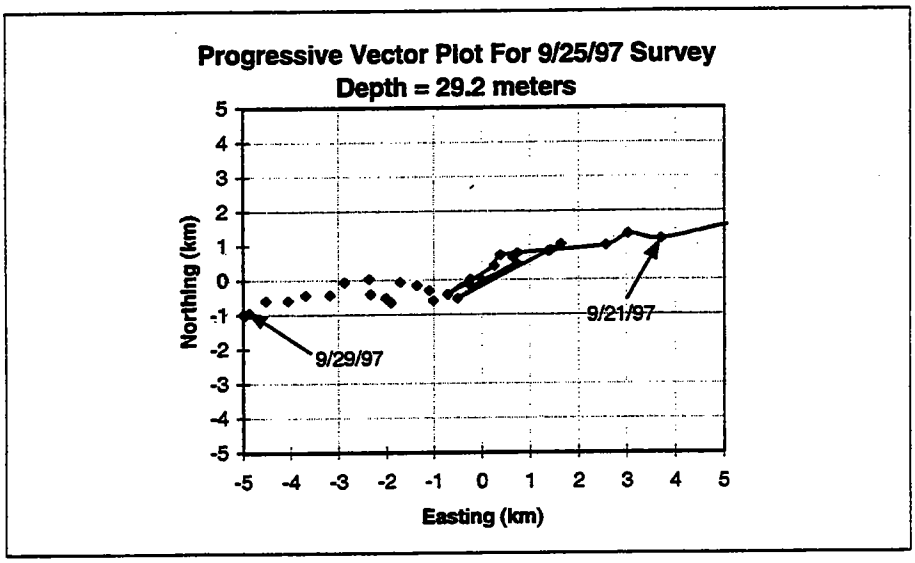

Note: The origin (0,0) is located at 42° 22.6' N latitude, 70° 47.0' W longitude.

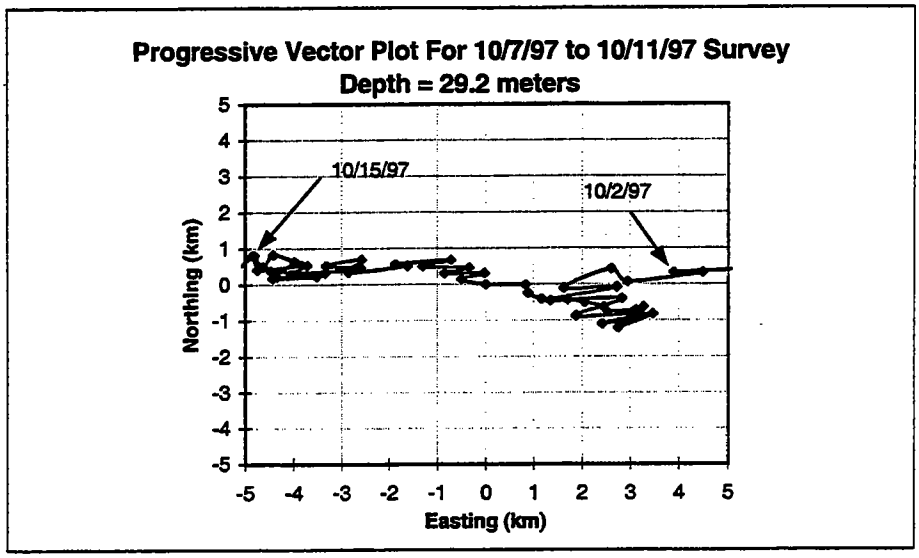

Note: The origin (0,0) is located at 42° 22.6' N latitude, 70° 47.0' W longitude.

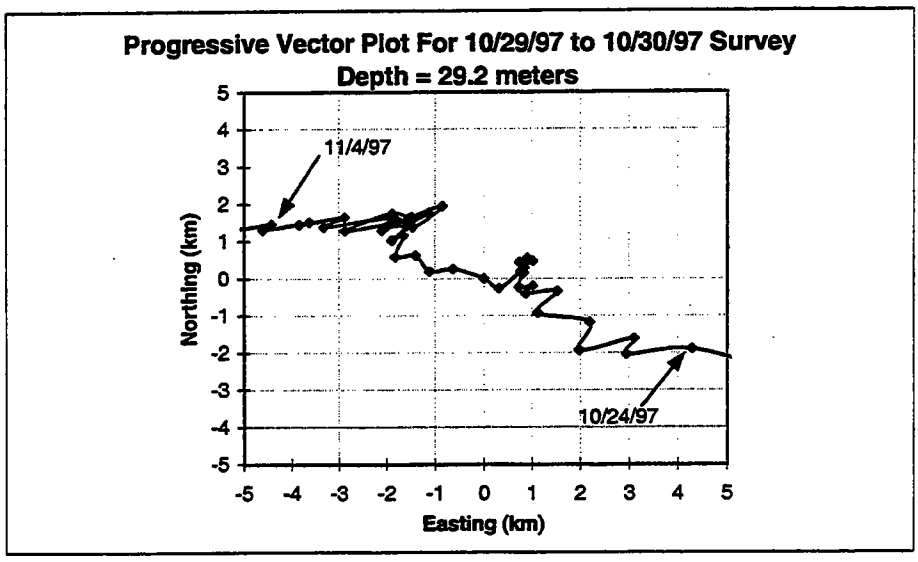

Note: The origin (0,0) is located at 42° 22.6' N latitude, 70° 47.0' W longitude.

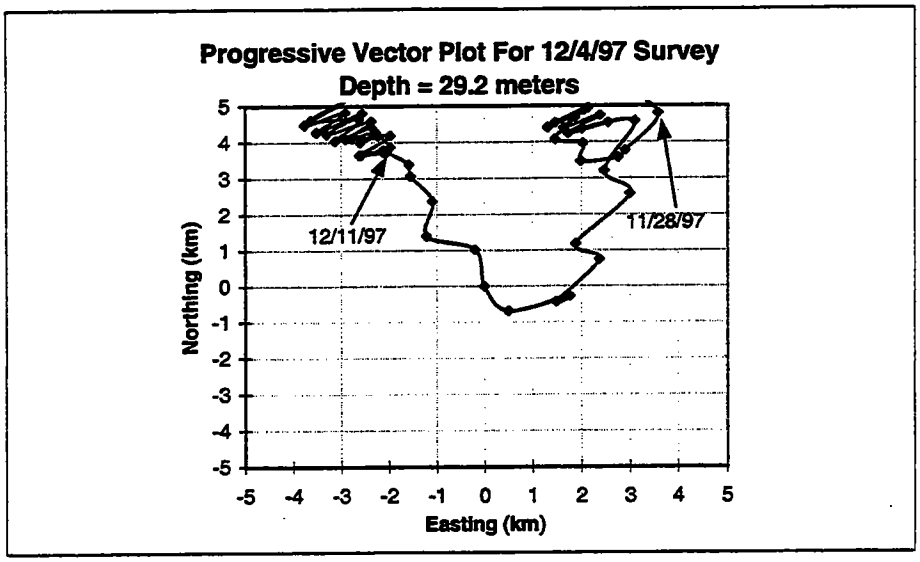

Note: The origin (0,0) is located at 42° 22.6' N latitude, 70° 47.0' W longitude.

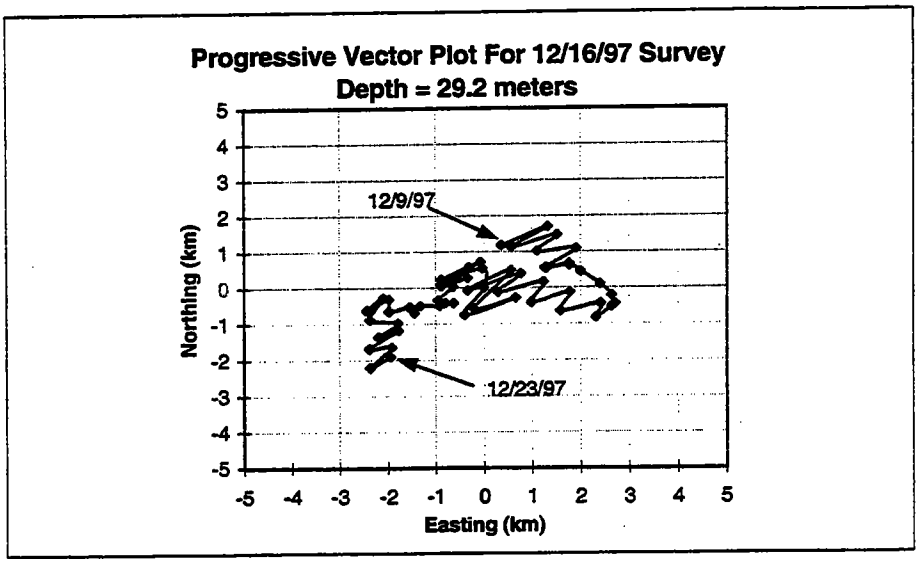

Note: The origin (0,0) is located at 42° 22.6' N latitude, 70° 47.0' W longitude.

Massachusetts Water Resources Authority
Charlestown Navy Yard
100 First Avenue
Boston, MA 02129
(617) 242-6000
http://www.mwra.state.ma.us